AWARD NUMBER: W81XWH-06-1-0585

TITLE: Rapid Translation of a Novel and Potent Vaccine in HER2+ Metastatic Breast Cancer Patients

PRINCIPAL INVESTIGATOR: H. Kim Lyerly, M.D.

CONTRACTING ORGANIZATION: Duke University
                                                    Durham, NC 27710

REPORT DATE: October 2013

TYPE OF REPORT: Final

PREPARED FOR: U.S. Army Medical Research and Materiel Command
                         Fort Detrick, Maryland 21702-5012

REPORT DOCUMENTATION PAGE

Public reporting burden for this collection of information is estimated to average 1 hour per response, including the time for reviewing instructions, searching existing data sources, gathering and maintaining the data needed, and completing and reviewing this collection of information. Send comments regarding this burden estimate or any other aspect of this collection of information, including suggestions for reducing this burden to Department of Defense, Washington Headquarters Services, Directorate for Information Operations and Reports (0704-0188), 1215 Jefferson Davis Highway, Suite 1204, Arlington, VA 22202-4302. Respondents should be aware that notwithstanding any other provision of law, no person shall be subject to any penalty for failing to comply with a collection of information if it does not display a currently valid OMB control number. **PLEASE DO NOT RETURN YOUR FORM TO THE ABOVE ADDRESS.**

1. REPORT DATE	2. REPORT TYPE	3. DATES COVERED
October 2013	Final	15 September 2006 – 14 September 2013

4. TITLE AND SUBTITLE

Rapid Translation of a Novel and Potent Vaccine in HER2+ Metastatic Breast Cancer Patients

5a. CONTRACT NUMBER

5b. GRANT NUMBER
W81XWH-06-1-0585

5c. PROGRAM ELEMENT NUMBER

6. AUTHOR(S)

H. Kim Lyerly, M.D.

Email: kim.lyerly@dm.duke.edu

5d. PROJECT NUMBER

5e. TASK NUMBER

5f. WORK UNIT NUMBER

7. PERFORMING ORGANIZATION NAME(S) AND ADDRESS(ES)

Duke University
Durham, NC 27710

8. PERFORMING ORGANIZATION REPORT NUMBER

9. SPONSORING / MONITORING AGENCY NAME(S) AND ADDRESS(ES)
U.S. Army Medical Research and Materiel Command
Fort Detrick, Maryland 21702-5012

10. SPONSOR/MONITOR'S ACRONYM(S)

11. SPONSOR/MONITOR'S REPORT NUMBER(S)

12. DISTRIBUTION / AVAILABILITY STATEMENT
Approved for Public Release; Distribution Unlimited

13. SUPPLEMENTARY NOTES

14. ABSTRACT

This clinical translation research award proposed to evaluate a novel viral vector vaccine combination for testing in Trastuzumab-refractory breast cancer patients. Both viral vectors express the human HER2 gene and individually promote potent immune responses mediated by cellular and antibody-mediated immunity. One is an adenovirus construct (Ad-HER2) and the other is an alphavirus VRP construct (VRP-HER2). We have demonstrated that both vectors elicit potent T cell and antibody responses and that these antibody responses are capable of both inhibiting the proliferation and directly killing Traztuzumab-refractory human breast cancer cells. The grant involves the manufacturing, safety testing, toxicology, and lot release testing, and submission of IND applications for the two vectors. Phase I safety studies were planned to evaluate primarily the safety of each vector in first in human studies. Our long term goal is to initiate a phase I/II study to evaluate the combination of the two vectors with the primary endpoint being clinical benefit.
.
.

15. SUBJECT TERMS
HER2, adenovirus, alphavirus, T cell, antibody, trastuzumab, immunotherapy, breast cancer, clinical trial

16. SECURITY CLASSIFICATION OF:			17. LIMITATION OF ABSTRACT	18. NUMBER OF PAGES	19a. NAME OF RESPONSIBLE PERSON USAMRMC
a. REPORT	b. ABSTRACT	c. THIS PAGE			
U	U	U	UU	143	19b. TELEPHONE NUMBER *(include area code)*

Table of Contents

1. **INTRODUCTION:** Narrative that briefly (one paragraph) describes the subject, purpose and scope of the research.

    This clinical translation research award proposed to evaluate a novel viral vector vaccine combination for testing in Trastuzumab-refractory breast cancer patients. Both viral vectors express the human HER2 gene and individually promote potent immune responses mediated by cellular and antibody-mediated immunity. One is an adenovirus construct (Ad-HER2) and the other is an alphavirus VRP construct (VRP-HER2). We have demonstrated that both vectors elicit potent T cell and antibody responses and that these antibody responses are capable of both inhibiting the proliferation and directly killing Traztuzumab-refractory human breast cancer cells. The grant involves the manufacturing, safety testing, toxicology, and lot release testing, and submission of IND applications for the two vectors. Phase I safety studies were planned to evaluate primarily the safety of each vector in first in human studies. Our long term goal is to initiate a phase I/II study to evaluate the combination of the two vectors with the primary endpoint being clinical benefit.

2. **KEYWORDS:** Provide a brief list of keywords (limit to 20 words).

    HER2, adenovirus, alphavirus, T cell, antibody, trastuzumab, immunotherapy, breast cancer, clinical trial

3. **OVERALL PROJECT SUMMARY:** Summarize the progress during appropriate reporting period (single annual or comprehensive final). This section of the report shall be in direct alignment with respect to each task outlined in the approved SOW in a summary of Current Objectives, and a summary of Results, Progress and Accomplishments with Discussion. Key methodology used during the reporting period, including a description of any changes to originally proposed methods, shall be summarized. Data supporting research conclusions, in the form of figures and/or tables, shall be embedded in the text, appended, or referenced to appended manuscripts. Actual or anticipated problems or delays and actions or plans to resolve them shall be included. Additionally, any changes in approach and reasons for these changes shall be reported. **Any change that is substantially different from the original approved SOW (e.g., new or modified tasks, objectives, experiments, etc.) requires review by the Grants Officer's Representative and final approval by USAMRAA Grants Officer through an award modification prior to initiating any changes.**

    Manufacture of clinical grade VRP and Adenoviral vectors

    In the first year of the grant, we held a pre-IND meeting with the FDA (12/19/06) for the Ad-HER2 virus vector and received important feedback on the Agency's stance on the use of the HER2 gene as a vaccine. The FDA requested that we perform further pre-clinical studies on the HER2 transgene sequence to demonstrate lack of "oncogenic potential" prior to selection of the HER2 transgene sequence for manufacture of clinical grade Adenovirus. This feedback was also relevant to the proposed VRP-HER2

construct and as a result, we have pursued a series of studies to develop the necessary data to provide the FDA.

To assess the potential oncogenicity of the mutated HER2Neu sequence we proposed to use, we developed stable mouse 3T3 cell lines expressing the HER2Neu wild-type or mutated sequences under the control of a Moloney-MuLV LTR or a CMV based promoter used in our adenovirus constructs. We assessed the HER2Neu expression of polyclonal populations as well as multiple individual clones and found three significant results. First, although both HER2 sequences are identical (except for the single amino acid mutation in the HER2Neu mutant) the expression of the mutated sequence is dramatically reduced in both the polyclonal population as well as the individual clones. This finding was confirmed in both the MuLV LTR or a CMV based promoter lines. Secondly, we found higher levels of HER2 (wild-type or mutant) expression using the MuLV LTR based promoter as opposed to the CMV based promoter. Thirdly, we also found that these HER2 stably transformed lines proliferate more rapidly in vitro compared to HER2mut and control lines, using a standard MTT based assay.

We then assessed the transformation potential in a normal, spontaneously transformed human breast epithelial cell line (MCF10A) which we reasoned was a better model than the murine NIH-3T3 cells. Using the constructs described above and also Adenovirus constructs expressing either ras (as a positive control, wild-type human HER2 full length, or our kinase-dead mutant HER2, we were able to demonstrate a 20-fold decrease in transformation potential with the kinase dead mutant compared to wild-type HER2. Indeed, the kinase-dead mutant showed no transforming potential in the colony forming assays compared to untreated controls (Table 1).

Table 1.

Vector	Plate 1	Plate 2	Plate 3	Average	Difference compared to mock (p value)
Mock	3	0	0	1	N/A
Ad-LacZ	0	0	1	<1	N/A
Ad-HER2 Wild Type	71	44	18	44	0.0452
Ad-HER2 kinase-dead	3	1	1	2	0.1481
Ad-ras	1299	2474	1959	1911	0.0049

This data provides evidence that the kinase-dead sequence we had proposed is indeed attenuated and lacks transformation potential. As an additional safeguard, we have also developed a kinase-dead mutant that lacks intracellular sequences and is thus more attenuated.
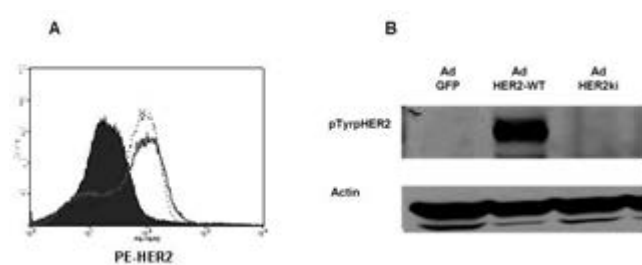
In order to avoid introducing further delays by waiting for the transformation studies to be completed with the Ad constructs prior to making the VRP constructs for vector downselection and titer optimization to ensure good yields in GMP manufacture, we

made the same constructs in VRP vectors and performed evaluation in parallel with the Ad studies.

Transgene downselection

The Ad-HER2-ki was first tested to demonstrate lack of signaling compared to full length human HER2 kinase inactive (Ad-HER2-ki) as shown in Figure 1. FACS analysis (Figure 1A) revealed similar surface expression levels of human HER2 on 40% of cells infected with the Ad-HER2-wild type (Ad-HER2-WT) and Ad-HER2-ki vectors respectively. Only the Ad-HER2-WT vector phosphorylates HER2 (pTyr) (Figure 1B). We also compared transcriptome profiles of human mammary epithelial cells (HMECs) transduced with the Ad-HER2-wt, Ad-HER2-ki, and Ad-GFP vectors using whole gene expression arrays (Figure 2). By 1-way ANOVA ($p < .05$ with Benjamini-Hochberg False Discovery Rate (BH FDR) Multiple Testing Correction) we found over 6,928 significantly different genes between Ad-HER2-wt and Ad-HER2-ki infected cells, but only 1,767 significantly different genes between Ad-HER2-ki and Ad-GFP infected cells. When those significantly different genes were filtered for fold differences (only those significantly different genes having more than 3 fold difference), 423 genes were statistically different between the Ad-HER2-wt and Ad-HER2-ki, while only 21 were different between Ad-HER2-ki and Ad-GFP (Figure 2). These results were confirmed by assessment of 12 individual gene targets by quantitative real-time PCR (Data not shown). These 423 differences between the Ad-HER2-wt and Ad-HER2-ki grouped into five Gene Ontology (GO) groups: systems development, EGF-like, chemotaxis, chemokine activity/GPCR activity, and angiogenesis.Thus confirmed, our results indicate that infection with Ad-HER2-wt elicited a much more profound transcription dysregulation compared to infection with Ad-HER2-ki and Ad-GFP.
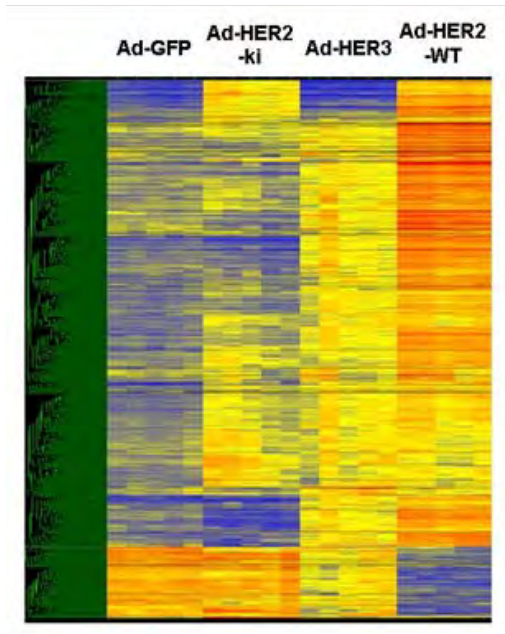
While we had demonstrated a lack of tyrosine kinase activity and differences in gene expression profile for the Ad-HER2-ki compared to Ad-HER2-WT, we also needed to demonstrate to the FDA that these differences reduced the transformation capability. Ad-HER2-ki had much less transforming capacity compared to Ad-HER2-WT in soft agar growth assays of transduced MCF10A cells, as shown in Figure 3. While Ad-HER2-WT resulted in increased colony formation (mean of 44 colonies), the Ad-HER2-ki gave similar levels of colonies to mock transfected cells (mean 1.7 colonies). Remarkably, the Ras gene used as a positive control resulted in >1900 colonies, indicating that the wild type HER2 is a relatively weak oncogene.
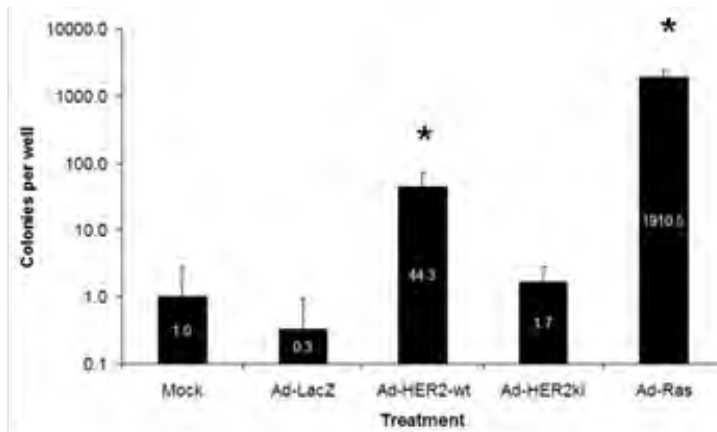

Figure 1A and B. The Ad-HER2-ki does not have kinase activity. A: Human mammary epithelial cells from reduction mammoplasties were serum starved for 36 hrs prior to infection for 18 hrs with Ad-HER2-WT (wildtype human HER2; dotted line), Ad-HER2-ki (kinase inactive human HER2 mutant; solid line), or Ad-GFP (as a negative control). B: Cell lysates were Western blotted with anti-HER2 pTyr and anti-Actin antibodies used to detect protein as previously described[3].

Figure 2. Gene expression analysis following infection of human mammary epithelial cells with Ad-GFP, Ad-HER2-ki, and Ad-HER2-wt respectively. In the color heat map, each gene is represented by a single row and each vertical column represents an individual sample (*n*), where *n* = 5 for Ad-GFP-infected HMEC, Ad-HER2-ki infected HMEC, or Ad-HER2-wt infected HMEC. The more transcriptionally active a gene is, the greater the intensity of the shade of red, while less transcriptionally active genes are depicted by greater intensity of shades of blue. In this heat map, the 2 groups of samples were hierarchically clustered (by relative level of gene expression) using a Pearson's correlation.

Figure 3. Diminished oncogenic potential of the Ad-HER2-ki vector was demonstrated in soft agar colony formation assays. Legend: Soft Agar Assay of Ad infected MCF-10A cells were performed as described in [4]. Briefly, MCF-10A were plated at 1×10^6 cells and infected at a MOI of 250 with the indicated adenoviral vectors. Twenty-four hours after infection, cells were typsinized and plated (50,000 in 35mm dish) in culture medium in soft agar (0.03%) and cultured for 2 weeks. Colonies containing more than 30 cells were counted (mean ± SD, n = 3). Ad-Ras was used as a positive control and mock infected MCF10A cells as a negative control. ***** denotes conditions that showed p<0.05 compared to the mock control.
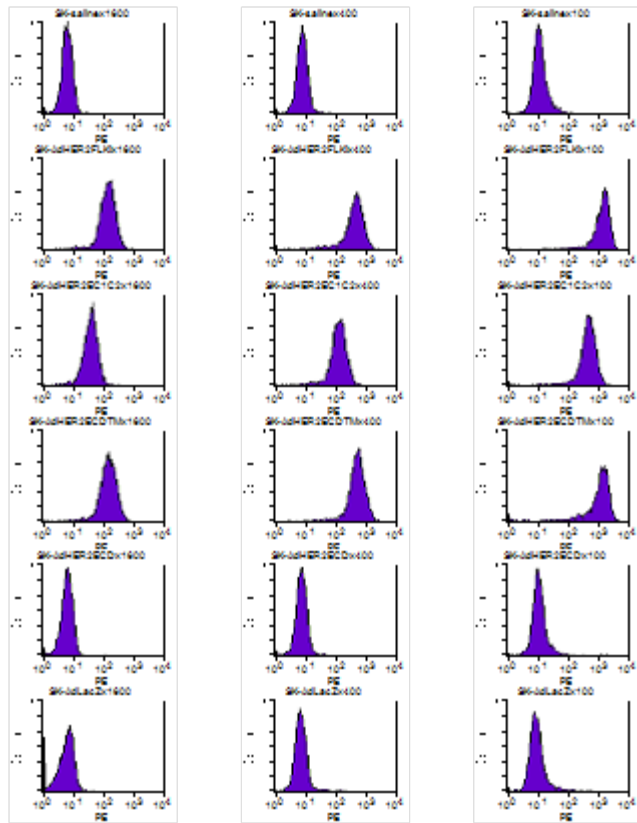
The original studies of HER2 biology relied upon overexpression of the wild type HER2 gene in permissive cell lines such as NIH-3T3 (mouse embryonic fibroblast) cells and used colony formation as a measure of tumorgenicity[1, 2]. Therefore, we used this NIH-3T3 transformation assay approach and cloned our HER2 wild type and HER2-ki genes into the same MoMLV LTR-driven plasmids that were used for those original studies. We found no proliferative enhancement of NIH-3T3 cells stably transfected with the HER2-ki gene (Data not shown).

6

As a final test to demonstrate lack of oncogenic potential, stably transfected NIH-3T3 cells were also implanted in vivo in SCID mice to assess tumor formation – studies funded outside of this DOD CTRA grant. Data from four experiments are summarized in the Table 2, which shows that while all mice injected with 3T3 cells expressing wild type human HER2 gene (HER2 wild type) developed tumors, no mice injected with 3T3 cells expressing the kinase inactive gene (HER2-ki) developed tumors. Collectively, these studies establish that our kinase inactive HER2ki gene is not oncogenic. This work is currently being written up for publication.
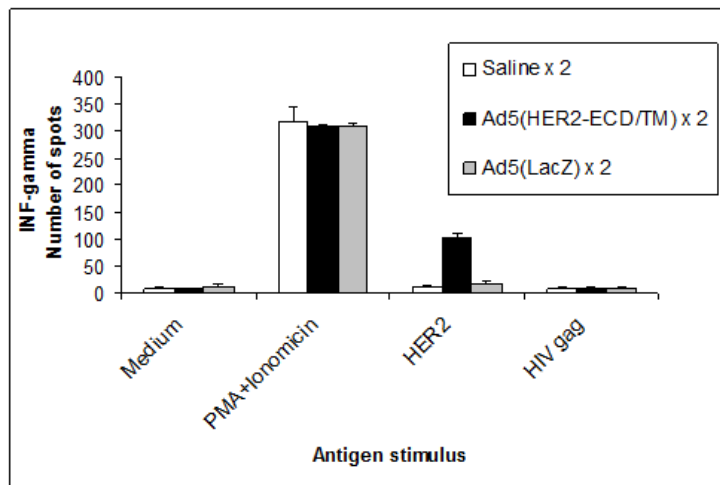
Table 2. Tumorgenicity assays demonstrate lack of oncogenic potential of the HER2-ki gene. 3T3 clone	Tumor formation at day 14-28 days	Stable 3T3 cells (and individual clones) were trypsinized, washed with PBS, and injected into the flank of SCID mice (NOD CB17-Prkdc SCID/J) at 100,000 cells resuspended in PBS as described in [1]. Tumors were measured at times 14-28 days post-injection from four independent experiments is shown. Stable clones expressing HER2-WT, HER2ki, empty plasmid, unmanipulated (mock) 3T3 cells were evaluated.
3T3-LTR/HER2 wild type	54/54 mice	
3T3-LTR/HER2-ki	0/30 mice	
3T3-LTR empty vector	1/10 mice	
3T3 cells mock	0/5 mice	

We finalized our selection based on immunogenicity and anti-tumor efficacy in vivo in our mouse models. This data is summarized in Figures 4, 5, and 6. Briefly, we vaccinated mice with various transgene sequences encoded by our Ad (Figures 4-6) or alphavirus vectors (Figure 7) and compared their ability to elicit anti-HER2 antibody, complement dependent cytotoxicity, and T cell responses. We also assayed anti-tumor activity (representative data is shown in Figure 8 for one such experiment with Ad-HER2-ECD/TM). Overall, these studies resulted in the selection of a final transgene sequence for our clinical vectors that combined lack of oncogenicity and optimal anti-HER2 immunity and anti-tumor activity. This transgene plasmid for the kinase ablated HER2-ECD/TM construct was submitted to SAFC PHARMA for initiation of Ad vector manufacturing and to AlphaVax Human Vaccines Inc. for initiation of Alphavirus replicon particle manufacturing.
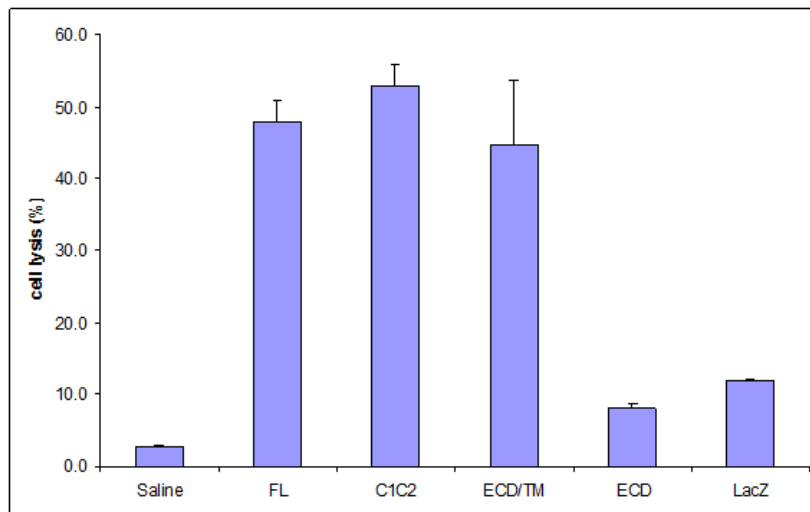
Figure 4. HER2-specific antibody binding to SKBR3 (human HER2+ breast cancer cells) is elicited by serum from mice vaccinated with the various Ad-HER2 constructs. HER2 constructs are FL - full length human HER2 transgene); C1C2 – exosomal targeted human HER2 extracellular domain; ECD/TM – human HER2 extracellular and transmembrane regions; ECD – Human HER2 extracellular domain. Serum from control mice vaccinated with saline (vehicle) or Ad-LacZ serves as negative controls.
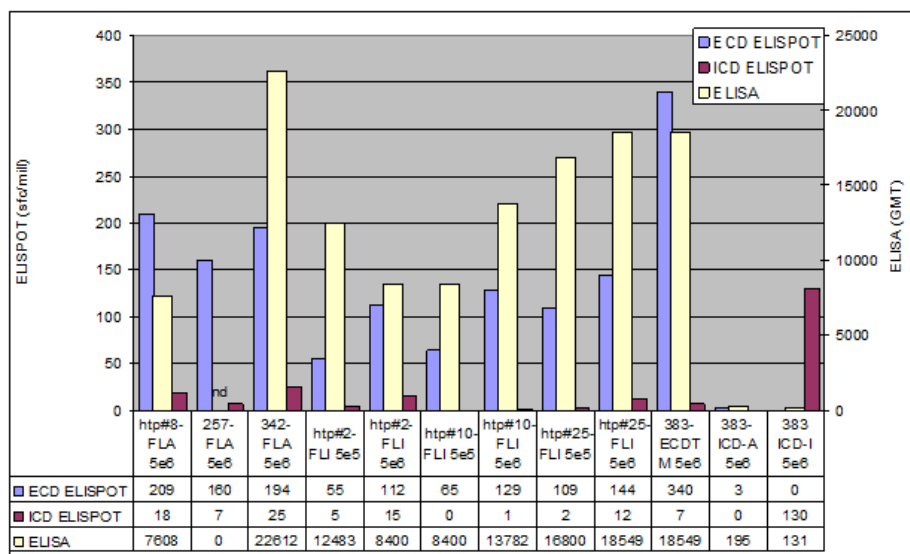

Figure 5. Interferon-gamma ELISPOT response of vaccinated mouse splenocytes demonstrates HER2-specific T cell responses induced by the Ad-HER2 vaccine. Vaccination with the *DUKE-001-Ad5(HuHER2-ECD+TM)* vaccine induces strong T cell immune responses to human HER2 in mice transgenic for human HER2. Mice were immunized via footpad with 2.6×10^{10} particles of either *DUKE-001-Ad5(HuHER2-ECD+TM)* vaccine, a control Ad expressing E. coli LacZ, or saline on day 0 and day 14. On day 28 mice were sacrificed and splenocytes were harvested for ELISPOT analysis. Data represents the mean of the eight mice per group. Error bars denote Std Dev. HER2 antigen is an overlapping polypeptide mix spanning the entire extracellular domain of human HER2, specifically 15 mers overlapping by eleven amino acids. HIV gag is an overlapping polypeptide mix spanning the entire HIV gag protein, specifically 15 mers overlapping by eleven amino acids. PMA/Ionomicin is a control mitogen used to demonstrate that splenocytes from all mice were functional in the assay. 6 replicate wells per antigen were performed for each mouse.
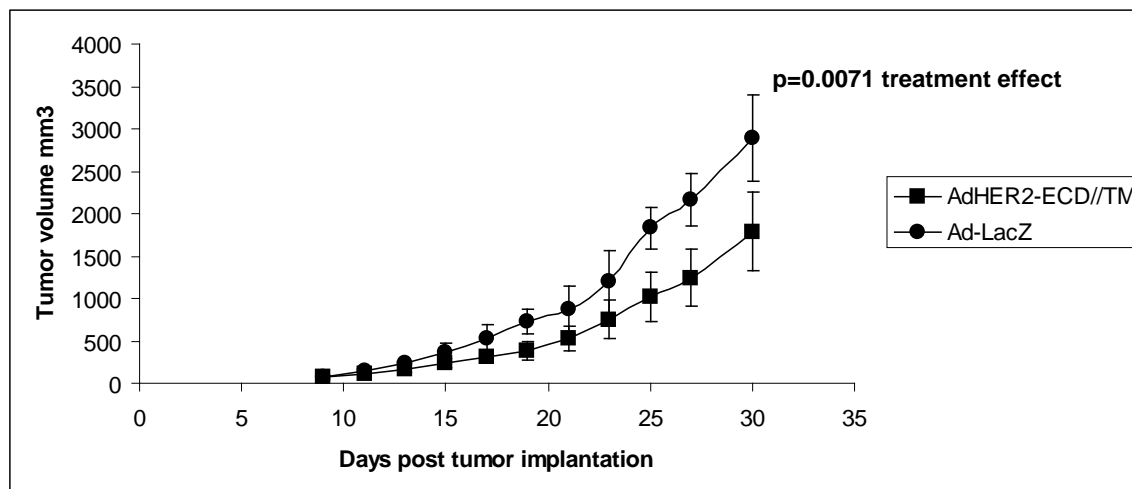
Figure 6. Complement dependent cytotoxicity is elicited by serum from mice vaccinated with the various Ad-HER2 constructs. HER2 constructs are FL - full length human HER2 transgene); C1C2 – exosomal targeted human HER2 extracellular domain; ECD/TM – human HER2 extracellular and transmembrane regions. Serum from control mice vaccinated with saline (vehicle) or Ad-LacZ serves as negative controls. Percent cell lysis of SKBR3 (Human HER2+) human breast cancer cells is denoted, with error bars representing Std. Dev.

	htp#8-FLA 5e6	257-FLA 5e6	342-FLA 5e6	htp#2-FLI 5e5	htp#2-FLI 5e6	htp#10-FLI 5e5	htp#10-FLI 5e6	htp#25-FLI 5e5	htp#25-FLI 5e6	383-ECDTM 5e6	383-ICD-A 5e6	383-ICD-I 5e6
ECD ELISPOT	209	160	194	55	112	65	129	109	144	340	3	0
ICD ELISPOT	18	7	25	5	15	0	1	2	12	7	0	130
ELISA	7608	0	22612	12483	8400	8400	13782	16800	18549	18549	195	131

Figure 7. HER2-specific antibody ELISA and HER2-intracellular domain and extracellular domain ELISPOT analysis of mice vaccinated with different VRP-HER2 transgene constructs. Splenocytes (ELISPOT) and serum (ELISA) from mice vaccinated with the various Ad-HER2 constructs were assayed. HER2 constructs are FLA - full length human HER2 transgene kinase active, FLI - full length human HER2 transgene kinase inactive); ECDT –HER2 extracellular domain and transmembrane region; ICDA – HER2 intracellular region kinase active; ICDI – intracellular region kinase inactive. Serum from control mice vaccinated with saline (vehicle) served as negative controls and showed <5 SFC in ELISPOT and <1:50 titer in ELISA.

Figure 8. Anti-tumor efficacy of Ad-HER2-ECD/TM vector. Tumor was administered on Day 0. On day 4 mice were randomized to receive either the Ad-HER2-ECD/TM vaccine or Ad-LacZ control vaccine. Administration of the Ad-HER2-ECD/TM vector retards the growth of established 4 day old tumors in HER2-tolerant (Human HER2-transgenic) mice. Error bars represent std. dev. There is significant retardation of tumor growth in HER2-tolerant human HER2-transgenic mice, with a statistical significance (p=0.0071) for fixed effects in a linear model.

Site Audits of SAFC PHARMA and AlphaVax Human Vaccines, Inc.
We performed a site audit of the SAFC PHARMA manufacturing facility on 20th May 2008 and confirmed that the facility is able to manufacture Ad vectors for clinical use and has SOPs in place that enable it to meet FDA requirements. The site audit was performed by Dr. Bruce Burnett, Director of Regulatory Affairs, Duke Translational Medicine Institute, Dr. Clay (PI of this grant), and Dr. Andrea Amalfitano, an Investigator on this grant and an adenovirus expert, and Dr. Frank Jones, a collaborator with Dr. Clay on other projects and an adenovirus vector expert. The audit demonstrated that the SAFC PHARMA facility met our requirements for clinical grade Ad vector manufacturing and the audit is a key component of the IND we will submit to FDA for clinical studies.
Auditing of AlphaVax Human Vaccines was completed/in place through involvement on another grant with AlphaVax., Inc.

In year 3 of the grant, we initiated the clinical grade GMP manufacture of both vectors. The Alphavirus VRP-HER2 vector manufacture was performed by sub-contractor AlphaVax Human Vaccines Inc. The Ad-HER2 vector was manufactured by sub-contractor SAFC PHARMA. We completed the clinical grade GMP manufacture of the Alphavirus VRP-HER2 vector and successfully completed the 5L scale pilot lot of the Ad-HER2 vector in year 4. The pilot lot of

10

Ad-HER2 was used for the preclinical animal toxicology studies. In year 5, clinical grade GMP manufacture of the Ad-HER2 vector was completed, vialed, and met final lot release criteria. Lot release testing was performed at Wuxi AppTec, our GMP testing sub-contractor.

Test clinical grade vector immunogenicity and perform toxicology in animal models for regulatory approval.

Pre-clinical animal toxicology studies for VRP-HER2 and Ad-HER2 were performed using clinical grade and pilot lot, respectively, at Avanza Laboratories, Inc (formerly Bridge Laboratories) (Gaithersburg, MD).

Results from the animal toxicology studies for VRP-HER2 are shown below. Similar study design and results were obtained with Ad-HER2. Dose level used for Ad-HER2 was 3.6×10^8 vp/site.

VRP-HER2 Toxicology Study
A toxicology study in mice was conducted in compliance with Good Laboratory Practices (GLP) using a total of 220 mice in two groups of 110 each (55 per sex per group) as outlined in Table 3.

Table 1:   AVX901 VRP Toxicity Study Design

Group	Treatment	Dose Level (IU/site)[a]	Dose volume	Route[b]	Injection Site Location	Dose Frequency (Study Days)
1	Placebo	0	0.05 mL	IM	Right hind limb Left hind limb	1 and 29 15
2	AVX901	1×10^6	0.05 mL	IM	Right hind limb Left hind limb	1 and 29 15

[a] IU = infectious units
[b] IM = intramuscular

With concurrence of the FDA after a pre-IND meeting, the test article was prepared with buffer containing mouse serum albumin (MSA), since mice receiving multiple injections of VRP formulated with 1% human serum albumin (HSA) routinely develop acute hypersensitivity reactions, due to the high concentration of HSA, but mice receiving multiple injections of VRP formulated with MSA do not develop acute hypersensitivity reactions.

Group 1 animals were treated with formulation buffer consisting of 200 mM NaCl, 0.1% MSA, 4% sucrose, 30mM sodium gluconate and 10mM sodium phosphate at pH 7.3, with 0.0018% residual HSA.. Group 2 animals were treated with AVX901 at a target dose of 1×10^6 IU. The test article was prepared by diluting AVX901 bulk vaccine to a concentration of 1×10^6 IU per 0.05 mL (2×10^7 IU per mL) in a formulation of 200 mM NaCl, 0.1% mouse serum albumin (MSA), 4% sucrose, 30 mM sodium gluconate and 10 mM sodium phosphate at pH 7.3, with approximately 0.0018% (17.6 µg per mL = 0.88 µg per 0.05 mL) residual HSA. On a IU per kg

basis, the target dose of 1 x 10^6 IU in a 25 gm mouse (4 x 10^7 IU/kg) was approximately seven times the highest anticipated clinical dose of 4 x 10^8 IU in a 70 kg person (5.7 x 10^6 IU/kg). Two hundred and twenty (110/sex) mice were randomly assigned to 2 groups (55 animals/sex/group). Animals were administered the placebo or HER2 VRP at 1 x 10^6 IU/site by IM injection in the biceps femoris of the right hind limb on Study Day (SD) 1, the left hind limb on SD 15, and the right hind limb on SD 29 (different location from the SD 1 injection). Animals were subjected to a full gross necropsy on SD 31 (first 5 animals/sex/group), 36 (fourth 5 animals/sex/group), or 43 (eighth 5 animals/sex/group). The remaining animals were used for blood collection and were discarded without necropsy.

Parameters evaluated during the study included mortality, clinical and cageside observations, dermal Draize observations, body weights and body weight changes, food consumption, clinical pathology, antibody analysis, gross pathology, organ weights and ratios, and histopathology. High titers of anti-HER2 antibodies were detected in all Group 2 animals that received AVX901 and in none of the Group 1 animals that received placebo.

Clinical Observations

Treatment with HER2 VRP at 1 x 10^6 IU/site had no effect on mortality, physical examinations, cageside observations, dermal Draize observations, body weight, body weight gains, food consumption, body temperatures, clinical pathology (clinical chemistry, hematology, and coagulation), gross pathology, absolute and relative organ weights, or histopathology.

Dermal Draize Observations

Dermal Draize reactions were categorized using a standardized scoring system (Table 4).

Table 2:   Dermal Draize Observation Scoring

Score	Grade	Edema	Erythema
0	None	No swelling	Normal color
1	Minimal	Slight swelling; indistinct border	Light pink; indistinct
2	Mild	Defined swelling; distinct border	Bright pink/pale red, distinct
3	Moderate	Defined swelling; raised border ($\leq$ 1 mm)	Bright red; distinct
4	Severe	Pronounced swelling; raised border (>1mm)	Dark red; pronounced

Treatment with HER2 VRP had no effect on dermal Draize observations.

After the first dose, male 13931 and female 14006 dosed with the placebo had erythema scores of 2 or 4 on SD 2-8 and the dose site appeared dark black in color from SD 2-3. After the second dose, males 13927 and 13937 (placebo), female 13982 (placebo), and female 14067 (HER2 VRP) had erythema scores of 1, 2, or 3 on SD 16, 17, 18, and/or 19. No edema was noted for any animal and no other instances of erythema were noted. These observations were likely related to the dosing procedure and not related to test article administration because they were mainly observed in the animals receiving placebo.

Body Temperatures

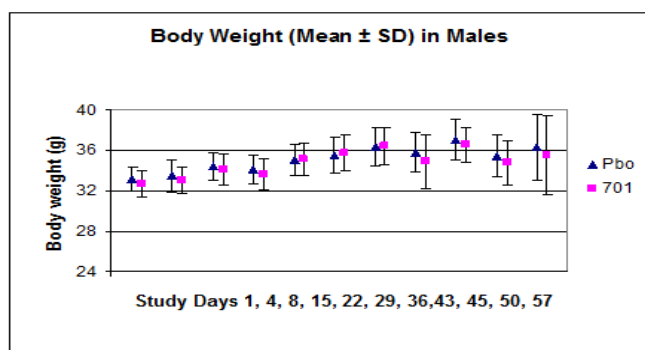Treatment with HER2 VRP had no effect on body temperatures.

A significant increase in body temperature was observed for HER2 VRP dosed males and females on SD 28, the day before the last dose. This increase in temperature was not observed on SD 31, two days after the dose, therefore this increase was not considered adverse or related to administration of HER2. A significant decrease in body temperature was observed for males dosed with HER2 VRP on SD 43. This decrease occurred ~2 weeks after the last dose and was not seen in the females, therefore this decrease was considered incidental and not related to administration of HER2 VRP.
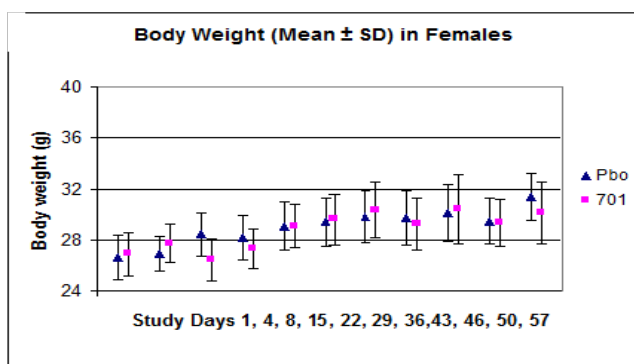
Body Weights and Body Weight Changes

Treatment with HER2 VRP had no adverse effect on body weights and body weight changes. There were no significant differences in mean absolute body weight gains during the SD 1 to 31 or SD 1 to 43 intervals.All changes noted were due to fasting and/or were not consistent between the genders.

Body weights are shown graphically in Figures 8 and 9.

Figure 8:   Body Weight by Study Day – Males

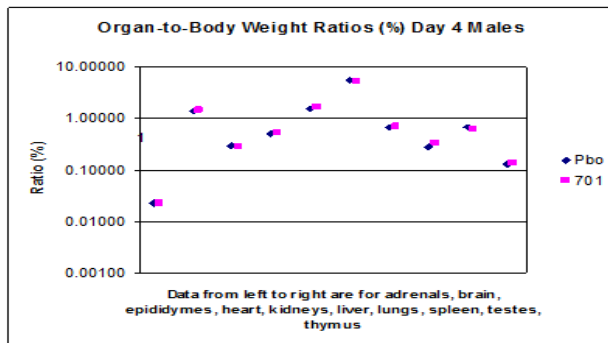**Figure 9:   Body Weight by Study Day – Females**
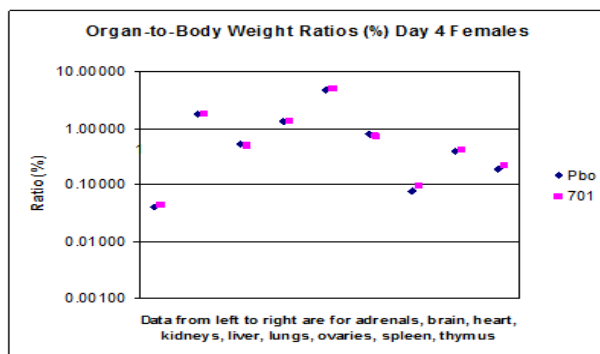

Organ Weights

Organs were weighed as soon as possible from all animals at scheduled necropsy. Paired organs were weighed together. Weights (and organ to body weight ratios) were determined for the

following organs; adrenal glands, brain, epididymides, heart, kidneys, liver (w/drained gallbladder), lung, ovaries, spleen, testes, thymus, and uterus. Organ-to-body weight ratios are shown graphically in Figure 10, Figure 11, Figure 12 Figure 13, Figure 14, and Figure 15.
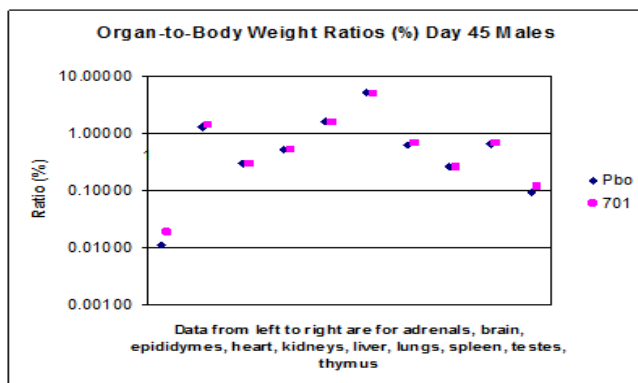
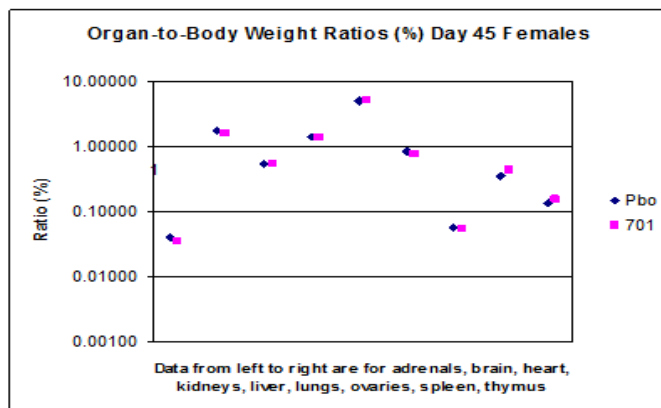**Figure 10   Organ to Body Weight Ratios – Day 4 Males**

Figure 11   Organ to Body Weight Ratios – Day 4 Females

Figure 12:   Organ to Body Weight Percentage – Day 45 Males

Figure 13: **Organ to Body Weight Percentage – Day 45 Females**

Organ-to-Body Weight Ratios (%) Day 45 Females

Data from left to right are for adrenals, brain, heart, kidneys, liver, lungs, ovaries, spleen, thymus

Figure 14: **Organ to Body Weight Percentage – Day 57 Males**

Organ-to-Body Weight Ratios (%) Day 57 Males

Data from left to right are for adrenals, brain, epididymes, heart, kidneys, liver, lungs, spleen, testes, thymus

Figure 15: **Organ to Body Weight Percentage – Day 57 Females**

Organ-to-Body Weight Ratios (%) Day 57 Females

Data from left to right are for adrenals, brain, heart, kidneys, liver, lungs, ovaries, spleen, thymus
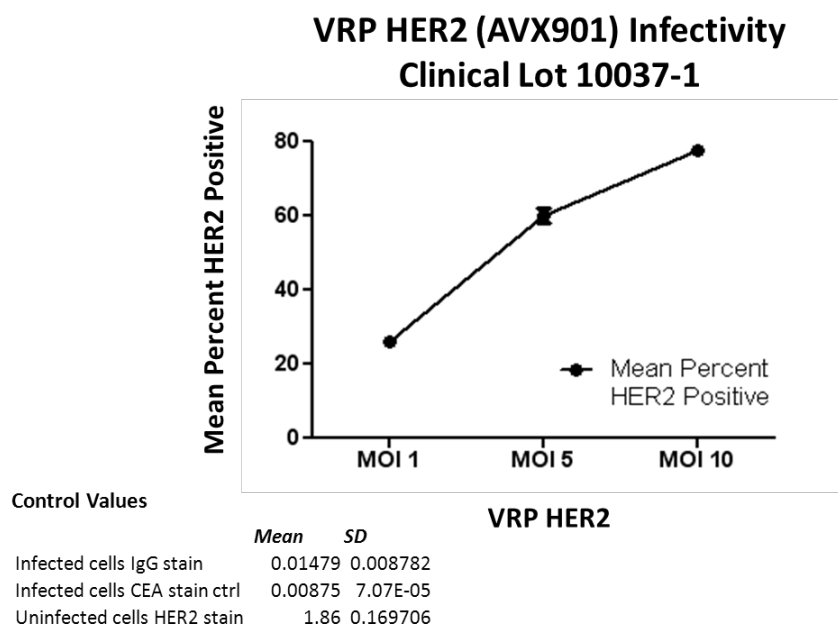
Pathology

Treatment with AVX901 had no effect on gross pathology, hematology, clinical chemistry or coagulation parameters, or on histopathology.
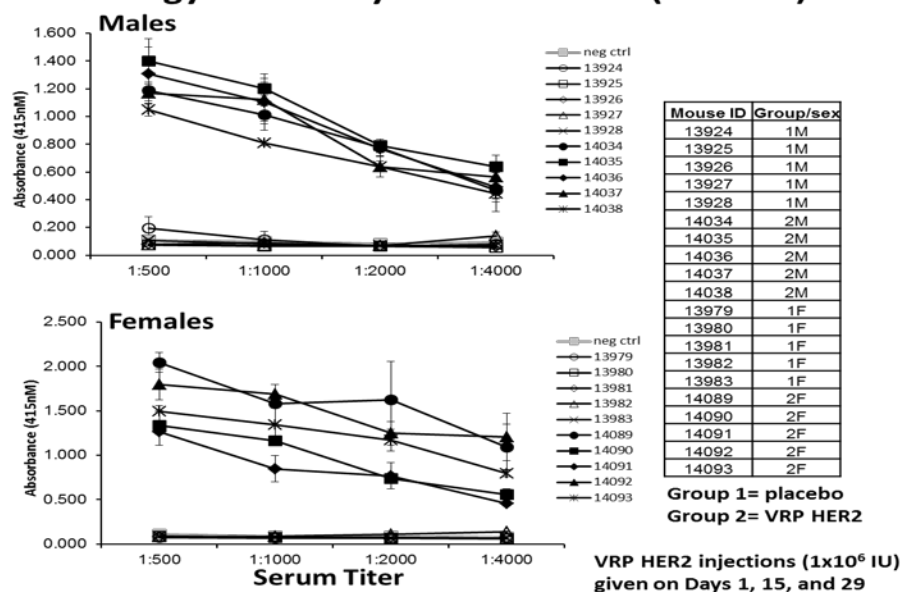
Infectivity Assays

Infectivity assays for testing the clinical grade Ad-HER and VRP-HER2 are performed annually to monitor vaccine stability and viral infectivity and transgene expression over time. Initial results from the clinical grade VRP-HER2 are shown in Figure 16 and clinical grade Ad-HER2 in Figure 18. HER2 specific ELISA results from serum from mice used in the toxicology reports are presented for VRP-HER2 in Figure 17. Similar results were seen with serum from mice used in toxicology studies with Ad-HER2.

Initial VRP-HER2 Infectivity Assay Results

VRP HER2 (AVX901) Infectivity Clinical Lot 10037-1

Control Values

	Mean	SD
Infected cells IgG stain	0.01479	0.008782
Infected cells CEA stain ctrl	0.00875	7.07E-05
Uninfected cells HER2 stain	1.86	0.169706

Figure 16: Infectivity of VRP-HER2 in Vero cells. 10^6 Vero cells were infected with clinical lot 1003701 VRP-HER2 at MOI of 0 (negative control), 1, 5, and 10 and incubated at 37^oC for 22 hours. Cells were harvested using cell dissociated buffer, washed with PBS, and stained for HER2 expression using anti-HER2-PE (BD Biosciences). HER2 expression data was acquired on a BD LSRII flow cytometer and analyzed using FloJo software. Results are the mean percent of HER2 expression by Vero cells for 2 replicates +/- SD.

Mouse Serology Data: Day 36 HER2 ELISA (AVX901)

Males

Absorbance (415nM)

neg ctrl
13924
13925
13926
13927
13928
14034
14035
14036
14037
14038

Mouse ID	Group/sex
13924	1M
13925	1M
13926	1M
13927	1M
13928	1M
14034	2M
14035	2M
14036	2M
14037	2M
14038	2M
13979	1F
13980	1F
13981	1F
13982	1F
13983	1F
14089	2F
14090	2F
14091	2F
14092	2F
14093	2F

Females

Absorbance (415nM)

neg ctrl
13979
13980
13981
13982
13983
14089
14090
14091
14092
14093

Group 1= placebo
Group 2= VRP HER2

Serum Titer: 1:500, 1:1000, 1:2000, 1:4000

VRP HER2 injections (1×10^6 IU) given on Days 1, 15, and 29

Figure 17: Murine HER2 ELISA. Serum collected from mice used in the VRP-HER2 pre-clinical toxicology studies were used in an ELISA to show HER2 antibody production following VRP-HER2 vaccination. 96 well plates were coated with HER2 recombinant protein (eBiosciences) and incubated with serial dilutions of serum from control mice (placebo) or VRP-HER2 vaccinated mice on day 36 following vaccination. Plates were developed with PNPP and read at 415 nM on a BioRad plate reader. Results shown are mean +/- SD for 2 replicates. Herceptin was used as a positive control. Similar results were seen for Day 43 serum (data not shown)

Ad HER2 ECDTM Infectivity 8 Hour Stability Test
Clinical Lot 079-11005 (2011)

Mean Percent HER2 Positive

- Fresh Thaw
- 8 hours at 4C

MOI 25, MOI 50, MOI 100

Ad HER2

Control Values

Ad-HER2 fresh thaw	*Mean*	*SD*
Infected cells IgG stain	0.0153	0.007212
Infected cells CEA stain ctrl	0.0051	0.007212
Uninfected cells HER2 stain	0.483	0.100409

Control Values

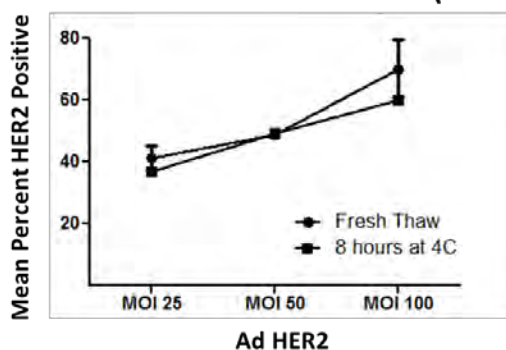| *Ad-HER2 thawed, 8 hrs at 4°C*	*Mean*	*SD*
Infected cells IgG stain	0.01755	0.010536
Infected cells CEA stain ctrl	0.00256	0.00362
Uninfected cells HER2 stain	0.483	0.100409

Figure 18: Infectivity of Ad-HER2 in Vero cells. 10^6 Vero cells were infected with clinical lot 079-11005 Ad-HER2 at MOI of 0 (negative control), 25, 50, and 100 and incubated at 37^oC for 22 hours. Cells were harvested using cell dissociated buffer, washed with PBS, and stained for HER2 expression using anti-HER2-PE (BD Biosciences). HER2 expression data was acquired on a BD LSRII flow cytometer and analyzed using FloJo software. Results are the mean percent of HER2 expression by Vero cells for 2 replicates +/- SD.

Submit IND's, prepare clinical protocols, and obtain regulatory approvals for the clinical trials with (a) Ad-HER2 and (b) VRP-HER2 vectors.

Regulatory approvals for a Phase I clinical trial of VRP-HER2 in patients with advanced or metastatic HER2 expressing cancers were received from the NIH-RAC, FDA, Duke IBC (Institutional BioSafety Committee), Duke CPC (Cancer protocol committee), and Duke IRB (Institutional Review Board). Reviewed by the NIH-RAC of a Phase I clinical trial of Ad-HER2 states the study does not require an in-depth review.

Perform individual phase I clinical trials of the (a) Ad-HER2 and (b) VRP-HER2 vectors in patients with metastatic, HER2 expressing breast cancer.

A Phase I study of VRP-HER2 entitled "A Phase I Study To Evaluate The Antitumor Activity And Safety Of Duke-002-VRP(HuHER2-ECD+TM), An Alphaviral Vector Encoding The HER2 Extracellular Domain And Transmembrane Region, In Patients With Locally Advanced Or Metastatic Human Epidermal Growth Factor Receptor 2-Positive (HER2+) Cancers Including Breast Cancer" is currently open for enrollment. The first patient was consented to the VRP-HER2 clinical study September 10, 2012. To date, 4 patients have been enrolled and received all 3 planned injections of VRP-HER2. No DLTs have been reported in these patients. The protocol has been amended to move forward into the proposed second cohort of patients that can receive concurrent HER2 targeted therapies.

Submit amendments to the existing IND's, and obtain regulatory approvals for the clinical heterologous prime-boost clinical trial and perform a phase I/II clinical trial of the heterologous vector prime-boost strategy.

Our long term goal is to initiate a phase I/II study to evaluate the combination of the two vectors with the primary endpoint being clinical benefit. Due to changes in the standard of care for breast patients during the course of this study and changes to our study design based on pre-IND discussions with the FDA, we did not reach the aim of testing the prime boost strategy of the Ad-HER2 and VRP-HER2 vectors in the current funding period, but are in the process of testing each vaccine individually.

We hope to apply for future funding to support completion of these studies.

4. **KEY RESEARCH ACCOMPLISHMENTS:** Bulleted list of key research accomplishments emanating from this research. Project milestones, such as simply completing proposed experiments, are not acceptable as key research accomplishments. Key research accomplishments are those that have contributed to the major goals and objectives and that have potential impact on the research field.

- Pre-IND teleconference held with FDA on 19 December, 2006 to discuss the project and obtain FDA comments on construct design and issues of concern to the Agency.
- We demonstrated lack of oncogenic potential of our kinase inactive HER2 construct (Hartman et al., 2010)
- Selection of the final transgene sequence for clinical vector production was made based upon lack of oncogenicity, and superior immunogencicity and anti-tumor efficacy.
- Pre-IND teleconference was held on 12 July, 2008 to confirm FDA approval of the proposed transgene, and to discuss clinical trial design.
- Plasmids encoding the transgene sequence were submitted to SAFC PHARMA and AlphaVax Human Vaccines, Inc. to initiate clinical grade vector production.
- We held a pre-IND meeting on 3-24-09 with the FDA to discuss one question we had about the "codon-optimized" vector being used for VRP-HER2 vaccine production. This "codon optimization" makes no change to the protein sequence produced by the vector but optimizes the yield of virus from the manufacturing and will ensure more "doses" of the vaccine can be made than otherwise. FDA did not have any issues with this vector and we proceeded to manufacture the VRP-HER2.
- The GMP clinical lot of alphavirus VRP-HER2 was manufactured vialed and underwent lot release testing. Pre-clinical toxicology testing was performed with Avanza (formerly Bridge Labs).
- We selected the plaque purified Ad-HER2 clone for pilot lot runs at SAFC PHARMA. Clone #11 was selected. Assays for HER2 expression were run at Duke and showed that HER2 protein was productively made by all 12 clones supplied for testing by SAFC. Clone 11 was chosen based on the production characteristics (titer, yield, etc.).
- SAFC PHARMA, our sub-contractor manufacturing the GMP clinical grade Ad-HER2 virus completed the Master Virus Bank (MVB) and the 5L scale WAVE pilot lot. This was scaled up to a 25L WAVE to produce the clinical lot. Ad-HER2 GMP clinical grade manufacturing, vialing and final lot release was completed.
- Pre-clinical toxicology studies were designed, with input from Pre-IND meetings with the FDA. Pre-clinical animal toxicology studies were completed for both VRP-HER2 and Ad-HER2.
- Vector infectivity assays and HER2 specific ELISA have been developed for testing of vector stability and infectivity and mouse immune response, respectively.
- VRP-HER2 study was submitted and approved by the DOD, IRB, FDA and NIH-RAC. Ad-HER2 study was submitted and reviewed by the NIH-RAC and does not need further in depth review.
- VRP-HER2 phase 1 clinical study was initiated. Four patients have been treated with VRP-HER2. The study remains open to enrollment.

5. **CONCLUSION:** Summarize the importance and/or implications with respect to medical and /or military significance of the completed research including distinctive contributions, innovations, or changes in practice or behavior that has come about as a result of the project. A brief description of future plans to accomplish the goals and objectives shall also be included.

Under this grant, we successfully responded to FDA's guidance and concerns regarding the HER2 transgene sequence and issues of potential oncogenicity in our proposed vectors by designing and selecting a HER2 kinase inactive transgene that induced both HER2 specific immune response and anti-tumor response in an animal model but did not exhibit oncogenic potential. This truncated HER2 transgene was used to manufacture both clinical grade Ad-HER2 and VRP-HER2 vectors. These vectors have been found to be safe and immunogenic in pre-clinical animal toxicology testing. We are currently enrolling patients into a Phase I clinical trial of VRP-HER2. To date, four patients have received all 3 proposed injections without DLTs.

We plan to complete Phase I studies of VRP-HER2 and Ad-HER2 including immune analysis following vaccination to test for HER2 specific immune responses.

Additionally, our long term goal remains to perform a phase I/II study to evaluate the combination of the two vectors in a prime boost strategy to reduce the effects possible neutralizing antibody to the viral vectors. We have a sufficient supply of both clinical grade vectors to complete these studies.

6. **PUBLICATIONS, ABSTRACTS, AND PRESENTATIONS:**

   a. List all manuscripts submitted for publication during the period covered by this report resulting from this project. Include those in the categories of lay press, peer-reviewed scientific journals, invited articles, and abstracts. Each entry shall include the author(s), article title, journal name, book title, editors(s), publisher, volume number, page number(s), date, DOI, PMID, and/or ISBN.

      (1) Lay Press:

Nothing to report.

      (2) Peer-Reviewed Scientific Journals:

Xia W, Petricoin EF 3rd, Zhao S, Liu L, Osada T, Cheng Q, Wulfkuhle JD, Gwin WR, Yang X, Gallagher RI, Bacus S, Lyerly HK, Spector NL. An heregulin-EGFR-HER3 autocrine signaling axis can mediate acquired lapatinib resistance in HER2+ breast cancer models. Breast Cancer Res. 2013 Sep 18;15(5):R85.

Ren XR, Wei J, Lei G, Wang J, Lu J, Xia W, Spector N, Barak LS, Clay TM, Osada T, Hamilton E, Blackwell K, Hobeika AC, Morse MA, Lyerly HK, Chen W. Polyclonal

HER2-specific antibodies induced by vaccination mediate receptor internalization and degradation in tumor cells. Breast Cancer Res. 2012 Jun 7;14(3):R89.

Amplification and high-level expression of heat shock protein 90 marks aggressive phenotypes of human epidermal growth factor receptor 2 negative breast cancer. Cheng Q, Chang JT, Geradts J, Neckers LM, Haystead T, Spector NL, Lyerly HK. Breast Cancer Res. 2012 Apr 17;14(2):R62.

Hamilton E, Blackwell K, Hobeika AC, Clay TM, Broadwater G, Ren XR, Chen W, Castro H, Lehmann F, Spector N, Wei J, Osada T, Lyerly HK, Morse MA. Phase 1 clinical trial of HER2-specific immunotherapy with concomitant HER2 kinase inhibition [corrected]. J Transl Med. 2012 Feb 10;10:28.

Hartman ZC, Wei J, Glass OK, Guo H, Lei G, Yang XY, Osada T, Hobeika A, Delcayre A, Le Pecq JB, Morse MA, Clay TM, Lyerly HK. Increasing vaccine potency through exosome antigen targeting. Vaccine. 2011 Nov 21;29(50):9361-7.

Hartman ZC, Yang XY, Glass O, Lei G, Osada T, Dave SS, Morse MA, Clay TM, Lyerly HK. HER2 overexpression elicits a proinflammatory IL-6 autocrine signaling loop that is critical for tumorigenesis. Cancer Res. 2011 Jul 1;71(13):4380-91.

Hartman ZC, Wei J, Osada T, Glass O, Lei G, Yang XY, Peplinski S, Kim DW, Xia W, Spector N, Marks J, Barry W, Hobeika A, Devi G, Amalfitano A, Morse MA, Lyerly HK, Clay TM. An adenoviral vaccine encoding full-length inactivated human Her2 exhibits potent immunogenicty and enhanced therapeutic efficacy without oncogenicity. Clin Cancer Res. 2010 Mar 1;16(5):1466-77. PMID: 20179231

Morse MA, Wei J, Hartman Z, Xia W, Ren XR, Lei G, Barry WT, Osada T, Hobeika AC, Peplinski S, Jiang H, Devi GR, Chen W, Spector N, Amalfitano A, Lyerly HK, Clay TM. Synergism from combined immunologic and pharmacologic inhibition of HER2 in vivo. Int J Cancer. 2010 Jun 15;126(12):2893-903.

(3) Invited Articles:

Clay TM, Osada T, Hartman ZC, Hobeika A, Devi G, Morse MA, Lyerly HK. Polyclonal immune responses to antigens associated with cancer signaling pathways and new strategies to enhance cancer vaccines. Immunol Res. 2011 Apr;49(1-3):235-47.

(4) Abstracts:

Nothing to report.

b. List presentations made during the last year (international, national, local societies, military meetings, etc.). Use an asterisk (*) if presentation produced a manuscript.
Nothing to report.

7. **INVENTIONS, PATENTS AND LICENSES:** List all inventions made and patents and licenses applied for and/or issued. Each entry shall include the inventor(s), invention title, patent application number, filing date, patent number if issued, patent issued date, national, or international.

   Nothing to report.

8. **REPORTABLE OUTCOMES:** Provide a list of reportable outcomes that have resulted from this research. Reportable outcomes are defined as a research result that is or relates to a product, scientific advance, or research tool that makes a meaningful contribution toward the understanding, prevention, diagnosis, prognosis, treatment and /or rehabilitation of a disease, injury or condition, or to improve the quality of life. This list may include development of prototypes, computer programs and/or software (such as databases and animal models, etc.) or similar products that may be commercialized.

   - A manuscript describing the transgene downselection and demonstration of the lack of oncogenic potential (Hartman et al., 2010); A manuscript reporting preclinical studies of the Ad-HER2 vaccine in the setting of concurrent lapatinib therapy (Morse et al., 2010); (see section 6.2 and 3 for a list of manuscripts supported by this grant)
   - The clinical grade VRP-HER2 vector was manufactured, completed lot release testing, tested in pre-clinical toxicology animal models, and is being used in human clinical trial.
   - The clinical grade Ad-HER2 vector was manufactured, completed lot release testing, and tested in pre-clinical toxicology animal models.
   - VRP-HER2 phase I clinical trial received regulatory (RAC, FDA, Duke IBC, Duke CPC, Duke IRB) and DOD approval. The study is currently open to enrollment. Four patients have received all 3 doses of VRP-HER2.

9. **OTHER ACHIEVEMENTS:** This list may include degrees obtained that are supported by this award, development of cell lines, tissue or serum repositories, funding applied for based on work supported by this award, and employment or research opportunities applied for and/or received based on experience/training supported by this award.

10. **REFERENCES:** List all references pertinent to the report using a standard journal format (i.e., format used in *Science*, *Military Medicine*, etc.).

1. Di Fiore, P. P. et al. erbB-2 is a potent oncogene when overexpressed in NIH/3T3 cells. Science 237, 178-82 (1987).
2. Hudziak, R. M., Schlessinger, J. & Ullrich, A. Increased expression of the putative growth factor receptor p185HER2 causes transformation and tumorigenesis of NIH 3T3 cells. Proc Natl Acad Sci U S A 84, 7159-63 (1987).
3. Xia, W. et al. A model of acquired autoresistance to a potent ErbB2 tyrosine kinase inhibitor and a therapeutic strategy to prevent its onset in breast cancer. Proc Natl Acad Sci U S A 103, 7795-800 (2006).
4. O'Hayer, K. M. & Counter, C. M. A genetically defined normal human somatic cell system to study ras oncogenesis in vivo and in vitro. Methods Enzymol 407, 637-47 (2006).

11. APPENDICES: Attach all appendices that contain information that supplements, clarifies or supports the text. Examples include original copies of journal articles, reprints of manuscripts and abstracts, a curriculum vitae, patent applications, study questionnaires, and surveys, etc.

Appendix 1: Copies of Journal Articles

Breast Cancer Research

An heregulin-EGFR-HER3 autocrine signaling axis can mediate acquired lapatinib resistance in HER2+ breast cancer models

Wenle Xia (Wenle.Xia@duke.edu)
Emanual F Petricoin III (epetrico@gmu.edu)
Sumin Zhao (sumin.zhao@duke.edu)
Leihua Liu (leihua.liu@duke.edu)
Takuya Osada (osada001@mc.duke.edu)
Qing Cheng (q.cheng@duke.edu)
Julia D Wulfkuhle (jwulfkuh@gmu.edu)
William R Gwin (william.gwin@duke.edu)
Xiaoyi Yang (xiao.yang@duke.edu)
Rosa I Gallagher (gallag3@gmu.edu)
Sarah Bacus (sarah.bacus@quintiles.com)
H Kim Lyerly (lyerl001@mc.duke.edu)
Neil L Spector (Neil.Spector@duke.edu)

This peer-reviewed article can be downloaded, printed and distributed freely for any purposes (see copyright notice below).

Articles in *Breast Cancer Research* are listed in PubMed and archived at PubMed Central.

For information about publishing your research in *Breast Cancer Research* go to

http://breast-cancer-research.com/authors/instructions/

An heregulin-EGFR-HER3 autocrine signaling axis can mediate acquired lapatinib resistance in HER2+ breast cancer models

Wenle Xia[1,2,*]
Email: Wenle.Xia@duke.edu

Emanual F Petricoin III[3]
Email: epetrico@gmu.edu

Sumin Zhao[2]
Email: sumin.zhao@duke.edu

Leihua Liu[2]
Email: leihua.liu@duke.edu

Takuya Osada[4,2]
Email: osada001@mc.duke.edu

Qing Cheng[4]
Email: q.cheng@duke.edu

Julia D Wulfkuhle[3]
Email: jwulfkuh@gmu.edu

William R Gwin[1,2]
Email: william.gwin@duke.edu

Xiaoyi Yang[4]
Email: xiao.yang@duke.edu

Rosa I Gallagher[3]
Email: gallag3@gmu.edu

Sarah Bacus[5]
Email: sarah.bacus@quintiles.com

H Kim Lyerly[4,2]
Email: lyerl001@mc.duke.edu

Neil L Spector[1,2,*]
Email: Neil.Spector@duke.edu

[1] Department of Medicine, Medical Science Research Building 1, Research Drive, Duke University Medical Center, Durham, NC 27710, USA

[2] Duke Cancer Institute, Duke University Medical Center, Durham, NC 27710, USA

[3] Center for Applied Proteomics and Molecular Medicine, George Mason University, 10900 University Blvd, Manassas, VA 20155, USA

[4] Department of Surgery, Medical Science Research Building 1, Research Drive, Duke University Medical Center, Durham, NC 27710, USA

[5] Targeted Molecular Diagnostics/Quintiles, 610 Oakmont Lane, Westmont, IL 60559, USA

[*] Corresponding author. Duke Cancer Institute, Duke University Medical Center, Durham, NC 27710, USA

Abstract

Introduction

The human epidermal growth factor receptor 2 (HER2) receptor tyrosine kinase (RTK) oncogene is an attractive therapeutic target for the treatment of HER2 addicted tumors. While lapatinib, an FDA-approved small molecule HER2 and epidermal growth factor receptor (EGFR) tyrosine kinase inhibitor (TKI), represents a significant therapeutic advancement in the treatment of HER2+ breast cancers, responses to lapatinib have not been durable. Consequently, elucidation of mechanisms of acquired therapeutic resistance to HER-directed therapies is of critical importance.

Methods

Using a functional protein pathway activation mapping strategy, along with targeted genomic knockdowns applied to a series of isogenic-matched pairs of lapatinib sensitive and resistant cell lines, we now report an unexpected mechanism of acquired resistance to lapatinib and other TKIs in class.

Results

The signaling analysis revealed that while HER2 was appropriately inhibited in lapatinib resistant cells, EGFR tyrosine phosphorylation was incompletely inhibited. Using a targeted molecular knockdown approach to interrogate the causal molecular underpinnings of EGFR persistent activation, we found that lapatinib resistant cells were no longer oncogene addicted to HER2-HER3-PI3K signaling as seen in the parental lapatinib sensitive cell lines, but instead were dependent upon an heregulin (HRG)-driven HER3-EGFR-PI3K-PDK1 signaling axis. Two FDA-approved EGFR TKIs could not overcome HRG-HER3 mediated activation of EGFR, or reverse lapatinib resistance. The ability to overcome EGFR-mediated acquired therapeutic resistance to lapatinib was demonstrated through molecular knockdown of EGFR and treatment with the irreversible pan-HER TKI neratinib, which blocked HRG-dependent phosphorylation of HER3 and EGFR, resulting in apoptosis of resistant cells. In addition, whereas HRG reversed lapatinib-mediated antitumor effects in parental HER2+ breast cancer cells, neratinib was comparatively resistant to the effects of HRG in parental cells. Finally, we showed that HRG expression is an independent negative predictor of clinical outcome in HER2^{+} breast cancers, providing potential clinical relevance to our findings.

Conclusions

Molecular analysis of acquired therapeutic resistance to lapatinib identified a new resistance mechanism based on incomplete and "leaky" inhibition of EGFR by lapatinib. The selective pressure applied by incomplete inhibition of the EGFR drug target resulted in selection of ligand-driven feedback that sustained EGFR activation in the face of constant exposure to the drug. Inadequate target inhibition driven by a ligand-mediated autocrine feedback loop may represent a broader mechanism of therapeutic resistance to HER TKIs and suggests adopting a different strategy for selecting more effective TKIs to advance into the clinic.

Keywords

EGFR, Tyrosine kinase inhibitor, Heregulin, Resistance

Introduction

Members of the human epidermal growth factor receptor (HER) family of transmembrane receptor tyrosine kinases (HER1/EGFR; HER2; HER3; HER4) and their respective ligands constitute a robust biological system that plays a key role in the regulation of cell proliferative growth, survival, and differentiation [1-6]. Ligand bound monomeric HER receptors form homo- or heterodimers, which in turn activate their respective autokinase activities leading to self-phosphorylation of c-terminus tyrosine residues serving as docking sites for adaptor proteins that activate downstream growth and survival signaling cascades [3-6]. HER2, the preferred dimerization partner for HER3 and EGFR, amplifies the signal generated through the dimer receptor complex [4]. HER3, on the other hand, is transactivated by its dimerization partner [7]. Importantly, HER3 contains six phosphotyrosine binding sites for the p85 subunit of PI3K (phosphoinositide 3-kinase), the most of all HER family members [8]. Consequently, HER2-HER3 dimers are potent activators of PI3K signaling, which in breast and other solid tumors, represents an important oncogenic signaling unit [9].

Deregulation of HER signaling, which can occur as a consequence of gene amplification (HER2) or gain-of-function mutation (EGFR) promotes solid tumor oncogenesis. In breast and ovarian cancers, HER2 overexpression (HER2+) predicts for a poor clinical outcome [10,11], findings that have prompted the development of HER2 targeted therapies including small molecule tyrosine kinase inhibitors (TKIs) designed to block the autokinase activity of the HER2 receptor. Lapatinib is a highly selective, small molecule inhibitor of the HER2 and EGFR tyrosine kinases [12]. It is currently the only FDA approved tyrosine kinase inhibitor (TKI) for the treatment of advanced stage HER2+ breast cancers [13]. Although lapatinib is considered an equipotent inhibitor of HER2 and EGFR based on data from *in vitro* kinase assays [14,15], its clinical efficacy to date has been limited to HER2+ breast cancers [16]. Despite representing a significant therapeutic advance in the treatment of aggressive HER2+ breast cancers, the clinical efficacy of lapatinib has been limited by the inevitable development of therapeutic resistance [13,16]. In this regard, several mechanisms of acquired therapeutic resistance have been reported, based primarily on data generated from preclinical models [17-23]. In contrast to other kinase inhibitors where mutations in the ATP binding pocket of the targeted kinase can lead to reactivation of the targeted protein [24,25], we and others have shown that HER2 mutation do not appear to play a role in resistance, and that phosphorylation of HER2 remains inhibited in models of acquired lapatinib resistance

[17,22,23]. Furthermore, previous work from our laboratory has shown that molecular knockdown of HER2 does not reverse lapatinib resistance providing additional evidence that resistant cells are no longer dependent upon HER2 for survival [17]. The recent decision to discontinue a lapatinib monotherapy treatment arm in the ALTTO study- an ongoing global phase III clinical trial of adjuvant HER2 targeted therapies in the treatment of early stage HER2^{+} breast cancers-due to an increased incidence of disease recurrence underscores the need to better understand the resistance conundrum. Elucidating mechanisms of acquired therapeutic resistance to HER TKIs and kinase inhibitors in general is therefore of critical importance in the management of kinase-driven diseases.

The tumor promoting PI3K cell signaling pathway has been shown to be persistently activated in models of acquired therapeutic resistance to lapatinib and similar HER TKIs in class [19,20]. The role of activating PI3KCA mutations or PTEN loss as a potential explanation for the persistent activation of PI3K signaling in lapatinib resistance remains controversial [19,26-28]. Here, we show that acquired therapeutic resistance to lapatinib in models of HER2+ breast cancer can be mediated by autocrine induction of the membrane-bound form of the HER3 ligand heregulin (HRG). Increased expression of full-length HRG in combination with inadequate inhibition of EGFR phosphorylation by lapatinib promotes an HRG-HER3-EGFR-PI3K signaling axis that not only contributes to lapatinib resistance, but also cross-resistance to FDA-approved EGFR TKIs. These findings could have a significant impact on not only the treatment of HER2 and EGFR-dependent tumors, but also relevance to the treatment of kinase-driven diseases in general.

Methods

Cell culture and reagents

Human breast cancer cell lines BT474, SKBR3, Au565 and SUM190 were obtained from the American Type Culture Collection (Manassas, VA). Lapatinib resistant cell lines (rBT474, rSKBR3, rAu565 and rSUM190) were generated and continuously maintained in 1 μM lapatinib as previously described [17,18]. The 4G10 anti-phosphotyrosine (p-tyr) antibody was purchased from Sigma-Aldrich (St. Louis, MO). Monoclonal antibodies to c-HER2 and EGFR were purchased from Neo Markers (Union City, CA). Phospho-specific primary antibodies to EGFR (Y992), EGFR (Y1148), EGFR (Y1173), EGFR (Y1068) and HER3 (Y1197), and PARP cleavage product were obtained from Cell Signaling (Beverly, MA). Anti PDK1 antibody was purchased from R&D System (Minneapolis MN). Antibodies to phosho-PI3Kp85 (Y508), Akt1/2, phospho-Akt1/2 (S473), phospho-Akt1/2 (T308), HRG and siRNA constructs (Akt1/2; PI3K subunits; PKC, PDK1, SGK, HRG and control siRNA-A) were purchased from Santa Cruz (Santa Cruz, CA). The PHLPP2 antibody was from Bethyl (Montgomery, TX). ADAM17 antibody was purchased from Abcam (Cambridge, MA). Erlotinib was obtained from Genentech (South San Francisco, CA). SU11274, neratinib and AZD0530 were from Selleck (Houston, TX). IRDye800 conjugated affinity purified anti-rabbit IgG and anti-mouse IgG were purchased from Rockland (Gilbertsville, PA). Alexa Fluor680 goat anti-rabbit IgG was obtained from Molecular Probes (Eugene, OR). NVP-BEZ 235 was obtained from Novartis (Basel, Switzland). Lapatinib and gefitinib were purchased from LC Laboratories (Woburn, CA).

siRNA Transfection

Cell transfections were performed in a 6 well format using 5 μl lipofectamine 2000 (Invitrogen Life Technologies) in OPTI-MEM I (Invitrogen Life Technologies, Carlsbad, CA) at 5×10^5 cells per well with individual siRNAs against target proteins, and non-specific siRNA (NSC) as controls, as described in the Invitrogen transfection protocol and in our previous publications [17,26]. The concentration of siRNA was 100 nM in a final volume of 2.5 ml. After 16-18 hours, the transfection media was removed and replaced with complete RPMI 1640 supplemented with 1 μM lapatinib for an additional 48 hours.

SDS-PAGE, and Western blot analysis

Details of the methods used for SDS-PAGE and Western blot analysis have been previously described [17,18,26]. Briefly, membranes were incubated with primary antibodies, washed several times in PBS and then incubated with a fluorescent-conjugated secondary antibody at a 1:10000 dilution with 5% try milk in PBS for 60 minute protected from light. After washing in PBS + 0.1% tween-20, the membranes were scanned and visualized using the Odyssey Infrared Imaging System (LI-COR, Inc., Lincoln, NE).

Cell growth and viability assay

The cell growth assay was performed in a 96 well plate format in a final volume of 100 μl/well cell culture medium with the cell proliferation reagent WST-1 from Roche Diagnostics (Mannheim, Germany). Details of the WST-1 assay have been previously described [17,18,26].

Reverse Phase Protein Microarray construction and analysis

Reverse phase protein microarrays were constructed as described previously [29]. A list of the antibodies used in this analysis and their sources are provided (Additional file 1). Briefly, denatured lysates were spotted onto nitrocellulose-coated glass slides (Whatman, Inc, Sanford, ME) using a 2470 Arrayer (Aushon BioSystems, Burlington, MA), outfitted with 185 μm pins. Each sample was printed in triplicate as a neat and 1:4 dilution two-point dilution series to ensure that one of the points was in the linear dynamic range of the fluorescent assay. A high and low internal control for antibody staining specificity, consisting of lysates derived from pervandate treated HeLa cells and calyculin treated Jurkat cells were used and spotted onto every array along with the experimental samples. Slides were stored desiccated at -20°C until staining. Blocked arrays were stained with antibodies on an automated slide stainer (Dako, Carpinteria, CA) using the Catalyzed Signal Amplification System kit (CSA; Dako) and streptavidin-conjugated IRDye680 (LI-COR Bioscience, Lincoln, NE) to generate a fluorescent signal. Each antibody used in the staining process was previously validated using Western blot procedure. Antibodies producing a single band in correspondence to the molecular weight of interest were considerate validated and eligible for use in immunostaining. All intensity values were normalized to total protein for each sample to account for differences in intensity due solely to starting lysate concentration variance. The total amount of protein present in each sample was estimated through Sypro Ruby Protein Blot Stain (Molecular Probes, Eugene, OR, USA) according to the manufacturer's instructions as previously described [29]. All Sypro and immunostained slides were scanned using a Revolution 4550 scanner (Vidar Corp., Herndon, VA) and acquired images were

analyzed using MicroVigene v2.9.9.9 (VigeneTech, Carlisle, MA) that performed spot finding, local background subtraction, replicate averaging and total protein normalization, producing a single value for each sample at each endpoint. Statistical analysis of the array data was performed by T-testing or Wilcoxon two-sample rank sum test using R v2.9.2 (R Foundation for Statistical Computing, Vienna, Austria) was used to compare values between groups, depending on normalcy distribution values. P-values < 0.05 were considered statistically significant.

Immunofluorescence microscopy

Cells were cultured on cover glass in 6 well plates. After washing with PBS, cells were fixed and permeabilized with methanol/acetone (1:1) and blocked with 2% goat serum, 0.3% triton X-100 in PBS at room temperature followed by washing with PBS and incubated with an anti HRG antibody at 4°C. After extensive washings, the cells were incubated with anti-rabbit IgG conjugated with Alexa Fluor 555 (Cell Signaling, Danvers, MA) followed by a liquid mountant application with ProLong Gold anti-fade reagent with DAPI nuclear stain (Life technologies, Grand Island, NY). A Zeiss Axio Observer was used for photographs.

Gene expression data analysis

We compiled a collection of 4010 breast tumor gene expression data derived from 23 datasets that have been posted on the NCBI Gene Expression Omnibus (GEO) database, as previously described [30]. In addition to the raw expression data, we also obtained recurrence-free survival data from a subset of the samples (n = 1372).

HRG (NRG1) expression was measured by probe set 208231_at. We assigned each of 4010 sample into Low (first quartile, lowest 25%), Intermediate (second quartile, intermediate 50%) and High (third quartile, highest 25%) subgroups according to HRG expression levels, and compared prognosis differences among these subgroups using Kaplan-Meier Estimates of recurrence-free survival analysis. Furthermore, we applied HRG expression signal as continuous variable and determined correlation of HRG expression and risk of recurrence among 204 HER2+ breast cancer samples, using Cox-regression survival analysis.

Statistical analysis

Data were expressed as means with standard error bars included. Student's *t*-test was used to determine statistical significance between 2 groups. A value of p < 0.05 was considered a statistically significant difference.

Results

PI3K pathway signaling is persistently activated in lapatinib resistant breast cancer cells

We used HER2+ breast cancer models of acquired therapeutic resistance to lapatinib established in our laboratory as previously described [17,18] to investigate how, and to what extent deregulation of the protein signaling network contributes to therapeutic resistance to HER2/EGFR TKIs. As previously shown, these cells are maintained in 1 μM lapatinib without decreased viability, compared with parental cell counterparts that are sensitive to the

antitumor effects of lapatinib (Additional file 2). In order to determine the activation state of the cell signaling network in lapatinib resistant tumor cells, we evaluated the expression of over 150 protein/phosphoprotein representing mediators of key cell processes using quantitative reverse-phase protein arrays (RPMA) [29]. Findings from the RPMA analysis were confirmed by Western blot analysis. For the purposes of the following studies, resistant cell lines were maintained in the continuous presence of 1 μM lapatinib, even when combined with other treatments. Consistent with our previous findings [17], HER2 phosphorylation remained inhibited in lapatinib resistant cells (Figure 1A). Using this strategy, we found that the PI3K pathway remained activated in our models of acquired lapatinib resistance as indicated by the persistent phosphorylation of PI3K-p85^{Y458}, Akt^{T308}, mTOR^{S2481}, p70S6K^{S371}, Bad^{S136} and 4EBP1^{S65} (Figure 1A and B; Additional file 3). In addition, protein expression of survivin, a member of the inhibitor of apoptosis family whose down-regulation in lapatinib treated HER2+ breast cancer cells we had previously shown to correlate with lapatinib antitumor activity in a PI3K-dependent manner [31], remained intact in lapatinib resistant cells.

Figure 1 Persistent activation of PI3K signaling promotes survival in lapatinib resistant cells. (A) pHER2, total HER2, Akt^{T308}, Akt^{S473}, p70S6K^{S371}, 4EBP1^{S65}, and survivin steady-state protein expression in untreated parental BT474, BT474 treated with 0.5 μM lapatinib for 48 hours, and rBT474 maintained in 1 μM lapatinib as determined by Western blot analysis from whole cell extracts. **(B)** Phospho-PI3K protein expression was determined by RPMA in the same treatment groups as described in (A). Results represent the mean +/- standard error of triplicate samples, and are representative of three independent experiments. *$P < 0.0018$. **(C)** Molecular knockdown of PI3K using pooled siRNA against PI3K subunits (*) in rBT474 cells was confirmed by Western blot analysis using subunit specific antibodies and an anti-PARP cleavage product antibody. Cells transfected with scrambled siRNA construct (NSC) served as controls. Actin steady-state protein levels served as a control to ensure for equal loading of protein. The results are representative of three independent experiments. **(D)** The effects of siRNA-mediated knockdown of PI3K on rBT474 cell growth ($P < 0.0058$). Non-specific siRNA construct (NSC) served as a control. Results represent the mean +/- standard error of triplicate samples, and are representative of three independent experiments.

A PI3K-PDK1-Akt^{T308} signaling axis maintains the survival of lapatinib resistant tumor cells

We used a molecular approach to knockdown specific targeted proteins in the PI3K signaling pathway in order to determine the functional role of PI3K in maintaining the resistant phenotype. As shown, small interfering RNA (siRNA)-mediated knockdown of PI3K, primarily targeting the p110 catalytic subunit, triggered resistant cells to undergo apoptosis as indicated by increased expression of cleaved PARP and significant inhibition of cell growth and viability ($P < 0.0058$) (Figure 1C and D). There are a number of downstream intermediaries that transduce the PI3K signaling effects e.g. Akt, PDK1, SGK, and PKCβ. Interestingly, phosphorylation of Akt serine 473 (S473), which is considered a hallmark of PI3K pathway activation, was inhibited in resistant cells despite persistent PI3K pathway activation (Figure 1A). Instead, phosphorylation of Akt threonine 308 remained intact, implicating a role for PDK1-the kinase responsible for phosphorylating Akt^{T308}- in resistant cells. To expand upon these findings, we individually knocked down Akt, PDK1, SGK, and PKCβ in order to determine each of their effects on the viability of resistant cells. We found that knockdown of Akt or PDK1, but not PKCβ or SGK had a significant antitumor effect in lapatinib resistant cells (Figure 2). The overlapping antitumor effects in response to knocking

down Akt or PDK1 implicated the role of a PI3K-PDK1-Akt^{T308} signaling axis in maintaining the survival of lapatinib resistant cells.

Figure 2 A PI3K-PDK1 signaling axis mediates the effects of PI3K signaling in lapatinib resistant cells. A comparison of the effects of siRNA-mediated knockdown of Akt, PDK1, PKC β and SGK on the growth of rBT474 cells. Cells transfected with scrambled siRNA construct (NSC) served as controls. Growth assays were performed as described in the Methods. Knockdown of targeted protein was confirmed by Western blot analysis (lower panels). Actin steady-state protein levels served as a control to ensure for equal loading of protein. Results represent the mean +/- standard error of triplicate samples, and are representative of three independent experiments.*$P < 0.005$; **$P < 0.002$.

The regulation of PI3K pathway activation and cell survival is switched from HER2-HER3 in the treatment naïve state to EGFR-HER3 signaling in lapatinib resistance

Lapatinib-naïve HER2+ breast cancer cells are addicted to HER2 signaling. Work from our laboratory and others has shown that regulation of pro-survival PI3K signaling in lapatinib resistant breast cancer cells appears to be mediated through a HER2-independent mechanism(s) [17,32]. Although loss of the PTEN tumor suppressor, or the presence of PI3KCA gain-of-function mutations can lead to constitutive activation of PI3K signaling in breast cancer [33,34], neither was found to be relevant in our models of resistance (data not shown). Similar to that reported by others, we found that redundant survival pathways previously linked to HER TKI resistance were phosphorylated in our models of resistance (e.g., c-src, c-met) [20,35,36]; however, we were unable to demonstrate their functional role in regulating the survival of resistant cells (Additional files 4 and 5).

HER2-HER3 heterodimers are potent activators of PI3K signaling [8]. HER3 was persistently phosphorylated on tyrosine 1197 in our models of lapatinib resistance (Figure 3A) despite inactivation of its preferred heterodimer partner HER2 (Figure 1A). HER3 knockdown in resistant cells led to inhibition of PI3K-p85^{Y508} phosphorylation, increased expression of cleaved PARP, and significant inhibition of cell growth and viability ($P < 0.013$ in rSKBR3; $P < 0.017$ in rBT474) (Figure 3A-D) revealing its central role in the maintenance of cell survival in our models. Unable to detect HER4 protein in resistant cells (data not shown), we speculated that EGFR, which is also expressed in lapatinib resistant cells, might be responsible for the persistent transactivation of HER3 in resistant cells. Since lapatinib is reported to be an equipotent inhibitor of the HER2 and EGFR kinases [14,15], we expected to find that phosphorylation of EGFR, similar to HER2, would be inhibited in resistant cells. However, analysis of individual EGFR phosphotyrosine sites in lapatinib resistant cells revealed a mixed pattern as evidenced by variably persistent phosphorylation of tyrosines 992 and 1148, and marked inhibition of other phosphotyrosine sites (Y1173, Y1068) (Figure 4).

Figure 3 EGFR-HER3 transactivation regulates resistant cell survival through PI3K signaling. (A) The effects of EGFR and HER3 knockdown on steady-state phospho-HER3^{Y1197} protein expression. The absolute optical density (OD) values attributed to the p-HER3 bands- determined using the Odyssey Infrared Imaging System-are indicated under each corresponding lane. **(B)** Western blot analysis with the indicated phosphospecific antibodies showing the effects of HER3 knockdown on EGFR^{Y992} and PI3K-p85^{Y508} in rBT474 and rSKBR3 cells. **(C)** Increased steady-state protein levels of cleaved PARP

product, and **(D)** inhibition of cell growth in response to HER3 knockdown in rBT474 and rSKBR3 cells. $P < 0.017$ (rBT474); $P < 0.013$ (rSKBR3). Results represent the mean +/- standard error of triplicate samples, and are representative of three independent experiments.

Figure 4 Lapatinib resistant cells exhibit a mixed pattern of EGFR tyrosine autophosphorylation. Reverse phase protein microarray analysis of EGFR Y992, Y1068, Y1148 and Y1173 in parental HER2+ breast cancer cell lines (BT474; SKBR3; Au565; SUM190), parental cells treated with 1 μM lapatinib for 24 hours, and lapatinib resistant cell counterparts (rBT474; rSKBR3; rAu565; rSUM190) maintained in 1 μM lapatinib. Results represent the mean +/- standard error of triplicate samples, and are representative of three independent experiments.

These findings made it tempting to speculate that escape from, or incomplete inhibition of EGFR tyrosine autophosphorylation sites in response to lapatinib, over time led to a switch in the regulation of cell survival from HER2-HER3-PI3K signaling in lapatinib-naive HER2$^+$ breast cancer cells, to EGFR-HER3-PI3K in cells that become resistance to lapatinib. To test this hypothesis, we molecularly knocked down EGFR in lapatinib resistant cells, which reduced HER3^{Y1197} phosphorylation and PI3K signaling, and led to increased apoptosis (cleaved PARP) with a statistically significant reduction in cell viability ($P < 0.018$ in rBT474; $P < 0.021$ in rSKBR3) (Figure 5A-C). Thus, the regulation of HER3 phosphorylation appears to switch from HER2 in treatment naïve cells, to EGFR in HER2+ breast cancer cell lines that have become resistant to lapatinib.

Figure 5 The effects of EGFR knockdown on steady-state levels of the indicated proteins and phosphoproteins using phosphospecific antibodies. (A) Western blot analysis with the indicated phosphospecific antibodies showing the effects of EGFR knockdown on EGFR^{Y992,} PI3K-p85^{Y508} and Akt^{T308} in rBT474 and rSKBR3 cells. **(B)** Western blot analysis of cleaved PARP product in rBT474 and rSKBR3 cells transfected with EGFR siRNA. Scrambled siRNA sequence (NSC) served as controls. Steady-state actin protein served as a control for equal loading of protein. Western blot data shown in A and B is representative of three independent experiments. **(C)** Effects of siRNA-mediated knockdown of EGFR on tumor cell growth in rBT474 and rSKBR3 cell lines. Results represent the mean +/- standard error of triplicate samples, and are representative of three independent experiments. $P < 0.018$ (rBT474) and $P < 0.021$ (rSKBR3).

Activation of a negative feedback loop in resistant tumor cells specifically dephosphorylates Akt^{S473} despite persistent PI3K pathway activation

Inhibition of Akt^{S473} phosphorylation in resistant cells appeared inconsistent with the persistent activation of the PI3K signaling pathway (Figure 1A). In this context, PHLPPL (PH domain leucine-rich repeat-containing phosphatase-like) is a protein phosphatase that is transcriptionally regulated by mTORC1 [37,38]. PHLPPL negatively feeds back on PI3K signaling by selectively dephosphorylating Akt on S473, not T308 [37,38], making it tempting to speculate that PHLPPL might be responsible for the pattern of Akt phosphorylation observed in lapatinib resistant cells. We found that expression of PHLPPL protein was increased in resistant cells compared with their parental cell counterparts (Additional file 6A). PHLPPL protein expression was decreased in parental cells treated with 1 μM lapatinib for 24 hours (Additional file 6A), consistent with inhibition of PI3K-mTOR signaling in lapatinib-treated parental cells. If the increased expression of PHLPPL in resistant cells was related to persistent PI3K-mTOR pathway activation, then inhibition of

PI3K signaling should block PHLPPL expression. Indeed, PHLPPL expression was inhibited in resistant cells growing in the presence of 1 μM lapatinib, following treatment with the dual PI3K-mTOR kinase inhibitor BEZ-NVP 235 [39] (Additional file 6A). In addition, molecular knockdown of EGFR, which blocked PI3K signaling, also inhibited PHLPPL protein expression (Additional file 6B). These findings suggest that Akt^{S473} phosphorylation may not necessarily represent a reliable pharmacodynamic readout to assess the effects of targeted therapies on PI3K signaling.

EGFR represents an attractive target in lapatinib resistant HER2+ breast cancer cells

Gefitinib and erlotinib are FDA approved EGFR TKIs [40-42]. In our hands, when used at a final concentration of 5 μM, neither drug was able to block persistent EGFR tyrosine phosphorylation in lapatinib resistant cells- maintained in 1 μM lapatinib- nor did they restore lapatinib sensitivity (Figure 6A and B). Neratinib, in contrast to lapatinib, gefitinib and erlotinib is an irreversible EGFR and HER2 TKI [43]. Consistent with previous reports [43], we found that neratinib was a potent inhibitor of parental HER2+ breast cancer cells (Additional file 7). Neratinib, when used at higher concentrations than in parental cell cultures, inhibited persistent phosphorylation of EGFR, HER3 and Akt^{T308} in resistant cells, triggering cell apoptosis (increased cleaved PARP), and inhibition of cell growth and viability ($P < 0.0008$ in rSKBR3; $P < 0.0025$ in rBT474) (Figure 6A and B). These findings suggest that persistent EGFR signaling, rather than incomplete inhibition HER2, can play a role in maintaining the lapatinib resistant phenotype.

Figure 6 Gefitinib and erlotinib do not reverse lapatinib resistance. (A) Cell growth of rBT474 and rSKBR3 cells after treatment with 5 μM gefitinib or erlotinib or 1 μM or 5 μM neratinib for 72 hours. Resistant cells were maintained in the presence of 1 μM lapatinib. Results represent the mean +/- standard error of triplicate samples, and are representative of three independent experiments. $P < 0.0025$ (rBT474) and $P < 0.0008$ (rSKBR3). **(B)** Western blot analysis showing steady-state $pEGFR^{Y992}$. $pHER3^{Y1197}$, $pAkt^{Y308}$ phosphoprotein and cleaved PARP product expression in rBT474 and rSKBR3 cells after 72 hours treatment with 5 μM gefitinib, erlotinib, or neratinib (1 and 5 μM), or vehicle (0.01% DMSO) alone. Steady-state actin protein levels served as a control for equal loading of protein. The results are representative of three independent experiments.

Auto-induction of heregulin in resistant cells drives the EGFR-HER3-PI3K signaling axis

We next sought to identify an underlying driver responsible for the persistent activation of the HER3-EGFR-PI3K signaling axis in lapatinib resistant HER2+ breast cancer cells. Previous work from our laboratory had shown that heregulin β1 (HRG)- a soluble ligand for HER3 and HER4- but not an EGFR ligand (EGF), can abrogate the inhibitory effects of lapatinib on cell signaling pathways in parental HER2+ breast cancer cells [44,45], findings that were recently confirmed by Settleman and colleagues [46]. We therefore speculated that autocrine induction of HRG might play a role in the development of lapatinib resistance by providing the HER3 activation input, which, in conjunction with concomitant persistent EGFR activation, results in the formation of HER3-EGFR heterodimers. As shown, HRG protein expression was indeed increased in lapatinib resistant cells compared with parental cell counterparts (Figure 7A and B). In contrast, we did not find increased expression of EGF

ligands (data not shown). Interestingly, we found the 105 kDa membrane-bound species (Figure 6B, labeled HRG1), which can activate HER3 [47], to be the predominant form of HRG increased in resistant cells. Moreover, protein expression of the 40 kDa soluble form of HRG was decreased in resistant cells compared to parental cell counterparts (Figure 7B, labeled HRG2). Importantly, targeted molecular knockdown of HRG in resistant cells induced apoptosis (cleaved PARP) and decreased cell growth and viability ($P < 0.009$ in rSKBR3; $P < 0.0023$ in rAu565) (Figure 7C and D).

Figure 7 Autocrine induction of HRG drives survival of resistant cells. (A) Immunofluorescence microscopy of HRG expression in the indicated cell lines using a primary rabbit anti-HRG antibody and visualized with an anti-rabbit IgG Alexa Fluor 555 (red) conjugated secondary antibody. Cell nuclei were visualized by DAPI staining (blue). These results are representative of other fields on the slide. **(B)** Western blot analysis of HRG type 1 (115 KD) and type 2 (40 KD) steady-state protein levels in lapatinib resistant (rSKBR3; rAu565; rBT474) maintained in 1 µM lapatinib, and untreated parental cell counterparts (SKBR3; BT474; Au565); actin served as a control for equal loading of protein. **(C)** Western blot analysis of survivin and cleaved PARP product following HRG knockdown in rAu565 and rSKBR3 cells. Cells transfected with scrambled siRNA construct (NSC) served as controls. Actin served as a control for equal loading of protein. **(D)** Effects of siRNA-mediated knockdown of HRG on tumor cell growth in rAu565 and rSKBR3 cell lines. Results represent the mean +/- standard error of triplicate samples, and are representative of three independent experiments. $P < 0.009$ (rSKBR3) and $P < 0.0023$ (rAu565). **(E)** Western blot analysis of ADAM17 protein level in parental BT474 and SKBR3 +/- lapatinib treatment as indicated in the figure. Resistant cells (rBT474 and rSKBR3) were growing in the presence of 1 µM lapatinib. Hela cell extract was used as a positive control. Two bands from 75 KD to 100 KD can be detected by a specific ADAM17 antibody. These results are representative of three independent experiments.

We next sought to gain a better understanding of the mechanism underlying the increased expression of membrane-bound HRG in resistant cells. Based on RT-PCR analysis, increased HRG resistant cells did not appear to be transcriptionally mediated (data not shown). ADAM17 is a metallopeptidase that proteolytically processes the 105 kDa membrane bound form to smaller molecular weight soluble forms of HRG [48]. A previous report suggested that transient inhibition of Akt phosphorylation in trastuzumab-treated HER2^{+} breast cancer cells can lead to increased expression of ADAM17 and consequently increased expression of the lower molecular weight (40 kDa) soluble form of HRG [49]. In contrast, here we show that the major forms of ADAM17 were inhibited over time in lapatinib-treated parental HER2+ breast cancer cell lines (Figure 7E, compare 1 hr and 24 hr treatments). Furthermore, ADAM17 was markedly reduced in lapatinib resistant cells compared with their untreated parental cell counterparts. These findings made it tempting to speculate that inhibition of ADAM17 by lapatinib blocks proteolytic processing of the 105 kDa membrane-bound form of HRG, leading to its increased expression and concomitant decreased expression of lower molecular weight forms in resistant cells.

Increased HRG expression predicts for a poor outcome in HER2+ breast cancer patients

To shed light on the potential clinical implications of the autocrine induction of HRG in lapatinib resistant HER2^{+} breast cancer cells, we analyzed the relationship between HRG gene expression and clinical outcome in women with HER2^{+} breast cancer. Our analysis of

the relationship between HRG gene expression and clinical outcome in women with HER2^{+} breast cancer (N = 204) revealed a linear correlation between HRG expression and risk of recurrence (p = 0.0036, Cox-regression analysis) and a statistically significant difference (p = 0.0034, Kaplan-Meier Estimates survival analysis) between high HRG expression and decreased recurrence-free survival (RFS) (Figure 8). Median RFS in tumors with high expression and others (Intermediate plus Low) was 2.84 and 10.04 years, respectively. Using clinical parameters that were associated with clinical outcome, such as tumor size, grade, nodal status, HER2, ER and PR status, we found that expressions of *HRG* was independent poor prognosis factor (comparing *HRG* high, intermediate and low expression groups, *P* = 0.049, n = 581, COXPH survival analysis). Thus, auto-induction of HRG in lapatinib resistant tumors could potentially contribute to a more aggressive tumor phenotype with a poorer clinical outcome.

Figure 8 Recurrence-free-survival in HER2+ breast cancer patients according to HRG expression levels. Tick marks in Kaplan-Meier Estimates of recurrence-free survival indicate patients whose data were censored by the time of last follow-up or owing to death. *P* < 0.0034 was calculated using log-rank Mantel-Cox test.

Discussion

The robustness of a biological system can be defined by its ability to maintain function when perturbed [50]. Accordingly, loss of HER2 signaling represents a significant perturbation to HER2-addicted breast cancer cells. Previous work from our laboratory and others has shown that the antitumor activity of lapatinib tracks with its ability to inhibit HER2 signaling [31,51]. Chronic exposure to lapatinib however leads to the development of acquired therapeutic resistance in models of HER2+ breast cancer and in patients. We and others have shown that resistance to lapatinib does not appear to be mediated by reactivation of HER2 [17,23,32]. Instead, we now show that an autocrine feedback mechanism involving membrane bound HRG can promote a previously unsuspected EGFR-HER3-PI3K-PDK1 signaling axis that is resistant to the effects of lapatinib and other FDA-approved EGFR TKIs. A key finding here is that the unopposed action of EGFR, which is incompletely inhibited by lapatinib, can transactivate HER3 in a manner driven by autocrine HRG. These findings demonstrate the robustness of the HER receptor-ligand system that enables HER2+ breast cancer cells to survive loss of HER2 signaling without the need to invoke mutations in the target kinase or its downstream intermediaries, or the activation of redundant signaling pathways.

In contrast to HRG, we were unable to demonstrate increased expression of EGFR ligands e.g. EGF, betacellulin in our models of lapatinib resistance. It is intriguing to speculate that the preferential induction of HRG reflects the drive of the tumor cell to maintain PI3K pathway activation in response to the loss of HER2-HER3 oncogenic signaling complex, which is a potent PI3K pathway activator. Induction of EGFR ligands could have led to the formation of EGFR homodimers, which are less potent activators of PI3K signaling compared with HER3-containing dimers. Indeed, lapatinib resistant cells may also be primed to respond to HRG stimulation as HER3, the cognate receptor for HRG, has been shown to be up-regulated in HER2+ breast cancer models of acquired lapatinib resistant [21].

The mechanism involved in the auto-induction of HRG in resistant cells described here differs from the transient activation of HRG previously reported in trastuzumab-treated cells [49]. First, activation of HRG by trastauzumab was not shown to be directly linked to the development of acquired therapeutic resistance to trastuzumab. Second, induction of HRG in trastuzumab-treated cells was reportedly mediated by activation of ADAM17. In contrast, we show that lapatinib inhibits expression of ADAM17, which may explain the increased expression of full-length membrane-bound HRG with a concomitant decrease in the expression of the lower molecular weight forms. Although lapatinib and trastuzumab both target HER2, our findings further underscore the distinct biological effects that each can have on HER2+ targeted breast cancer cells.

The findings reported here highlight the importance of the cell context in the interpretation of predictive or correlative biological readouts. For example, we previously reported that the phosphorylation state of HER3 could discriminate those patients with HER2+ inflammatory breast cancers who were more likely to respond to lapatinib monotherapy [16]. In that lapatinib-naïve setting, HER3 was likely transactivated by HER2 and therefore more sensitive to the antitumor activity of a potent HER2 tyrosine kinase inhibitor such as lapatinib. However, in HER2+ breast cancer cells that have become resistant to lapatinib, HER3 phosphorylation can be regulated by EGFR-HER3 dimers, which were not responsive to inhibition by lapatinib or other EGFR TKIs. Thus, monitoring tumors for the presence of increased HER3 phosphorylation, and perhaps phosphorylated EGFR too, during lapatinib treatment may be an effective biomarker to identify patients whose tumors are becoming HRG-rewired. In addition, phosphorylation of Akt^{S473}, which has long been considered a hallmark of PI3K pathway activation, was inhibited in lapatinib resistant cells despite persistent activation of the PI3K pathway. An explanation for this apparent discrepancy can be attributed to the increased expression of a PI3K-mTOR regulated phosphatase (PHLPPL) that dephosphorylates Akt on S473, in lapatinib resistant cells (Additional file 6A). Thus, the predictive power of biomarkers such as phosphorylated HER3 or phospho-Akt^{S473} would need to be placed into the context of the signals regulating its activation for clinical implementation. Consequently, clinical confirmation of the predictive nature of the elucidated pathway biomarker architecture would have to take place within that same context- in this instance tumor tissue from patients who relapsed after initially responding to lapatinib therapy and not from more easily obtained pre-treatment biopsy samples. Our findings provide the scientific rationale to collect these tumor specimens so that validation of biomarkers of acquired resistance could be rigorously interrogated.

We previously showed that the antitumor activity of lapatinib in HER2+ breast cancer cells was not affected by EGF stimulation [44]. Here however, increased expression of HRG can not only promote acquired therapeutic resistance to HER TKIs, it can also mediate primary resistance to lapatinib (Additional file 8) [44-46]. The frequent expression of HRG in solid tumors [52], including triple negative breast cancers may provide an explanation as to why current FDA approved HER TKIs have had limited clinical impact in the treatment of the majority of HER2-overexpressing and EGFR-expressing solid tumors, with the exception of head and neck cancers [53]. Importantly, we identified HRG expression as an independent negative predictor of clinical outcome in patients with HER2$^+$ breast cancers (Figure 8). Thus, targeting ligand-mediated feedback loops represents a new treatment strategy to overcome therapeutic resistance established through this mechanism.

Although current FDA approved EGFR TKIs did not suppress HRG-driven EGFR activation in our models of resistance, siRNA-mediated knockdown of EGFR and treatment with the

irreversible pan-HER TKI neratinib exerted antitumor effects in resistant cells (Figure 6A and B). Furthermore, whereas HRG can reverse the antitumor effects of lapatinib in parental HER2+ breast cancer cells (Additional file 8) [44-46], the antitumor effects of neratinib in parental HER2+ breast cancer cells are more resistant to HRG (Additional file 8). These findings are consistent with the ability of neratinib to exert antitumor effects on HRG-expressing resistant cells. Although neratinib is described as a pan-HER inhibitor, at clinically relevant concentrations it can affect non-HER receptor kinases that contain homologous ATP kinase domains. Whereas lapatinib has been shown to be a highly specific TKI for HER2 and EGFR, neratinib and many other FDA-approved TKIs exhibit promiscuous inhibitory effects on non-HER kinases at clinically relevant concentrations [54]. These effects may contribute to the antitumor effects of neratinib in resistant cells, particularly at higher concentrations. Indeed, preliminary clinical data indicates that neratinib remains clinically active in the treatment of HER2$^+$ breast cancers that have progressed on prior lapatinib-based therapy (Chow L, et al. Efficacy and safety of neratinib (HKI-272) in combination with paclitaxel in HER2+ metastatic breast cancer. San Antonio Breast Cancer Symposium 2010). Furthermore, it is not surprising that parental HER2+ breast cancer cells were more sensitive to the antitumor effects of neratinib compared with lapatinib resistant cells. Resistance to HER2 TKIs does not appear to be mediated by one underlying mechanism, as we and others have shown [17-23,55,56]. Therefore, completely reversing established resistance will likely require more than a single targeted intervention e.g. neratinib. It will require a combination approach, which, based on the findings reported here, should include inhibitors that block HRG-HER3-EGFR-PI3K-PDK1 signaling. These findings suggest that inhibition of wild-type EGFR remains an attractive therapeutic strategy awaiting the development of more effective EGFR inhibitors.

The findings presented here have broad implications for the development of TKIs used to treat cancer and other kinase-driven diseases. As we have demonstrated, selection of clinical candidates based on activity profiles from *in vitro* kinase assays can be misleading. To the extent that lapatinib, erlotinib, and gefitinib are considered potent EGFR kinase inhibitors, none were able to neutralize HRG-mediated activation of EGFR. In contrast, neratinib appears to be a more effective inhibitor of EGFR phosphorylation and activation, even in the presence of HRG in resistant and parental cells. It is tempting to suggest that the use of PI3K or mTOR selective inhibitors will prevent the development of ligand-mediated resistance. However, given the complex feedback mechanisms that govern these cytoplasmic signaling events, and the potential for HRG to exert promiscuous effects on cell signaling pathways in a PI3K-independent manner [57], combination therapies that target both proximal and distal signaling are more likely to yield better clinical outcomes. Progressing TKIs into the clinic based on their ability to inhibit multiple tyrosine autophosphorylation sites may lead to the identification of more effective drugs with a reduced risk of developing therapeutic resistance, and better candidates for personalized, combination therapies.

Conclusions

Molecular targeted therapies that are directed against tyrosine kinases and receptor tyrosine kinases represent an important class of cancer drugs. However, development of TKI resistance remains a significant clinical dilemma that has limited the clinical impact of this class of targeted drugs in a broad range of solid tumors where they were predicted to be effective. Past descriptions of mechanisms of TKI resistance have been attributed to mutations in targeted kinases or compensatory activation of signaling pathways that circumvent the target. Here we demonstrate the robustness of the HER biological system to

respond to a significant perturbation in cell signaling in the context of describing an entirely new mechanism of resistance to HER TKIs, including the FDA-approved dual HER2/EGFR TKI lapatinib which is triggered by autocrine induction of the HER3 ligand, heregulin β1 (HRG). While lapatinib, a supposed equipotent HER2 and EGFR kinase inhibitor based on data from *in vitro* kinase assays appropriately inhibited HER2 signaling, EGFR on the other hand was incompletely inactivated. Persistent EGFR signaling coupled with the autocrine induction of membrane bound HRG contributed to a switch in the regulation of cell survival from HER2-HER3-PI3K in treatment naïve HER2+ breast cancer cells to and HRG-driven EGFR-HER3-PI3K-PDK1 signaling axis in lapatinib resistant tumor cells. Importantly, the FDA approved EGFR TKIs gefitinib and erlotinib failed to block EGFR signaling and restore lapatinib sensitivity. Wild type EGFR did however remain an attractive target as molecular knockdown of EGFR and treatment with the irreversible pan-HER TKI neratinib blocked residual EGFR signaling, exerting an antitumor effect in resistant cells. We further showed the clinical relevance of increased HRG expression in TKI resistant tumor cells in a large breast cancer dataset (N = 204) of women with HER2+ breast cancers where increased HRG expression was an independent predictor for a significantly poorer clinical outcome (recurrence free survival) compared to women whose tumors expressed moderate to low levels of HRG ($P < 0.0036$). Thus, incomplete inhibition and persistent signaling of the target itself, driven by a ligand-mediated autocrine feedback loop may have broad implications for the treatment of diseases using TKI therapies. These findings underscore potential inadequacies associated with the current approach of selecting clinical TKI candidates based on activity profiles from *in vitro* kinase assays. If incomplete target inhibition driven by autocrine ligand induction can mediate resistance to a selective inhibitor such as lapatinib, then induction of ligand-driven autocrine feedback loops in response to promiscuous kinase inhibitors may be a new major causal factor of resistance. Selecting clinical lead candidates based on their ability to inhibit multiple tyrosine autophosphorylation sites instead of inhibition from *in vitro* kinase assays may lead to the identification of more effective drugs with a reduced risk of developing therapeutic resistance.

Abbreviations

ADAM17, ADAM Metallopeptidase 17; Akt, Protein Kinase B; ALLTO, Adjuvant Lapatinib and/or Trastuzumab Treatment Optimization; ATP, Adenosine triphosphate; 4EBP1, eIF4E-Binding Protein 1; EGF, Epidermal Growth Factor; EGFR, Epidermal Growth Factor Receptor; FDA, Food and Drug Administration; HER2, Human Epidermal Growth Factor Receptor 2; HER2+, HER2 overexpression; HER3, Human Epidermal Growth Factor Receptor 3; HER4, Human Epidermal Growth Factor Receptor 4; HRG, Heregulin β 1; mTOR, Mammalian target of rapamycin; p70S6K, p70S6 Kinase; PDK1, Phosphoinositide-dependent kinase 1; PARP, Poly (ADP-ribose) polymerase; PHLPPL, PH domain leucine-rich repeat-containing phosphatase-like; PI3K, Phosphoinositide 3-kinase; PI3KCA, Catalytic subunit of PI3K; PKC, Protein kinase C; PTEN, Phosphatase and tensin homolog; RPMA, reverse phase protein microarray; RTK, Receptor Tyrosine Kinase; siRNA, Small interfering RNA; SGK, Serum-glucocorticoid regulated kinase; TKI, Tyrosine Kinase Inhibitor.

Competing interests

Authors' contributions

WX, SZ, LL, and WG maintained all of the cell cultures, designed and performed treatment interventions with small molecule inhibitors, and ran SDS-PAGE Western blots. WX, SZ, LL, XY designed and performed siRNA experiments. XY and TO, helped SZ perform immunofluorescence microscopy. SB helped with data analysis and provided critical review of the manuscript. KL and QC mined the breast cancer database QC had generated for the HRG genomic data, and provided statistical input on analysis. EP, JW, and RG performed and analyzed the RPMA studies. NLS conceived of the ideas of the manuscript. NLS, WX, and EP oversaw the conduct of the experiments, data analysis, and wrote the manuscript. NLS and EP provided funding for the experiments performed in the manuscript. All authors read and approved the manuscript for publication.

Acknowledgements

References

1. Burden S, Yarden Y: **Neuregulins and their receptors: a versatile signalling module in organogenesis and oncogenesis.** *Neuron* 1997, **18:**847–855.

2. Riese DJ II, van Raaij TM, Plowman GD, Andrews GC, Stern DF: **The cellular response to neuregulins is governed by complex interactions of the ErbB receptor family.** *Mol Cell Biol* 1995, **15:**5770–5776.

3. Tzahar E, Waterman H, Chen X, Levkowitz G, Karunagaran D, Lavi S, Ratzkin BJ, Yarden Y: **A hierarchical network of interreceptor interactions determines signal transduction by Neu differentiation factor/neuregulin and epidermal growth factor.** *Mol Cell Biol* 1996, **16:**5276–5287.

4. Graus Porta D, Beerli RR, Daly JM, Hynes NE: **ErbB2, the preferred heterodimerization partner of all ErbB receptors, is a mediator of lateral signalling.** *EMBO J* 1997, **16:**1647–1655.

5. Yarden Y, Sliwkowski MX: **Untangling the ErbB signalling network.** *Nat Rev Mol Cell Biol* 2001, **2:**127–137.

6. Hynes NE, McDonald G: **ErbB receptors and signaling pathways in cancer.** *Curr Opin Cell Biol* 2009, **21:**177–184.

7. Guy PM, Platko JV, Cantley LC, Cerione RA, Carraway KL: **Insect cell-expressed p180ErbB3 possesses an impaired tyrosine kinase activity.** *Proc Natl Acad Sci U S A* 1994, **91:**8132–8136.

8. Fedi P, Pierce J, Di Fiore PP, Kraus MH: **Efficient coupling with phosphatidylinositol 3-kinase, but not phospholipase C gamma or GTPase-activating protein, distinguishes ErbB3 signalling from that of other ErbB/EGFR family members.** *Mol Cell Biol* 1994, **14:**492–500.

9. Holbro T, Beerli RR, Maurer F, Koziczak M, Barbas CF 3rd, Hynes NE: **The ErbB2/ErbB3 heterodimer functions as an oncogenic unit: ErbB2 requires ErbB3 to drive breast tumor cell proliferation.** *Proc Natl Acad Sci U S A* 2003, **100:**8933–8938.

10. Slamon DJ, Clark GM, Wong SG, Levin WJ, Ullrich A, McGuire WL: **Human breast cancer: correlation of relapse and survival with amplification of the HER-2/neu oncogene.** *Science* 1987, **235:**177–182.

11. Slamon DJ, Godolphin W, Jones LA, Holt JA, Wong SG, Keith DE, Levin WJ, Stuart SG, Udove J, Ullrich A, Press MF: **Studies of the HER-2/neu proto-oncogene in human breast and ovarian cancer.** *Science* 1989, **244:**707–712.

12. Rusnak DW, Affleck K, Cockerill SG, Stubberfield C, Harris R, Page M, Smith KJ, Guntrip SB, Carter MC, Shaw RJ, Jowett A, Stables J, Topley P, Wood ER, Brignola PS, Kadwell SH, Reep BR, Mullin RJ, Alligood KJ, Keith BR, Crosby RM, Murray DM, Knight WB, Gilmer TM, Lackey K: **The characterization of novel, dual ErbB-2/EGFR, tyrosine kinase inhibitors: potential therapy for cancer.** *Cancer Res* 2001, **61:**7196–7203.

13. Geyer CE, Forster J, Lindquist D, Chan S, Romieu CG, Pienkowski T, Jagiello-Gruszfeld A, Crown J, Chan A, Kaufman B, Skarlos D, Campone M, Davidson N, Berger M, Oliva C, Rubin SD, Stein S, Cameron D: **Lapatinib plus capecitabine for HER2-positive advanced breast cancer.** *N Engl J Med* 2006, **355:**2733–2743.

14. Rusnak D, Lackey K, Affleck K, Wood ER, Alligood KJ, Rhodes N, Keith BR, Murray DM, Glennon K, Knight WB, Mullin RJ, Gilmer TM: **The effects of the novel, reversible epidermal growth factor receptor/ErbB-2 Tyrosine Kinase inhibitor, GW2016, on the growth of human normal and tumor-derived cell lines *in Vitro* and *in Vivo*.** *Mol Cancer Ther* 2001, **1:**85–94.

15. Wood ER, Truesdale AT, McDonald OB, Yuan D, Hassell A, Dickerson SH, Ellis B, Pennisi C, Horne E, Lackey K, Alligood KJ, Rusnak DW, Gilmer TM, Shewchuk L: **A unique structure for epidermal growth factor receptor bound to GW572016 (Lapatinib): relationships among protein conformation, inhibitor off-rate, and receptor activity in tumor cells.** *Cancer Res* 2004, **64:**6652–6659.

16. Johnston S, Trudeau M, Kaufman B, Boussen H, Blackwell K, LoRusso P, Lombardi DP, Ben Ahmed S, Citrin DL, DeSilvio ML, Harris J, Westlund RE, Salazar V, Zaks TZ, Spector NL: **Targeting HER2 in advanced inflammatory breast cancer with lapatinib monotherapy: A phase II study with biomarker profiles that predict for response.** *J Clin Oncol* 2008, **26:**1066–1072.

17. Xia W, Bacus S, Hegde P, Husain I, Strum J, Liu L, Paulazzo G, Lyass L, Trusk P, Hill J, Harris J, Spector NL: **A model of acquired autoresistance to ErbB2 tyrosine kinase inhibitors and a therapeutic strategy to prevent its onset in breast cancer.** *Proc Natl Acad Sci U S A* 2006, **103:**7795–7800.

18. Xia W, Liu Z, Zong R, Liu L, Zhao S, Bacus SS, Mao Y, He J, Wulfkuhle JD, Petricoin EF III, Osada T, Yang X-Y, Hartman ZC, Clay TM, Blackwell KL, Lyerly HK, Spector NL: **Truncated ErbB2 Expressed in Tumor Cell Nuclei Contributes to Acquired Therapeutic Resistance to ErbB2 Kinase Inhibitors.** *Mol Cancer Therap* 2011, **10:**136–1374.

19. Eichhorn PJ, Gili M, Scaltriti M, Serra V, Guzman M, Nijkamp W, Beijersbergen RL, Valero V, Seoane J, Bernards R, Baselga J: **Phosphatidylinositol 3-kinase hyperactivation results in lapatinib resistance that is reversed by the mTOR/phosphatidylinositol 3-kinase inhibitor NVP-BEZ235.** *Cancer Res* 2008, **68:**9221–9230.

20. Rexer BN, Ham AJ, Rinehart C, Hill S, Granja-Ingram Nde M, González-Angulo AM, Mills GB, Dave B, Chang JC, Liebler DC, Arteaga CL: **Phosphoproteomic mass spectrometry profiling links Src family kinases to escape from HER2 tyrosine kinase inhibition.** *Oncogene* 2011, **30:**4163–4174.

21. Garrett JT, Olivares MG, Rinehart C, Granja-Ingram ND, Sánchez V, Chakrabarty A, Dave B, Cook RS, Pao W, McKinely E, Manning HC, Chang J, Arteaga CL: **Transcriptional and posttranslational up-regulation of HER3 (ErbB3) compensates for inhibition of the HER2 tyrosine kinase.** *Proc Natl Acad Sci U S A* 2011, **108:**5021–5026.

22. Huang C, Park CC, Hilsenbeck SG, Ward R, Rimawi MF, Wang YC, Shou J, Bissell MJ, Osborne CK, Schiff R: **β1 integrin mediates an alternative survival pathway in breast cancer cells resistant to lapatinib.** *Breast Cancer Res* 2011, **13:**R84.

23. Martin AP, Miller A, Emad L, Rahmani M, Walker T, Mitchell C, Hagan MP, Park MA, Yacoub A, Fisher PB, Grant S, Dent P: **Lapatinib resistance in HCT116 cells is mediated by elevated MCL-1 expression and decreased BAK activation and not by ERBB receptor kinase mutation.** *Mol Pharmacol* 2008, **74:**807–822.

24. Shah NP, Nicoll JM, Nagar B, Gorre ME, Paquette RL, Kuriyan J, Sawyers CL: **Multiple BCR-ABL kinase domain mutations confer polyclonal resistance to the tyrosine kinase inhibitor imatinib (STI571) in chronic phase and blast crisis chronic myeloid leukemia.** *Cancer Cell* 2002, **2:**117–125.

25. Pao W, Miller VA, Politi KA, Riely GJ, Somwar R, Zakowski MF, Kris MG, Varmus H: **Acquired resistance of lung adenocarcinomas to gefitinib or erlotinib is associated with a second mutation in the EGFR kinase domain.** *PLoS Med* 2005, **2:**225–235.

26. Xia W, Husain I, Liu L, Bacus S, Saini S, Spohn J, Pry K, Westlund R, Stein SH, Spector NL: **Lapatinib antitumor activity is not dependent upon phosphatase and tensin homologue deleted on chromosome 10 in ErbB2-overexpressing breast cancers.** *Cancer Res* 2007, **67:**1170–1175.

27. Dave B, Migliaccio I, Gutierrez MC, Wu MF, Chamness GC, Wong H, Narasanna A, Chakrabarty A, Hilsenbeck SG, Huang J, Rimawi M, Schiff R, Arteaga C, Osborne CK, Chang JC: **Loss of phosphatase and tensin homolog or phosphoinositol-3 kinase activation and response to trastuzumab or lapatinib in human epidermal growth factor receptor 2-overexpressing locally advanced breast cancers.** *J Clin Oncol* 2011, **29:**166–173.

28. O'Brien NA, Browne BC, Chow L, Wang Y, Ginther C, Arboleda J, Duffy MJ, Crown J, O'Donovan N, Slamon DJ: **Activated phosphoinositide 3-kinase/AKT signaling confers resistance to trastuzumab but not lapatinib.** *Mol Cancer Ther* 2010, **9:**1489–1502.

29. Wulfkuhle JD, Speer R, Pierobon M, Laird J, Espina V, Deng J, Mammano E, Yang SX, Swain SM, Nitti D, Esserman LJ, Belluco C, Liotta LA, Petricoin EF 3rd: **Multiplexed cell signaling analysis of human breast cancer: applications for personalized therapy.** *J Prot Res* 2008, **7:**1508–1517.

30. Cheng Q, Chang JT, Geradts J, Neckers LM, Haystead T, Spector NL, Lyerly HK: **Amplification and high-level expression of heat shock protein 90 marks aggressive phenotypes of human epidermal growth factor receptor 2 negative breast cancer.** *Breast Cancer Res* 2012, **14R:**62.

31. Xia W, Bisi J, Strum J, Liu L, Carrick K, Graham KM, Treece AL, Hardwicke MA, Dush M, Liao Q, Westlund RE, Zhao S, Bacus S, Spector NL: **Regulation of survivin by ErbB2 signaling: Therapeutic implications for ErbB2-overexpressing breast cancers.** *Cancer Res* 2006, **66:**1640–1647.

32. Wang YC, Morrison G, Gillihan R, Guo J, Ward RM, Fu X, Botero MF, Healy NA, Hilsenbeck SG, Phillips GL, Chamness GC, Rimawi MF, Osborne CK, Schiff R: **Different mechanisms for resistance to trastuzumab versus lapatinib in HER2-positive breast cancers–role of estrogen receptor and HER2 reactivation.** *Breast Cancer Res* 2011, **13:**R121.

33. Samuels Y, Wang Z, Bardelli A, Silliman N, Ptak J, Szabo S, Yan H, Gazdar A, Powell SM, Riggins GJ, Willson JK, Markowitz S, Kinzler KW, Vogelstein B, Velculescu VE: **High Frequency of Mutations of the *PIK3CA* Gene in Human Cancers.** *Science* 2004, **304:**554.

34. Lu Y, Lin YZ, LaPushin R, Cuevas B, Fang X, Yu SX, Davies MA, Khan H, Furui T, Mao M, Zinner R, Hung MC, Steck P, Siminovitch K, Mills GB: **The PTEN/MMAC1/TEP tumor suppressor gene decreases cell growth and induces apoptosis and anoikis in breast cancer cells.** *Oncogene* 1999, **18:**7034–7045.

35. Mueller KL, Hunter LA, Ethier SP, Boerner JL: **Met and c-src cooperate to compensate for loss of epidermal growth factor receptor kinase activity in breast cancer cells.** *Cancer Res* 2008, **68:**3314–3322.

36. Engelman JA, Zejnullahu K, Mitsudomi T, Song Y, Hyland C, Park JO, Lindeman N, Gale CM, Zhao X, Christensen J, Kosaka T, Holmes AJ, Rogers AM, Cappuzzo F, Mok T, Lee C, Johnson BE, Cantley LC, Jänne PA: *MET* **amplification leads to Gefitinib resistance in lung cancer by activating ERBB3 signaling.** *Science* 2007, **316:**1039–1043.

37. Gao T, Furnari F, Newton AC: **PHLPP: a phosphatase that directly dephosphorylates Akt, promotes apoptosis, and suppresses tumor growth.** *Mol Cell* 2005, **18:**13–24.

38. Liu J, Stevens PT, Gao T: **mTOR-dependent regulation of PHLPP expression controls the rapamycin sensitivity in cancer cells.** *J Biol Chem* 2005, **286:**6510–6520.

39. Maira S-M, Maira SM, Stauffer F, Brueggen J, Furet P, Schnell C, Fritsch C, Brachmann S, Chène P, De Pover A, Schoemaker K, Fabbro D, Gabriel D, Simonen M, Murphy L, Finan P, Sellers W, García-Echeverría C: **Identification and characterization of NVP-BEZ235, a new orally available dual phosphatidylinositol 3-kinase/mammalian target of rapamycin inhibitor with potent in vivo antitumor activity.** *Mol Cancer Ther* 2008, **7:**1851–1863.

40. Lynch TJ, Bell DW, Sordella R, Gurubhagavatula S, Okimoto RA, Brannigan BW, Harris PL, Haserlat SM, Supko JG, Haluska FG, Louis DN, Christiani DC, Settleman J, Haber DA: **Activating mutations in the epidermal growth factor receptor underlying responsiveness of non-small-cell lung cancer to gefitinib.** *N Engl J Med* 2004, **350:**2129–2139.

41. Paez JG, Jänne PA, Lee JC, Tracy S, Greulich H, Gabriel S, Herman P, Kaye FJ, Lindeman N, Boggon TJ, Naoki K, Sasaki H, Fujii Y, Eck MJ, Sellers WR, Johnson BE, Meyerson M: **EGFR mutations in lung cancer: correlation with clinical response to gefitinib therapy.** *Science* 2004, **304:**1497–1500.

42. Herbst RS, Bunn PA Jr: **Targeting the epidermal growth factor receptor in non-small cell lung cancer.** *Clin Cancer Res* 2003, **9:**5813–5824.

43. Rabindran SK, Discafani CM, Rosfjord EC, Baxter M, Floyd MB, Golas J, Hallet WA, Johnson BD, Nilakantan R, Overbeek E, Reich MF, Shen R, Shi X, Tsou HR, Wang WF, Wissner A: **Antitumor activity of HKI-272, an orally active, irreversible inhibitor of the HER-2 tyrosine kinase.** *Cancer Res* 2004, **64:**3958–3965.

44. Xia W, Mullin R, Keith B, Liu L-H, Alligood K, Ma H, Rusnak DW, Spector NL: **Anti-tumor activity of GW2016, a dual tyrosine kinase inhibitor blocks EGF activation of EGFR/erbB2 and downstream Erk1/2 and AKT pathways.** *Oncogene* 2002, **21:**6255–6263.

45. Xia W, Liu LH, Ho P, Spector NL: **Truncated ErbB2 receptor (p95ErbB2) is regulated by heregulin through heterodimer formation with ErbB3 yet remains sensitive to the dual EGFR/ErbB2 kinase inhibitor GW572016.** *Oncogene* 2004, **23:**646–653.

46. Wilson TR, Fridlyand J, Yan Y, Penuel E, Burton L, Chan E, Peng J, Lin E, Wang Y, Sosman J, Ribas A, Li J, Moffat J, Sutherlin DP, Koeppen H, Merchant M, Neve R, Settleman J: **Widespread potential for growth-factor-driven resistance to anticancer kinase inhibitors.** *Nature* 2012, **487:**505–509.

47. Aguilar Z, Slamon DJ: **The transmembrane heregulin precursor is functionally active.** *J Biol Chem* 2001, **276:**44099–44107.

48. Horiuchi K, Zhou HM, Kelly K, Manova K, Blobel CP: **Evaluation of the contributions of ADAMs 9, 12, 15, 17, and 19 to heart development and ectodomain shedding of neuregulins beta1 and beta2.** *Dev Biol* 2005, **283:**459–471.

49. Gijsen M, King P, Perera T, Parker PJ, Harris AL, Larijani B, Kong A: **HER2 phosphorylation is maintained by a PKB negative feedback loop in response to anti-HER2 herceptin in breast cancer.** *PLoS Biol* 2010, **8:**e1000563.

50. Kitano H: **Towards a theory of Biological Robustness.** *Mol Syst Biol* 2007, **3:**1–7.

51. Konecny GE, Pegram MD, Venkatesan N, Finn R, Yang G, Rahmeh M, Untch M, Rusnak DW, Spehar G, Mullin RJ, Keith BR, Gilmer TM, Berger M, Podratz KC, Slamon DJ: **Activity of the dual kinase inhibitor lapatinib (GW572016) against HER-2-overexpressing and trastuzumab-treated breast cancer cells.** *Cancer Res* 2006, **66:**1630–1639.

52. Montero JC, Rodríguez-Barrueco R, Ocaña A, Díaz-Rodríguez E, Esparís-Ogando A, Pandiella A: **Neuregulins and cancer.** *Clin Cancer Res* 2008, **14:**3237–3241.

53. Wilson TR, Lee DY, Berry L, Shames DS, Settleman J: **Neuregulin-1-mediated autocrine signaling underlies sensitivity to HER2 kinase inhibitors in a subset of human cancers.** *Cancer Cell* 2011, **20:**158–172.

54. Fabian MA, Biggs WH 3rd, Treiber DK, Atteridge CE, Azimioara MD, Benedetti MG, Carter TA, Ciceri P, Edeen PT, Floyd M, Ford JM, Galvin M, Gerlach JL, Grotzfeld RM, Herrgard S, Insko DE, Insko MA, Lai AG, Lélias JM, Mehta SA, Milanov ZV, Velasco AM, Wodicka LM, Patel HK, Zarrinkar PP, Lockhart DJ: **A small molecule–kinase interaction map for clinical kinase inhibitors A small molecule–kinase interaction map for clinical kinase inhibitors.** *Nat Biotechnol* 2005, **23:**329–336.

55. Xia W, Bacus S, Husain I, Liu L, Zhao S, Liu Z, Moseley MA III, Thompson JW, Chen KL, Koch KM, Spector NL: **Resistance to ErbB2 tyrosine kinase inhibitors in breast cancer is mediated by calcium-dependent activation of RelA.** *Mol Cancer Ther* 2010, **9:**292–299.

56. Kurokawa M, Kim J, Geradts J, Mastuura K, Liu L, Xia W, Ribar TJ, Dewhirst MW, Kim W-J, Lucas JE, Wang S, Spector NL, Kornbluth S: **A network of substrastes of the E3 ubiquitin ligases MDM2 and HUWE1 control apoptosis independently of p53.** *Sci Signal* 2013, **6:**ra32.

57. Escher P, Lacazette E, Courtet M, Blindenbacher A, Landmann L, Bezakova G, Lloyd KC, Mueller U, Brenner HR: **Synapses form in skeletal muscles lacking neuregulin receptors.** *Science* 2005, **308:**1920–1923.

Additional files

Additional_file_1 as ZIP
Additional file 1 List of Antibodies used in the RPMA analysis.

Additional_file_2 as JPEG
Additional file 2 Lapatinib resistant cells remain viable in concentrations of lapatinib lethal to parental cells. Cell growth and viability in parental cells (BT474; SKBR3) treated with 1 μM lapatinib for 72 hours, compared with resistant cells (rBT474; rSKBR3) continuously cultured in the presence of 1 μM lapatinib. Parental cells treated with vehicle alone (0.01% DMSO) served as controls. Results represent the mean +/- standard error of triplicate samples, and are representative of three independent experiments.
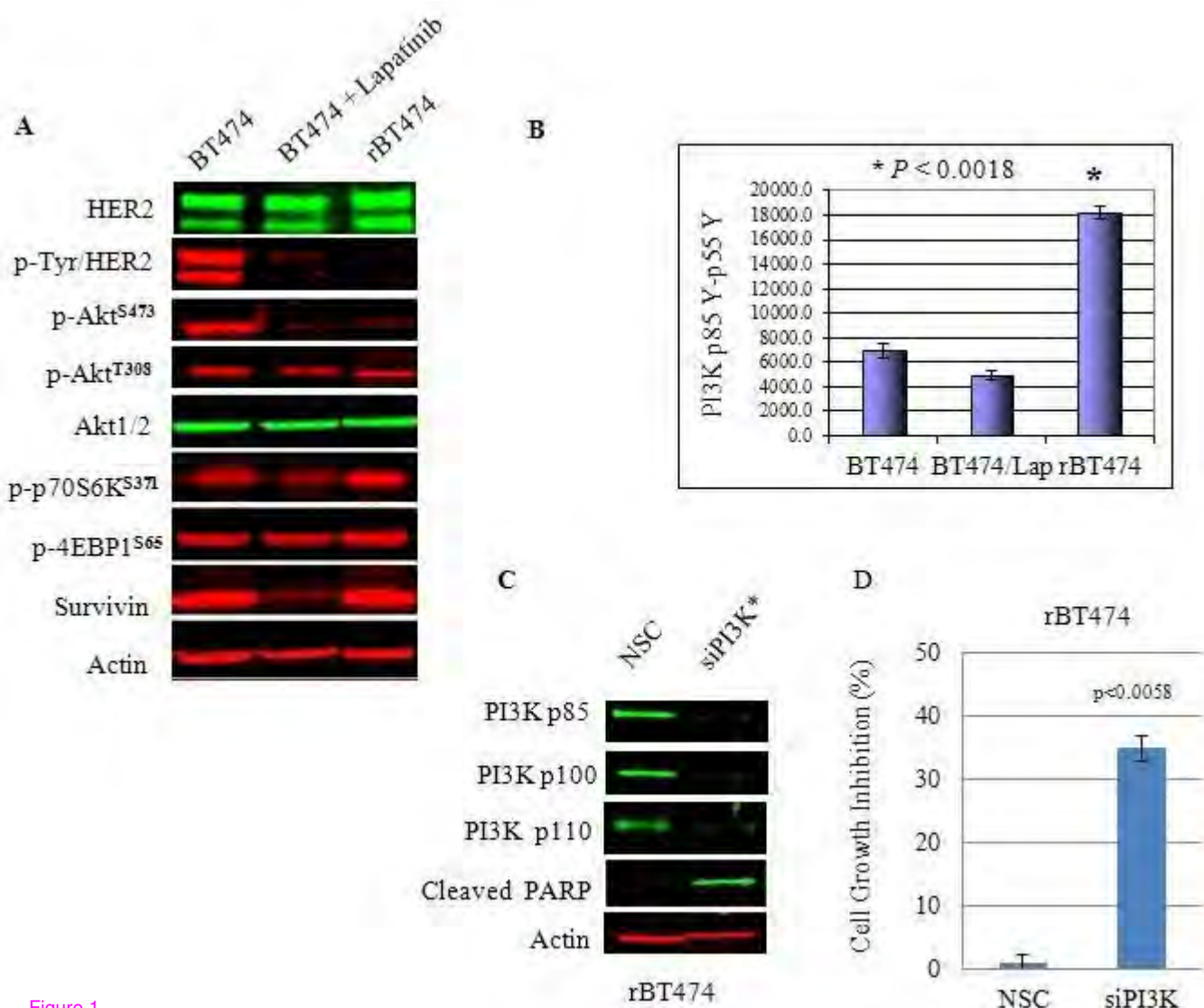
Additional_file_3 as JPEG

Additional file 3 Persistent PI3K signaling in lapatinib resistant cells. Reverse phase protein microarray analysis of the indicated phosphorylated proteins using the indicated phosphotyrosine specific antibodies. Results represent the mean +/- standard error of triplicate samples, and are representative of three independent experiments.

Additional_file_4 as JPEG

Additional file 4 Inhibition of c-src does not reverse lapatinib resistance. Treatment of rBT474 and rSKBR3 with a specific src inhibitor (AZD0530) had relatively little effect on cell growth. Top panels show the activation of Src in rBT474 and rSKBR3 compared with parental cells following treatment with 1 μM lapatinib for 24 hours as demonstrated by Western blotting using a phosphospecific antibody to src^{Y416}. Actin steady-state protein served as a control for equal loading of protein. The middle panels demonstrate inhibition of src^{Y416} by a specific src kinase inhibitor AZD0530 used at 10 μM for 72 hours, and the lower bar graph shows the effects of AZD0530 on the growth of rBT474 and rSKBR3 cells. Resistant cells were maintained in the presence of 1 μM lapatinib. Results represent the mean +/- standard error of triplicate samples, and are representative of three independent experiments.

Additional_file_5 as JPEG

Additional file 5 Inhibition of c-met does not reverse lapatinib resistance. rBT474 and rSKBR3 cells were treated with a selective c-met inhibitor, SU11274 at 10 μM for 72 hours and then analyzed for cell viability and proliferation. Resistant cells were maintained in the presence of 1 μM lapatinib. Results represent the mean +/- standard error of triplicate samples, and are representative of three independent experiments.

Additional_file_6 as JPEG

Additional file 6 EGFR knockdown and inhibition of PI3K/mTOR signaling block PHLPPL2 protein expression. (**A**) The effects of EGFR knockdown on steady-state levels of the indicated proteins/phosphoproteins was determined using specific primary antibodies (see Methods). The absolute optical density (OD) values attributed to the PHLPPL2 protein-determined using the Odyssey Infrared Imaging System-are indicated under each corresponding lane. (**B**) Inhibition of PI3K/mTOR signaling blocks PHLPPL2 protein expression. The effects of 0.2 μM NVP-BEZ 235 for 48 hours on the expression of PHLPPL2 protein in rBT474 and rSKBR3 cells as determined by Western blot. Actin protein levels served as a control to ensure for equal loading of protein. Resistant cells were maintained in the presence of 1 μM lapatinib. Parental cells (BT474; SKBR3) were treated with 1 μM lapatinib for 24 hours. Results are representative of three independent experiments.

Additional_file_7 as JPEG

Additional file 7 Sensitivity of parental HER2+ breast cancer cells line to neratinib. Parental BT474 and SKBR3 were treated with neratinib at the indicated concentrations (0.1; 0.5; 1; 5 μM) for 72 hours, and then growth and viability was determined. Results represent the mean +/- standard error of triplicate samples, and are representative of three independent experiments

Additional_file_8 as JPEG
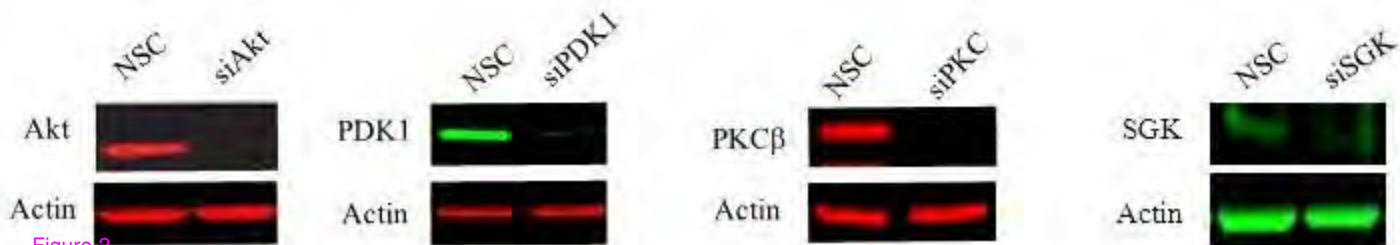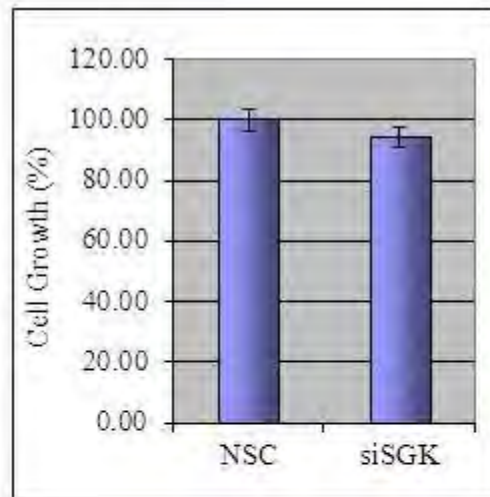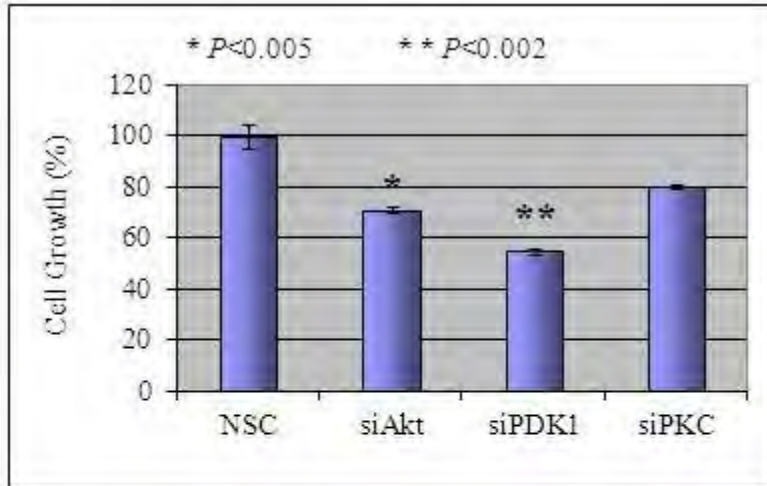
Additional file 8 HRG reverses the antitumor effects of lapatinib, but not neratinib in parental HER2+ breast cancer cells. Cell growth and viability was assessed in parental BT474 cells treated with 1 μM lapatinib or neratinib in the presence or absence of HRG (50 ng/ml) for 72 hours. Cells treated with vehicle alone (0.01% DMSO) served as controls. Results represent the mean +/- standard error of triplicate samples, and are representative of three independent experiments.

A

	BT474	BT474 + Lapatinib	rBT474
HER2			
p-Tyr/HER2			
p-Akt^{S473}			
p-Akt^{T308}			
Akt1/2			
p-p70S6K^{S371}			
p-4EBP1^{S65}			
Survivin			
Actin			

B

$* P < 0.0018$

PI3K p85 Y-p55 Y

BT474   BT474/Lap   rBT474

C

rBT474

	NSC	siPI3K*
PI3K p85		
PI3K p100		
PI3K p110		
Cleaved PARP		
Actin		

rBT474

D

rBT474

Cell Growth Inhibition (%)

$p < 0.0058$

NSC   siPI3K

Figure 1

Figure 2

A

	rSKBR3			rBT474		
p-HER3^{Y1197}						
Actin						
siRNA	NSC	EGFR	HER3	NSC	EGFR	HER3
p-HER3 OD	1.01	0.65	0.39	0.80	0.55	0.20

B

	rBT474		rSKBR3	
HER3				
p-EGFR^{Y992}				
p-PI3K-p85^{Y508}				
Actin				
siRNA	NSC	HER3	NSC	HER3

C

	rBT474		rSKBR3	
Cleaved PARP				
Actin				
siRNA	NSC	HER3	NSC	HER3

D

rSKBR3 — Cell Growth Inhibition (%): NSC, siHER3, p<0.013

rBT474 — p<0.017

Figure 3

Figure 4

A

	rBT474	rSKBR3
p- EGFR^{Y992}		
p-PI3K-p85^{Y508}		
p-Akt^{T308}		
Akt		
Actin		
siRNA	NSC EGFR	NSC EGFR

B

Cleaved PARP — rBT474, rSKBR3
Actin
siRNA   NSC   EGFR   NSC   EGFR

C

rBT474 — Cell Growth Inhibition (%), p<0.018, NSC, siEGFR
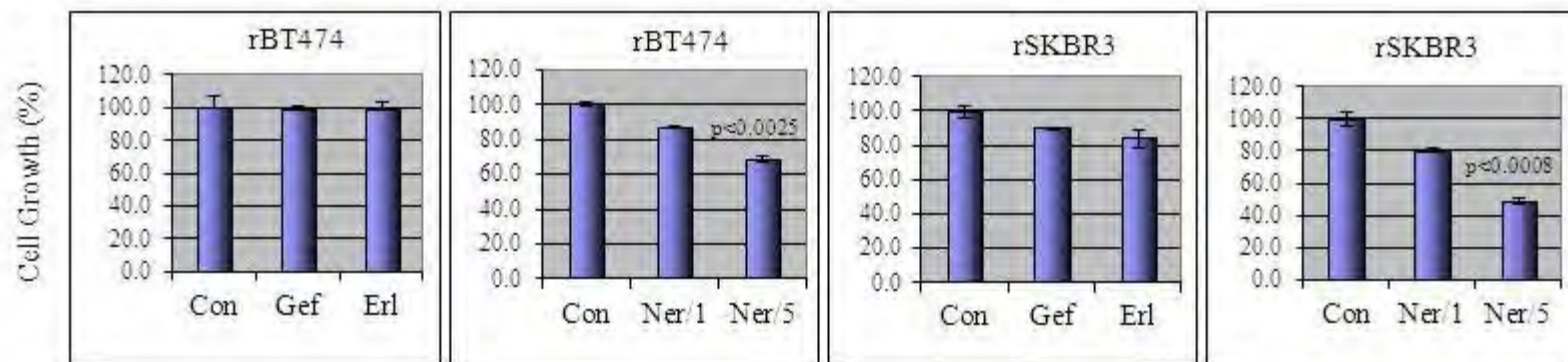
rSKBR3 — p<0.021, NSC, siEGFR

Figure 5

Figure 6

Figure 7

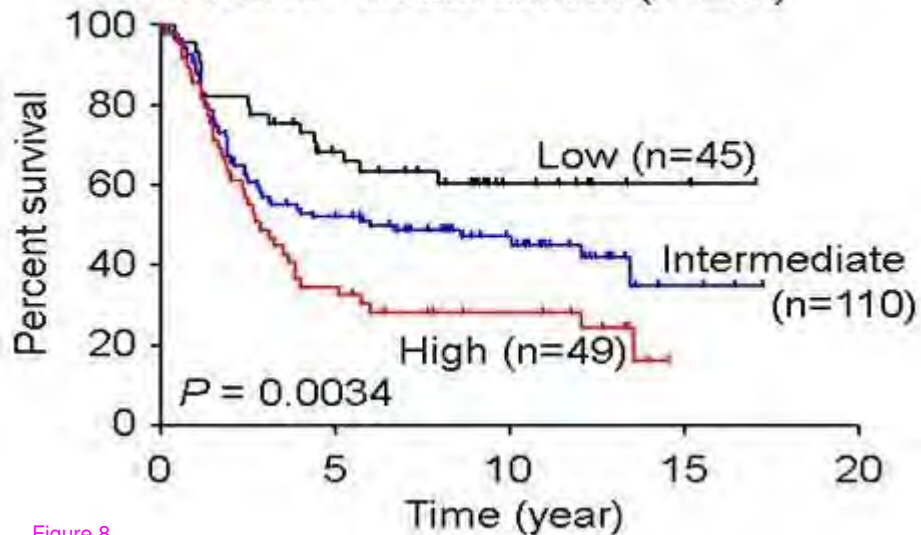Recurrence-free survival of HRG in HER2+ breast cancer (n=204)

Low (n=45)

Intermediate (n=110)

High (n=49)

$P = 0.0034$

Figure 8

Additional files provided with this submission:

Additional file 1: 1077757776849634_add1.zip, 310K
http://breast-cancer-research.com/imedia/1960922115105812/supp1.zip
Additional file 2: 1077757776849634_add2.jpeg, 46K
http://breast-cancer-research.com/imedia/1384991013105812/supp2.jpeg
Additional file 3: 1077757776849634_add3.jpeg, 44K
http://breast-cancer-research.com/imedia/7027561821058123/supp3.jpeg
Additional file 4: 1077757776849634_add4.jpeg, 40K
http://breast-cancer-research.com/imedia/1566400803105812/supp4.jpeg
Additional file 5: 1077757776849634_add5.jpeg, 27K
http://breast-cancer-research.com/imedia/2242786571058123/supp5.jpeg
Additional file 6: 1077757776849634_add6.jpeg, 32K
http://breast-cancer-research.com/imedia/3275603010581234/supp6.jpeg
Additional file 7: 1077757776849634_add7.jpeg, 32K
http://breast-cancer-research.com/imedia/9298413391058123/supp7.jpeg
Additional file 8: 1077757776849634_add8.jpeg, 29K
http://breast-cancer-research.com/imedia/2133926987105812/supp8.jpeg

Breast Cancer
R E S E A R C H

Polyclonal HER2-specific antibodies induced by vaccination mediate receptor internalization and degradation in tumor cells

Xiu-Rong Ren[1], Junping Wei[2], Gangjun Lei[2], Jiangbo Wang[1], Jiuyi Lu[1], Wenle Xia[3], Neil Spector[2,3], Larry S Barak[4], Timothy M Clay[5], Takuya Osada[2], Erika Hamilton[6], Kimberly Blackwell[6], Amy C Hobeika[2], Michael A Morse[2,3], H Kim Lyerly[2,7*] and Wei Chen[1,2*]

Abstract

Introduction: Sustained HER2 signaling at the cell surface is an oncogenic mechanism in a significant proportion of breast cancers. While clinically effective therapies targeting HER2 such as mAbs and tyrosine kinase inhibitors exist, tumors overexpressing HER2 eventually progress despite treatment. Thus, abrogation of persistent HER2 expression at the plasma membrane to synergize with current approaches may represent a novel therapeutic strategy.

Methods: We generated polyclonal anti-HER2 antibodies (HER2-VIA) by vaccinating mice with an adenovirus expressing human HER2, and assessed their signaling effects *in vitro* and anti-tumor effects in a xenograft model. In addition, we studied the signaling effects of human HER2-specific antibodies induced by vaccinating breast cancer patients with a HER2 protein vaccine.

Results: HER2-VIA bound HER2 at the plasma membrane, initially activating the downstream kinases extracellular signal-regulated protein kinase 1/2 and Akt, but subsequently inducing receptor internalization in clathrin-coated pits in a HER2 kinase-independent manner, followed by ubiquitination and degradation of HER2 into a 130 kDa fragment phosphorylated at tyrosine residues 1,221/1,222 and 1,248. Following vaccination of breast cancer patients with the HER2 protein vaccine, HER2-specific antibodies were detectable and these antibodies bound to cell surface-expressed HER2 and inhibited HER2 signaling through blocking tyrosine 877 phosphorylation of HER2. In contrast to the murine antibodies, human anti-HER2 antibodies induced by protein vaccination did not mediate receptor internalization and degradation.

Conclusion: These data provide new insight into HER2 trafficking at the plasma membrane and the changes induced by polyclonal HER2-specific antibodies. The reduction of HER2 membrane expression and HER2 signaling by polyclonal antibodies induced by adenoviral HER2 vaccines supports human clinical trials with this strategy for those breast cancer patients with HER2 therapy-resistant disease.

Introduction

Breast cancers overexpressing HER2 have an aggressive clinical course. Despite the proven effectiveness of the HER2-specific mAb trastuzumab (Herceptin) and the dual epidermal growth factor receptor (EGFR) and HER2

receptor tyrosine kinase inhibitor lapatinib (Tykerb), disease progression and the rate of cancer-related deaths remain unacceptably high. HER2 remains overexpressed on cells that develop resistance to either anti-HER2 mAbs or tyrosine kinase inhibitor, which may be partly responsible for these failures in therapy, because additional blockade by combining trastuzumab and lapatinib provides clinical benefit [1,2]. Recent preclinical and clinical studies using novel mAbs that prevent HER2 and HER3 dimerization also appear to be effective, suggesting

* Correspondence: lyerl001@mc.duke.edu; w.chen@duke.edu
[1]Department of Medicine, Duke University Medical Center, 595 Lasalle Street, Durham, NC 27710, USA
[2]Duke Comprehensive Cancer Center, Duke University Medical Center, 203 Research Drive, Durham, NC 27710, USA
Full list of author information is available at the end of the article

that persistent HER2 signaling is a cause of treatment failure [3,4]. The depletion of HER2 from the surface of resistant tumors cells by novel agents may therefore provide a means for reducing tumor aggressiveness and improving patient survival.

HER2/neu together with HER1 (EGFR), HER3, and HER4 comprise the EGFR family of plasma membrane tyrosine kinases [5,6]. HER2, in contrast to the other three receptors, is an orphan with no recognized endogenous ligand; nevertheless, plasma membrane-localized HER2 signals as a consequence of intrinsic tyrosine kinase activity. The HER2 receptor forms homodimers as well as heterodimer pairs with HER1, HER3, or HER4 [7-9]. HER2/3 heterodimers are the most potent activators of the phosphatidylinositol-3-kinase (PI3K)-Akt cell survival pathway. The binding of the HER1 ligand epidermal growth factor (EGF) and the HER3 ligand neuregulin to extracellular domains of HER1 and HER3, respectively, leads to receptor activation and the formation of homodimers or heterodimers. The increased kinase activity of heterodimeric partners leads to the transactivation of HER2 and phosphorylation of tyrosine residues including tyrosines 1,221/1,222 and 1,248 in the cytosolic tail of HER2. These phosphotyrosine residues serve as docking sites for SH2-containing and PTB-containing adaptor proteins that link HERs to downstream intracellular signaling cascades, including Ras, extracellular signal-regulated protein (ERK) kinase, phospholipase C gamma, PI3K, Akt and signal transducer and activator of transcription (STAT3)3 pathways.

HER1 undergoes a rapid and pronounced EGF-induced internalization from the plasma membrane as part of a dynamic clathrin-directed trafficking process that plays a key role in regulating its membrane expression, intracellular signaling, and downregulation [10]. HER1 contains canonical motifs that, following its autophosphorylation, directly bind to clathrin and clathrin-associated adaptor proteins. While it has been reported that HER2 co-internalizes with HER1 [11], internalization of HER2 alone from a population of HER2 homodimers has not been observed, even though HER2 contains intracellular motifs that are localized similarly to those present in HER1 [12].

In this report we show that, in comparison with the mAb trastuzumab, exposure of cell-surface HER2 to polyclonal anti-HER2 antibody generated in mice promotes rapid receptor internalization and degradation, accompanied by phosphorylation of the downstream kinasesERK1/2 and Akt. Prolonged exposure to the polyclonal anti-HER2 antibody is characterized by significant HER2 internalization, ubiquitination and degradation, a dramatic reduction in plasma membrane HER2 expression and signaling, and profound anti-tumor activity *in vitro* and *in vivo*. As we reported before, the polyclonal anti-HER2 antibody had a synergistic effect with small-molecule

HER2 kinase inhibitors [13]. In addition to antibodies induced by potent adenoviral vectors, we studied HER2-specific antibodies induced by a HER2 protein vaccine being tested in clinical trials in breast cancer patients. The HER2-specific antibodies were detected in the serum of vaccinated patients. These human anti-HER2-specific antibodies were capable of binding to surface expressed HER2 and inhibiting HER2 phosphorylation but did not mediate receptor internalization.

Materials and methods
Reagents and antibodies
Vaccine-induced anti-HER2 antibodies (HER2-VIA), LacZ-VIA and GFP-VIA were generated as previously described [13]. Briefly, pooled serum from a large quantity of mice was purified using saturated ammonium sulfate buffer and the concentration of total serum proteins in stock for all of the studies was measured and adjusted to 20 mg/ml in saline.

Trastuzumab was obtained from the Duke University Medical Center Pharmacy (Durham, NC, USA). Neuregulin was purchased from R&D systems (Minneapolis, MN, USA). Mouse and rabbit IgG beads were from eBioscience (San Diego, CA, USA). HER2 antibody 3B5 and ubiquitin antibodies were from Santa Cruz Biotechnology (Santa Cruz, CA, USA). HER2 (29D8), HER3, Akt, pAkt, and surviving antibodies were from Cell Signaling (Beverly, MA, USA). Phospho-specific HER2 antibodies (Y877, Y1221/1222 and Y1248) were also purchased from Cell Signaling. These antibodies were used at 1:500 dilutions in western blotting.

Lamin B1 rabbit antibody was from Abcam (Cambridge, MA, USA). EZ-Link™ Sulfo-NHS-SS Biotin and Streptavidin beads were from Pierce (Rockford, IL, USA). β-actin, *N*-ethylmaleimide, and MG132 were purchased from Sigma (St Louis, MO, USA). Lapatinib was obtained from the Duke University Medical Center Pharmacy.

Treatment of established HER2-positive human tumor xenografts by passive transfer of vaccine-induced antibodies
These studies were performed under a protocol approved by the Duke University Institutional Animal Care and Use Committee (IACUC) (Durham, NC, USA). Eight-week-old to 10-week-old NOD.CB17-*Prkdc^{scid}*/J mice (Jackson Laboratories, Bar Harbor, ME, USA) were implanted with 17β-estradiol pellets (0.72 mg 60-day continuous release pellets; Innovative Research of American, Sarasota, FL, USA) in the flank 1 week prior to the implantation of 5 million BT474M1 tumor cells (kindly provided by Mien-Chie Hung, The University of Texas MD Anderson Cancer Center, Houston, TX, USA). Tumors were allowed to develop for 14 days and then mice were randomized to receive intravenous injection of

either GFP-VIA or HER2-VIA (five mice per group). Then 100 to 150 μl vaccine-induced antibodies were injected intravenously at 2-day to 3-day intervals for a total of 10 administrations. Tumor growth was measured in two dimensions using calipers, and the tumor volume was determined using the formula:

$$\text{Volume} = \text{width}^2 \times \text{length}$$

The study was terminated on day 39.

Flow cytometry analysis

We adapted a methodology reported by Piechocki and colleagues to measure HER2-VIA in vaccinated mouse serum by flow cytometry [14]. Briefly, 3×10^5 HCC1569 cells were incubated with a mouse anti-human-HER2 mAb or isotype control (Becton Dickinson, San Jose, CA, USA) or with diluted (1:200) mouse serum antibodies (HER2-VIA or LacZ-VIA) for 1 hour at 4°C and then washed with 1% BSA-PBS. The cells exposed to mouse serum containing vaccine-induced antibodies were further stained with phycoerythrin-conjugated anti-mouse IgG (catalogue number R0480; Dako (Carpinteria, CA, USA)) for 30 minutes at 4°C, and washed again. Samples were then analyzed on a Becton Dickinson LSRII flow cytometer with results represented as histograms.

Cell culture

HEK293 cells were grown at 37°C, 5% CO_2 in MEM supplemented with 10% fetal bovine serum (Atlanta Biologicals, Lawrenceville, GA, USA), 200 U/ml penicillin, and 50 ng/ml streptomycin (Invitrogen, Carlsbad, CA, USA). SK-BR-3 cells (American Type Culture Collection: HTB-30™) were grown at 37°C, 5% CO_2 in McCoy's 5A medium supplemented with 10% FCS, 200 U/ml penicillin, and 50 ng/ml streptomycin. HCC1569 cells (American Type Culture Collection: CRL-2330™) were grown at 37°C, 5% CO_2 in RPM-1640 medium also supplemented with 10% FCS, 1 mM sodium pyruvate, 10 mM Hepes, 0.25% glucose, 200 U/ml penicillin, and 50 ng/ml streptomycin. All cell lines were purchased from American Type Culture Collection (Manassas, VA, USA).

Construction of fluorescent HER2 construct

HER2-YFP was constructed using a LTR-2/erbB-2(HER2) construct (provided by Dr LE Samelson, NCI, Bethesda, MD, USA) as a PCR template and a pcDNA3.1-mYFP construct as a vector (gift from Roger Y Tsien, University of California at San Diego, USA). HER2 was PCR amplified using the primers 5'-CCCAAGCTTAGCACCATG-GAGCTGGCGGCC-3' and 5'-CCGCTCGAGCACTGG CACGTCCAGACCCAG-3', and was inserted into the vector by *Hind*III and *Xho*I restriction sites. HER2 cDNA was verified by sequencing.

Assay of HER2 endocytosis

Endocytosis of HER2 was assayed using cleavable biotin as described previously [15]. Briefly, SK-BR-3 cells were biotinylated with 1.5 mg/ml sulfo-NHS-SS-biotin (Pierce) in PBS with calcium and magnesium at 4°C for 1 hour. After washing with cold PBS three times, cells were incubated at 37°C for 1 hour in McCoy's 5A medium with or without antibodies (50 μg/ml) to allow endocytosis to occur. Cell-surface biotin was cleaved by incubation (twice, 15 minutes each) in the glutathione cleavage buffer (50 mM glutathione, 75 mM NaCl, 10 mM ethylene-diamine tetraacetic acid, 1% BSA, and 0.075 N NaOH). Cells were washed with PBS three times and scraped into the modified RIPA buffer (150 mM NaCl, 50 mM Tris-HCl, pH 7.5, 0.25% (w/v) deoxycholate, 1% NP-40, 5 mM sodium orthovanadate, 2 mM sodium fluoride, and a protease inhibitor cocktail). Cell lysates were incubated with streptavidin beads (Pierce) on a rocking platform overnight at 4°C. After washing, the beads were mixed with the sample buffer and biotinylated proteins were analyzed by immunoblotting using antibodies against HER2.

Western blotting

The protein samples were subjected to SDS-PAGE using 4-12% Novex® Tris-Glycine Gels (Invitrogen), transferred to nitrocellulose membranes (Bio-Rad Laboratories, Hercules, CA, USA) blocked with 5% nonfat milk powder in TBS-0.2% Tween-20 for 20 minutes, followed by incubation with primary antibodies and then horseradish peroxidase-conjugated secondary antibodies (Amersham Biosciences, Piscataway, NJ, USA). Imaging and quantification of bands were performed using Supersignal (Pierce Biotechnology, Rockford, IL, USA) and AlphaImager™ (Alpha Innotech, Santa Clara, CA, USA).

Microscopy

HEK293 cells plated on 35-mm, poly-D-lysine-coated, glass-bottom microwell dishes (MatTek Cultureware, Ashland, MA, USA) were allowed to grow for 24 hours and transfected (Fugene6; Roche, Indianapolis, IN, USA) with HER2-YFP construct. Twenty-four hours after transfections, the cells were incubated in culture medium for live cell imaging with 100 μg/ml HER2-VIA, LacZ-VIA, trastuzumab, 20 ng/ml neuregulin or 10 ng/ml EGF. SK-BR-3 and HCC1569 cells plated on the dishes were allowed to grow for 24 hours and were treated as above for the indicated time at 37°C before fixation in 4% paraformaldehyde. Fixed cells were permeabilized and blocked in buffer (5% BSA with 0.2% saponin in PBS) for 20 minutes at room temperature and washed in PBS. Where indicated, cells were incubated with primary antibody (rabbit monoclonal sc-13584; Santa Cruz) in blocking buffer for 1 hour at room temperature, washed, incubated with secondary

antibody (Alexa-594-conjugated goat anti-rabbit; Invitrogen) in blocking buffer for 60 minutes at room temperature, washed, and mounted with mounting medium (Vector Laboratories, Inc., Burlingame, CA, USA).

Live cells were studied at 37°C using a heated microscope stage. All slides were examined using a LSM 510-Meta confocal microscope (Carl Zeiss, Thornwood, NY, USA) equipped with 40 × and 100 × apochromat objectives. YFP was excited using a 488-nm argon laser line. Alexa fluorophores were excited at 543 nm using a NeHe laser. Images were processed using the LSM software Image Browser (Carl Zeiss).

Assay of HER2 degradation and ubiquitination
A total of 0.15 million SK-BR-3 cells or HCC1569 cells plated in six-well plates were allowed to grow for 24 hours in medium with 10% fetal bovine serum and incubated with 100 μg/ml HER2-VIA, LacZ-VIA and trastuzumab in serum-free medium for the indicated time. Cells were washed twice with PBS and lysed with 2 × SDS sample buffer, and the cell lysates were subjected to western blot analysis. For ubiquitination assays, the cells were cultured as described above and then treated with 10 μM MG132 in serum-free medium for 1 hour before incubation with 100 μg/ml HER2-VIA, LacZ-VIA and trastuzumab for the indicated time. After washing twice with PBS, the cells were collected into glycerol lysis buffer (50 mM Hepes, 250 mM NaCl, 0.5% NP40, 10% glycerol, 2 mM ethylenediamine tetraacetic acid) with 5 mM *N*-ethylmaleimide and incubated with 25 μl mouse and rabbit IgG beads for at least 1 hour. The cell lysate was then spun at 18,000 g for 10 minutes to remove the beads, and the supernatant was incubated overnight with 1 μl anti-HER2 antibody 29D8 (Cell Signaling). This was followed by addition of 25 μl rabbit IgG beads for another 2 hours, washing the mix three times with glycerol lysis buffer, and subsequent western blot analysis.

Patients and treatment/monitoring
The human clinical trial enrolled patients aged 18 or older with stage IV HER2-overexpressing (HER2 3+ or fluorescence *in situ* hybridization-positive) breast cancer who had documented disease progression or relapse following at least one prior standard therapy containing trastuzumab [16]. These patients were immunized with dHER2, a recombinant protein consisting of the extracellular domain and a portion of the intracellular domain of HER2 combined with the adjuvant AS15, containing MPL, QS21, CpG and liposome. Lapatinib (1,250 mg/day) was administered concurrently. Serum was collected at various times pre and post immunization and antibodies were purified from the serum using ammonium sulfate precipitation.

Statistical analysis
A mixed-effects model was fit to fold-change measurements, with a regression model used to describe the tumor volume by treatment over time. Treatment and mouse were considered categorical variables. Day was considered a continuous variable. Day-squared and the day×treatment and day-squared×treatment interactions were also considered. Treatment and day were considered as fixed effects, and volume measurements for each mouse were considered as repeated measures within treatment. Tumor volume was measured on days 8, 10, 12, 14, 16, 18, and 20 post inoculation. Covariance was modeled as autoregressive. The likelihood ratio test was highly significant ($\chi^2 = 28.27$ with 2 degrees of freedom; $P <0.01$), such that one concludes there is a sharp treatment difference in tumor growth over time.
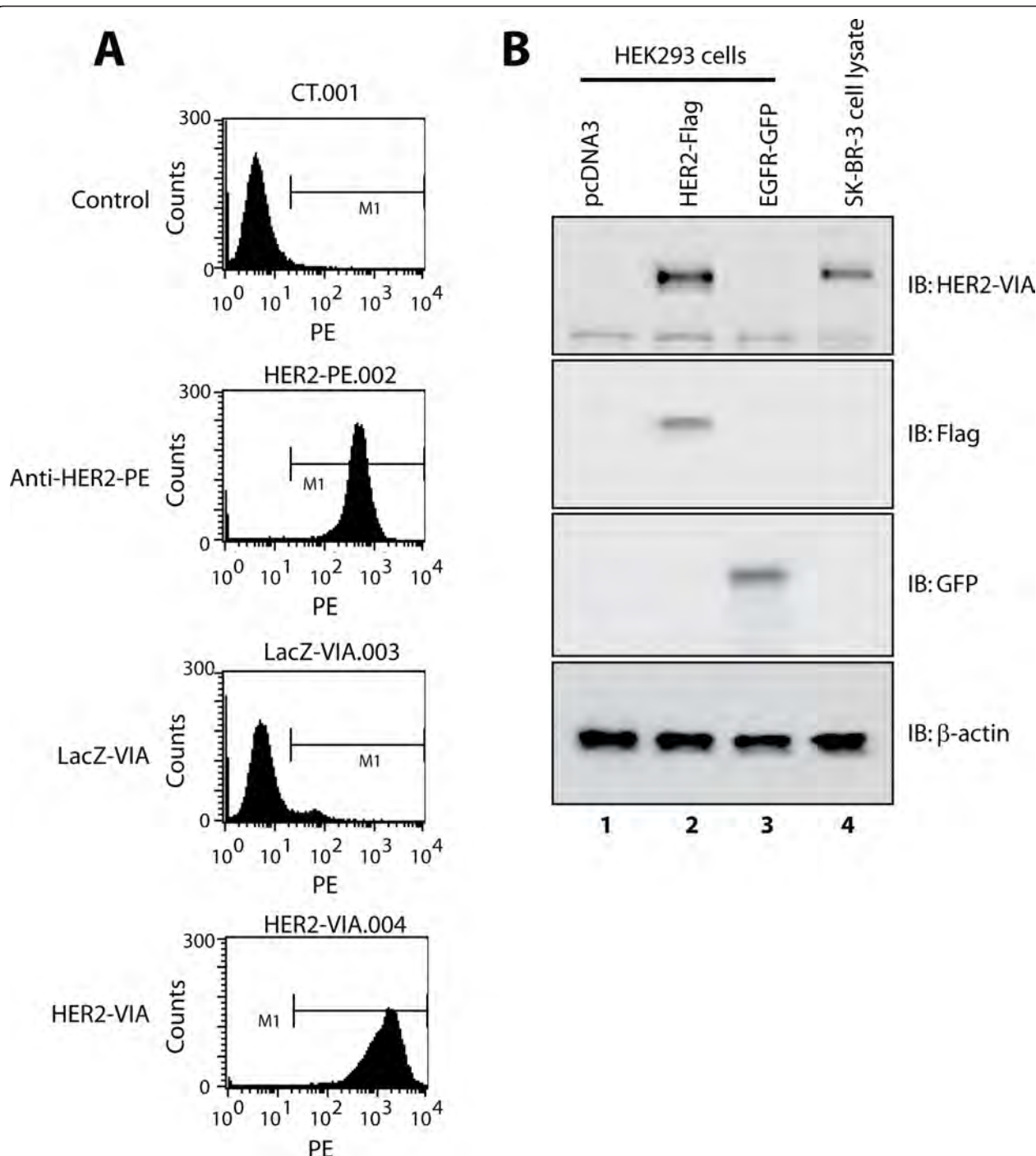
Results
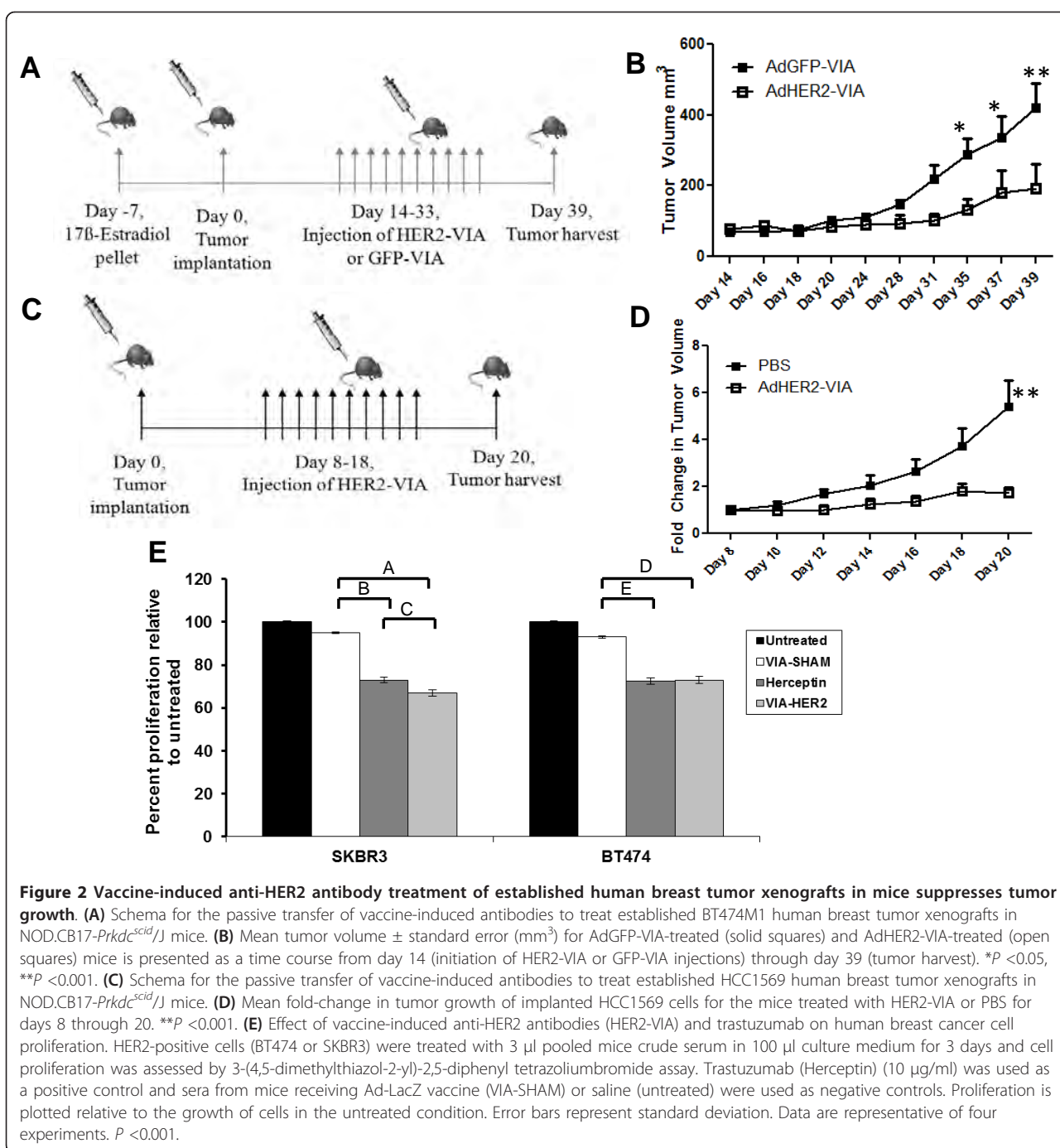### Generation of HER2-VIA antibodies against HER2
We developed adenovirus vectors encoding human HER2/neu with a kinase-inactivating mutation in order to ablate oncogenicity (K753A) [17-21]. The recombinant adenoviruses expressing HER2 were then injected into C57BL/6 mice for anti-HER2 antibody generation. The resulting HER2-VIA were assessed for activity against the extracellular portion of the receptor by flow cytometry, and significant affinity for HER2 at the cell surface was observed (Figure 1A). Based on the flow cytometric assessment of the relative affinity of HER2-VIA compared with trastuzumab in SK-BR-3 cells, we calculated that HER2-VIA-containing crude serum at ~30 μg/ml concentration had the same binding capacity for HER2 as trastuzumab at 1 μg/ml concentration (see Additional file 1). Since the concentration of specific antibodies in crude serum is usually less than 1% of total serum proteins, the affinity of HER2-VIA for HER2 is similar to, if not higher than, that of trastuzumab. Furthermore, overexpressed HER2 or endogenous HER2 protein in SK-BR-3 cells, but not EGFR protein in HEK293 cells, can be detected by HER2-VIA using western blotting, demonstrating the specificity of HER2-VIA for HER2 recognition (Figure 1B).

Anti-tumor effects of HER2-VIA
We found that passive immunotherapy with HER2-VIA retards the growth of established HER2-positive human tumor xenografts of BT474M1 cells *in vivo*. Starting at day 21 post inoculation, the average tumor volume in the HER2-VIA-treated group was significantly reduced when compared with mice treated with control GFP-VIA (Figure 2A,B). We also wanted to test the effect of HER2-VIA on tumors expressing HER2 but resistant to trastuzumab and lapatinib. HCC1569 cells are highly resistant to trastuzumab and lapatinib treatment *in*

Figure 1 Characterization of vaccine-induced anti-HER2 antibodies by flow cytometry and western blot analysis. **(A)** Recognition of cell-surface HER2 by vaccine-induced anti-HER2 antibodies (HER2-VIA). HCC1569 cells were incubated with a mouse anti-human-HER2 mAb (HER2-phycoerythrin (PE)) or isotype control (Becton Dickinson (BD), San Jose, CA, USA), or with diluted (1:200) mouse serum antibodies (HER2-VIA or LacZ-VIA) for 1 hour at 4°C. Samples were then analyzed by BD LSRII flow cytometry, with results represented as histograms. **(B)** Recognition of total HER2 but not epidermal growth factor receptor (EGFR)-GFP by HER2-VIA. HER293 cells expressing vector (lane 1), HER2-FLAG (lane 2) or EGFR-GFP (lane 3) as well as SK-BR-3 cells lysates were western blotted with HER2-VIA (top panel), anti-FLAG antibody (upper middle panel), and anti-GFP antibody (lower middle panel). β-actin was used as a loading control (bottom panel). IB, immunoblot.

Figure 2 Vaccine-induced anti-HER2 antibody treatment of established human breast tumor xenografts in mice suppresses tumor growth. **(A)** Schema for the passive transfer of vaccine-induced antibodies to treat established BT474M1 human breast tumor xenografts in NOD.CB17-*Prkdc^scid^*/J mice. **(B)** Mean tumor volume ± standard error (mm^3) for AdGFP-VIA-treated (solid squares) and AdHER2-VIA-treated (open squares) mice is presented as a time course from day 14 (initiation of HER2-VIA or GFP-VIA injections) through day 39 (tumor harvest). *P <0.05, **P <0.001. **(C)** Schema for the passive transfer of vaccine-induced antibodies to treat established HCC1569 human breast tumor xenografts in NOD.CB17-*Prkdc^scid^*/J mice. **(D)** Mean fold-change in tumor growth of implanted HCC1569 cells for the mice treated with HER2-VIA or PBS for days 8 through 20. **P <0.001. **(E)** Effect of vaccine-induced anti-HER2 antibodies (HER2-VIA) and trastuzumab on human breast cancer cell proliferation. HER2-positive cells (BT474 or SKBR3) were treated with 3 μl pooled mice crude serum in 100 μl culture medium for 3 days and cell proliferation was assessed by 3-(4,5-dimethylthiazol-2-yl)-2,5-diphenyl tetrazoliumbromide assay. Trastuzumab (Herceptin) (10 μg/ml) was used as a positive control and sera from mice receiving Ad-LacZ vaccine (VIA-SHAM) or saline (untreated) were used as negative controls. Proliferation is plotted relative to the growth of cells in the untreated condition. Error bars represent standard deviation. Data are representative of four experiments. P <0.001.

vitro. HER2-VIA was adoptively transferred into HCC1569 tumor-bearing recipient mice and significantly (P <0.001) suppressed tumor growth relative to control treated mice (Figure 2C,D, tumor volume fold-change). Accordingly, HER2-VIA - like trastuzumab - inhibits cell proliferation in breast cancer SK-BR-3 and BT474 cells *in vitro*, as shown in Figure 2E. However, HER2-VIA treatment had little effect on HCC1569 cell proliferation *in vitro* (data not shown), suggesting that HER2-

VIA functions more effectively against HCC1569 cells *in vivo*. Future studies are needed to determine whether higher concentrations of HER2-VIA are needed to inhibit HCC1569 cells *in vitro*. Based on these anti-tumor effects, we hypothesized that the polyclonal HER2 antibodies may have a direct effect on receptor internalization and degradation. We therefore proceeded to study the molecular events following antibody-receptor interaction.

Activation of HER2 by HER2-VIA

Despite a lack of identified HER2-soluble ligands, HER2 phosphorylation on multiple tyrosine sites (including residues 877, 1,221, 1,222 and 1,248) has been established from HER2 activation by homodimerization or heterodimerization [18,22-24]. In SK-BR-3 breast cancer cells transiently stimulated with HER2-VIA, phosphorylation of HER2 on sites 877, 1,221, 1,222 and 1,248, as well as phosphorylation of the downstream HER2 signaling molecules Akt and ERK, was detected (Figure 3, lanes 1 to 5). The HER2 and EGFR tyrosine kinase inhibitor lapatinib abolished tyrosine phosphorylation at these sites, as well as blocking activation of Akt and ERK (Figure 3, lanes 6 to 10). These data indicate that HER2-VIA initially behaves as a HER2 agonist, similar to trastuzumab [25-27].

Internalization of HER2 upon HER2-VIA stimulation

To characterize the effect of antibodies on HER2 receptor internalization, HEK293 cells transfected with HER2-YFP were incubated with 100 μg/ml HER2-VIA antibody for 1 hour prior to observation. HER2-VIA-induced internalization of HER2-YFP resulted in the formation of fluorescent cytosolic aggregates (Figure 4A, a vs. b). As shown in Additional file 1, 100 μg/ml HER2-VIA antibody exhibits a HER2 fluorescence staining intensity comparable with 5 μg/ml trastuzumab. However, a 20-fold excess of trastuzumab (100 μg/ml) behaved similarly to LacZ-negative control antibody and was unable to internalize receptor, because YFP fluorescence remained at the plasma membrane (Figure 4A, c to 4f).

We next sought to confirm the findings of Figure 4A for endogenous HER2 receptor internalization using breast cancer cell lines SK-BR-3 and HCC1569, which each express abundant HER2 protein but are sensitive or resistant to trastuzumab treatment, respectively [28]. As is shown (Figure 4B, a to 4c), HER2-VIA induced HER2 internalization in SK-BR-3 cells while LacZ control antibody had little to no effect. Trastuzumab produced only a small complement of internalized HER2 receptors in SK-BR-3 cells (Figure 4B, d). Similarly, treatment of HCC1569 cells with HER2-VIA caused a significant amount of endogenous HER2 internalization while LacZ-VIA and trastuzumab had no effect (Figure 4B, e to 4h). Counterstaining cells with the nuclear membrane marker lamin B indicates that the internalized endogenous HER2 localizes exclusively to the cytosol (see Additional file 2), suggesting that HER2 internalization does not lead to HER2 nuclear translocation as reported [29].

We further studied the effect of antibodies on endogenous HER2 receptor endocytosis using a biotin method to label HER2 at the cell surface, as shown in Figure 4C. Western blotting of biotin-labeled internalized receptors that originated at the cell surface demonstrates that HER2-VIA induces robust HER2 in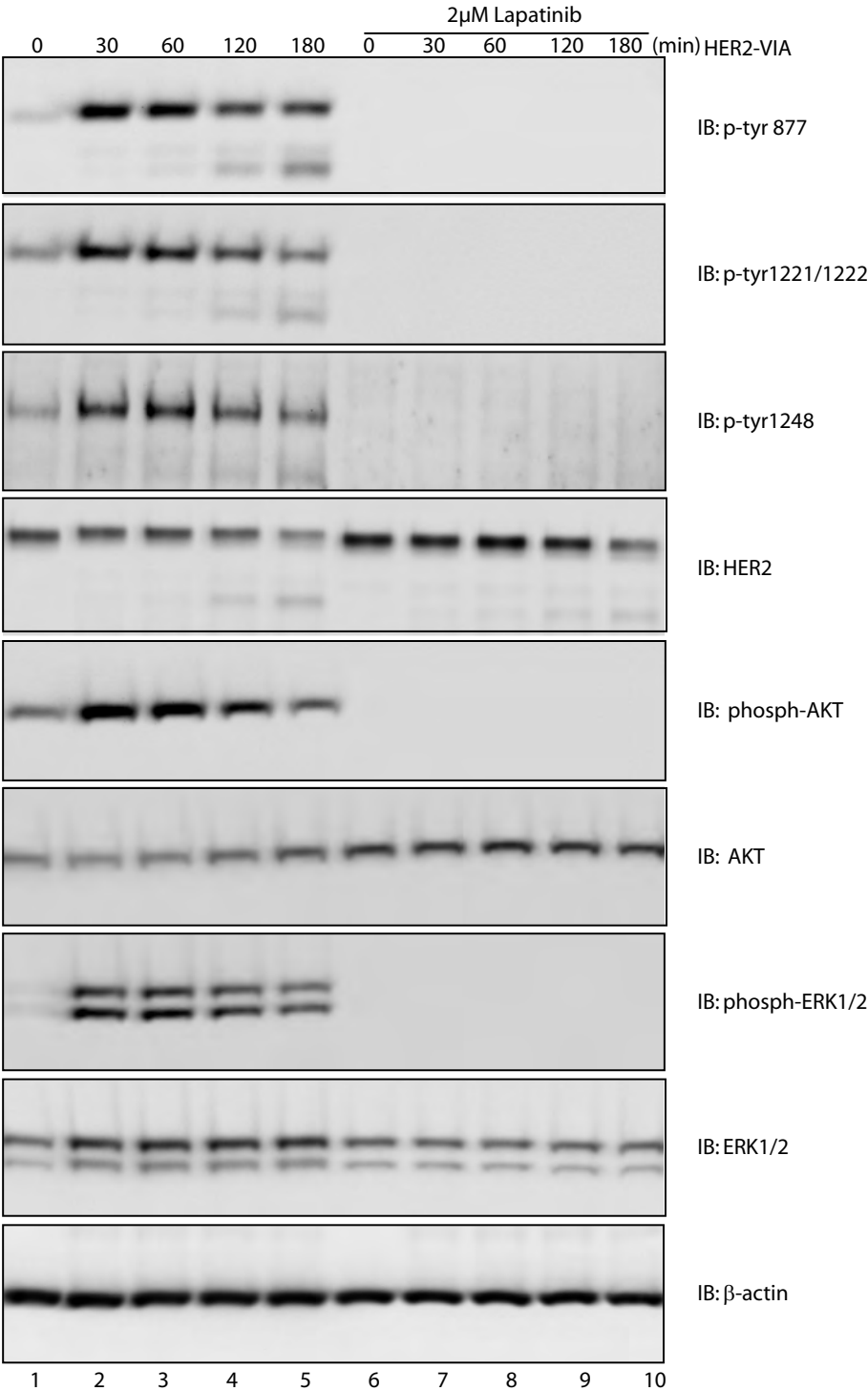ternalization (Figure 4C, lane 3 vs. rest of the lanes). Note also that raising the temperature of the cells from 4 to 37°C induces a small amount of HER2 internalization (Figure 4C, lanes 1 and 2) [15]. In addition, HER2 internalization induced by HER2-VIA is tyrosine kinase independent, because it occurs in the presence of the kinase inhibitor lapatinib (Figure 4D,E).

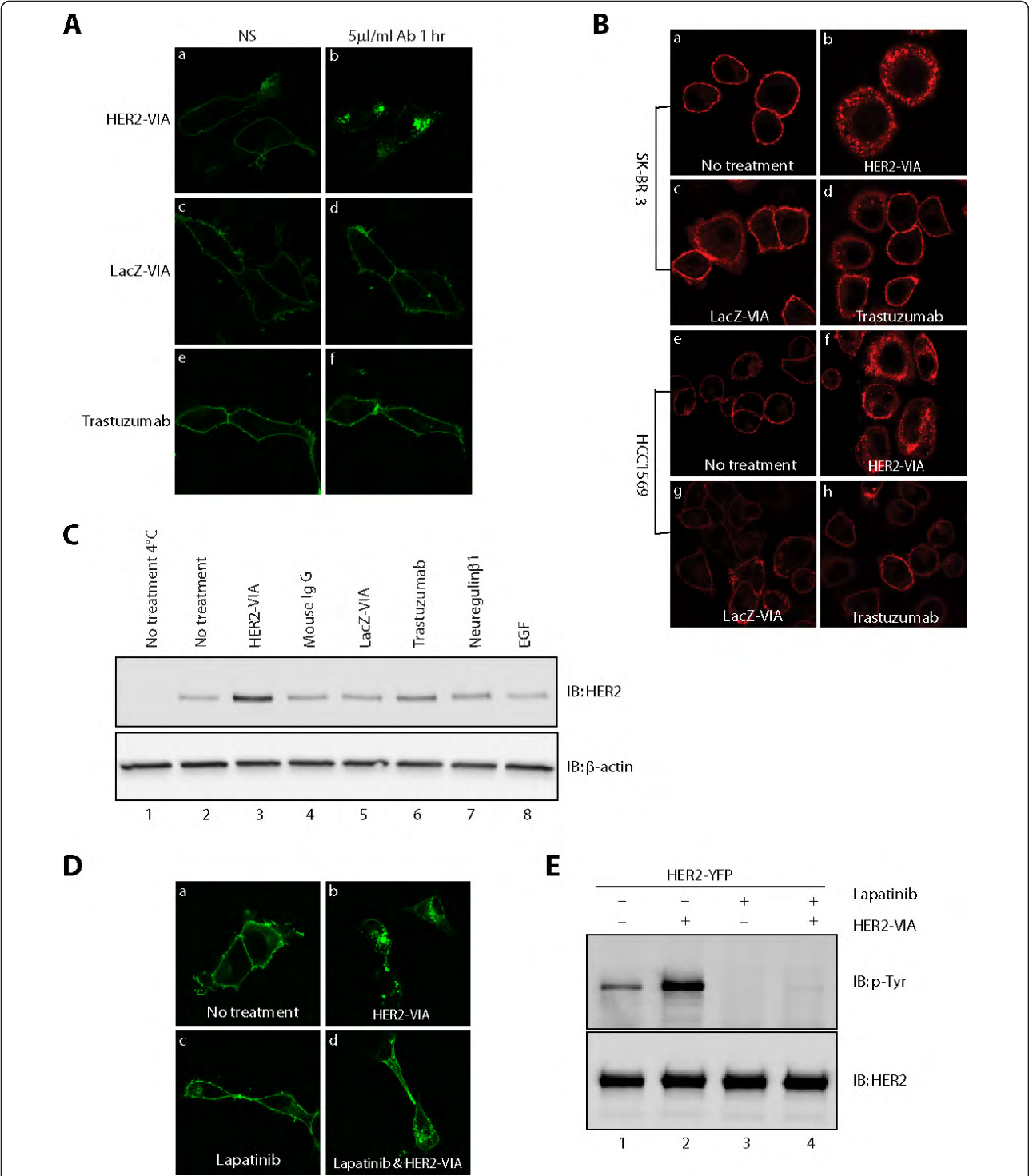## Internalization of HER2 through clathrin-coated pits/vesicles

Upon EGF stimulation, HER1 (EGFR) undergoes internalization through clathrin-coated pits/vesicles where it co-internalizes with HER2 [30-32]. To elucidate the HER2 internalization process, we examined the capacity of HER2-VIA to modulate trafficking of heterodimers of EGFR and HER2 (Figure 5A). GFP protein was fused to the C-terminus of EGFR (EGFR-GFP) and RFP protein was fused to the C terminus of HER2 (HER2-RFP). In addition to membrane localization, a small percentage of the EGR receptors were localized to the cytoplasm basally when co-expressed with HER2 in HEK293 cells (Figure 5A, a, g and 5m). This is probably due to the constitutive endocytosis and recycling of EGFRs that is known to be ligand independent [33,34]. HER2-VIA treatment of HEK293 cells transiently co-expressing HER1-GFP (EGFR-GFP) and HER2-RFP caused robust HER2-RFP internalization (Figure 5A, a to 5f). However, the overall distribution and the membrane localized EGFR were not altered by the HER2-VIA treatment, suggesting that the HER2-VIA-induced endocytosis is specific for HER2 (Figure 5A, d). In contrast, EGF ligand treatment caused robust EGFR-GFP internalization but had little or no effect on HER2 distribution (Figure 5A, g to 5l). When cells were treated simultaneously with HER2-VIA and EGF, internalization of both HER2 and EGFR was observed and the two markers extensively overlapped within the cells (Figure 5A, m to 5r). These data are also suggestive of HER2 utilizing the same clathrin mechanism for receptor internalization as EGFR [10].

β_2-adrenergic receptors are prototypical for clathrin-dependent internalization of G-protein-coupled receptors [35,36], and transferrin is a well-documented standard for clathrin-mediated internalization in general [37]. The demonstration that internalized HER2-YFP co-localizes with either β_2-adrenergic receptor-RFP or transferrin in intracellular vesicles would further confirm that HER2 also internalizes in manner similar to these other proteins. As shown in Figure 5B, in cells expressing both β_2-adrenergic receptor-RFP and HER2-YFP receptors and prior to activation, the two receptors are not intracellularly co-localized (Figure 5B, a to 5c). Exposure to isoproterenol and HER2-VIA for 1 hour resulted in multiple overlapping intracellular distributions of these receptors (Figure 5B, d to 5f). Similarly, internalized transferrin at 1
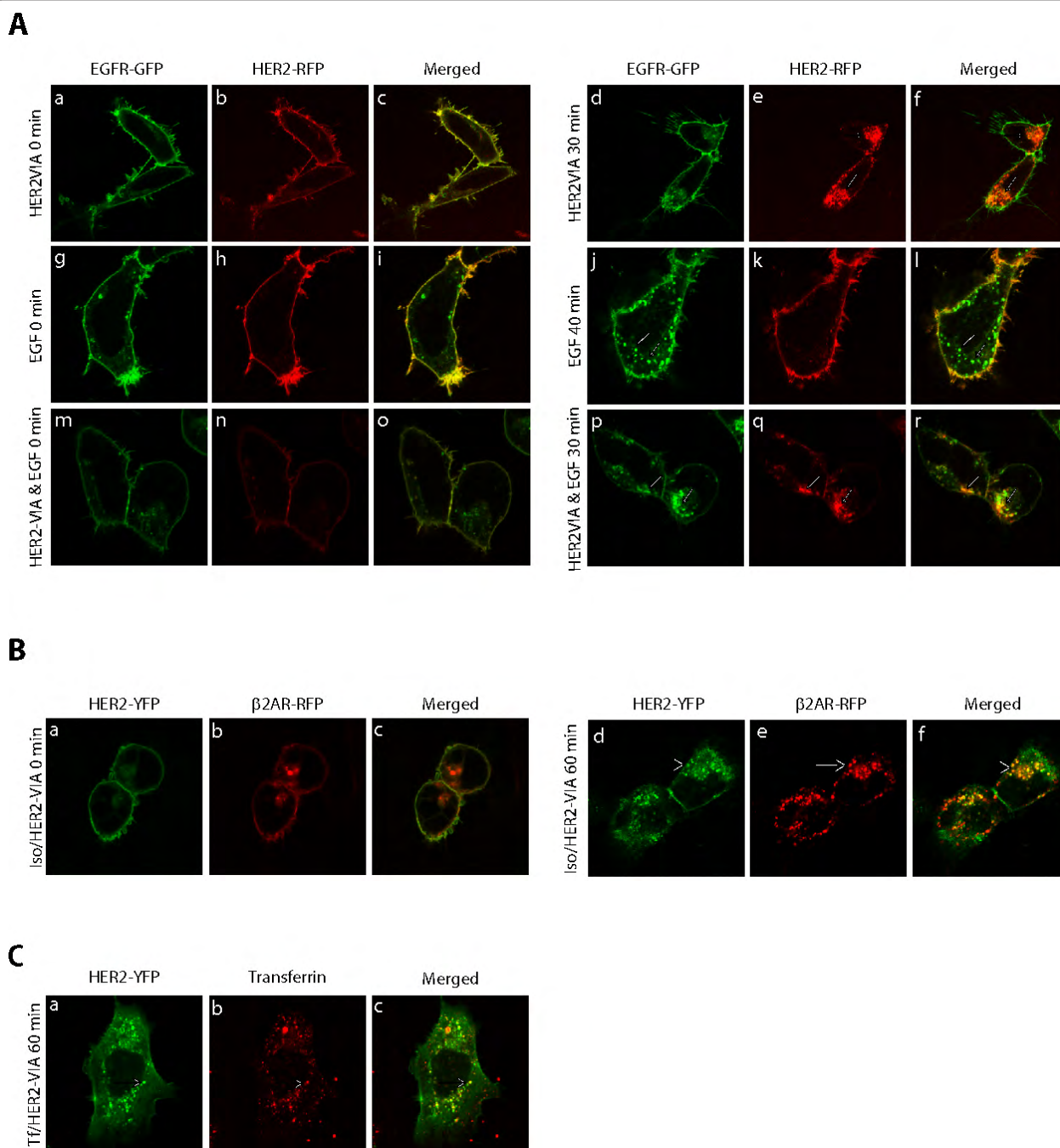
Figure 3 Activation of multiple signaling molecules by vaccine-induced anti-HER2 antibodies and inhibition of activation by lapatinib.
SK-BR-3 cells were left untreated (lanes 1 to 5) or were pretreated with 2 μM lapatinib for 3 hours (lanes 6 to 10) followed by 100 μg/ml
vaccine-induced anti-HER2 antibodies (HER2-VIA) stimulation at 37ºC for the indicated time. After treatment, cells were washed and then lysed in
2 × SDS sample buffer followed by sonication. Equal amounts of protein from each sample were used to visualize the indicated molecules by
immunoblotting. ERK, extracellular signal-regulated protein kinase.

Figure 4 Effects of vaccine-induced anti-HER2 antibodies on HER2 internalization. **(A)** Internalization of HER2-YFP by vaccine-induced anti-HER2 antibodies (HER2-VIA). HEK 293 cells transiently expressing HER2-YFP were stimulated with **(a, b)** HER2-VIA, **(c, d)** LacZ-VIA, or **(e, f)** trastuzumab, respectively for 1 hour. Confocal images from the same cells were taken before and after antibody incubation. Formation of vesicles in the cells indicated receptor internalization. The experiment was repeated three times. NS, non-stimulated. **(B)**. Imaging endogenous HER2 internalization by HER2-VIA. SK-BR-3 and HCC1569 cells were allowed to grow for 24 hours and were treated as described in Materials and methods. Confocal images of cells that **(a, e)** were left untreated, or were treated with **(b, f)** HER2-VIA, **(c, g)** LacZ-VIA or **(d, h)** trastuzumab. **(C)** Endogenous HER2 internalization by HER2-VIA as assessed by cell surface Biotin-labeling. Upper panel: immunoblot (IB) for protected (internalized) biotin-labeled HER2 in cells treated with indicated agents/conditions. Lower panel: β-actin serves as loading control to ensure equal amounts of cell lysate. EGF, epidermal growth factor. **(D)** Effect of lapatinib on HER2-YFP internalization induced by HER2-VIA. Confocal images of HEK293 cells expressing HER2-YFP that **(a)** were left untreated, or were treated with **(b)** HER2-VIA, **(c)** lapatinib or **(d)** lapatinib then HER2-VIA for 1 hour. **(E)** The same transfected cells were immunoblotted (IB) for HER2 tyrosine phosphorylation (upper panel) and total HER2 expression (lower panel).

Figure 5 HER2 internalizes through a clathrin-coated mechanism. **(A)** Effect of HER2 and epidermal growth factor receptor (EGFR) trafficking by vaccine-induced anti-HER2 antibodies (HER2-VIA) and epidermal growth factor (EGF). HEK 293 cells transiently expressing HER2-RFP and EGFR-GFP were **(a to c, g to i, m to o)** left untreated, or were stimulated with **(d to f)** HER2-VIA, **(j to l)** EGF and **(p to r)** HER2-VIA/EGF at 37°C for 30 minutes. Confocal images from the same cells were taken before and after HER2-VIA and/or EGF ligand stimulation. Arrowheads indicate internalized receptors. Representative images from three experiments are presented. **(B)** Co-localization of HER2-VIA-stimulated HER2-YFP with the β_2-adrenergic receptor (β_2AR). Confocal images of unstimulated HEK293 cells expressing both **(a)** HER2-YFP and **(b)** β_2AR-RFP. **(c)** Merged image of (a) and (b). **(d to f)** Confocal images of cells simultaneously stimulated with 0.1 μM isoproterenol (Iso) and 100 μg/ml HER2-VIA at 37°C for 1 hour. **(f)** Merged image of (d) and (e). Arrowheads indicate co-localized vesicles. **(C)** Co-localization of HER2-VIA-stimulated HER2-YFP with transferrin. **(a to c)** Confocal images of cells expressing the HER2-YFP and treated simultaneously with Alexa-546 transferrin (Tf) (100 μg/ml) and HER2-VIA (100 μg/ml) for 1 hour at 37°C. (c) Merged picture. Arrowheads indicate co-localized vesicles.

hour has significant co-localization with internalized HER2-YFP (Figure 5C). To further demonstrate that HER2-VIA-induced HER2 internalization occurs through clathrin-coated pits, SK-BR-3 cells were treated with sucrose, a known inhibitor of clathrin-dependent endocytosis [38]. As shown in Additional file 3, HER2-VIA-induced internalization of HER2 was effectively blocked by sucrose, and this inhibition was reversible because removing sucrose from the cells allowed the internalization of HER2 to proceed. Taken together, these data suggest that HER2-VIA-induced HER2 internalization occurs through a clathrin-coated pit mechanism.

Ubiquitination of HER2 upon HER2-VIA stimulation

Receptor internalization is often associated with receptor ubiquitination and targeting to proteasomes for degradation. In SK-BR-3 cells transiently expressing exogenous Myc-tagged ubiquitin, HER2-VIA treatment resulted in increased HER2-ubiquitin-Myc in the presence of 10 μM of the protease inhibitor MG132, as assessed by western blotting (Figure 6A). HER2-VIA also led to ubiquitination of endogenous HER2 receptor in SK-BR-3 cells in the presence of MG132 (Figure 6B). Interestingly, we found that the ubiquitination of HER2 induced by HER2-VIA treatment was effectively blocked by 1 μM lapatinib (see Additional file 4). It has also been shown previously that lapatinib is capable of stabilizing HER2 proteins by inhibiting basal-induced and trastuzumab-induced ubiquitination of HER2 [26]. Our results are consistent with the notion that HER-VIA functions by activating HER2 receptors and subsequently triggers internalization and ubiquitination.

Degradation of HER2 upon HER2-VIA stimulation

To explore the stability of HER2 after internalization, SK-BR-3 cells were incubated with HER2-VIA and harvested. Using western blot analysis we demonstrated that HER2-VIA treatment for 3 hours induced a significant reduction of total HER2 (Figure 6C). A 9-hour treatment reduced HER2 protein expression by about 70%. In contrast, the amount of HER2 protein did not decrease after treatment with control antibody LacZ-VIA. Trastuzumab also did not reduce HER2 protein expression (Figure 6C). Similar results were obtained in HCC1569 cells (Figure 6D), suggesting that HER2-VIA is an effective antibody for promoting HER2 degradation.

Truncation of HER2 upon HER2-VIA stimulation

HER2 is a 1,255-amino-acid protein that migrates at 185 kDa. Similar to other EGF family receptors, the extracellular domain of HER2 can be cleaved, reportedly at amino acid site R647, A644 or N530 [39]. Following HER2-VIA stimulation we observed the formation of a 130 kDa fragment of HER2 that was associated with a

reduction in full-length HER2 expression (Figure 6E). Blockade of proteasome digestion prevented the appearance of this cleaved form of HER2 (Figure 6E). Moreover, this fragment was phosphorylated at tyrosine residues (referenced to full-length HER2) 877, 1,221, 1,222 and 1,248 as detected by phospho-specific antibodies (Figure 6F, lanes 1 and 2). Since tyrosine 1,248 is present in this 130 kDa fragment, the cleavage must take place at the amino-terminal end of HER2. Lapatinib treatment had no effect on the appearance of the 130 kDa fragment (Figure 6F, lanes 3 and 4) while the protease inhibitor MG132 blocked its formation (Figure 6F, lanes 5 and 6). However, HER2-VIA-induced tyrosine phosphorylation of the fragment was abolished with lapatinib treatment (Figure 6F, lanes 3 and 4). Taken together, these data suggest that this 130 kDa fragment is cleaved from the HER2 N-terminus and may represent a novel cleavage site, distinct from those observed previously [40] (Figure 6E).
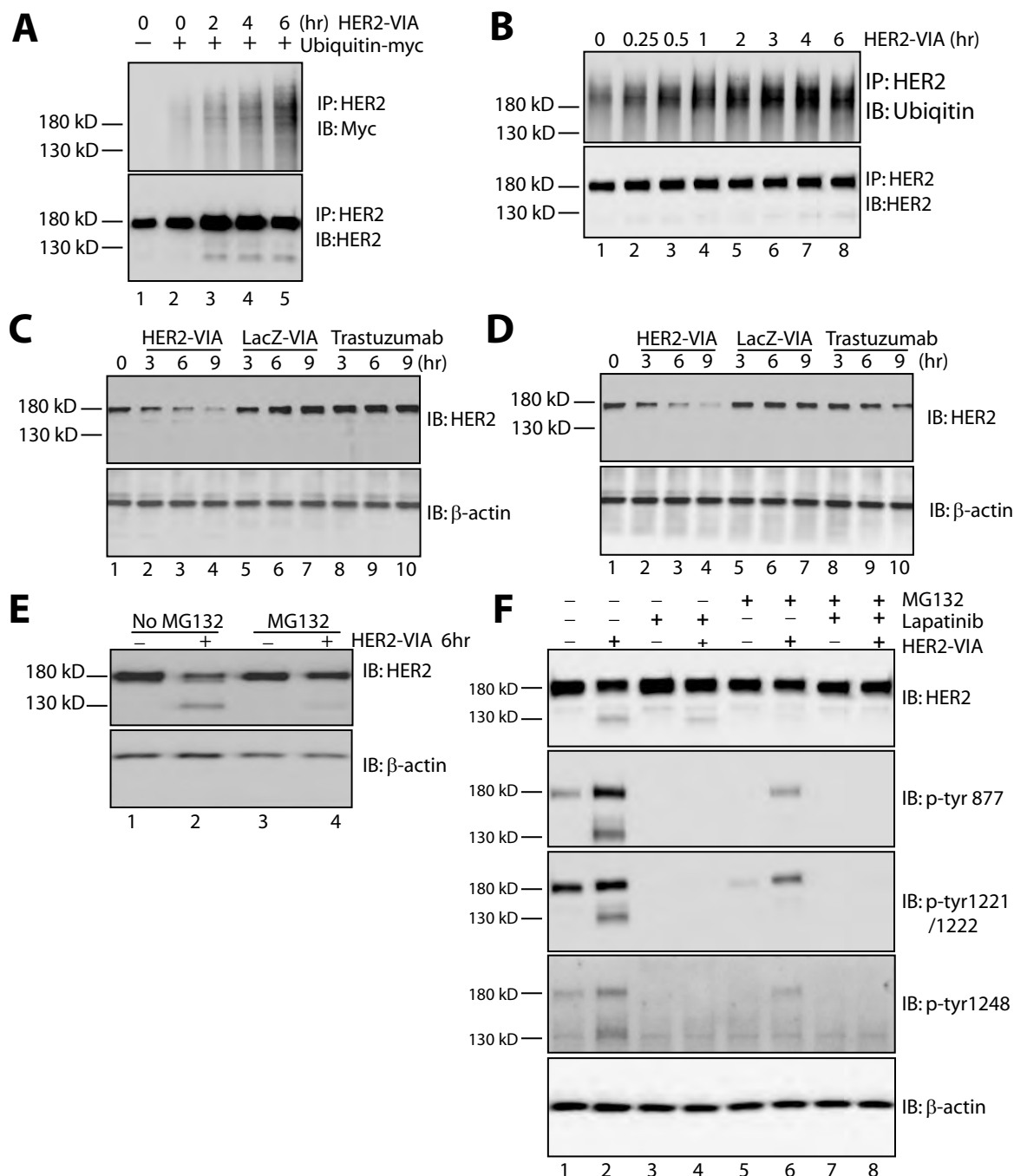
Reduced signaling by HER2 following prolonged-HER2-VIA treatment

In SK-BR-3 breast cancer cells transiently exposed to HER2-VIA, phosphorylation of HER2 on sites 877, 1,221, 1,222, and 1,248 as well as phosphorylation of the downstream HER2 signaling molecules AKT and ERK was detected (Figure 3, lanes 1 to 5). However, prolonged HER2-VIA binding (up to 72 hours stimulation) resulted in decreased AKT phosphorylation, probably due to the decreased HER2 expression after prolonged treatment (Figure 7A,B).

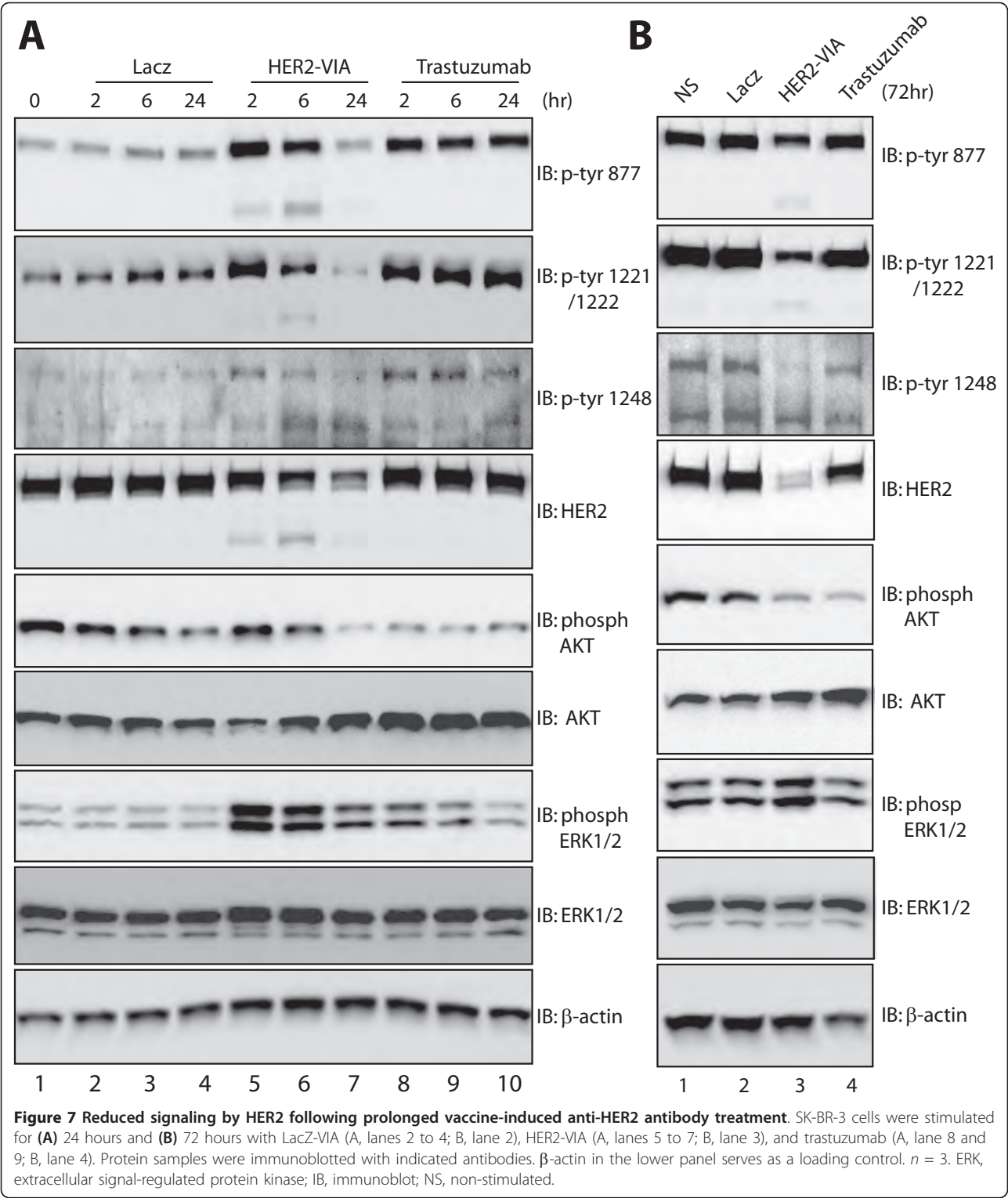### Effects of human HER2-specific antibodies

As an extension of the above experiments, we were interested in studying the signaling effects of human antibodies generated against HER2 in the setting of tyrosine kinase inhibition, Prior to utilizing our recombinant viral vectors expressing HER2 with lapatinib in humans, important safety issues regarding combination HER2-specific vaccination and kinase inhibition needed assessment. We therefore proceeded to study the concept of vaccination with concomitant kinase inhibition using a HER2 protein vaccine (dHER2) that was in clinical trial development in combination with lapatinib for this first study in humans. The vaccine we proposed to test, dHER2, consists of the extracellular domain and part of the intracellular domain of HER2 combined with the adjuvant AS15 containing MPL, QS21, CpG and liposome.

In this study, women with metastatic, trastuzumab-refractory HER2-overexpressing breast cancer were immunized six times at 2-week intervals with dHER2 concomitantly with oral lapatinib (1,250 mg/day). The clinical results and primary immune analysis of this study are reported elsewhere [16]. The specificity of human serum samples against HER2 receptors has been verified

Figure 6 HER2 ubiquitination, degradation, and fragmentation induced by vaccine-induced anti-HER2 antibodies. **(A)** Vaccine-induced anti-HER2 antibodies (HER2-VIA) stimulation led to HER2 ubiquitination. SK-BR-3 cells expressing ubiquitin-Myc were pretreated with MG132 for 2 hours and then treated with HER2-VIA for the indicated time. The ubiquitinated HER2 was detected by anti-Myc antibody. **(B)** HER2-VIA stimulation leads to HER2 ubiquitination. SK-BR-3 cells were pretreated with MG132 for 2 hours before HER2-VIA stimulation. Cell lysates were immunoprecipitated with anti-HER2 29D8 antibody. The endogenous ubiquitinated HER2 was detected by the anti-ubiquitin antibody and the total HER2 was visualized by anti-HER2 3B5 antibody. **(C), (D)** HER2-VIA stimulation causes HER2 degradation: (C) SK-BR-3 and (D) HCC1569 cells were stimulated with HER2-VIA, LacZ-VIA, or trastuzumab for the indicated time, and an equal amount of cell lysates was subjected to western blot analysis. Expression levels of HER2 and β-actin were detected by corresponding antibodies. **(E)** HER2-VIA stimulation produces HER2 fragmentation. SK-BR-3 cells were treated with HER2-VIA for 6 hours in the absence or presence of prior MG132 treatment for 2 hours. Full-length and truncated HER2 are detected by anti-HER2 3B5 antibody. β-actin serves as loading control. **(F)** HER2-VIA stimulation produces tyrosine phosphorylation of the 130 kDa HER2 C-terminal fragment. SK-BR-3 cells were incubated with HER2-VIA for 6 hours after pretreatment with lapatinib, MG132, or lapatinib plus MG132 for 2 hours. Full-length and truncated HER2 are detected by anti-HER2 3B5 antibody, which recognizes the C-terminus (top panel). Phosphorylated full-length and truncated HER2 were recognized by tyrosine site-specific phospho-antibodies for phosphorylated tyrosine 877, 1,221/1,222 and 1,248 (middle three panels). IB, immunoblot.

Figure 7 Reduced signaling by HER2 following prolonged vaccine-induced anti-HER2 antibody treatment. SK-BR-3 cells were stimulated for **(A)** 24 hours and **(B)** 72 hours with LacZ-VIA (A, lanes 2 to 4; B, lane 2), HER2-VIA (A, lanes 5 to 7; B, lane 3), and trastuzumab (A, lane 8 and 9; B, lane 4). Protein samples were immunoblotted with indicated antibodies. β-actin in the lower panel serves as a loading control. *n* = 3. ERK, extracellular signal-regulated protein kinase; IB, immunoblot; NS, non-stimulated.

using ELISAs as described in the previous study [16]. To further determine the molecular mechanism of human HER2 antibodies, crude serum antibodies from three patients with the highest titer of antibodies to the HER2

extracellular domain were obtained via ammonium sulfate precipitation to deplete lapatinib and then tested for binding to HER2-expressing cells. Although human HER2 antibodies are capable of binding to HER2 as

shown previously [16], no receptor internalization was observed after 1 hour of incubation in contrast to the rapid receptor internalization and degradation noted with the murine HER2-VIA (Figure 8A). Even after 6 hours of treatment, no HER2 internalization was observed in SK-BR-3 cells incubated with human antibodies (data not shown). Nonetheless, phosphorylation of HER2 (tyrosine 877) was markedly decreased by patients' serum upon 6 hours of treatment (Figure 8B); meanwhile, the phosphorylation of HER2 (tyrosine 877) remained relatively unchanged upon short-term stimulation of SK-BR-3 with patient antibodies, unlike murine HER2-VIA, which possesses agonistic effect on HER2 signaling (see Additional file 5).

In summary, our studies suggest that HER2-VIA antibodies possess some properties characteristic of agonists, such as promoting HER2 signaling, but that this is soon followed by receptor internalization, ubiquitination and, finally, degradation and downregulation of signaling.
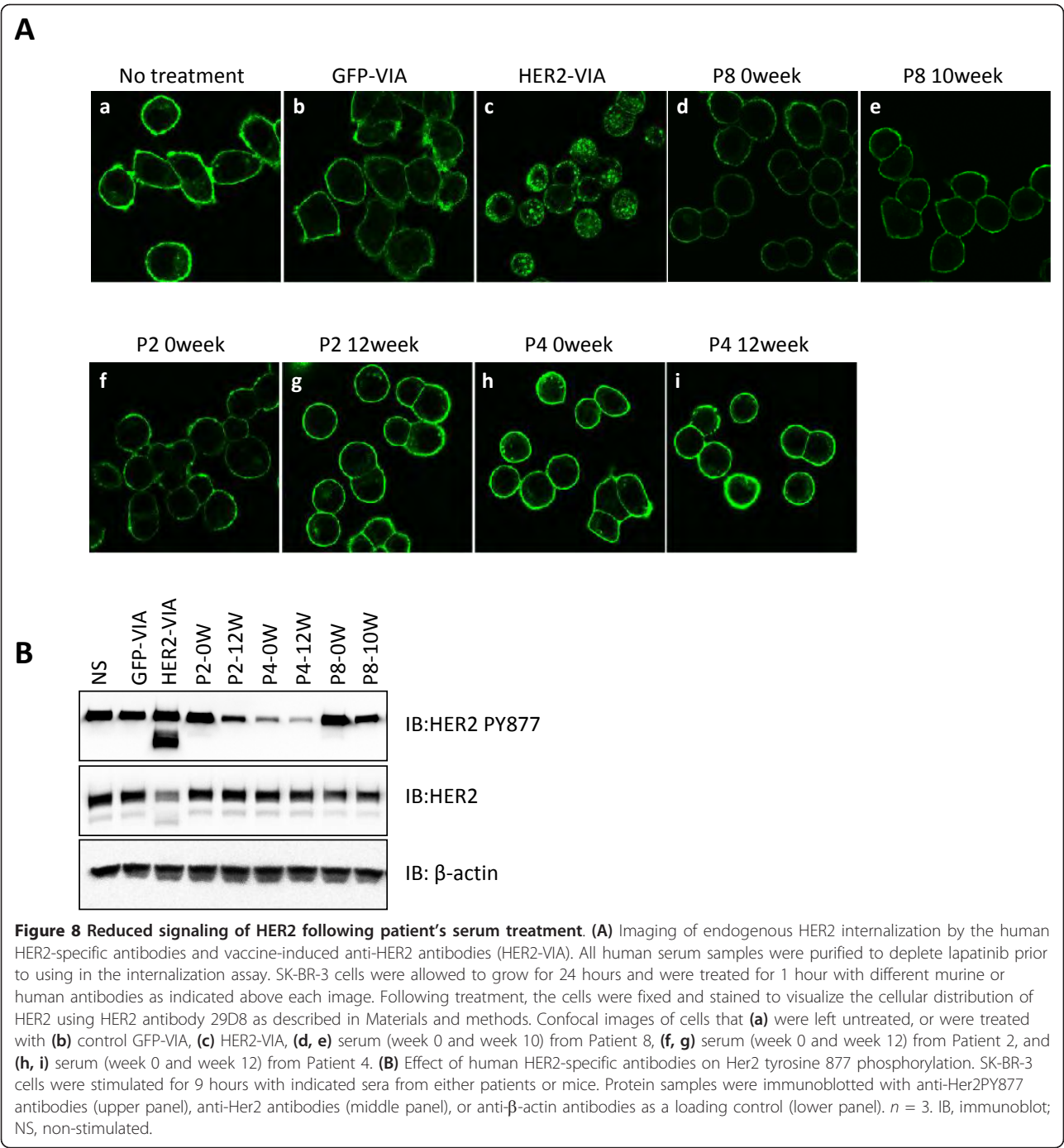
Discussion

Constitutive HER2 internalization and membrane recycling normally occur at a very slow rate in many cell systems in the absence of a recognized agonist. A recent report indicates that one mAb or multiple mAbs against HER2, alone or in combination, were able to induce HER2 internalization over intervals as short as 4 hours, but the mechanisms underlying the internalization were not determined [41]. Interestingly, even slow HER2 internalization is associated with reductions in HER2 signaling and decreases in tumor growth rates. We found that polyclonal anti-HER2 antibodies were remarkably more potent than the mAb trastuzumab in causing HER2 internalization and degradation. Our data indicate that HER2-VIA antibodies are HER2 agonists that bind and internalize the receptor, signal through ERK1/2 and Akt, and deplete HER2 from the plasma membrane by the same clathrin-mediated mechanisms utilized by other HER family members exposed to cognate agonists.

Although polyclonal antibodies specific to HER2 are not clinically available, active immunotherapy targeting tumor antigens can lead to tumor antigen-specific immune responses. We have administered HER2 protein-loaded autologous dendritic cells to patients with advanced HER2-overexpressing tumors. Remarkably, we found that all patients were long-term survivors, and six out of seven patients had developed HER2-specific antibodies that inhibited tumor growth *in vitro* [13]. Alternatives to autologous dendritic cell vaccines include tumor antigen-expressing recombinant vectors. We have developed a potent novel recombinant vector expressing kinase-inactivated HER2 that induced high levels of HER2-specific antibodies [17], and vaccination with this

vaccine demonstrated synergy when combined with HER2 kinase inhibition with lapatinib [13], consistent with clinical observations that combinations of antibodies and small-molecule tyrosine kinase inhibitor are more effective than monotherapy.

The HER2-VIA binding sites that are both necessary and sufficient for rapid HER2 removal from the plasma membrane remain unidentified, but these sites could become future targets for small molecules or could be important to elucidation of structure-activity relationships. Other agents are known to produce HER2 internalization but with slower kinetics, suggesting that allosteric modulation of receptor conformation may be sufficient to achieve desired therapeutic goals in the absence of an identified HER2 agonist. Exposure of cells to the ansamysin antibiotic geldanamycin results in HER2 degradation with cleavage of a 130 kDa C-terminus fragment, the separation of HER2 from Hsp90, and within 2 hours the accumulation of HER2 in cytoplasmic vesicles [40]. It is unclear whether the vesicular compartmentalization of HER2 is a consequence of enhanced receptor internalization or an inhibition of receptor recycling, but recent evidence points to the latter. It also has not been determined whether geldanamycin leads to HER2 activation or whether HER2 trafficking is clathrin dependent or independent, asboth explanations have been proposed [42-44].

Interestingly, our western blotting data indicate that the majority of HER2 receptors remain intact following HER2-VIA treatment. However, in contrast to geldanamycin treatment, a 130 kDa fragment truncated at the N-terminus of HER2 is observed in cells that are treated with HER2-VIA, while mAb treatment does not produce a similar fragment. Moreover, we show that HER2-VIA-induced internalization of HER2 receptors precedes HER2 degradation. The internalized HER2-containing vesicles (observed in Figure 4A, b) may represent the receptors localized in the endosome compartment, where the receptors are waiting to be further sorted and can still signal. The level of HER2 remains relatively unchanged until the receptors traffic to the lysosome at a later time point where the protein degradation occurs. Our finding is consistent with a recent study showing that geldanamycin-induced HER2 internalization can be observed within 2 hours whereas the degradation of HER2 did not occur until 6 hours after the treatment [45]. The half-life of HER2 in HER2-VIA-treated cells is around 3 hours, which is similar to that observed in geldanamycin-treated cells [40]. Interestingly, the time course of Akt dephosphorylation tightly correlates with the time course of HER2-VIA-induced dephosphorylation and degradation of HER2. In HER2-overexpressing cells such as SK-BR-3, the termination of downstream signaling probably only occurs after the level of HER2 is

Figure 8 Reduced signaling of HER2 following patient's serum treatment. **(A)** Imaging of endogenous HER2 internalization by the human HER2-specific antibodies and vaccine-induced anti-HER2 antibodies (HER2-VIA). All human serum samples were purified to deplete lapatinib prior to using in the internalization assay. SK-BR-3 cells were allowed to grow for 24 hours and were treated for 1 hour with different murine or human antibodies as indicated above each image. Following treatment, the cells were fixed and stained to visualize the cellular distribution of HER2 using HER2 antibody 29D8 as described in Materials and methods. Confocal images of cells that **(a)** were left untreated, or were treated with **(b)** control GFP-VIA, **(c)** HER2-VIA, **(d, e)** serum (week 0 and week 10) from Patient 8, **(f, g)** serum (week 0 and week 12) from Patient 2, and **(h, i)** serum (week 0 and week 12) from Patient 4. **(B)** Effect of human HER2-specific antibodies on Her2 tyrosine 877 phosphorylation. SK-BR-3 cells were stimulated for 9 hours with indicated sera from either patients or mice. Protein samples were immunoblotted with anti-Her2PY877 antibodies (upper panel), anti-Her2 antibodies (middle panel), or anti-β-actin antibodies as a loading control (lower panel). n = 3. IB, immunoblot; NS, non-stimulated.

reduced substantially. Taken together, our findings indicate that although HER2-VIA shares certain similarities with trastuzumab and geldanamycin in its ability to inhibit HER signaling, it affects HER2 behavior in a manner quite distinct from either trastuzumab or geldanamycin.

The responses we observed with polyclonal anti-HER2 antibodies suggest that their mechanism of action may underlie new strategies for cancer immunotherapy. Most active immunotherapy strategies have not resulted in large clinical reductions of tumors. Nonetheless, recent reports have suggested that, despite the absence of classical clinical responses to active immunotherapy, there have been long-term survival benefits [46,47]. We anticipated that the generation of HER2-specific antibodies in patients with breast cancer would have similar effects to the murine HER2-specific antibodies. While we were preparing our recombinant HER2-expressing adenoviral vaccine for human testing, we performed a pilot study

of vaccination of breast cancer patients with a combination of HER2 protein vaccine and lapatinib. Although this vaccine induced detectable HER2-specific antibodies that could recognize HER2 expressed on the surface of tumor cells, we did not see receptor internalization and degradation. We were able to document that the antibodies had an inhibitory effect on HER2 signaling *in vitro*, as had been previously reported with peptide-based vaccines. Nonetheless, more potent vaccines targeting HER2 may be capable of generating higher-titer HER2-specific antibodies, and antibodies that not only bind but mediate receptor internalization and degradation, and the resultant loss of HER2 signaling.

Our studies provide new insights into the mechanisms underlying HER2 receptor trafficking and provide proof-of-principle that HER2 can be rapidly removed from the cell surface by agonist-like mimetics that have agonist effects. The absence of HER2 agonists has impeded development of therapies that exploit the relationship between plasma membrane HER2 expression and inappropriate HER2 signaling, but our findings suggest a long-term clinical benefit from oncogenic signaling ablation. Our results with HER2-VIA provide a basis for developing new classes of HER2 signaling inhibitors for patients that are resistant to current modes of therapy. These data also support the clinical evaluation of cancer vaccine strategies targeting HER2, with overall survival rather than tumor shrinkage/progression-free survival as an endpoint.

Conclusions

We have found that polyclonal anti-HER2 antibodies (HER2-VIA) generated by vaccinating mice with an adenovirus expressing human HER2 can retard the growth of established HER2-positive human tumor xenografts *in vivo*, bind to HER2 at the plasma membrane, induce HER2 internalization, ubiquitination and degradation, and eventually inactivate downstream kinase Akt. We have also demonstrated that low-titer HER2-specific antibodies induced by vaccinating breast cancer patients with a HER2 protein vaccine can bind to receptor and inhibit HER2 signaling through blocking tyrosine 877 phosphorylation of HER2, but did not induce receptor internalization and degradation. These data support the testing of more potent HER2-specific vaccines in human clinical trials.

Additional material

Additional file 1: Figure S1 showing flow cytometric assessment of the relative HER2-VIA and trastuzumab binding intensity to HER2-positive SK-BR-3 human breast tumor cells. SK-BR-3 cells were incubated with the indicated dilution of **(A)** HER2-VIA (1:100 to 1:102,400) or **(B)** trastuzumab (20 to 0.02 μg/ml) and then stained with the appropriate phycoerythrin-conjugated anti-IgG secondary antibody. Mean fluorescence intensity, as

a measure of antibody binding to HER2, was plotted. LacZ-VIA as a negative control showed an MFI (mean fluorescence intensity) of less than 50 at all dilutions (1:100 to 1:102,400) (data not shown).

Additional file 2: Figure S2 showing HER2-VIA drives HER internalization to the cytoplasm but not to the nucleus. Confocal images of SK-BR-3 cells were **(a to c)** left untreated, or **(d to f)** treated with HER2-VIA for 60 minutes. Cells were stained with anti-HER2 antibody (a, d) and lamin B (b, e). (c, f) Merged pictures.

Additional file 3: Figure S3 showing sucrose inhibits HER2-VIA-induced internalization of HER2. SK-BR-3 cells were treated with 20 μl HER2-VIA and then incubated with FITC 488-conjugated goat anti-mouse antibody on ice. The cells were then exposed to the following conditions and were then imaged by confocal microscopy: **(a)** incubation on ice for 1 hour; **(b)** incubation at 37°C for 1 hour; **(c)** incubation in 0.45 M sucrose on ice; **(d)** incubation in 0.45 M sucrose at 37°C for 1 hour; **(e)** incubation in 0.45 M sucrose on ice for 30 minutes followed by washing and then incubation of the cells at 37°C for 1 hour.

Additional file 4: Figure S4 showing inhibition of HER2-VIA-induced HER2 ubiquitination by lapatinib. SK-BR-3 cells were pretreated with the proteasome inhibitor MG132 (10 μM) and lapatinib for 30 minutes before HER2-VIA application for 2 hours. After the indicated treatment, cells were lysed and HER2 was precipitated using anti-HER2 rabbit antibody 29D8. Precipitated proteins were subjected to western blot analysis. Upper panel: ubiquitinated HER; lower panel: total HER2 visualized by anti-HER2 rabbit antibody 29D8.

Additional file 5: Figure S5 showing the effect of human HER2-specific antibodies on HER2 tyrosine 877 phosphorylation. SK-BR-3 cells were stimulated for 1 hour with the indicated sera from either patients or mice. Protein samples were immunoblotted with anti-HER2 PY877 antibodies (upper panel) or anti-HER2 antibodies (lower panel).

Abbreviations

BSA, bovine serum albumin; EGF, epidermal growth factor; EGFR, epidermal growth factor receptor; ERK, extracellular signal-regulated protein kinase; FCS, fetal calf serum; GFP, green fluorescent protein; HER, human epidermal growth factor receptor; HER2-VIA, vaccine-induced anti-HER2 antibodies; mAb, monoclonal antibody; MEM, modified Eagle's medium; PBS, phosphate-buffered saline; PCR, polymerase chain reaction; RFP, red fluorescent protein; YFP, yellow fluorescent protein.

Author details

[1]Department of Medicine, Duke University Medical Center, 595 Lasalle Street, Durham, NC 27710, USA. [2]Duke Comprehensive Cancer Center, Duke University Medical Center, 203 Research Drive, Durham, NC 27710, USA. [3]Division of Medical Oncology, Department of Medicine, Duke University Medical Center, 203 Research Drive, Durham, NC 27710, USA. [4]Department of Cell Biology, Duke University Medical Center, 171 Research Drive, Durham, NC 27710, USA. [5]GlaxoSmithKline Biologicals S.A, 1330 Rixensart, Belgium. [6]Department of Medicine, Oncology, Duke University Medical Center, 40 Duke Medicine Circle, Durham, NC 27710, USA. [7]Division of General Surgery, Department of Surgery, Duke Comprehensive Cancer Center, Duke University Medical Center, 203 Research Drive, Durham, NC 27710, USA.

Authors' contributions

X-RR participated in the design and coordination of the study, data acquisition and analysis, and helped draft the manuscript. JuW participated in the data acquisition and analysis. GL participated in the data acquisition and analysis. JiW participated in the coordination of the study and helped draft the manuscript. JL participated in the coordination of the study and helped draft the manuscript. WX participated in the design of the study and

helped draft the manuscript. NS participated in the design of the study and helped draft the manuscript. LB participated in the design of the study and helped draft the manuscript. TC participated in the design of the study and helped draft the manuscript. TO helped with manuscript revision. EH participated in the design of the study, participated in the recruitment of patients, managed specimen acquisition and preparation from the human study, and helped draft the manuscript. KB participated in the recruitment of patients and helped draft the manuscript. AH participated in the coordination of the study, immune analysis of human specimens, and helped draft the manuscript. MAM participated in the design the study, managed specimen acquisition and preparation from the human study and helped draft the manuscript. HKL participated in the design and coordination of the study, and help draft the manuscript. WC participated in the overall design and coordination of the study and drafted the manuscript. All authors gave final approval of the manuscript for publication.

References
1. Ferrer-Soler L, Vazquez-Martin A, Brunet J, Menendez JA, De Llorens R, Colomer R: **An update of the mechanisms of resistance to EGFR-tyrosine kinase inhibitors in breast cancer: Gefitinib (Iressa)-induced changes in the expression and nucleo-cytoplasmic trafficking of HER-ligands [review].** *Int J Mol Med* 2007, **20**:3-10.
2. Blackwell KL, Burstein HJ, Storniolo AM, Rugo H, Sledge G, Koehler M, Ellis C, Casey M, Vukelja S, Bischoff J, Baselga J, O'Shaughnessy J: **Randomized study of Lapatinib alone or in combination with trastuzumab in women with ErbB2-positive, trastuzumab-refractory metastatic breast cancer.** *J Clin Oncol* 2010, **28**:1124-1130.
3. Scheuer W, Friess T, Burtscher H, Bossenmaier B, Endl J, Hasmann M: **Strongly enhanced antitumor activity of trastuzumab and pertuzumab combination treatment on HER2-positive human xenograft tumor models.** *Cancer Res* 2009, **69**:9330-9336.
4. Baselga J, Gelmon KA, Verma S, Wardley A, Conte P, Miles D, Bianchi G, Cortes J, McNally VA, Ross GA, Fumoleau P, Gianni L: **Phase II trial of pertuzumab and trastuzumab in patients with human epidermal growth factor receptor 2-positive metastatic breast cancer that progressed during prior trastuzumab therapy.** *J Clin Oncol* 2010, **28**:1138-1144.
5. Hsieh AC, Moasser MM: **Targeting HER proteins in cancer therapy and the role of the non-target HER3.** *Br J Cancer* 2007, **97**:453-457.
6. Moasser MM: **The oncogene HER2: its signaling and transforming functions and its role in human cancer pathogenesis.** *Oncogene* 2007, **26**:6469-6487.
7. Dikic I: **Mechanisms controlling EGF receptor endocytosis and degradation.** *Biochem Soc Trans* 2003, **31**:1178-1181.
8. Wiley HS: **Trafficking of the ErbB receptors and its influence on signaling.** *Exp Cell Res* 2003, **284**:78-88.
9. Bazley LA, Gullick WJ: **The epidermal growth factor receptor family.** *Endocr Relat Cancer* 2005, **12(Suppl 1)**:S17-S27.
10. Sorkin A, Goh LK: **Endocytosis and intracellular trafficking of ErbBs.** *Exp Cell Res* 2008, **314**:3093-3106.
11. Breuleux M, Schoumacher F, Rehn D, Kung W, Mueller H, Eppenberger U: **Heregulins implicated in cellular functions other than receptor activation.** *Mol Cancer Res* 2006, **4**:27-37.
12. Jones SM, Foreman SK, Shank BB, Kurten RC: **EGF receptor downregulation depends on a trafficking motif in the distal tyrosine kinase domain.** *Am J Physiol Cell Physiol* 2002, **282**:C420-C433.
13. Morse MA, Wei J, Hartman Z, Xia W, Ren XR, Lei G, Barry WT, Osada T, Hobeika AC, Peplinski S, Jiang H, Devi GR, Chen W, Spector N, Amalfitano A, Lyerly HK, Clay TM: **Synergism from combined immunologic and pharmacologic inhibition of HER2 in vivo.** *Int J Cancer* 2010, **126**:2893-2903.
14. Piechocki MP, Pilon SA, Wei WZ: **Quantitative measurement of anti-ErbB-2 antibody by flow cytometry and ELISA.** *J Immunol Methods* 2002, **259**:33-42.
15. Yang XL, Huang YZ, Xiong WC, Mei L: **Neuregulin-induced expression of the acetylcholine receptor requires endocytosis of ErbB receptors.** *Mol Cell Neurosci* 2005, **28**:335-346.
16. Hartman ZC, Wei J, Osada T, Glass O, Lei G, Yang XY, Peplinski S, Kim DW, Xia W, Spector N, Marks J, Barry W, Hobeik A, Devi G, Amalfitano A, Morse MA, Lyerly HK, Clay TM: **An adenoviral vaccine encoding full-length inactivated human Her2 exhibits potent immunogenicty and enhanced therapeutic efficacy without oncogenicity.** *Clin Cancer Res* 2010, **16**:1466-1477.
17. Akiyama T, Matsuda S, Namba Y, Saito T, Toyoshima K, Yamamoto T: **The transforming potential of the c-erbB-2 protein is regulated by its autophosphorylation at the carboxyl-terminal domain.** *Mol Cell Biol* 1991, **11**:833-842.
18. Messerle K, Schlegel J, Hynes NE, Groner B: **NIH/3T3 cells transformed with the activated erbB-2 oncogene can be phenotypically reverted by a kinase deficient, dominant negative erbB-2 variant.** *Mol Cell Endocrinol* 1994, **105**:1-10.
19. Ben-Levy R, Paterson HF, Marshall CJ, Yarden Y: **A single autophosphorylation site confers oncogenicity to the Neu/ErbB-2 receptor and enables coupling to the MAP kinase pathway.** *EMBO J* 1994, **13**:3302-3311.
20. Wei WZ, Shi WP, Galy A, Lichlyter D, Hernandez S, Groner B, Heilbrun L, Jones RF: **Protection against mammary tumor growth by vaccination with full-length, modified human ErbB-2 DNA.** *Int J Cancer* 1999, **81**:748-754.
21. Segatto O, Lonardo F, Pierce JH, Bottaro DP, Di Fiore PP: **The role of autophosphorylation in modulation of erbB-2 transforming function.** *New Biol* 1990, **2**:187-195.
22. Muthuswamy SK, Gilman M, Brugge JS: **Controlled dimerization of ErbB receptors provides evidence for differential signaling by homo- and heterodimers.** *Mol Cell Biol* 1999, **19**:6845-6857.
23. Hazan R, Margolis B, Dombalagian M, Ullrich A, Zilberstein A, Schlessinger J: **Identification of autophosphorylation sites of HER2/neu.** *Cell Growth Differ* 1990, **1**:3-7.
24. Junttila TT, Akita RW, Parsons K, Fields C, Lewis Phillips GD, Friedman LS, Sampath D, Sliwkowski MX: **Ligand-independent HER2/HER3/PI3K complex is disrupted by trastuzumab and is effectively inhibited by the PI3K inhibitor GDC-0941.** *Cancer Cell* 2009, **15**:429-440.
25. Scaltriti M, Verma C, Guzman M, Jimenez J, Parra JL, Pedersen K, Smith DJ, Landolfi S, Ramon y, Cajal S, Arribas J, Baselga J: **Lapatinib, a HER2 tyrosine kinase inhibitor, induces stabilization and accumulation of HER2 and potentiates trastuzumab-dependent cell cytotoxicity.** *Oncogene* 2009, **28**:803-814.
26. Gijsen M, King P, Perera T, Parker PJ, Harris AL, Larijani B, Kong A: **HER2 phosphorylation is maintained by a PKB negative feedback loop in response to anti-HER2 herceptin in breast cancer.** *PLoS Biol* 2010, **8**:e1000563.
27. Neve RM, Chin K, Fridlyand J, Yeh J, Baehner FL, Fevr T, Clark L, Bayani N, Coppe JP, Tong F, Speed T, Spellman PT, DeVries S, Lapuk A, Wang NJ, Kuo WL, Stilwell JL, Pinkel D, Albertson DG, Waldman FM, McCormick F, Dickson RB, Johnson MD, Lippman M, Ethier S, Gazdar A, Gray JW: **A collection of breast cancer cell lines for the study of functionally distinct cancer subtypes.** *Cancer Cell* 2006, **10**:515-527.
28. Giri DK, Ali-Seyed M, Li LY, Lee DF, Ling P, Bartholomeusz G, Wang SC, Hung MC: **Endosomal transport of ErbB-2: mechanism for nuclear entry of the cell surface receptor.** *Mol Cell Biol* 2005, **25**:11005-11018.
29. Worthylake R, Wiley HS: **Structural aspects of the epidermal growth factor receptor required for transmodulation of erbB-2/neu.** *J Biol Chem* 1997, **272**:8594-8601.
30. Worthylake R, Opresko LK, Wiley HS: **ErbB-2 amplification inhibits down-regulation and induces constitutive activation of both ErbB-2 and epidermal growth factor receptors.** *J Biol Chem* 1999, **274**:8865-8874.
31. Kornilova ES, Taverna D, Hoeck W, Hynes NE: **Surface expression of erbB-2 protein is post-transcriptionally regulated in mammary epithelial cells by epidermal growth factor and by the culture density.** *Oncogene* 1992, **7**:511-519.
32. Katz M, Shtiegman K, Tal-Or P, Yakir L, Mosesson Y, Harari D, Machluf Y, Asao H, Jovin T, Sugamura K, Yarden Y: **Ligand-independent degradation of epidermal growth factor receptor involves receptor ubiquitylation and Hgs, an adaptor whose ubiquitin-interacting motif targets ubiquitylation by Nedd4.** *Traffic* 2002, **3**:740-751.

33. Chin LS, Raynor MC, Wei X, Chen HQ, Li L: **Hrs interacts with sorting nexin 1 and regulates degradation of epidermal growth factor receptor.** *J Biol Chem* 2001, **276**:7069-7078.

34. Cardullo RA: **Theoretical principles and practical considerations for fluorescence resonance energy transfer microscopy.** *Methods Cell Biol* 2007, **81**:479-494.

35. Kallal L, Gagnon AW, Penn RB, Benovic JL: **Visualization of agonist-induced sequestration and down-regulation of a green fluorescent protein-tagged β2-adrenergic receptor.** *J Biol Chem* 1998, **273**:322-328.

36. Mellman I: **Endocytosis and molecular sorting.** *Annu Rev Cell Dev Biol* 1996, **12**:575-625.

37. Hansen SH, Sandvig K, van Deurs B: **Clathrin and HA2 adaptors: effects of potassium depletion, hypertonic medium, and cytosol acidification.** *J Cell Biol* 1993, **121**:61-72.

38. Yuan CX, Lasut AL, Wynn R, Neff NT, Hollis GF, Ramaker ML, Rupar MJ, Liu P, Meade R: **Purification of Her-2 extracellular domain and identification of its cleavage site.** *Protein Expr Purif* 2003, **29**:217-222.

39. Tikhomirov O, Carpenter G: **Geldanamycin induces ErbB-2 degradation by proteolytic fragmentation.** *J Biol Chem* 2000, **275**:26625-26631.

40. Hamilton E, Blackwell K, Hobeika AC, Clay TM, Broadwater G, Ren XR, Chen W, Castro H, Lehmann F, Spector N, Wei J, Osada T, Lyerly HK: **Phase I clinical trial of HER2-specific immunotherapy with concomitant HER2 kinase inhibition.** *J Transl Med* 2012, **10**:28.

41. Ben-Kasus T, Schechter B, Lavi S, Yarden Y, Sela M: **Persistent elimination of ErbB-2/HER2-overexpressing tumors using combinations of monoclonal antibodies: relevance of receptor endocytosis.** *Proc Natl Acad Sci USA* 2009, **106**:3294-3299.

42. Lerdrup M, Hommelgaard AM, Grandal M, van Deurs B: **Geldanamycin stimulates internalization of ErbB2 in a proteasome-dependent way.** *J Cell Sci* 2006, **119**:85-95.

43. Austin CD, De Maziere AM, Pisacane PI, van Dijk SM, Eigenbrot C, Sliwkowski MX, Klumperman J, Scheller RH: **Endocytosis and sorting of ErbB2 and the site of action of cancer therapeutics trastuzumab and geldanamycin.** *Mol Biol Cell* 2004, **15**:5268-5282.

44. Barr DJ, Ostermeyer-Fay AG, Matundan RA, Brown DA: **Clathrin-independent endocytosis of ErbB2 in geldanamycin-treated human breast cancer cells.** *J Cell Sci* 2008, **121**:3155-3166.

45. Marx C, Held JM, Gibson BW, Benz CC: **ErbB2 trafficking and degradation associated with K48 and K63 polyubiquitination.** *Cancer Res* 2010, **70**:3709-3717.

46. Small EJ, Schellhammer PF, Higano CS, Redfern CH, Nemunaitis JJ, Valone FH, Verjee SS, Jones LA, Hershberg RM: **Placebo-controlled phase III trial of immunologic therapy with sipuleucel-T (APC8015) in patients with metastatic, asymptomatic hormone refractory prostate cancer.** *J Clin Oncol* 2006, **24**:3089-3094.

47. Kantoff PW, Schuetz TJ, Blumenstein BA, Glode LM, Bilhartz DL, Wyand M, Manson K, Panicali DL, Laus R, Schlom J, Dahut WL, Arlen PM, Gulley JL, Godfrey WR: **Overall survival analysis of a phase II randomized controlled trial of a Poxviral-based PSA-targeted immunotherapy in metastatic castration-resistant prostate cancer.** *J Clin Oncol* 2010, **28**:1099-1105.

Breast Cancer
R E S E A R C H

RESEARCH ARTICLE   **Open Access**

Amplification and high-level expression of heat shock protein 90 marks aggressive phenotypes of human epidermal growth factor receptor 2 negative breast cancer

Qing Cheng[1*], Jeffrey T Chang[5], Joseph Geradts[2], Leonard M Neckers[6], Timothy Haystead[3], Neil L Spector[4] and H Kim Lyerly[1,2*]

Abstract

Introduction: Although human epidermal growth factor receptor 2 (HER2) positive or estrogen receptor (ER) positive breast cancers are treated with clinically validated anti-HER2 or anti-estrogen therapies, intrinsic and acquired resistance to these therapies appears in a substantial proportion of breast cancer patients and new therapies are needed. Identification of additional molecular factors, especially those characterized by aggressive behavior and poor prognosis, could prioritize interventional opportunities to improve the diagnosis and treatment of breast cancer.

Methods: We compiled a collection of 4,010 breast tumor gene expression data derived from 23 datasets that have been posted on the National Center for Biotechnology Information (NCBI) Gene Expression Omnibus (GEO) database. We performed a genome-scale survival analysis using Cox-regression survival analyses, and validated using Kaplan-Meier Estimates survival and Cox Proportional-Hazards Regression survival analyses. We conducted a genome-scale analysis of chromosome alteration using 481 breast cancer samples obtained from The Cancer Genome Atlas (TCGA), from which combined expression and copy number data were available. We assessed the correlation between somatic copy number alterations and gene expression using analysis of variance (ANOVA).

Results: Increased expression of each of the heat shock protein (HSP) 90 isoforms, as well as HSP transcriptional factor 1 (*HSF1*), was correlated with poor prognosis in different subtypes of breast cancer. High-level expression of *HSP90AA1* and *HSP90AB1*, two cytoplasmic HSP90 isoforms, was driven by chromosome coding region amplifications and were independent factors that led to death from breast cancer among patients with triple-negative (TNBC) and HER2-/ER+ subtypes, respectively. Furthermore, amplification of *HSF1* was correlated with higher *HSP90AA1* and *HSP90AB1* mRNA expression among the breast cancer cells without amplifications of these two genes. A collection of *HSP90AA1*, *HSP90AB1* and *HSF1* amplifications defined a subpopulation of breast cancer with up-regulated HSP90 gene expression, and up-regulated HSP90 expression independently elevated the risk of recurrence of TNBC and poor prognosis of HER2-/ER+ breast cancer.

Conclusions: Up-regulated HSP90 mRNA expression represents a confluence of genomic vulnerability that renders HER2 negative breast cancers more aggressive, resulting in poor prognosis. Targeting breast cancer with up-regulated HSP90 may potentially improve the effectiveness of clinical intervention in this disease.

* Correspondence: q.cheng@duke.edu; kim.lyerly@dm.duke.edu
[1]Department of Surgery, Duke University Medical Center, Box 2606, 203 Research Drive, Durham, NC 27710, USA
Full list of author information is available at the end of the article

BioMed Central

Introduction

Despite the progress that has been made in reducing mortality rates of breast cancer in the most recent time period, more than 40,000 breast cancer deaths occur in the United States annually [1]. Substantial progress in treatment requires identification of a specific set of actionable genomic abnormalities that drive or facilitate tumorigenesis, resistance to a given treatment and recurrence. Although significant amounts of gene expression profile analyses have been performed in breast cancers, assessing expression levels as the primary parameter to characterize breast cancers may be confounded by the phenotypic heterogeneity that arises as a consequence of abnormal signaling nodes and extensive biological cross-talk and redundancy. On the other hand, copy number aberrations in cancer cells can quantitatively affect gene function [2], and multiple copy number aberrations collectively regulate clinical phenotypes and cancer prognosis [3]. Analyses of chromosomal copy number aberrations (CNAs) have been proposed as a critical indicator of the possible location of aggressive cancer phenotype related genes [4,5]. Therefore, we undertook an integrative analysis of copy number and gene expression in a large population study to identify molecular factors abundant in breast cancer cells, especially in those characterized by aggressive behavior and poor prognosis, by which to prioritize interventional opportunities to transform breast cancer diagnosis, characterization, treatment and ultimately prevention.

Although a number of aberrant signaling pathways in breast cancer have been identified, heat shock protein 90 (HSP90), which is one of the most abundant proteins in mammalian cells [6], plays an important role in folding newly synthesized proteins or stabilizing and refolding denatured proteins after stress, and would influence a large number of signaling pathways. To date, more than 200 HSP90 clients have been identified, including key regulators in signal transduction and cell cycle control, steroid hormone receptors, and tyrosine and serine/threonine kinases [7-9]. HSP90 exists as multiple isoforms that include HSP90AA1 (an inducible form) and HSP90AB1 (a constitutive form) in cytoplasm, HSP90B1 in endoplasmic reticulum and TRAP1 in mitochondria [10]. However, unlike HSP90AA1 and HSP90AB1, the client proteins selectively interacting with HSP90B1 or TRAP1 chaperones have yet to be defined.

HSP90 contains an N-domain ATP binding site and its ATPase activity is necessary for all of its cellular functions [11]. *In vivo* Hsp90 does not function alone but acts in concert with co-chaperones such as Sba1/p23 and Cdc37[8]. Interactions with co-chaperones are thought to be important to direct Hsp90 function for specific physiological processes such as regulation of cell cycle progression, apoptotic responses, or kinase-mediated signaling cascades [10]. The protein is regulated both at the expression level and through posttranslational modifications such as phosphorylation, acetylation and methylation. These processes control its ATPase activity, and its ability to interact with its clients and co-chaperones, as well as its degradation [6,7]. In addition, HSP90 has a higher affinity for amino–terminal ligands in cancer cells, compared with the HSP90 in normal cells[12].

In breast cancer, HSP90 is required for the stabilization of many proteins in pathways that play key roles in cancer growth and survival, such as estrogen receptor (ER), progesterone receptor (PR), essential components of HER2 signaling (HER2, AKT, c-SRC, RAF and HIF-1α), and EGFR [9,13]. For example, HER2 is among the most sensitive client proteins of HSP90 [14,15], and HSP90 inhibition mediates degradation of HER2, as well as PI3K and AKT in HER2-overexpressing cancer cells [16]. Consequently, HSP90 inhibitors plus trastuzumab have significant anticancer activity in patients with HER2-positive, metastatic breast cancer previously progressing on trastuzumab[17]. Although a number of agents are in development for HER2+ and ER+ breast cancers, HSP90 inhibitors also represent therapeutic opportunities in other molecular subtypes. Triple negative breast cancer (TNBC) is defined by the clinical laboratory evaluation revealing a lack of expression of ER, PR and HER2 receptors, accounts for 10% to 20% of all breast cancer[18], and has a higher rate of distant recurrence and a poorer prognosis than other breast cancer subtypes [19,20]. Unfortunately, the lack of expression of a credentialed therapeutic target in this subtype of breast cancer limits the effective treatment options. Of interest, TNBCs often express increased EGFR protein, but in early clinical trials, response rates to EGFR inhibitors were minimal.

One potential therapeutic opportunity in tumor subtypes that do not have a known therapeutic target could include targeting Hsp90 function. Although Hsp90 protein expression was reported to be relatively low in TNBC compared to other subtypes, this early report only evaluated nine tumors [21]. More encouragingly, in pre-clinical models, TNBCs have been sensitive to Hsp90 inhibitors [22,23]. Similarly to HER2 positive tumors, TNBCs were sensitive to Hsp90 inhibition through down-regulation of components of the Ras/Raf/MARK pathway in preclinical and *in vitro* studies [23]. Being a central integrator of multiple pathways, activation of HSP90 may maintain the malignant phenotype, facilitate metastasis, and promote treatment-resistance under the stress of cancer therapy in multiple breast

cancer subtypes. It has been suggested that Hsp90 up-regulation may be a sign of poor disease prognosis [24] and a recent study has demonstrated that co-expression of HSP90 and PI3K or expression of HSP90 in combination with the loss of PTEN were associated with significantly worse recurrence-free survival in patients with breast cancer [25]. However, adequately powered population studies correlating up-regulated HSP90 with prognosis in breast cancer patients have not been performed to date.

In this study, we exploited the availability of publicly available data and performed a genome scan for somatic copy number aberrations and gene expression profiling of primary breast tumors to address the general prognostic significance of gene amplification and high-level expression in breast cancer. We found that up-regulated HSP90 was one of the most significant poor prognosis factors in triple negative and HER2-/ER+ breast cancer subtypes. Our result suggested that targeting breast cancer with up-regulated HSP90 would potentially reduce the risk of lethal recurrence and distant metastasis.

Materials and methods
Human breast tumor samples and data collection
A total of 4,010 breast cancer gene expression profiles were collected from 23 independent data sets (GSE22093, GSE17705, GSE11121, GSE12093, GSE7390, GSE5327, GSE6532, GSE1456, GSE2034, GSE3494, GSE26639, GSE20685, GSE23720, GSE21653, GSE16446, GSE23177, GSE19615, GSE12276, GSE9195, GSE17907, GSE16391, GSE22035 and GSE5460) that were on NCBI Gene Expression Omnibus (GEO). Primary breast tumor samples were obtained before treatment and gene expression profiles were measured using Affymetrix U133A or U133 Plus 2.0 expression array. Each dataset selected for this study should have either clinical outcome data and/or HER2, ER or PR status determined by immunohistochemistry (Additional file 1). Patients' unique IDs were also collected from series matrix files (GEO) to ensure there is no redundant sample set. In addition, we successfully processed somatic copy number alterations (CNAs) of 481 breast invasive carcinoma samples that were measured using Affymetrix Genome-Wide Human SNP Array 6.0, of which gene expression profiles of the same set of primary tumor samples were also measured using Agilent Expression 244 K microarrays by The Cancer Genome Atlas Project (TCGA).

Processing of gene expression data
Raw Affymetrix expression CEL files from each dataset were RMA (Robust Multi-array Average) normalized independently using Expression Console Version 1.1 (Affymetrix). All data were filtered to include those
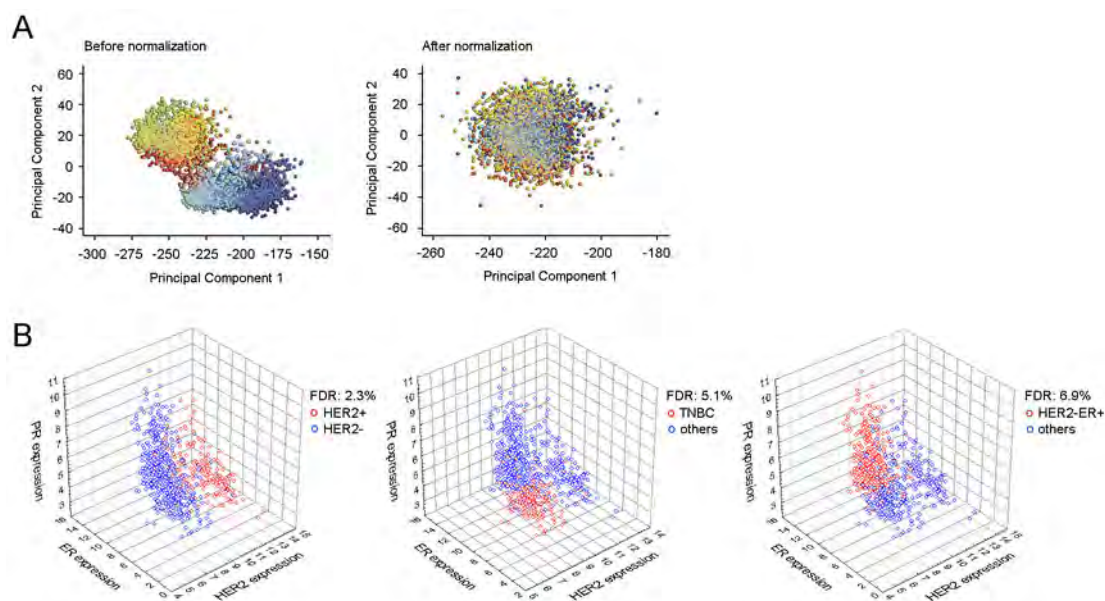
probes on the HG-U133A platform. Assuming that the signal from the 69 Affymetrix control probes should be invariant, we found the structure in those probes by taking the first 15 principal components, and then removed the contribution of those patterns in the expression of genes using Bayesian Factor Regression Modeling (BFRM) [26]. A Principal Component Analysis (PCA) and Heatmap were used to confirm dataset normalization (Figure 1 and Additional file 2). By this procedure, we generated a normalized gene expression dataset compiling 4,010 breast tumor samples.

Copy number analyses
Somatic copy number alterations (CNAs) of invasive breast cancer samples collected from 517 female patients were measured using Affymetrix Genome-Wide Human SNP Array 6.0. CEL files were available from TCGA. SNP array data from matched blood lymphocytes or matched normal tissue were also available for 494 patients. We generated a canonical genotype cluster using a data set of 799 Affymetrix Genome-Wide Human SNP 6.0 arrays that measured from normal blood lymphocytes obtained from TCGA. In total, 1,831,105 SNP and copy number markers were analyzed to construct canonical clustering positions and Log R ratio (LRR) and B allele frequency (BAF) from raw CEL files were calculated using PennCNV-Affy [27]. Matched normal samples were genotyped using Affymetrix genotyping console (version 4) and all samples were compared to ensure there was no duplication. All copy number markers and SNPs with genotype call rate higher than 90% were selected for tumor copy number analysis, and CNA calls were generated using genoCN software [28]. Genotype calls from normal tissues of the same individual were applied for genoCNA analysis, if they were available. Thirty-six samples that failed to obtain estimated parameters after 200 iterations of EM were removed from further study. All probe coordinates were mapped to the human genome assembly build 36 (hg18). In total, tumor copy number on chromosome 1-22 and chromosome X were successfully measured in 481 TCGA breast tumor samples, and normalized gene expression data from the same set of samples were downloaded from TCGA.

Statistics analyses
We downloaded the Affymetrix U133A annotation file (hg18) from Affymetrix and removed probe sets that do not have a matched gene symbol or whose probe set's alignment did not match with gene chromosome location (pseudogenes). Using all 4,010 samples, we defined the gene expression level at each probe set as low-level expression (bottom 10% low expression value), intermediate-level expression (middle 80% expression value)

Figure 1 Analysis of 4,010 breast cancer sample. **(A)** PCA plots of before normalization and after normalization. These plots show the gene expression profiles of the samples plotted on the first two principal components. Each point represents a sample, and samples from the same data set have the same color. If there are batch effects, the samples from the same data set (the same color) will cluster together. If there are no batch effects, the colors should be mixed. **(B)** Prediction of HER2+, TNBC and HER-/ER+ breast cancer subtypes using HER2, ER and PR mRNA expression levels.

and high-level expression (top 10% high expression value), and compared survival differences among those three groups using Cox-regression survival analyses. Co-efficiency was used to ensure if high-level expression was associated with poor prognosis and low-level expression was correlated with better outcome. A total of 11,761 known genes were analyzed. Statistical analyses were performed using R Project for Statistical Computing (Augasse, Austria), Matlab (Natick, MA, USA) or STATISTICA (Tulsa, OK, USA). Kaplan-Meier survival analyses on selected genes were conducted using GraphPad (La Jolla, CA, USA).

To measure the correlation between copy number aberration and gene expression, we generated copy number calls at 1,794,774 probes on chromosome 1-22 and chromosome X from all samples, including 857,551 SNPs and 937,223 CN markers. We determined copy number calls at each marker site as homozygous deletion (CN = 0), hemizygous deletion (CN = 1), normal copy number (CN = 2), low level amplification (CN = 3) and high level amplification (CN ≥4). We downloaded normalized expression data (level 2) from the TCGA database and analyzed the association between copy number and gene expression using analysis of variance (ANOVA). Associated region was defined as the region that should cover at least five consecutive SNPs or CN markers and should be longer than 10 kb. Direct correlation was defined as amplification associated with high-

level expression and deletion was correlated with low-level expression.

Results

Analysis of 4,010 breast cancer samples

To conduct a genome wide survey for poor prognosis-associated genes in breast cancer, we compiled a collection of breast tumor gene expression data ($n = 4,010$) derived from 23 datasets that were posted on the NCBI Gene Expression Omnibus (GEO, Table 1) and normalized by Bayesian Factor Regression Modeling (BFRM) to remove technical variation (Figure 1A; Additional file 2) [26]. In addition to the raw expression data, we also obtained clinical outcome data from a subset of the samples (Additional file 1), which included data on overall survival ($n = 1,027$), recurrence-free survival ($n = 1,372$), and distant metastasis free survival ($n = 2,187$), as well as disease specific survival (event of death from breast cancer, $n = 395$).

As shown in Table 1, the majority of samples lacked the molecular analysis of HER2, ER and PR expression as measured by immunohistochemistry (IHC) or fluorescent *in situ* hybridization (FISH) analysis. Nevertheless, we found significant correlations between mRNA expression level and reported HER2, ER or PR status measured by IHC ($P < 1 \times 10^{-8}$, Mann-Whitney U test, Additional file 3), which was consistent with previous reports that ER, HER2 and PR biochemical status was concordant with Affymetrix microarray data [29,30]. By

Table 1 Summary of 23 data sets.

Data set	Institution	Array Platform	number of array	prognosis	IHC	Ref.
GSE22093	UT MD Anderson, TX, USA	HG-U133A	82		ER	[43]
GSE17705	Nuvera Biosciences, MA, USA	HG-U133A	298	dmfs	ER	[44]
GSE11121	Bayer Technology Services GmbH, Leverkusen, Germany	HG-U133A	200	dmfs		[45]
GSE12093	Veridex LLC, CA, USA	HG-U133A	136	dmfs		[46]
GSE7390	Institut Jules Bordet, Bruxelles, Belgium	HG-U133A	198	os, rfs, dmfs	ER	[47]
GSE5327	University of Chicago, IL, USA	HG-U133A	58	dmfs		[48]
GSE6532	Institut Jules Bordet, Bruxelles, Belgium	HG-U133A, HG-U133_Plus_2	414	rfs, dmfs	ER, PR	[49]
GSE1456	Karolinska Institutet, Stockholm, Sweden	HG-U133A	159	os, rfs, dmfs, Death_fromBC		[50]
GSE2034	Veridex, CA, USA	HG-U133A	286	rfs	ER	[51]
GSE3494	Genome Institute of Singapore, Singapore	HG-U133A	251	Death_fromBC	ER, PR	[52]
GSE26639	Institut Curie, Paris, France	HG-U133_Plus_2	226		HER, ER, PR	[53]
GSE20685	Koo Foundation SYS Cancer Center, Taiwan	HG-U133_Plus_2	327	os, mfs		[54]
GSE23720	Institut Paoli-Calmettes, Marseille, France	HG-U133_Plus_2	197		ER, PR	[55]
GSE21653	Institut Paoli-Calmettes, Marseille, France	HG-U133_Plus_2	266	dmfs	HER2, ER, PR	[56]
GSE16446	Institut Jules Bordet, Bruxelles, Belgium	HG-U133_Plus_2	120	os, dmfs	HER2, PR	[57]
GSE23177	Flanders Institute for Biotechnology, Leuven, Belgium	HG-U133_Plus_2	116		HER2, ER	[58]
GSE19615	Dana-Farber Cancer Institute, MA, USA	HG-U133_Plus_2	115	dmfs	HER2, ER, PR	[59]
GSE12276	Erasmus Medical Centre, Rotterdam, Netherlands	HG-U133_Plus_2	204	rfs		[60]
GSE9195	Institut Jules Bordet, Bruxelles, Belgium	HG-U133_Plus_2	77	rfs, dmfs	ER, PR	[61]
GSE17907	Institut Paoli-Calmettes, Marseille, France	HG-U133_Plus_2	55	mfs	HER2, ER, PR	[62]
GSE16391	Institut Jules Bordet, Bruxelles, Belgium	HG-U133_Plus_2	55	rfs	HER2, ER, PR	[63]
GSE22035	Centre Rene Huguenin, SAINT-CLOUD, France	HG-U133_Plus_2	43		ER	[64]
GSE5460	Dana-Farber Cancer Institute, MA, USA	HG-U133_Plus_2	127		HER2, ER	[65]

fitting two normal distributions of mRNA expression into IHC positive and negative groups, we identified a bimodal cutoff that represents maximum likelihood of IHC status, using samples where the biochemical status of HER2 ($n = 1,004$), ER ($n = 2,771$) and PR ($n = 1,559$) was available [29], and then applied this predictive cutoff to the entire set of 4,010 samples (Additional file 4). Clinical outcomes of gene expression defined subtypes were highly concordant with IHC subtypes (Additional file 4). When mRNA expression of *HER2*, *ER* and *PR* were applied together, the over-all accuracy for HER2+, triple-negative and HER2-/ER+ was 91.7%, 91.5%, and 89.6%, respectively, comparing with the biochemical defined breast cancer subtypes (Figure 1).

Genome-scan of copy number aberration in 481 breast cancer samples

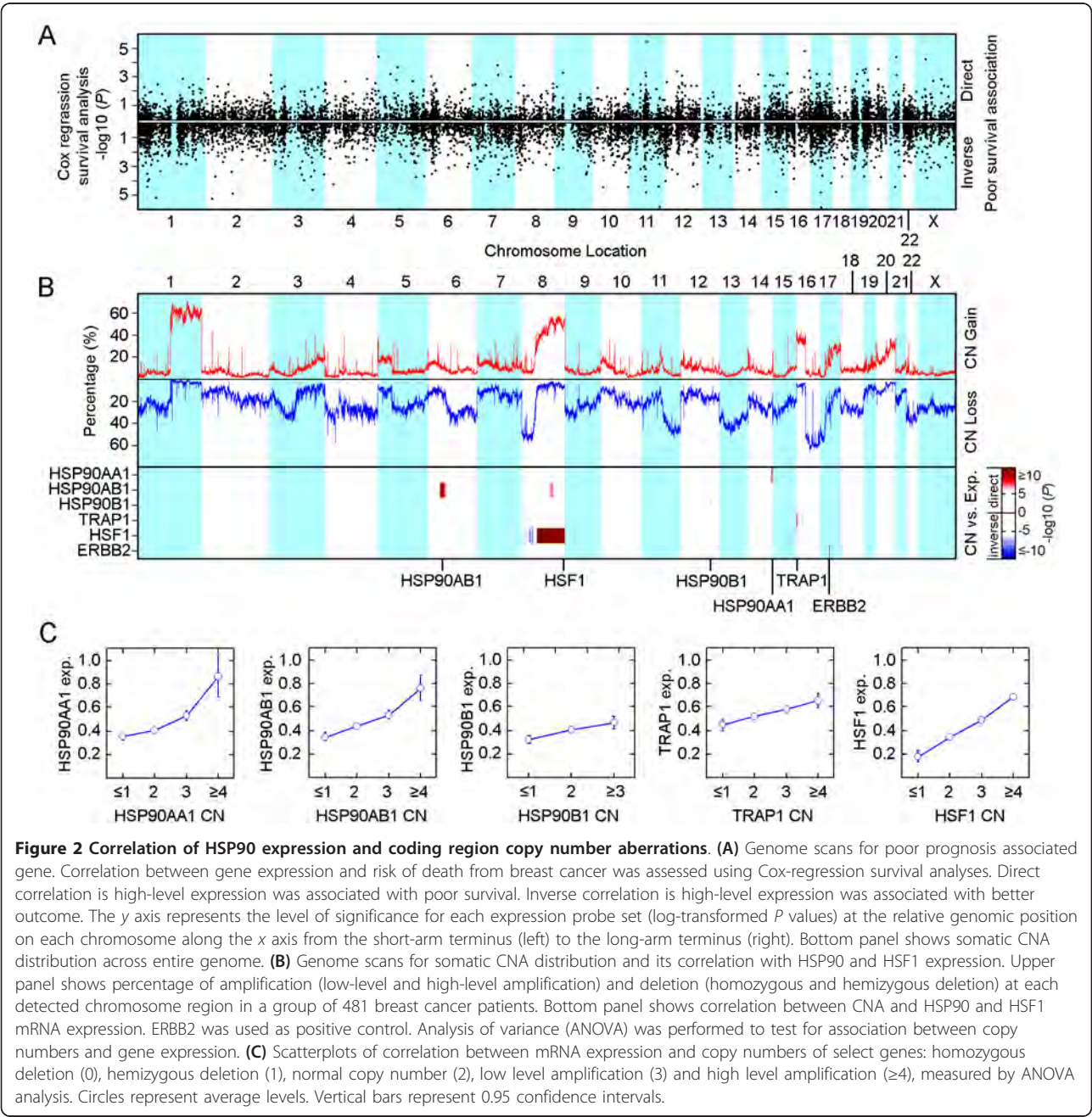Chromosomal aberrations reflect oncogene activation and loss of tumor suppressor genes. Surveys of DNA gain or loss have been considered a fertile area to search for determinants of treatment response and disease outcome in human cancer cells. In breast cancer, it has been reported that 44% to 62% of highly amplified genes were over-expressed [31,32] and at least 12% of the total variation in gene expression was directly attributed to copy number aberrations [33]. TCGA data provide a unique opportunity to enable different and potentially complementary forms of analysis of cancer phenotypes given the comprehensive nature of the datasets generated in this effort. We were particularly interested in the opportunity to link genomic copy number alterations with the observed gene expression profile and clinical data as a strategy to identify genomic determinants of poor prognosis. We therefore performed a genome-scale analysis of chromosome alteration using 481 breast cancer samples obtained from the TCGA project, from which combined expression and copy number data were

available. We revealed the distribution of copy number amplifications and deletions across the entire genome (Figure 2). As expected, we observed that 23.7% of breast cancer samples had amplification (CN ≥3) on the *HER2* coding region. Although copy number abnormalities on chromosome 1, 8, 11 and 16 are more common in studied populations (n = 481), we found that in most chromosome regions, both amplifications (CN ≥3) and deletions (CN ≤1) occurred in approximately 10% of analyzed samples (Figure 2).

Identification of genes that were correlated with risk of death from breast cancer

The large cohort of 4,010 gene expression samples provided an opportunity to define a subpopulation of patients containing either extremely high or low expression levels of candidate genes and to identify genes whose high-level expression is predominant in a poor prognosis stage compared to a better prognosis stage. To determine poor prognosis-associated genes, we performed two stage analyses. In the first stage, we selected

Figure 2 Correlation of HSP90 expression and coding region copy number aberrations. **(A)** Genome scans for poor prognosis associated gene. Correlation between gene expression and risk of death from breast cancer was assessed using Cox-regression survival analyses. Direct correlation is high-level expression was associated with poor survival. Inverse correlation is high-level expression was associated with better outcome. The *y* axis represents the level of significance for each expression probe set (log-transformed *P* values) at the relative genomic position on each chromosome along the *x* axis from the short-arm terminus (left) to the long-arm terminus (right). Bottom panel shows somatic CNA distribution across entire genome. **(B)** Genome scans for somatic CNA distribution and its correlation with HSP90 and HSF1 expression. Upper panel shows percentage of amplification (low-level and high-level amplification) and deletion (homozygous and hemizygous deletion) at each detected chromosome region in a group of 481 breast cancer patients. Bottom panel shows correlation between CNA and HSP90 and HSF1 mRNA expression. ERBB2 was used as positive control. Analysis of variance (ANOVA) was performed to test for association between copy numbers and gene expression. **(C)** Scatterplots of correlation between mRNA expression and copy numbers of select genes: homozygous deletion (0), hemizygous deletion (1), normal copy number (2), low level amplification (3) and high level amplification (≥4), measured by ANOVA analysis. Circles represent average levels. Vertical bars represent 0.95 confidence intervals.

a universal cut-off and assigned each of the 4,010 samples into low, intermediate and high expression categories for each of 11,761 known genes. Then, we carried out an unbiased, genome wide Cox-regression survival analysis, comparing the prognosis difference among those three groups. By doing this, poor prognosis-associated genes should show a poor prognosis in the high expression group and a better outcome in the low expression group. In the second stage, we further assessed the poor prognosis correlation of the identified genes using gene-expression as a continuous variable and sought to correlate copy number aberrations with gene expression by measuring if amplification was correlated with high-level expression and deletion was associated with low-level expression.

Starting with the extreme, we defined the lowest 10% of expression values across the entire 4,010 samples as low-level expression and the highest 10% of expression values as high-level expression. Using death from breast cancer as the incident event, we carried out a genome wide Cox-regression survival analysis and identified 152 genes whose high-level expression was significantly associated with higher risk of death from breast cancer ($P < 0.01$, Figure 2 and Additional file 5). In addition, we assigned each of the 4,010 samples into first quartile (lowest 25%), second quartile (intermediate 50%) and third quartile (highest 25%) subgroups according to the expression levels of the 152 identified genes, and compared prognosis differences among these subgroups. Furthermore, we applied expression signal as a continuous variable to measure the distribution of the identified genes. A total of 47 of the 152 genes showed linear correlation between increased expression and poor prognosis. The highest risk of death from breast cancer was observed in patients with either top 10% or 25% higher level gene expression ($P < 0.05$, Additional file 5).

Since amplifications or deletions are likely to control the expression of genes within the corresponding region, and the correlation between copy number and expression has been recently suggested as an approach to predict the authentic molecular drivers in carcinogenesis [34], we then extended this analysis of gene expression to assess the correlation between somatic copy number alterations and gene expression using 481 invasive breast cancer samples obtained from TCGA. We found that 26 of 47 poor prognosis-associated genes showed a significant correlation between copy number aberrations and mRNA expression ($P < 1 \times 10^{-8}$, ANOVA, Additional file 5 and Additional file 6). To support this modeling, we analyzed the expression of HER2, a well known oncogene associated with poor prognosis based on increased copy number and high gene expression. As expected, high-level expression of *HER2* was driven by coding region amplification and was significantly

associated with poor prognosis (Additional file 5). Importantly, we found both cytoplasmic HSP90 isoforms, *HSP90AA1* and *HSP90AB1*, were among the most significant factors that led to higher risk of death from breast cancer, indicating that HSP90 plays an important role in modulating poor prognosis phenotypes in breast cancer (Additional file 5).

Increasing expression of HSP90 was correlated with poor prognosis of breast cancer

To address the extent to which HSP90 is a prognostic factor in breast cancer, we analyzed the correlation between HSP90 expression and clinical disease outcomes, such as survival, recurrence, and metastasis, in different subtypes of breast cancer. Other HSP90 isoforms, such as *HSP90B1* and *TRAP1*, may affect treatment responses in specific subtypes of breast cancer and this effect could be largely diluted in the analysis of a heterologous population. Therefore, *HSP90B1* and *TRAP1*, as well as HSP transcriptional factor 1 (*HSF1*), were also included.

We assessed the correlation between mRNA expression and poor prognosis in different breast cancer subtypes using Cox-regression survival analysis and compared survival differences between high-level expression (top 10% or 25%) and low-level expression groups using Kaplan-Meier Estimated survival analysis. To elucidate if high-level expression of HSP90 isoforms were truly independent prognostic factors, we conducted Cox Proportional-Hazards Regression (COXPH) survival analyses to quantify the weight of the hazard ratios associated with high expression and their significance when considered alongside other clinical variables, such as size, grade, nodal status, age, HER2, ER and PR, in the whole cohort and in the relevant subtype of cancer.

We found that high-level expression of *HSP90AA1* independently led to higher risk of death from breast cancer in TNBC, while *HSP90AB1* caused poor survival among patients with the HER2-/ER+ breast cancer subtype through increased risk of distant metastasis (Table 2 and Additional file 7). High-level expression of *HSP90AB1* was an independent factor affecting disease-specific survival (death from breast cancer) and over-all survival of breast cancer (Table 2). In addition to these findings, we found that a higher risk of recurrence in HER2+ and HER2-/ER+ breast cancer subtypes was significantly correlated with increased expression of *HSP90AA1* and *HSP90B1*; and increasing expression of *HSP90AA1* and *HSP90AB1* were significantly associated with a higher chance of distant metastasis in patients with HER2-/ER+ tumor (Additional file 7).

Among patients with TNBC, higher expression of HSP90 isoforms (*HSP90AA1, HSP90AB1, HSP90B1* and *TRAP1*) was correlated with higher risk of recurrence.

Table 2 Prognosis of HSP90AA1 and HSP90AB1 in different subtypes of breast cancer.

| Subtype | Gene | Cox-regression analysis | | Kaplan-Meier survival analysis | | | | | COXPH survival analysis | | |
| | | | | High 25% vs. others | | High 10% vs. others | | | High 10% vs. others | | |
		P-value	n	*P*-value	HR(95%CI)	*P*-value	HR(95%CI)	n	*P*-value	*P*-adjusted	n
All samples	HSP90AA1	0.0020	395	0.0499	1.75(1.00-3.06)	0.0241	2.81 (1.15-6.90)	395	0.0193	0.3320	225
(dss)	HSP90AB1	0.0136		0.0404	1.72(1.02-2.90)	0.0011	3.69 (1.68-8.07)		0.0022	0.0008	
All samples	HSP90AA1	0.0081	1072	0.0384	1.39(1.02-1.89)	0.0002	2.55(1.55-4.21)	1072	0.0048	0.1069	421
(os)	HSP90AB1	0.0175		0.0401	1.36(1.01-1.83)	0.0024	2.06(1.29-3.28)		0.0010	0.0022	
HER2+	HSP90AA1	0.7459	194	0.694	0.89(0.50-1.60)	0.1523	2.07(0.76-5.61)	194	0.4364	0.2703	63
(os)	HSP90AB1	0.5693		0.6728	1.15(0.59-2.24)	0.3733	1.76(0.51-6.13)		4.90E-08	0.1839	
HER2-ER+	HSP90AA1	0.1057	506	0.0706	1.52(0.97-2.39)	0.0563	1.92(0.98-3.75)	506	0.1593	0.5829	228
(os)	HSP90AB1	0.0015		0.0918	1.44(0.94-2.20)	0.0005	3.04 (1.63-5.68)		1.53E-05	0.0004	
TNBC	HSP90AA1	0.0049	282	0.0302	2.07(1.07-3.98)	< 0.0001	16.9(4.66-60.9)	282	0.0079	0.0394	105
(os)	HSP90AB1	0.1328		0.0483	1.82(1.00-3.30)	0.2936	1.83 0.59-5.66)		0.4344	0.9968	

Cox-regression survival analysis was performed using gene expression signal as continuing variable. CI, confidence interval; Dss, disease specific survival (death from breast cancer); HR, Hazard Ratio; n: number of samples; os, over-all survival.

However, these significant interactions were not observed after adjusted multiple clinical availables. This might be affected by the fact that the entire set of clinical variables were only available in a small proportion of the samples. It also indicated that a single HSP90 isoform might only have a slight influence on disease outcome, such that when several interactions occur together, the combined effect becomes clinically significant. Nevertheless, high-level expression of *HSF1* was an independent factor for recurrence in TNBC (Additional file 7).

Amplifications of *HSP90AA1*, *HSP90AB1* and *HSF1* collectively defined a subpopulation of breast cancer samples with up-regulated HSP90 gene expression

We found a significant association between gene expression and copy number aberrations in *HSP90AA1*, *HSP90AB1*, *TRAP1* and *HSF1* ($P < 1 \times 10^{-8}$, ANOVA; Figure 2) and a trend for significant correlation in *HSP90B1* ($P < 1 \times 10^{-5}$, ANOVA; Figure 2), indicating that high-level expression of HSP90 and HSF1 was driven by gene amplification. Although hemizygous deletion of HSP90 isoforms and *HSF1* were found in 4.37% to 18.09% of breast cancer samples, homozygous deletion was uncommon. Only 1 of 481 (2%) breast cancer samples had two allele deletions on the *TRAP1* coding region, and no patients carried a homozygous deletion of other HSP90 isoforms and HSF1, suggesting that loss of expression of HSP90 is a rare event in breast cancer.

We observed that 8% of breast cancer samples carried amplifications (both high-level and low-level amplifications, CN ≥3) of *HSP90AA1*, leading to a higher expression of *HSP90AA1*, compared with samples without *HSP90AA1* amplifications ($P = 7.67 \times 10^{-8}$, $n = 481$, Mann-Whitney U Test; Figure 3A). Similarly, amplifications (CN ≥3) of *HSP90AB1* were found in 11% of the

population, and were correlated with significantly higher expression of *HSP90AB1* ($P = 1.02 \times 10^{-8}$, $n = 481$, Mann-Whitney U Test, Figure 3A). Although amplification (CN ≥3) of *HSF1* coding regions was a common event in the studied samples (54.1%), high-level amplification (CN ≥4) of *HSF1* was found in 16% of the population, in which 75% of the samples did not have a co-amplification of either *HSP90AA1* or *HSP90AB1* (Figure 3B). Among the samples without amplifications of *HSP90AA1* or *HSP90AB1*, high-level amplification of *HSF1* was significantly correlated with higher expression of *HSP90AA1* ($P = 0.0052$, $n = 422$, Mann-Whitney U Test) and *HSP90AB1* ($P = 4.5 \times 10^{-7}$, $n = 428$, Mann-Whitney U Test), respectively (Figure 3A). Furthermore, amplification of *HSP90AA1* and/or high-level amplification of *HSF1* collectively represents a group of breast cancer samples with up-regulated *HSP90AA1* mRNA expression ($P = 9.62 \times 10^{-8}$, $n = 481$, Mann-Whitney U Test, Figure 3A). Up-regulated *HSP90AB1* mRNA expression was also seen in samples with amplification of *HSP90AB1* and/or high-level amplification of *HSF1* ($P = 5.72 \times 10^{-14}$, $n = 481$, Mann-Whitney U Test, Figure 3A).

On the other hand, we found that amplification of *HSP90AA1* and *HSP90AB1* was a predominant genomic feature of the highest 10% of *HSP90AA1* ($P = 0.0001$, $n = 481$, Fisher's exact Test) and *HSP90AB1* ($P = 2.71 \times 10^{-6}$, $n = 481$, Fisher's exact Test) expressing tumors. High-level amplification of *HSF1* (CN ≥4) was significantly enriched in the samples with the highest 20% of *HSF1* ($P = 3.30 \times 10^{-10}$, $n = 481$, Fisher's exact Test) expressing tumors. When samples with the highest 10% of *HSP90AA1* and/or highest 10% of *HSP90AB1* expressing tumors were combined with the highest 20% of *HSF1* expressing tumors, this collective set of samples clearly captured the subpopulation of amplified HSP90

Figure 3 Prognosis of up-regulated HSP90. (A) Correlation between *HSP90AA1*, *HSP90AB1* and *HSF1* copy number aberrations and *HSP90AA1* and *HSP90AB1* expression. Differences between up-regulated HSP90 and others were assessed using the exact Mann-Whitney U test. Boxes represent the 25% to 75% quartiles, lines *in the boxes* represent the median level, whiskers represent the non-outlier range, and circles represent the outliers. **(B)** Distribution of *HSP90AA1*, *HSP90AB1* and *HSF1* copy number aberrations across 481 TCGA samples. **(C)** Prognosis of high-level expression of *HSP90AA1* or *HSP90AB1*, and up-regulated HSP90. Kaplan-Meier estimates of disease specific survival (event of death from breast cancer) in 395 breast cancer patients (number of events, *n* = 83) and over-all survival in 1,027 breast cancer patients (number of events, *n* = 248). *P* values were calculated using log-rank Mantel-cox test. Tick marks indicate patients whose data were censored by the time of last follow-up.

(P = 3.99 × 10^{-25}, *n* = 481, Fisher's exact Test). Because high expression of *HSP90AA1*, *HSP90AB1* and *HSF1* was driven by amplification, and high-level amplification of *HSF1* was associated with higher expression of HSP90 in un-amplified HSP90 samples, we defined up-regulated HSP90 as a collection of samples with the top 10% high expression value of *HSP90AA1* and/or *HSP90AB1*, and the top 20% higher expression of *HSF1*. Using these definitions, up-regulated HSP90 accounted for 31% of the breast cancer population (Additional file 1) and up-regulated HSP90 was significantly correlated with higher expression of all HSP90 isoforms ($P < 1 \times 10^{-8}$, Mann-Whitney U test, Additional file 8).

Up-regulated HSP90 was independently correlated with poor prognosis in HER2 negative breast cancer subtypes

To investigate the correlation of up-regulated HSP90 and poor breast cancer prognosis, we performed a univariate Kaplan-Meier survival analysis and a multivariate Cox Proportional-Hazards Regression (COXPH) survival analysis using other poor clinical outcome-associated clinical cofactors, such as tumor size, grade, nodal status, age, HER2, ER and PRstatus, as co-variants. We found that up-regulated HSP90 was significantly associated with a higher risk of death from breast cancer (P = 0.0049, *n* = 395, Figure 3B) and poor overall survival in a subset of 1,027 patients in which overall survival

data were available ($P = 0.0034$, log-rank Mantel-cox test, Figure 3C). This poor prognosis phenotype was independent of clinical cofactors ($P = 0.0062$, $n = 421$, COXPH test, Table 3 and Additional file 9). Furthermore, we found that up-regulated HSP90 was significantly associated with a higher risk of recurrence and distant metastasis in TNBC and breast cancer with the HER2-/ER+ phenotype (Additional file 10). Up-regulated HSP90 was an independent factor that led to higher risk of death from breast cancer in the HER2-/ER+ breast cancer subtype ($P = 0.0042$, $n = 421$, COXPH test, Table 3), with a trend of significantly higher risk of distant metastasis in this subtype (Table 3). Particularly, up-regulated HSP90 independently increased risk of recurrence in TNBC ($P = 0.0101$, $n = 421$, COXPH test, Table 3; Additional file 9), and more than 70% of TNBC patients with up-regulated HSP90 had disease recurrence within eight years after initial treatment (Additional file 10).

Discussion

The phenotypic heterogeneity of cancer arises as a consequence of numerous genetic abnormalities (such as somatic mutations and chromosomal aberrations) acquired during tumor development and results in the formation of a disease that is enormously complex and highly variable between patients. An ability to dissect this heterogeneity will facilitate a deeper understanding of the relevance of these alterations for disease phenotypes by which to develop rational therapeutic strategies that can be matched with the characteristics of the individual patient's tumor. In fact, this has already been achieved in some instances of breast cancer where HER2-positive tumors are treated with trastuzumab or lapatinib, and ER-positive tumors are treated with anti-hormonal therapy. To identify additional molecular characteristics for a more effective treatment of breast cancer, an approach to rapidly and efficiently leverage available breast cancer genomic data and correlate both genetic and clinical features and outcomes is urgently needed.

Gene expression profiling has become a major tool for the study of breast cancer and substantial amounts of data are available from public databases. To date, microarray data from more than 6,000 primary breast cancer samples have been posted on the Gene Expression Omnibus (GEO) database. To capture the complexity of breast cancer heterogeneity and pinpoint molecular factors that can be therapeutically targeted, we compiled a large collection of breast tumor gene expression data ($n = 4,010$) derived from 23 datasets that were published from October 2005 to February 2011, including subsets of samples in which clinical prognosis data were available. We identified a series of genes whose high-level expression increased the risk of death from breast cancer, which may be exploited to improve the effectiveness of clinical intervention in this disease. We found that HSP90AA1 and HSP90AB1, two cytoplasmic HSP90 isoforms, were among the most significant factors of poor prognosis in different breast cancer subtypes. As one of the most abundant proteins in malignant cells and a key factor that stabilizes oncoproteins involved in cancer growth and survival, our results suggest that increased HSP90 expression may play an important role in promoting aggressive breast cancer phenotypes. Furthermore, we found that highly expressed *HSP90AA1*, *HSP90AB1* and *HSF1* were driven by somatic amplifications, which collectively were found in approximately 30% of tumors, which we classified as up-regulated HSP90. We revealed that up-regulated HSP90 was significantly associated with risk of death from breast cancer among patients with HER2-/ER+ breast cancer, and greatly increased the chance of disease recurrence in TNBC, and these interactions were independent of clinical variables.

Perhaps the most significant challenge presented by the complexity of breast cancer is the ability to design

Table 3 Prognosis of up-regulated HSP90 in different subtypes of breast cancer.

Subtype	Event phenotype	Kaplan-Meier survival analysis			COXPH survival analysis			
		P-value	HR (95%CI)	n	*P*-value	Co-efficiency	*P*-adjusted	n
All samples	Death	0.0034	1.57 (1.16-2.12)	1072	0.0007	0.5714	0.0062	421
HER2+	Death	0.3118	1.40 (0.73-2.71)	194	0.2564	0.7433	0.1405	63
	Recurrence	0.475	0.87 (0.58-1.29)	204	0.9528	-0.2160	0.6705	72
	Distant metastasis	0.2292	0.77 (0.50-1.18)	347	0.5383	-0.6461	0.2330	90
HER2-/ER+	Death	0.0148	1.71 (1.11-2.63)	506	0.0003	0.8373	0.0042	228
	Recurrence	0.0183	1.31 (1.05-1.65)	832	0.1790	0.2077	0.3054	361
	Distant metastasis	0.0002	1.65 (1.27-2.15)	1223	0.0098	0.4050	0.0705	415
TNBC	Death	0.0604	1.76 (0.98-3.19)	282	0.5693	0.2586	0.5869	105
	Recurrence	0.0002	2.29 (1.49-3.52)	285	0.0008	0.9924	0.0101	122
	Distant metastasis	0.0195	1.60 (1.08-2.37)	516	0.6722	-0.0323	0.9390	158

CI: confidence interval; HR: hazard ratio; n: number of samples

and develop therapeutic regimens that can match the characteristics of the individual patient's tumor – to achieve the goal of personalized cancer treatment. In addition to the well credentialed or previously described genes HER2 and GRB7, we found additional factors associated with an increased risk of death from breast cancer, such as CUTL1 [35], CTTN [36] and GINS2 [37] that have been previously linked with poor prognosis of breast cancer. This reflects the nature of cancer heterogeneity in which multiple mutations and alterations generate the cancer phenotype. The development of therapeutic strategies that can completely and precisely match the complexity of breast cancer with equally complex combinations of regimens will be clinically challenging, particularly considering the need to utilize combinations of drugs that must be shown to be safe when combined together. A more practical approach would prioritize the more universal molecular factors associated with aggressive behavior and poor prognosis, upon which more general therapeutic regimens can be developed for use in combinations. Previous reports have indicated that high expression of HSP90, assessed by protein expression analysis, is associated with a poor overall prognosis in breast cancer patients [24]. High HSP90 expression was associated with high expression of HER2 and ER, large tumors, high nuclear grade, and lymph node involvement [9]. Our results demonstrated that up-regulation of multiple isoforms of HSP90 in primary breast cancer were independent poor prognosis factors, indicating that HSP90 targeted therapies in combination with cytotoxic chemotherapies or other targeted agents, may improve diagnosis and treatment of highly aggressive breast cancers.

Because HSP90 is a key component of oncogenic signaling, an increasing number of candidate HSP90 inhibitors have been developed and evaluated, both in preclinical models and in clinical trials. Although HSP90 inhibitors have exhibited clinical activity in the treatment of breast and other cancers, targeting HSP90 alone generally results in cytostatic rather than cytotoxic effects on tumors. In the majority of patients, disease progression occurs following cessation of treatment with an HSP90 inhibitor [8]. Our results suggest that up-regulated HSP90 might not be an independent poor prognosis factor among patients with HER2-positive breast cancer, as no statistically significant correlation was observed between poor survival and high-level expression of any HSP90 isoforms, which is consistent with the previous finding that the most common clinical response in patients with HER2-positive breast cancer who received HSP90 monotherapy is stable disease. In contrast, multiple studies using cell-based or various tumor xenograft models of breast cancer have shown a large degree of synergy by combining HSP90 inhibitors with therapies targeting HER2 (such as trastuzumab or lapatinib) [38,39]. Indeed, in animal xenograft models, tumors often do not immediately re-grow upon drug withdrawal, and often significant tumor regression can be observed[17]. In clinical trials, chronic administration of the majority of HSP90 inhibitors is well tolerated by humans, with manageable toxicity. At first glance this seems surprising given the essential role of the protein in numerous normal cellular processes; however, the apparent lack of toxicity of HSP90 inhibitors may be related to the recent realization that cancer cells are addicted to HSP90–a prime example of tumor cell non-oncogene addiction [8]. This may provide a sufficiently large therapeutic window for the safe use of HSP90 inhibitors in cancer. Additionally, there is evidence that oncogenic clients can alter the conformation of HSP90. Several inhibitors of the protein have been developed that only recognize this activated conformation [40,41] suggesting an even greater therapeutic index.

TNBC has been considered a more aggressive breast cancer subtype with a higher rate of distant recurrence and a poorer prognosis [19,20]. We found that increased expression of each of the HSP90 isoforms was correlated with a higher risk of recurrence and more than 70% of patients with up-regulated HSP90 experienced disease recurrence within eight years after initial treatment, suggesting that TNBC patients might benefit from therapies that target multiple HSP90 isoforms, such as HSP90AA1, HSP90AB1 and TRAP1. In fact, in pre-clinical models, TNBC have been sensitive to Hsp90 inhibitors [22,23]. Similar to HER2 positive tumors, TNBCs were sensitive to Hsp90 inhibition through down-regulation of components of the Ras/Raf/MAPK pathway in preclinical and *in vitro* studies [23]. Furthermore, our results demonstrated that up-regulated HSP90 was also a significant prognostic factor in HER2-/ER+ breast cancers, suggesting a broad application of HSP90 targeted therapies in the 80% of breast cancers that do not over-express HER2. In addition, other hormone receptors, such as androgen receptor, utilized HSP90, which provides a rationale for the use of HSP90 inhibitors and AR antagonist in the subset of AR+ breast cancers. Given the fact that HSP90 is one of the most abundant proteins in breast cancer cells, and HSP90 has been proposed as a potential therapeutic target for other cancers, including non-small cell lung cancer [42], our results indicate that HSP90 is an important oncogenic signaling node in breast cancer, whose high expression is associated with aggressive behavior and poor prognosis of breast cancer. Diagnostic and therapeutic strategies directed to cancer expressing high levels of HSP90 are warranted.

Conclusions

High-level expression of two cytoplasmic HSP90 iso-forms, HSP90AA1 and HSP90AB1, were predominantly driven by gene amplifications. Using clinical parameters that were associated with poor clinical outcome, such as tumor size, grade, nodal status, age, HER2, ER and RP status, we demonstrated that high-level expressions of *HSP90AA1* and *HSP90AB1* were independent poor prognosis factors affecting triple-negative and HER2-/ER+ breast cancer subtypes. Furthermore, up-regulated HSP90 that was defined as a collection of *HSP90AA1*, *HSP90AB1* and *HSF1* amplifications was one of the most significant factors that independently associated with risk of death from breast cancer, and greatly increased the incidence of recurrence and distant metastasis in triple negative and HER2-/ER+ breast cancer subtypes.

Additional material

Additional file 1: Clinical data of 4,010 breast cancer samples and expression of selected genes. This table lists clinical data that was downloaded from NCBI GEO database, and normalized expression signal of HER2 (216836_s_at), ER (205225_at), PR (208305_at), HSP90AA1 (214328_s_at), HSP90AB1 (214359_s_at), HSP90B1 (200598_s_at) and HSF1 (213756_s_at), as well as defined up-regulated HSP90.

Additional file 2: Heatmaps. These heatmaps show the expression patterns in the data before **(A)** and after **(B)** normalization. The rows contain the 1,000 genes that exhibit the highest variance in gene expression profile across the original data set. The columns contain the samples in the data sets provided. The genes and samples are in the same order in both heatmaps. Warm colors indicate high expression of the gene and cool colors indicate low expression.

Additional file 3: Distribution of HER2, ER and PR mRNA expression and its correlation with IHC measure molecular status. This figure shows **(A)** histograms of HER2, ER and PR mRNA expression in 4,010 breast cancer samples and **(B)** the correlation between mRNA expression and IHC status. Differences between positive and negative groups were assessed using the exact Mann-Whitney U test. Boxes represent the 25% to 75% quartiles, lines *in the boxes* represent the median level, whiskers represent the non-outlier range, and circles represent the outliers.

Additional file 4: Expression defined breast cancer subtypes. This figure shows **(A)** Bimodal selection for HER2, ER and PR cutoff according to the distribution of expression values stratified by IHC/biochemical status. **(B)** Distribution of HER2, ER and PR mRNA expression in combined dataset. **(C)** Distant metastasis-free survival analyses were stratified according to IHC/biochemical status or expression derived status using samples with available IHC/biochemical status and outcome data. Tick marks in Kaplan-Meier Estimates distant-metastasis free survival indicate patients whose data were censored by the time of last follow-up or owing to death. *P* values were calculated using log-rank Mantel-cox test.

Additional file 5: Breast cancer poor prognosis associated gene. This table lists breast cancer poor prognosis -ssociated genes. Cox-regression survival analyses were performed using 395 samples in which event of death from breast cancer was available. Analysis of variance (ANOVA) was performed to test for an association between copy numbers and gene expression using 481 TCGA breast cancer samples.

Additional file 6: Genome scans for poor prognosis associated gene. This figure shows the correlation between copy number aberrations and gene expression of identified genes that were associated with breast cancer poor prognosis. Upper panel shows percentage of amplification (low-level and high-level amplification) and deletion

(homozygous and hemizygous deletion) at each detected chromosome region in a group of 481 breast cancer patients. Bottom panel shows correlation between CNA and mRNA expression of poor prognosis associated genes that were identified from each chromosome. Analysis of variance (ANOVA) was performed to test for association between copy numbers and gene expression.

Additional file 7: Prognosis of HSP90 and HSF1 in different breast cancer subtypes. This table lists the results of survival analyses. Breast cancer subtype specific disease-specific survival (dss, event of death from breast cancer), over-all survival (os), recurrence-free survival (rfs), and distant metastasis-free survival (dmfs) were assessed using Cox-regression survival analysis, Kaplan-Meier Estimates survival analysis and Cox Proportional-Hazards (COXPH) Regression survival analysis.

Additional file 8: Correlation between HSP90 and HSF1 mRNA expression and up-regulated HSP90. This figure shows HSP90 and HSF1 expression difference between samples defined as up-regulated HSP90 and not up-regulated HSP90. Differences for each pairwise comparison were assessed by the Mann-Whitney U test. Boxes represent the 25% to 75% quartiles, lines *in the boxes* represent the median level, whiskers represent the non-outlier range, and circles represent the outliers.

Additional file 9: Cox univariate and multivariate analyses of up-regulated HSP90. This table lists **the** results of Cox Proportional-Hazards (COXPH) Regression survival analyses of up-regulated HSP90 using samples where the entire set of clinical data was available.

Additional file 10: Prognosis of up-regulated HSP90 in different breast cancer subtypes. This figure shows Kaplan-Meier estimates curve of up-regulated HSP90 in different breast cancer subtypes. Number of recurrence events: TNBC, *n* = 142; HER2-/ER+, *n* = 331; HER2+, *n* = 112. Number of distant metastasis events: TNBC, *n* = 133; HER2-/ER+, *n* = 260; HER2+, *n* = 111. Tick marks in Kaplan-Meier estimates of recurrence-free survival and distant-metastasis free survival indicate patients whose data were censored by the time of last follow-up or owing to death. *P* values were calculated using log-rank Mantel-cox test.

Abbreviations

ANOVA: analysis of variance; CNAs: copy number aberrations; COXPH: Cox Proportional-Hazards Regression survival analyses; ER: estrogen receptor; GEO: Gene Expression Omnibus; HER2: human epidermal growth factor receptor 2; HSF1: HSP transcriptional factor 1; HSP90: heat shock protein 90; PR: progesterone receptor; RMA: Robust Multi-array Average; TCGA:The Cancer Genome Atlas; TNBC: triple negative breast cancer.

Author details

[1]Department of Surgery, Duke University Medical Center, Box 2606, 203 Research Drive, Durham, NC 27710, USA. [2]Department of Pathology, Duke University Medical Center, 3108 Meyer Ward, Durham, NC 27710, USA. [3]Department of Pharmacology & Cancer Biology, Duke University Medical Center, C118 LSRC, Durham, NC 27710, USA. [4]Department of Medicine, Duke University Medical Center, 101B MSRB, Durham, NC 27710, USA. [5]Department of Integrative Biology and Pharmacology, University of Texas Health Science Center, 6431 Fannin Street, Houston, TX 77030, USA. [6]Urologic Oncology Branch, Center for Cancer Research, National Cancer Institute, 9000 Rockville Pike Bethesda, MD 20892, USA.

Authors' contributions

QC, TH, LMN and HKL designed the study. QC and JTC contributed to the data analyses. JG, NLS and HKL provided expertise in clinical breast oncology. All authors contributed to the preparation of the manuscript. All authors have read and approved the final manuscript for publication.

Competing interests

Dr. Timothy Haystead was founding scientist of Serenex Inc, Durham NC. Dr. Timothy Haystead declares a technology has been developed for the detection of up regulated/activated Hsp90 at the protein level in tumors. This technology has been disclosed to Duke University in accordance with its patenting policies. He is a tenured Associate Professor at Duke University and receives an annual salary from this organization. All other co-authors declare no competing interests.

References

1. Jemal A, Siegel R, Xu J, Ward E: Cancer statistics, 2010. *CA Cancer J Clin* 2010, **60**:277-300.
2. Cheng Q, Yang W, Raimondi SC, Pui CH, Relling MV, Evans WE: Karyotypic abnormalities create discordance of germline genotype and cancer cell phenotypes. *Nat Genet* 2005, **37**:878-882.
3. Diouf B, Cheng Q, Krynetskaia NF, Yang W, Cheok M, Pei D, Fan Y, Cheng C, Krynetskiy EY, Geng H, Chen S, Thierfelder WE, Mullighan CG, Downing JR, Hsieh P, Pui CH, Relling MV, Evans WE: Somatic deletions of genes regulating MSH2 protein stability cause DNA mismatch repair deficiency and drug resistance in human leukemia cells. *Nat Med* 2011, **17**:1298-1303.
4. Albertson DG, Collins C, McCormick F, Gray JW: Chromosome aberrations in solid tumors. *Nat Genet* 2003, **34**:369-376.
5. Beroukhim R, Mermel CH, Porter D, Wei G, Raychaudhuri S, Donovan J, Barretina J, Boehm JS, Dobson J, Urashima M, McHenry KT, Pinchback RM, Ligon AH, Cho YJ, Haery L, Greulich H, Reich M, Winckler W, Lawrence MS, Weir BA, Tanaka KE, Chiang DY, Bass AJ, Loo A, Hoffman C, Prensner J, Liefeld T, Gao Q, Yecies D, Signoretti S, *et al*: The landscape of somatic copy-number alteration across human cancers. *Nature* 2010, **463**:899-905.
6. Welch WJ, Feramisco JR: Purification of the major mammalian heat shock proteins. *J Biol Chem* 1982, **257**:14949-14959.
7. Picard D, Khursheed B, Garabedian MJ, Fortin MG, Lindquist S, Yamamoto KR: Reduced levels of hsp90 compromise steroid receptor action in vivo. *Nature* 1990, **348**:166-168.
8. Trepel J, Mollapour M, Giaccone G, Neckers L: Targeting the dynamic HSP90 complex in cancer. *Nat Rev Cancer* 2010, **10**:537-549.
9. Neckers L, Ivy SP: Heat shock protein 90. *Curr Opin Oncol* 2003, **15**:419-424.
10. Chen B, Piel WH, Gui L, Bruford E, Monteiro A: The HSP90 family of genes in the human genome: insights into their divergence and evolution. *Genomics* 2005, **86**:627-637.
11. Taipale M, Jarosz DF, Lindquist S: HSP90 at the hub of protein homeostasis: emerging mechanistic insights. *Nat Rev Mol Cell Biol* 2010, **11**:515-528.
12. Kamal A, Thao L, Sensintaffar J, Zhang L, Boehm MF, Fritz LC, Burrows FJ: A high-affinity conformation of Hsp90 confers tumour selectivity on Hsp90 inhibitors. *Nature* 2003, **425**:407-410.
13. Zhang H, Burrows F: Targeting multiple signal transduction pathways through inhibition of Hsp90. *J Mol Med (Berl)* 2004, **82**:488-499.
14. Basso AD, Solit DB, Munster PN, Rosen N: Ansamycin antibiotics inhibit Akt activation and cyclin D expression in breast cancer cells that overexpress HER2. *Oncogene* 2002, **21**:1159-1166.
15. Xu W, Mimnaugh E, Rosser MF, Nicchitta C, Marcu M, Yarden Y, Neckers L: Sensitivity of mature Erbb2 to geldanamycin is conferred by its kinase domain and is mediated by the chaperone protein Hsp90. *J Biol Chem* 2001, **276**:3702-3708.
16. Workman P, Burrows F, Neckers L, Rosen N: Drugging the cancer chaperone HSP90: combinatorial therapeutic exploitation of oncogene addiction and tumor stress. *Ann N Y Acad Sci* 2007, **1113**:202-216.
17. Modi S, Stopeck A, Linden H, Solit D, Chandarlapaty S, Rosen N, D'Andrea G, Dickler M, Moynahan ME, Sugarman S, Ma W, Patil S, Norton L, Hannah AL, Hudis C: HSP90 inhibition is effective in breast cancer: a phase II trial of tanespimycin (17-AAG) plus trastuzumab in patients with HER2-positive metastatic breast cancer progressing on tastuzumab. *Clin Cancer Res* 2011, **17**:5132-5139.
18. Morris GJ, Naidu S, Topham AK, Guiles F, Xu Y, McCue P, Schwartz GF, Park PK, Rosenberg AL, Brill K, Mitchell EP: Differences in breast carcinoma characteristics in newly diagnosed African-American and Caucasian patients: a single-institution compilation compared with the National Cancer Institute's Surveillance, Epidemiology, and End Results database. *Cancer* 2007, **110**:876-884.
19. Haffty BG, Yang Q, Reiss M, Kearney T, Higgins SA, Weidhaas J, Harris L, Hait W, Toppmeyer D: Locoregional relapse and distant metastasis in conservatively managed triple negative early-stage breast cancer. *J Clin Oncol* 2006, **24**:5652-5657.
20. Dent R, Trudeau M, Pritchard KI, Hanna WM, Kahn HK, Sawka CA, Lickley LA, Rawlinson E, Sun P, Narod SA: Triple-negative breast cancer: clinical features and patterns of recurrence. *Clin Cancer Res* 2007, **13**:4429-4434.
21. Zagouri F, Sergentanis TN, Nonni A, Papadimitriou CA, Michalopoulos NV, Domeyer P, Theodoropoulos G, Lazaris A, Patsouris E, Zografos E, Pazaiti A, Zografos GC: Hsp90 in the continuum of breast ductal carcinogenesis: evaluation in precursors, preinvasive and ductal carcinoma lesions. *BMC Cancer* 2010, **10**:353.
22. Mehta PP, Whalen P, Baxi SM, Kung PP, Yamazaki S, Yin MJ: Effective targeting of triple-negative breast cancer cells by PF-4942847, a novel oral inhibitor of Hsp 90. *Clin Cancer Res* 2011, **17**:5432-5442.
23. Caldas-Lopes E, Cerchietti L, Ahn JH, Clement CC, Robles AI, Rodina A, Moulick K, Taldone T, Gozman A, Guo Y, Wu N, De SE, White J, Gross SS, Ma Y, Varticovski L, Melnick A, Chiosis G: Hsp90 inhibitor PU-H71, a multimodal inhibitor of malignancy, induces complete responses in triple-negative breast cancer models. *Proc Natl Acad Sci USA* 2009, **106**:8368-8373.
24. Pick E, Kluger Y, Giltnane JM, Moeder C, Camp RL, Rimm DL, Kluger HM: High HSP90 expression is associated with decreased survival in breast cancer. *Cancer Res* 2007, **67**:2932-2937.
25. Song CH, Park SY, Eom KY, Kim JH, Kim SW, Kim JS, Kim IA: Potential prognostic value of heat-shock protein 90 in the presence of phosphatidylinositol-3-kinase overexpression or loss of PTEN, in invasive breast cancers. *Breast Cancer Res* 2010, **12**:R20.
26. Carvalho CM, Chang J, Lucas JE, Nevins JR, Wang Q, West M: High-dimensional sparse factor modeling: applications in gene expression genomics. *J Am Stat Assoc* 2008, **103**:1438-1456.
27. Wang K, Li M, Hadley D, Liu R, Glessner J, Grant SF, Hakonarson H, Bucan M: PennCNV: an integrated hidden Markov model designed for high-resolution copy number variation detection in whole-genome SNP genotyping data. *Genome Res* 2007, **17**:1665-1674.
28. Sun W, Wright FA, Tang Z, Nordgard SH, Van LP, Yu T, Kristensen VN, Perou CM: Integrated study of copy number states and genotype calls using high-density SNP arrays. *Nucleic Acids Res* 2009, **37**:5365-5377.
29. Karn T, Metzler D, Ruckhaberle E, Hanker L, Gatje R, Solbach C, Ahr A, Schmidt M, Holtrich U, Kaufmann M, Rody A: Data-driven derivation of cutoffs from a pool of 3,030 Affymetrix arrays to stratify distinct clinical types of breast cancer. *Breast Cancer Res Treat* 2010, **120**:567-579.
30. Lehmann BD, Bauer JA, Chen X, Sanders ME, Chakravarthy AB, Shyr Y, Pietenpol JA: Identification of human triple-negative breast cancer subtypes and preclinical models for selection of targeted therapies. *J Clin Invest* 2011, **121**:2750-2767.
31. Hyman E, Kauraniemi P, Hautaniemi S, Wolf M, Mousses S, Rozenblum E, Ringner M, Sauter G, Monni O, Elkahloun A, Kallioniemi OP, Kallioniemi A: Impact of DNA amplification on gene expression patterns in breast cancer. *Cancer Res* 2002, **62**:6240-6245.
32. Pollack JR, Sorlie T, Perou CM, Rees CA, Jeffrey SS, Lonning PE, Tibshirani R, Botstein D, Borresen-Dale AL, Brown PO: Microarray analysis reveals a major direct role of DNA copy number alteration in the transcriptional program of human breast tumors. *Proc Natl Acad Sci USA* 2002, **99**:12963-12968.
33. Solvang HK, Lingjaerde OC, Frigessi A, Borresen-Dale AL, Kristensen VN: Linear and non-linear dependencies between copy number aberrations and mRNA expression reveal distinct molecular pathways in Breast Cancer. *BMC Bioinformatics* 2011, **12**:197.
34. Akavia UD, Litvin O, Kim J, Sanchez-Garcia F, Kotliar D, Causton HC, Pochanard P, Mozes E, Garraway LA, Pe'er D: An integrated approach to uncover drivers of cancer. *Cell* 2010, **143**:1005-1017.

35. Michl P, Ramjaun AR, Pardo OE, Warne PH, Wagner M, Poulsom R, D'Arrigo C, Ryder K, Menke A, Gress T, Downward J: **CUTL1 is a target of TGF(beta) signaling that enhances cancer cell motility and invasiveness.** *Cancer Cell* 2005, **7**:521-532.

36. Hashimoto S, Hirose M, Hashimoto A, Morishige M, Yamada A, Hosaka H, Akagi K, Ogawa E, Oneyama C, Agatsuma T, Okada M, Kobayashi H, Wada H, Nakano H, Ikegami T, Nakagawa A, Sabe H: **Targeting AMAP1 and cortactin binding bearing an atypical src homology 3/proline interface for prevention of breast cancer invasion and metastasis.** *Proc Natl Acad Sci USA* 2006, **103**:7036-7041.

37. Rantala JK, Edgren H, Lehtinen L, Wolf M, Kleivi K, Vollan HK, Aaltola AR, Laasola P, Kilpinen S, Saviranta P, Iljin K, Kallioniemi O: **Integrative functional genomics analysis of sustained polyploidy phenotypes in breast cancer cells identifies an oncogenic profile for GINS2.** *Neoplasia* 2010, **12**:877-888.

38. Arteaga CL: **Why is this effective HSP90 inhibitor not being developed in HER2+ breast cancer?** *Clin Cancer Res* 2011, **17**:4919-4921.

39. Raja SM, Clubb RJ, Bhattacharyya M, Dimri M, Cheng H, Pan W, Ortega-Cava C, Lakku-Reddi A, Naramura M, Band V, Band H: **A combination of Trastuzumab and 17-AAG induces enhanced ubiquitinylation and lysosomal pathway-dependent ErbB2 degradation and cytotoxicity in ErbB2-overexpressing breast cancer cells.** *Cancer Biol Ther* 2008, **7**:1630-1640.

40. Fadden P, Huang KH, Veal JM, Steed PM, Barabasz AF, Foley B, Hu M, Partridge JM, Rice J, Scott A, Dubois LG, Freed TA, Silinski MA, Barta TE, Hughes PF, Ommen A, Ma W, Smith ED, Spangenberg AW, Eaves J, Hanson GJ, Hinkley L, Jenks M, Lewis M, Otto J, Pronk GJ, Verleysen K, Haystead TA, Hall SE: **Application of chemoproteomics to drug discovery: identification of a clinical candidate targeting hsp90.** *Chem Biol* 2010, **17**:686-694.

41. Huang KH, Veal JM, Fadden RP, Rice JW, Eaves J, Strachan JP, Barabasz AF, Foley BE, Barta TE, Ma W, Silinski MA, Hu M, Partridge JM, Scott A, Dubois LG, Freed T, Steed PM, Ommen AJ, Smith ED, Hughes PF, Woodward AR, Hanson GJ, McCall WS, Markworth CJ, Hinkley L, Jenks M, Geng L, Lewis M, Otto J, Pronk B, *et al*: **Discovery of novel 2-aminobenzamide inhibitors of heat shock protein 90 as potent, selective and orally active antitumor agents.** *J Med Chem* 2009, **52**:4288-4305.

42. Gallegos Ruiz MI, Floor K, Roepman P, Rodriguez JA, Meijer GA, Mooi WJ, Jassem E, Niklinski J, Muley T, van ZN, Smit EF, Beebe K, Neckers L, Ylstra B, Giaccone G: **Integration of gene dosage and gene expression in non-small cell lung cancer, identification of HSP90 as potential target.** *PLoS ONE* 2008, **3**:e0001722.

43. Iwamoto T, Bianchini G, Booser D, Qi Y, Coutant C, Shiang CY, Santarpia L, Matsuoka J, Hortobagyi GN, Symmans WF, Holmes FA, O'Shaughnessy J, Hellerstedt B, Pippen J, Andre F, Simon R, Pusztai L: **Gene pathways associated with prognosis and chemotherapy sensitivity in molecular subtypes of breast cancer.** *J Natl Cancer Inst* 2011, **103**:264-272.

44. Symmans WF, Hatzis C, Sotiriou C, Andre F, Peintinger F, Regitnig P, Daxenbichler G, Desmedt C, Domont J, Marth C, Delaloge S, Bauernhofer T, Valero V, Booser DJ, Hortobagyi GN, Pusztai L: **Genomic index of sensitivity to endocrine therapy for breast cancer.** *J Clin Oncol* 2010, **28**:4111-4119.

45. Schmidt M, Bohm D, von Torne C, Steiner E, Puhl A, Pilch H, Lehr HA, Hengstler JG, Kolbl H, Gehrmann M: **The humoral immune system has a key prognostic impact in node-negative breast cancer.** *Cancer Res* 2008, **68**:5405-5413.

46. Zhang Y, Sieuwerts AM, McGreevy M, Casey G, Cufer T, Paradiso A, Harbeck N, Span PN, Hicks DG, Crowe J, Tubbs RR, Budd GT, Lyons J, Sweep FC, Schmitt M, Schittulli F, Golouh R, Talantov D, Wang Y, Foekens JA: **The 76-gene signature defines high-risk patients that benefit from adjuvant tamoxifen therapy.** *Breast Cancer Res Treat* 2009, **116**:303-309.

47. Desmedt C, Piette F, Loi S, Wang Y, Lallemand F, Haibe-Kains B, Viale G, Delorenzi M, Zhang Y, d'Assignies MS, Bergh J, Lidereau R, Ellis P, Harris AL, Klijn JG, Foekens JA, Cardoso F, Piccart MJ, Buyse M, Sotiriou C: **Strong time dependence of the 76-gene prognostic signature for node-negative breast cancer patients in the TRANSBIG multicenter independent validation series.** *Clin Cancer Res* 2007, **13**:3207-3214.

48. Minn AJ, Gupta GP, Padua D, Bos P, Nguyen DX, Nuyten D, Kreike B, Zhang Y, Wang Y, Ishwaran H, Foekens JA, van de Vijver M, Massague J: **Lung metastasis genes couple breast tumor size and metastatic spread.** *Proc Natl Acad Sci USA* 2007, **104**:6740-6745.

49. Loi S, Haibe-Kains B, Desmedt C, Lallemand F, Tutt AM, Gillet C, Ellis P, Harris A, Bergh J, Foekens JA, Klijn JG, Larsimont D, Buyse M, Bontempi G, Delorenzi M, Piccart MJ, Sotiriou C: **Definition of clinically distinct molecular subtypes in estrogen receptor-positive breast carcinomas through genomic grade.** *J Clin Oncol* 2007, **25**:1239-1246.

50. Pawitan Y, Bjohle J, Amler L, Borg AL, Egyhazi S, Hall P, Han X, Holmberg L, Huang F, Klaar S, Liu ET, Miller L, Nordgren H, Ploner A, Sandelin K, Shaw PM, Smeds J, Skoog L, Wedren S, Bergh J: **Gene expression profiling spares early breast cancer patients from adjuvant therapy: derived and validated in two population-based cohorts.** *Breast Cancer Res* 2005, **7**: R953-R964.

51. Wang Y, Klijn JG, Zhang Y, Sieuwerts AM, Look MP, Yang F, Talantov D, Timmermans M, Meijer-van Gelder ME, Yu J, Jatkoe T, Berns EM, Atkins D, Foekens JA: **Gene-expression profiles to predict distant metastasis of lymph-node-negative primary breast cancer.** *Lancet* 2005, **365**:671-679.

52. Miller LD, Smeds J, George J, Vega VB, Vergara L, Ploner A, Pawitan Y, Hall P, Klaar S, Liu ET, Bergh J: **An expression signature for p53 status in human breast cancer predicts mutation status, transcriptional effects, and patient survival.** *Proc Natl Acad Sci USA* 2005, **102**:13550-13555.

53. de Cremoux P, Valet F, Gentien D, Lehmann-Che J, Scott V, Tran-Perennou C, Barbaroux C, Servant N, Vacher S, Sigal-Zafrani B, Mathieu MC, Bertheau P, Guinebretiere JM, Asselain B, Marty M, Spyratos F: **Importance of pre-analytical steps for transcriptome and RT-qPCR analyses in the context of the phase II randomised multicentre trial REMAGUS02 of neoadjuvant chemotherapy in breast cancer patients.** *BMC Cancer* 2011, **11**:215.

54. Kao KJ, Chang KM, Hsu HC, Huang AT: **Correlation of microarray-based breast cancer molecular subtypes and clinical outcomes: implications for treatment optimization.** *BMC Cancer* 2011, **11**:143.

55. Bekhouche I, Finetti P, Adelaide J, Ferrari A, Tarpin C, Charafe-Jauffret E, Charpin C, Houvenaeghel G, Jacquemier J, Bidaut G, Birnbaum D, Viens P, Chaffanet M, Bertucci F: **High-resolution comparative genomic hybridization of inflammatory breast cancer and identification of candidate genes.** *PLoS ONE* 2011, **6**:e16950.

56. Sabatier R, Finetti P, Cervera N, Lambaudie E, Esterni B, Mamessier E, Tallet A, Chabannon C, Extra JM, Jacquemier J, Viens P, Birnbaum D, Bertucci F: **A gene expression signature identifies two prognostic subgroups of basal breast cancer.** *Breast Cancer Res Treat* 2011, **126**:407-420.

57. Juul N, Szallasi Z, Eklund AC, Li Q, Burrell RA, Gerlinger M, Valero V, Andreopoulou E, Esteva FJ, Symmans WF, Desmedt C, Haibe-Kains B, Sotiriou C, Pusztai L, Swanton C: **Assessment of an RNA interference screen-derived mitotic and ceramide pathway metagene as a predictor of response to neoadjuvant paclitaxel for primary triple-negative breast cancer: a retrospective analysis of five clinical trials.** *Lancet Oncol* 2010, **11**:358-365.

58. Smeets A, Daemen A, Vanden Bempt I, Gevaert O, Claes B, Wildiers H, Drijkoningen R, Van HP, Lambrechts D, De Moor B, Neven P, Sotiriou C, Vandorpe T, Paridaens R, Christiaens MR: **Prediction of lymph node involvement in breast cancer from primary tumor tissue using gene expression profiling and miRNAs.** *Breast Cancer Res Treat* 2011, **129**:767-776.

59. Li Y, Zou L, Li Q, Haibe-Kains B, Tian R, Li Y, Desmedt C, Sotiriou C, Szallasi Z, Iglehart JD, Richardson AL, Wang ZC: **Amplification of LAPTM4B and YWHAZ contributes to chemotherapy resistance and recurrence of breast cancer.** *Nat Med* 2010, **16**:214-218.

60. Bos PD, Zhang XH, Nadal C, Shu W, Gomis RR, Nguyen DX, Minn AJ, van de Vijver MJ, Gerald WL, Foekens JA, Massague J: **Genes that mediate breast cancer metastasis to the brain.** *Nature* 2009, **459**:1005-1009.

61. Loi S, Haibe-Kains B, Majjaj S, Lallemand F, Durbecq V, Larsimont D, Gonzalez-Angulo AM, Pusztai L, Symmans WF, Bardelli A, Ellis P, Tutt AN, Gillett CE, Hennessy BT, Mills GB, Phillips WA, Piccart MJ, Speed TP, McArthur GA, Sotiriou C: **PIK3CA mutations associated with gene signature of low mTORC1 signaling and better outcomes in estrogen receptor-positive breast cancer.** *Proc Natl Acad Sci USA* 2010, **107**:10208-10213.

62. Sircoulomb F, Bekhouche I, Finetti P, Adelaide J, Ben HA, Bonansea J, Raynaud S, Innocenti C, Charafe-Jauffret E, Tarpin C, Ben AF, Viens P, Jacquemier J, Bertucci F, Birnbaum D, Chaffanet M: **Genome profiling of ERBB2-amplified breast cancers.** *BMC Cancer* 2010, **10**:539.

63. Desmedt C, Giobbie-Hurder A, Neven P, Paridaens R, Christiaens MR, Smeets A, Lallemand F, Haibe-Kains B, Viale G, Gelber RD, Piccart M, Sotiriou C: **The Gene Expression Grade Index: a potential predictor of relapse for endocrine-treated breast cancer patients in the BIG 1-98 trial.** *BMC Med Genomics* 2009, **2**:40.

64. Cizkova M, Cizeron-Clairac G, Vacher S, Susini A, Andrieu C, Lidereau R, Bieche I: **Gene expression profiling reveals new aspects of PIK3CA mutation in ERalpha-positive breast cancer: major implication of the Wnt signaling pathway.** *PLoS ONE* 2010, **5**:e15647.

65. Lu X, Lu X, Wang ZC, Iglehart JD, Zhang X, Richardson AL: **Predicting features of breast cancer with gene expression patterns.** *Breast Cancer Res Treat* 2008, **108**:191-201.

RESEARCH   **Open Access**

Phase I clinical trial of HER2-specific immunotherapy with concomitant HER2 kinase inhibtion

Erika Hamilton[1], Kimberly Blackwell[1], Amy C Hobeika[2], Timothy M Clay[3], Gloria Broadwater[4], Xiu-Rong Ren[5], Wei Chen[5], Henry Castro[3], Frederic Lehmann[3], Neil Spector[1], Junping Wei[6], Takuya Osada[6] and H Kim Lyerly[2*]

Abstract

Background: Patients with HER2-overexpressing metastatic breast cancer, despite initially benefiting from the monoclonal antibody trastuzumab and the EGFR/HER2 tyrosine kinase inhibitor lapatinib, will eventually have progressive disease. HER2-based vaccines induce polyclonal antibody responses against HER2 that demonstrate enhanced anti-tumor activity when combined with lapatinib in murine models. We wished to test the clinical safety, immunogenicity, and activity of a HER2-based cancer vaccine, when combined with lapatinib.

Methods: We immunized women (n = 12) with metastatic, trastuzumab-refractory, HER2-overexpressing breast cancer with dHER2, a recombinant protein consisting of extracellular domain (ECD) and a portion of the intracellular domain (ICD) of HER2 combined with the adjuvant AS15, containing MPL, QS21, CpG and liposome. Lapatinib (1250 mg/day) was administered concurrently. Peripheral blood antibody and T cell responses were measured.

Results: This regimen was well tolerated, with no cardiotoxicity. Anti-HER2-specific antibody was induced in all patients whereas HER2-specific T cells were detected in one patient. Preliminary analyses of patient serum demonstrated downstream signaling inhibition in HER2 expressing tumor cells. The median time to progression was 55 days, with the majority of patients progressing prior to induction of peak anti-HER2 immune responses; however, 300-day overall survival was 92% (95% CI: 77-100%).

Conclusions: dHER2 combined with lapatinib was safe and immunogenic with promising long term survival in those with HER2-overexpressing breast cancers refractory to trastuzumab. Further studies to define the anticancer activity of the antibodies induced by HER2 vaccines along with lapatinib are underway.

Trial registry: ClinicalTrials.gov NCT00952692

Keywords: HER2, Antitumor immunity, Immunization, Breast cancer

Introduction

The human epidermal growth factor receptor 2 (HER2), overexpressed in 20-30% of breast cancers, is associated with more aggressive tumor behavior [1]. Treatment with combinations of the anti-HER2 antibody trastuzumab and chemotherapy lengthens survival in patients with metastatic HER2-overexpressing breast cancer [2]. However, progressive disease typically occurs within one

year. Lapatinib, a potent reversible inhibitor of HER2 and epidermal growth factor receptor (EGFR) tyrosine kinases [3], in conjunction with chemotherapy, increases time to progression in these patients [4]. Unfortunately, responses to lapatinib are generally short-lived, and progression remains a significant clinical problem.

Intriguingly, the overexpression of HER2 persists in trastuzumab and lapatinib-refractory tumors [5,6], and thus, targeting HER2 with cancer immunotherapy is a potentially effective strategy. A variety of vaccines targeting HER2, based on proteins, peptides, modified tumor cells, viral vectors, pDNA and dendritic cells

* Correspondence: lyerl001@mc.duke.edu
[2]Department of Surgery, Division of General Surgery, Duke University Medical Center, Durham, NC, USA
Full list of author information is available at the end of the article

(DC) have been developed. Results from phase I and II studies of HER2-targeting cancer vaccines [7] have demonstrated that HER2 is immunogenic, and that immune responses against HER2 may be associated with an improved clinical outcome [8-13].

One protein-based vaccine, dHER2 Antigen-Specific Cancer Immunotherapeutic (ASCI) a recombinant HER2 protein, including a truncated intracellular domain (ICD) and the complete extracellular domain (ECD), combined with the immunological adjuvant AS15, containing MPL, QS21, CpG and liposome, was evaluated in two early phase clinical studies of patients with HER2-overexpressing breast cancer (NCT 00058526 and NCT 00140738) [14]. In both studies, the data showed that dHER2 immunizations were well tolerated, consistently immunogenic at the 500 µg dose and that clinical activity (including prolonged stable disease) was associated with antibody and T cell responses.

One important observation from the prior dHER2 ASCI studies was that the polyclonal antibody-containing serum from immunized patients had functional activity against signaling pathways mediated by HER2. Specifically, incubation of breast cancer cell lines with serum from two immunized patients demonstrated an impact on molecular pathways resembling that of trastuzumab [14]. Because clinical trials have demonstrated that combinations of lapatinib and trastuzumab lead to enhanced clinical activity and combined effects on signaling pathways [15], there has been interest in combining the polyclonal anti-HER2 serum with trastuzumab and indeed, increased apoptosis of human HER2-overexpressing breast cancer cells was observed when lapatinib was combined with HER2-specific polyclonal antisera generated from rabbits immunized with dHER2 ASCI [16]. We therefore hypothesized that the lapatinib would enhance the anti-signaling activity of the polyclonal Abs induced by the dHER2 vaccine in humans. First, it was necessary to establish that the induction of anti-HER2 antibodies by the dHER2 vaccine was not affected by lapatinib and this was the primary purpose of this study.

Methods
Patients
Patients provided consent under a protocol approved by the Duke University Medical Center Institutional Review Board. Enrollment requirements were age 18 or older, stage IV HER2- overexpressing (HER2 3+ or FISH +) breast cancer, documented disease progression or relapse following at least one prior standard therapy containing trastuzumab, ECOG status of 0 or 1, adequate hematologic counts, hepatic and renal function and an LVEF of 50% or greater. Concurrent bisphosphonates and hormonal therapy were permitted. Prior chemotherapy and/or trastuzumab were required to have

been discontinued no sooner than four and three weeks, respectively, before the first ASCI administration. Initially, prior lapatinib was not permitted; however, this severely limited enrollment and therefore, an amendment was made to permit prior and ongoing lapatinib use. Known autoimmune disease, immunosuppressive therapies or HIV, significant cardiovascular disease or arrhythmias were exclusionary criteria.

Treatment/Monitoring
The dHER2 ASCI containing 500 µg of recombinant dHER2 protein (a truncated intra-cellular sequence (ICD) and the complete extracellular sequence (ECD)), reconstituted in the AS15 adjuvant, a liposomal formulation containing MPL, QS21 and CpG, was administered intramuscularly every 2 weeks for 6 administrations (See Figure 1 depicting one cycle). Up to three total cycles of immunization were permitted unless discontinued due to progression of disease. Clinical tumor evaluations were conducted at baseline and at the end of the cycles (e.g., week 12, week 26). Lapatinib (1250 mg) was taken by mouth daily.

Cardiac monitoring consisted of a 12-lead ECG at screening, and at week 12, week 26, and follow-up visit #1 and a MUGA evaluation of ejection fraction (EF) at screening, week 6, 12, 20, 26, follow-up visits #1 and #4.

Analysis of anti-HER2 antibody binding by ELISA
Serum was collected pre- (week 0) and every 2 weeks while on study. 96-well plates were coated with HER2 ICD protein (5 µg/well) or HER2 ECD protein (5 µg/well) and incubated with 100 µl of serially diluted patient serum or trastuzumab. Plates were then incubated with mouse anti-human IgG conjugated alkaline phosphatase (AP) (Sigma) and developed using p-nitrophenyl phosphate (Sigma). Absorbance (415 nm) was read using a BioRad microplate reader. Titers were defined as the greatest dilution at which the mean absorbance was at least twice negative control.

ELISPOT analysis
IFN-γ ELISPOT assays (Mabtech Inc., Cincinnati, OH) were performed according to the manufacturer's instructions as previously described 16]. Briefly, PBMC (250,000 cells/well) were added to each well and stimulated overnight with HER2 ICD or HER2 ECD overlapping peptide mixes (1 µg/ml) to detect HER2-specific responses, or CMV peptide mix (2.6 µg/ml), HIV peptide mix (2.6 µg/ml) (both from BD Bioscience) and a mixture of PMA (50 ng/ml) and Ionomycin (1 µg/ml) as controls. Results were normalized to the number of spots per 1×10^6 PBMC. Based on our previously reported experience [17], a positive response was defined as an increase by ≥ 40 spots from baseline.

Figure 1.

CR: Complete Response, PR: Partial Response, SD: Stable Disease, MR: Mixed Response, TE: Tumor Evaluation.

Figure 1 Study treatment schematic.

Statistical analyses

Descriptive statistics are presented. Progression-free interval was defined as time from trial enrollment to disease progression or death, whichever came first. Overall survival was defined from time of enrollment until death due to any cause. Progression-free and overall survival was calculated using the Kaplan-Meier product limit method.

Results

Patient demographics

Twelve (12) patients were enrolled and received treatment on trial. Demographics are listed for each patient in Table 1. Of note, the patients had substantial metastatic disease burden and had been heavily pretreated, all having progressed on prior trastuzumab and 10/12 having progressed on a lapatinib-containing regimen. Four patients completed one full cycle and one completed two full cycles of immunization.

dHER2 ASCI vaccination in combination with lapatinib was well tolerated. The most common adverse events (AE) encountered were "constitutional symptoms" such as musculoskeletal pain (8/12, 66% with 0% grade 3), injection site reactions (6/12, 50% with 0% grade 3), myalgia (5/12,

42% with 0% grade 3) and fatigue (5/12, 42% with 1/12, 9% grade 3 due to progression of disease). There were only two serious adverse events (SAE) on study: one patient experienced chest pain which was determined to be secondary to progression with mediastinal lymphadenopathy and one patient suffered a pulmonary embolism deemed not related to treatment. There was one additional grade 3 AE: epistaxis after a lacrimal duct repair. There were no grade 4 AEs observed.

Cardiac function was closely monitored during this study with two evaluations of left ventricular ejection fraction (LVEF) at the beginning of every cycle. No heart failure or any decrease in left ventricular cardiac ejection fraction ≥ 20% relative to baseline was seen for any patient at any time point on trial.

Antigen specific T Cell and antibody responses

We analyzed HER2 ICD and ECD specific antibody responses by ELISA. All patients had a detectable anti-ICD-antibody response (ranging from 1:200 to 1:6400) following vaccination in the context of lapatinib treatment. We observed an increase in HER2 ICD antibody titer starting as early as week 4 (after 2 injections; 9 of 12 patients) (Figure 2).

Table 1 Patient characteristics

Pt #	Age	Race	ER or PR +	# prior lines tx	# met sites	Trastuzumab in prior regimen (days since)	Prior Lapatinib	# injections	PFS (d)	OS (d)
001	45	W	Y	4	2	Y (23)	N	4	53	615+
002	50	W	Y	3	3	Y (34)	P	6	82	484
003	48	W	N	3	4	Y (24)	C	6	85	596+
004	53	W	N	6	1	N	C	6	86	549+
005	63	W	Y	2	2	N	C	4	48	540+
006	60	W	N	5	4	Y (37)	C	6	86	531+
007	46	B	N	4	1	Y (33)	P	5	69	486+
008	65	W	N	8	3	Y (27)	C	3	41	456+
012	55	W	N	3	2	N	C	5	69	216
013	65	W	N	4	2	Y (27)	C	4	55	316+
014	56	W	N	3	2	Y (25)	C	12	188	310+
015	46	B	Y	3	4	Y (21)	N	4	69	274+
Median	54			3.5	2			5	69	

1) Prior Lapatinib Use (N = no prior use, P = previous progression on lapatinib, but not on regimen immediately prior, C = continued use, patient was on lapatinib in immediately prior regimen and continued the medication onto trial). 2) OS (overall survival): "+" indicates that the patient was still alive at the last follow-up date

As expected, detection of dHER2 vaccine-induced ECD-specific antibodies was complicated by detection of pre-vaccination HER2-ECD specific antibodies (due to residual trastuzumab) in the sera of 9 of the 12 patients who had been receiving trastuzumab 23 to 60 days prior to study entry (Figure 3). The 3 patients who did not receive trastuzumab within 2 months of starting the study (patients 4, 5, 12) did not exhibit pre-existing antibodies to HER2-ECD, but had detectable post vaccination HER2-ECD specific responses ranging from 1:100 to 1:1600 (Figure 3). For these 3 patients, the dynamics of the HER2-ICD and -ECD antibody responses over time indicate that HER2-specific antibodies were detectable between 4 to 6 weeks after initiating the vaccinations (i.e., following 3-4 vaccinations) with a greater antibody titer specific for HER2-ICD compared to HER2-ECD (Figures 2 and 3). An additional two patients with detectable pre-vaccination anti-ECD antibodies demonstrated an increase in HER2-ECD antibody titer following vaccination (Figure 3). In the remainder of patients, the pre-vaccination HER2 ECD titers levels were not increased after vaccination, making an accurate assessment of the vaccine induced HER2 ECD-specific response difficult.

HER2 specific T cell responses were analyzed by IFNγ ELISPOT assay on cryopreserved, non-restimulated peripheral blood specimens obtained at each timepoint. There were increments in the ECD-specific T cell precursor frequency in one patient and in the ICD-specific T cell precursor frequency in four patients; however, using a pre-specified definition of a positive response as an increase in 40 spots over pre-vaccination frequency, there was a single patient with an ECD-specific T cell

response and none with an ICD-specific T cell response (Additional file 1: Table S1). This patient appears to have had a pre-existing ECD-specific response which was boosted with the vaccine.

Clinical outcome

There were no objective clinical responses. One patient remained progression free on trial for 6 months. Median time to progression was 55 days (range: 41-188) (Figure 4a). Ten of 12 patients remain alive in follow-up. Overall survival at 300 days was 92% (95% CI: 77-100%) (Figure 4b). Because of the small numbers of patients, we could not statistically compare TTP or overall survival with immune responses; however, there were no obvious correlations.

Discussion

The purpose of this study was to determine the clinical and immunologic effects of immunization against HER2 concurrent administration of the HER2 tyrosine kinase inhibitor lapatinib. Previously, we reported that a HER2-targeting vaccine could induce antibody and T cell responses when administered concomitantly with lapatinib in a murine model [18]. We extended this work in the present study confirming for the first time in humans that concomitant administration of lapatinib did not appear to affect the immune response induced by the HER2 immunotherapy. Although we are not aware of other data regarding the effect of lapatinib on the immune response in humans, other tyrosine kinase inhibitors have demonstrated negative effects on the immune response, such as sorafenib (which targets RAF protein in the EGFR pathway as well as other targets)
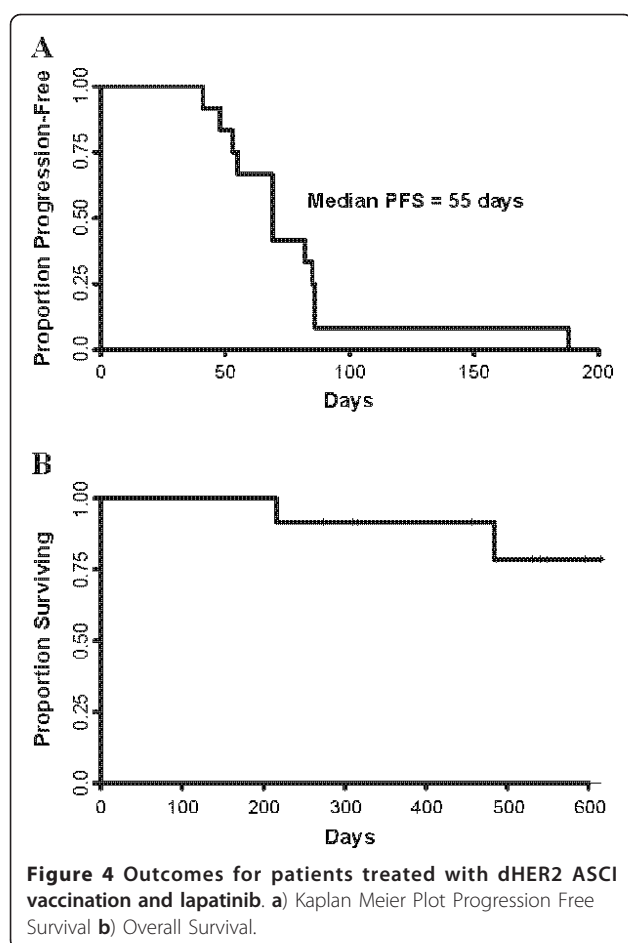
Figure 2 HER2-ICD specific antibody response. Serum from patients receiving dHER2-ASCI + lapatinib was analyzed for HER2-ICD specific antibodies by ELISA. Plates were coated with HER2-ICD protein and incubated with serial dilutions of patient sera (1:25-1:6400), along with negative control serum. Individual graphs of the HER2-ICD titer over time are presented for each patient (indicated by study number) with arrows indicating final dHER2ASCI injection.

while others, such as sunitinib, have had no detrimental effects or potentially improve immune responses [19,20].

We observed potent antibody responses to HER2 ECD and ICD, suggesting that we could still break tolerance to a self-antigen in the context of lapatinib. In the prior phase I/II studies of dHER2 ASCI, antibody responses were consistently observed, and CD4+ and CD8+ T cell responses were also reported. The preferential induction of antibodies using HER2 protein-based vaccines has been already reported. In a series of patients immunized with the truncated 146HER2 protein complexed with cholesteryl pullulan alone or with various adjuvants [21-23], antibody responses against HER2 were detected in 14 of 15 patients, but only 5 out of 9 developed detectable HER2-specific CD8+ and/or CD4+ T-cell immune responses. Because the development of antibodies generally requires Th2 cells, but our method for

measuring IFN-gamma ELISPOT identifies Tc1 and Th1, and not Th2 responses, it is possible that a Th2 response occurred, but was not detectable. It is also possible, as has been reported by others using protein-based vaccines, that regulatory T cells (Treg), typically increased in advanced cancer patients, caused decreases in T cell responses [24]. Future strategies to induce greater T cell responses could be warranted as some authors have suggested the T cell responses correlate with clinical outcome [25]. We have developed a series of recombinant viral vectors expressing HER2 that have been evaluated preclinically and were shown to induce HER2-specific CD8+ T cells. These vectors will be entering clinical trials shortly [26]. We have also reported strategies for depleting Treg [27].

One emerging aspect of cancer immunotherapy is that long periods (between 4 to 6 immunizations) are needed

Figure 3. HER2 ECD ELISA

Arrows indicate time of final dHER2ASCI injection

*Restarted Herceptin

Figure 3 HER2-ECD specific antibody response. Serum from patients receiving dHER2-ASCI + lapatinib was analyzed for HER2-ECD specific antibodies by ELISA. Plates were coated with HER2-ECD protein and incubated with serial dilutions of patient sera (1:25- 1:6400), along with negative control serum and Herceptin as a positive control. Individual graphs of the HER2-ECD titer over time is represented for each patient (indicated by study number) with arrows indicating final dHER2ASCI injection. Although all patients had received trastuzumab at some point in the past, nine patients had received trastuzumab with their immediately prior systemic treatment regimen (range 21 to 37 days), while three had received the trastuzumab during a more distant systemic treatment reginmen. The numbers of days between receiving trastuzumab and starting study drug is noted on each graph as applicable. A * indicates samples taken once trastuzumab was restarted by the patient

to reach an optimal humoral or cellular response. We noted that some patients rapidly progressed during immunization, but prior to development of detectable HER2 specific antibody responses, or until the antibody responses are of sufficient quantity or quality to impact disease. In most cases these were patients who had been maintained on trastuzumab prior to participation. The decline in anti-ECD Ab responses in the early weeks of the study likely represents trastuzumab levels declining. This suggests that for future vaccine studies, patients may need to receive concomitant trastuzumab until they have an adequate induction of antibody responses. Disis *et al*. showed that patients could be vaccinated in the setting of trastuzumab without additional toxicity. The

expected immune responses including epitope and antigen spreading were observed [28]. Indeed, in our study, two patients with detectable pre-vaccination anti-ECD antibodies demonstrated an increase in HER2-ECD antibody titer following vaccination (Figure 3), suggesting we could also induce antibody responses against the dHER2 despite the presence of trastuzumab.

Recent clinical trials have established longer survival for patients receiving trastuzumab plus lapatinib, suggesting clinical benefit for antibody plus tyrosine kinase inhibition of HER2. Because this was not a randomized trial, we are not able to determine the clinical benefit of combined dHER2 ASCI plus lapatinib; however, our observed median PFS and overall survival in a heavily

Figure 4 Outcomes for patients treated with dHER2 ASCI vaccination and lapatinib. **a**) Kaplan Meier Plot Progression Free Survival **b**) Overall Survival.

pretreated population with multiple sites of metastasis who had progressive disease on trastuzumab and prior lapatinib compares favorably with other clinical data. For example, although there is insufficient data in the literature regarding the outcome of patients refractory to both drugs, among patients who have progressive disease while receiving trastuzumab therapy, overall survival has ranged from 10 - 19 months [29-31]. In the EGF104900 study, which randomized patients who had progressed on trastuzumab to either lapatinib alone or lapatinib in combination with trastuzumab, PFS of 8 weeks and OS of 39 weeks (or 273 days) was reported for the lapatinib only arm [31]. It has also been observed in some immunotherapy studies, that OS is improved despite a lack of effect on PFS suggesting that delayed effects of the vaccine might have led us to prematurely discontinue immunization. Future studies should permit a greater extent of progression (such as 50% growth) in asymptomatic progression as has been suggested in the literature [32].

Another important aspect of the strategy of combining a HER2 immunotherapy with lapatinib is the potential combined inhibition of HER2 signaling. A detailed analysis of effects of anti-HER2 serum by our group is reported elsewhere (Rong et al., manuscript submitted). For the current manuscript, we performed a preliminary analysis in which antibodies, purified from post-vaccination serum from selected patients (P002, P004, and P008), were tested for their ability to reduce phosphorylation of the downstream molecule AKT in the HER2 overexpressing cell line SKBR3. In the patient with the highest titer of ECD among the three (P004), pAKT was decreased by antibodies purified from the post-vaccination serum, providing a suggestion that there are anti-signaling effects of the dHER2-induced antibodies (Additional file 2: Figure S1). Serum from patients in the previous phase I/II studies of dHER2 alone bound HER2-overexpressing breast cancer cell lines and inhibited growth of these cell lines with an effect on molecular pathways resembling that of trastuzumab [14]. We previously reported that the polyclonal sera induced in mice by a HER2 vaccine were superior to monoclonal antibodies in mediating receptor internalization and degradation, resulting in ablation of HER2 signaling over time. Furthermore, there was increased anti-tumor activity when this vaccine was administered concomitantly with lapatinib to mice [18]. These data suggest a potential advantage to our approach. First, the vaccine may provide durable periods of exposure to biologic levels of anti-HER2 antibody, whereas trastuzumab must continue to be administered. Second, the vaccine induces polyclonal antibody responses which could have immunologic functions (such as antibody dependent cellular cytotoxicity) as well as direct functions on HER2 signaling. Recently, it was reported that lapatinib induced HER2 surface expression in HER2-positive breast cancer cell lines, leading to the enhancement of trastuzumab-mediated ADCC [33]. These potential advantages strongly support the further assessment of HER2-targeting immunotherapies with concomitant lapatinib and/or trastuzumab in human clinical trials.

One potential disadvantage of the vaccine strategy is that the antibody titers are lower than those achieved during trastuzumab administration, suggesting future vaccine strategies may need to enhance the titer of antibody induced. Based on the tolerability and safety established in the current study, we will be embarking on a study to evaluate the use of viral vector-based vaccine encoding HER2 along with lapatinib. The potential benefits of such immunotherapeutic strategies over a monoclonal antibody approach (e.g., induction of both T cell and polyclonal antibody responses with multiple mechanisms of action) warrant this testing. More broadly, we believe that targeting receptor molecules using immunotherapy as a mean to perturb signaling offers potential new opportunities to target cancer beyond the conventional lytic killing of tumors by the immune system.

In summary, the data presented is consistent with prior preclinical and clinical observations and supports the expansion of combination studies. However, the limited numbers of patients, the inability to assess clinical responses compared with controls, and the potential effects of waning trastuzumab levels are challenges that would be best addressed in a randomized trial.

Additional material

Additional file 1: Table S1. dHER2ASCI ELISpot results: Number of IFNg producing.

Additional file 2: Figure S1. Reduced phosphorylation of AKT following dHER ASCI immunization.

Abbreviations
HER2: human epidermal growth factor receptor 2; EGFR: epidermal growth factor receptor; DC: dendritic cells; ASCI: Antigen-Specific Cancer Immunotherapeutic; ICD: intracellular domain; ECD: extracellular domain; EF: ejection fraction; AP: alkaline phosphatase; AE: adverse events; SAE: serious adverse events; LVEF: left ventricular ejection fraction

Author details
[1]Department of Medicine, Division of Medical Oncology, Duke University Medical Center, Durham, NC, USA. [2]Department of Surgery, Division of General Surgery, Duke University Medical Center, Durham, NC, USA. [3]GlaxoSmithKline Biologicals, Rixensart, Belgium. [4]Cancer Statistical Center, Duke Cancer Institute, Durham, NC, USA. [5]Department of Medicine, Division of Gastroenterology, Duke University Medical Center, Durham, NC, USA. [6]Department of Surgery, Division of Surgical Sciences, Duke University Medical Center, Durham, NC, USA.

Authors' contributions
EH participated in the design and coordination of the study, data acquisition and analysis, recruitment of patients and helped draft the manuscript, KB participated in the design of the study, recruitment of patients and helped draft the manuscript, AH participated in the coordination of the study, data acquisition, immune data analysis, and helped draft the manuscript, TM participated in the design and helped draft the manuscript, GB performed statistical analysis, HC participated in the design and helped draft the manuscript, FL participated in the design and helped draft the manuscript, NS participated in the design and helped draft the manuscript, JW participated in the data acquisition and analysis, TO participated in the data acquisition and analysis, HKL participated in the design and helped draft the manuscript. All authors gave final approval of the manuscript for publication. Funding

Competing interests
EH, KB, ACH, GB, NS, TO, HKL and MAM received financial support from GSK to support the research described in the manuscript. HC, FL, and TC are employed by and/or stockholders of GSK.

References
1. Paik S, Hazan R, Fisher ER, Sass RE, Fisher B, Redmond C, Schlessinger J, Lippman ME, King CR: Pathologic findings from the National Surgical Adjuvant Breast and Bowel Project: prognostic significance of erbB-2 protein overexpression in primary breast cancer. *J Clin Oncol* 1990, **8**:103-112.
2. Slamon DJ, Leyland-Jones B, Shak S, Fuchs H, Paton V, Bajamonde A, Fleming T, Eiermann W, Wolter J, Pegram M, Baselga J, Norton L: Use of chemotherapy plus a monoclonal antibody against HER2 for metastatic breast cancer that overexpresses HER2. *N Engl J Med* 2001, **344**:783-792.
3. Xia W, Mullin RJ, Keith BR, Liu LH, Ma H, Rusnak DW, Owens G, Alligood KJ, Spector NL: Anti-tumor activity of GW572016: a dual tyrosine kinase inhibitor blocks EGF activation of EGFR/erbB2 and downstream Erk1/2 and AKT pathways. *Oncogene* 2002, **21**:6255-6263.
4. Geyer CE, Forster J, Lindquist D, Chan S, Romieu CG, Pienkowski T, Jagiello-Gruszfeld A, Crown J, Chan A, Kaufman B, Skarlos D, Campone M, Davidson N, Berger M, Oliva C, Rubin SD, Stein S, Cameron D: Lapatinib plus capecitabine for HER2-positive advanced breast cancer. *N Engl J Med* 2006, **355**:2733-2743.
5. Ritter CA, Perez-Torres M, Rinehart C, Guix M, Dugger T, Engelman JA, Arteaga CL: Human breast cancer cells selected for resistance to trastuzumab in vivo overexpress epidermal growth factor receptor and ErbB ligands and remain dependent on the ErbB receptor network. *Clin Cancer Res* 2007, **3**:4909-4919.
6. Martin AP, Miller A, Emad L, Rahmani M, Walker T, Mitchell C, Hagan MP, Park MA, Yacoub A, Fisher PB, Grant S, Dent P: Lapatinib resistance in HCT116 cells is mediated by elevated MCL-1 expression and decreased BAK activation and not by ERBB receptor kinase mutation. *Mol Pharmacol* 2008, **74**:807-822.
7. Emens LA, Reilly RT, Jaffee EM: Breast cancer vaccines: maximizing cancer treatment by tapping into host immunity. *Endocr Relat Cancer* 2005, **12**:1-17.
8. Peoples GE, Gurney JM, Hueman MT, Woll MM, Ryan GB, Storrer CE, Fisher C, Shriver CD, Ioannides CG, Ponniah S: Clinical trial results of a HER2/neu (E75) vaccine to prevent recurrence in high-risk breast cancer patients. *J Clin Oncol* 2005, **23**:7536-7545.
9. Disis ML, Schiffman K, Guthrie K, Salazar LG, Knutson KL, Goodell V, dela Rosa C, Cheever MA: Effect of dose on immune response in patients vaccinated with an her-2/neu intracellular domain protein-based vaccine. *J Clin Oncol* 2004, **22**:1916-1925.
10. Murray JL, Gillogly ME, Przepiorka D, Brewer H, Ibrahim NK, Booser DJ, Hortobagyi GN, Kudelka AP, Grabstein KH, Cheever MA, Ioannides CG: Toxicity, immunogenicity, and induction of E75-specific tumor-lytic CTLs by HER-2 peptide E75 (369-377) combined with granulocyte macrophage colony-stimulating factor in HLA-A2+ patients with metastatic breast and ovarian cancer. *Clin Cancer Res* 2002, **8**:3407-3418.
11. Salazar LG, Fikes J, Southwood S, Ishioka G, Knutson KL, Gooley TA, Schiffman K, Disis ML: Immunization of cancer patients with HER-2/neu-derived peptides demonstrating high-affinity binding to multiple class II alleles. *Clin Cancer Res* 2003, **9**:5559-5565.
12. Disis ML, Gooley TA, Rinn K, Davis D, Piepkorn M, Cheever MA, Knutson KL, Schiffman K: Generation of T-cell immunity to the HER-2/neu protein after active immunization with HER-2/neu peptide-based vaccines. *J Clin Oncol* 2002, **20**:2624-2632.
13. Morse MA, Hobeika A, Osada T, Niedzwiecki D, Marcom PK, Blackwell KL, Anders C, Devi GR, Lyerly HK, Clay TM: Long Term Disease-Free Survival and T Cell and Antibody Responses in Women with High-Risk HER2+ Breast Cancer Following Vaccination Against HER2+. *J Transl Med* 2007, **5**:42-51.
14. Limentani SA, Curigliano G, Campone M, Dorval T, Romieu G, Tan-Chiu E, White S, De Boer R, Lehmann F, Cormont F, Louahed J: dHER2 cancer immunotherapeutic: Clinical responses in breast cancer patients is associated with an induction of functional antibodies and the generation of specific T-cells [Abstract]. *SABCS* 2007, **106**:s7.
15. O'Donovan N, Byrne AT, O'Connor AE, McGee S, Gallagher WM, Crown J: Synergistic interaction between trastuzumab and EGFR/HER-2 tyrosine kinase inhibitors in HER-2 positive breast cancer cells. *Invest New Drugs* 2011, **29**:752-759.
16. Xia W, Gerard CM, Liu L, Baudson NM, Ory TL, Spector NL: Combining lapatinib (GW572016), a small molecule inhibitor of ErbB1 and ErbB2 tyrosine kinases, with therapeutic anti-ErbB2 antibodies enhances apoptosis of ErbB2-overexpressing breast cancer cells. *Oncogene* 2005, **24**:6213-6221.
17. Morse MA, Hobeika AC, Osada T, Serra D, Niedzwiecki D, Lyerly HK, Clay TM: Depletion of human regulatory T cells specifically enhances antigen-specific immune responses to cancer vaccines. *Blood* 2008, **112**:610-618.

18. Morse MA, Wei J, Hartman Z, Xia W, Ren XR, Lei G, Barry WT, Osada T, Hobeika AC, Peplinski S, Jiang H, Devi GR, Chen W, Spector N, Amalfitano A, Lyerly HK, Clay TM: **Synergism from combined immunologic and pharmacologic inhibition of HER2 in vivo.** *Int J Cancer* 2010, **126**:2893-2903.

19. Zhao W, Gu YH, Song R, Qu BQ, Xu Q: **Sorafenib inhibits activation of human peripheral blood T cells by targeting LCK phosphorylation.** *Leukemia* 2008, **22**:1226-1233.

20. Hipp MM, Hilf N, Walter S, Werth D, Brauer KM, Radsak MP, Weinschenk T, Singh-Jasuja H, Brossart P: **Sorafenib, but not sunitinib, affects function of dendritic cells and induction of primary immune responses.** *Blood* 2008, **111**:5610-5620.

21. Kageyama S, Kitano S, Hirayama M, Nagata Y, Imai H, Shiraishi T, Akiyoshi K, Scott AM, Murphy R, Hoffman EW, Old LJ, Katayama N, Shiku H: **Humoral immune responses in patients vaccinated with 1-146 HER2 protein complexed with cholesteryl pullulan nanogel.** *Cancer Sci* 2008, **99**:601-607.

22. Aoki M, Ueda S, Nishikawa H, Kitano S, Hirayama M, Ikeda H, Toyoda H, Tanaka K, Kanai M, Takabayashi A, Imai H, Shiraishi T, Sato E, Wada H, Nakayama E, Takei Y, Katayama N, Shiku H, Kageyama S: **Antibody responses against NY-ESO-1 and HER2 antigens in patients vaccinated with combinations of cholesteryl pullulan (CHP)-NY-ESO-1 and CHP-HER2 with OK-432.** *Vaccine* 2009, **27**:6854-6861.

23. Kitano S, Kageyama S, Nagata Y, Miyahara Y, Hiasa A, Naota H, Okumura S, Imai H, Shiraishi T, Masuya M, Nishikawa M, Sunamoto J, Akiyoshi K, Kanematsu T, Scott AM, Murphy R, Hoffman EW, Old LJ, Shiku H: **HER2-specific T-cell immune responses in patients vaccinated with truncated HER2 protein complexed with nanogels of cholesteryl pullulan.** *Clin Cancer Res* 2006, **12**:7397-7405.

24. Nicholaou T, Ebert LM, Davis ID, McArthur GA, Jackson H, Dimopoulos N, Tan B, Maraskovsky E, Miloradovic L, Hopkins W, Pan L, Venhaus R, Hoffman EW, Chen W, Cebon J: **Regulatory T-cell-mediated attenuation of T-cell responses to the NY-ESO-1 ISCOMATRIX vaccine in patients with advanced malignant melanoma.** *Clin Cancer Res* 2009, **15**:2166-2173.

25. Disis ML, Strickler JH, Wallace D, Goodell V, Salazar LG, Higgins D, Childs J, Tietje K, Dang Y, Slota M: **Cellular immune parameters associated with improved long-term survival in advanced stage breast cancer patients after active immunization with a HER2-specific vaccine [Abstract].** *J Clin Oncol* 2008, **26**:3015.

26. Hartman ZC, Wei J, Osada T, Glass O, Lei G, Yang XY, Peplinski S, Kim DW, Xia W, Spector N, Marks J, Barry W, Hobeika A, Devi G, Amalfitano A, Morse MA, Lyerly HK, Clay TM: **An adenoviral vaccine encoding full-length inactivated human Her2 exhibits potent immunogenicty and enhanced therapeutic efficacy without oncogenicity.** *Clin Cancer Res* 2010, **16**:1466-1477.

27. Morse MA, Hobeika A, Serra D, Aird K, McKinney M, Aldrich A, Clay T, Mourich D, Lyerly HK, Iversen PL, Devi GR: **Depleting regulatory T cells with arginine-rich, cell-penetrating, peptide-conjugated morpholino oligomer targeting FOXP3 inhibits regulatory T-cell function.** *Cancer Gene Ther* 2012, **19**:30-37.

28. Disis ML, Wallace DR, Gooley TA, Dang Y, Slota M, Lu H, Coveler AL, Childs JS, Higgins DM, Fintak PA, dela Rosa C, Tietje K, Link J, Waisman J, Salazar LG: **Concurrent trastuzumab and HER2/neu-specific vaccination in patients with metastatic breast cancer.** *J Clin Oncol* 2009, **27**:4685-4692.

29. Waddell T, Kotsori A, Constantinidou A, Yousaf N, Ashley S, Parton M, *et al*: **Trastuzumab beyond progression in HER2-positive advanced breast cancer: The Royal Marsden experience.** *Br J Cancer* 2011, **104**:1675-1679.

30. Blackwell KL, Pegram MD, Tan-Chiu E, Schwartzberg LS, Arbushites MC, Maltzman JD, Forster JK, Rubin SD, Stein SH, Burstein HJ: **Single-agent lapatinib for HER2-overexpressing advanced or metastatic breast cancer that progressed on first- or second-line trastuzumab-containing regimens.** *Ann Oncol* 2009, **20**:1026-1031.

31. Blackwell KL, Burstein HJ, Storniolo AM, Rugo H, Sledge G, Koehler M, Ellis C, Casey M, Vukelja S, Bischoff J, Baselga J, O'Shaughnessy J: **Randomized study of Lapatinib alone or in combination with trastuzumab in women with ErbB2-positive, trastuzumab-refractory metastatic breast cancer.** *J Clin Oncol* 2010, **28**:1124-1130.

32. Hoos A, Eggermont AM, Janetzki S, Hodi FS, Ibrahim R, Anderson A, Humphrey R, Blumenstein B, Old L, Wolchok J: **Improved endpoints for cancer immunotherapytrials.** *J Natl Cancer Inst* 2010, **102**:1388-1397.

33. Maruyama T, Mimura K, Izawa S, Inoue A, Shiba S, Watanabe M, Kawaguchi Y, Inoue M, Nogata H, Inoue S, Fujii H, Kono K: **Lapatinib**

enhances herceptin-mediated antibody-dependent cellular cytotoxicity by up-regulation of cell surface HER2 expression. *Anticancer Res* 2011, **31**:2999-3005.

Increasing vaccine potency through exosome antigen targeting☆

Zachary C. Hartman [a,1], Junping Wei [a,1], Oliver K. Glass [a], Hongtao Guo [a], Gangjun Lei [a], Xiao-Yi Yang [a], Takuya Osada [a], Amy Hobeika [a], Alain Delcayre [d], Jean-Bernard Le Pecq [d], Michael A. Morse [b], Timothy M. Clay [a,c], Herbert K. Lyerly [a,*]

[a] Duke Comprehensive Cancer Center, Department of Surgery, Duke University Medical Center, Durham, NC 27710, USA
[b] Department of Medicine, Division of Medical Oncology, Duke University Medical Center, Durham, NC 27710, USA
[c] Department of Immunology, Duke University Medical Center, Durham, NC 27710, USA
[d] ExoThera L.L.C, Menlo Park, CA, USA

ABSTRACT

While many tumor associated antigens (TAAs) have been identified in human cancers, efforts to develop efficient TAA "cancer vaccines" using classical vaccine approaches have been largely ineffective. Recently, a process to specifically target proteins to exosomes has been established [1] which takes advantage of the ability of the factor V like C1C2 domain of lactadherin to specifically address proteins to exosomes. Using this approach, we hypothesized that TAAs could be targeted to exosomes to potentially increase their immunogenicity, as exosomes have been demonstrated to traffic to antigen presenting cells (APC) [2]. To investigate this possibility, we created adenoviral vectors expressing the extracellular domain (ECD) of two non-mutated TAAs often found in tumors of cancer patients, carcinoembryonic antigen (CEA) and HER2, and coupled them to the C1C2 domain of lactadherin. We found that these C1C2 fusion proteins had enhanced expression in exosomes in vitro. We saw significant improvement in antigen specific immune responses to each of these antigens in naïve and tolerant transgenic animal models and could further demonstrate significantly enhanced therapeutic anti-tumor effects in a human HER2+ transgenic animal model. These findings demonstrate that the mode of secretion and trafficking can influence the immunogenicity of different human TAAs, and may explain the lack of immunogenicity of non-mutated TAAs found in cancer patients. They suggest that exosomal targeting could enhance future anti-tumor vaccination protocols. This targeting exosome process could also be adapted for the development of more potent vaccines in some viral and parasitic diseases where the classical vaccine approach has demonstrated limitations.

© 2011 Elsevier Ltd. All rights reserved.

1. Introduction

In most infectious diseases, soluble or particle antigens are circulating in the blood and can easily be captured by the professional antigen presenting cells (APC). Vaccines delivering these antigens in a native or inactivated form associated with proper adjuvant typically elicit a very potent immune response. This classical vaccine approach has been used widely and successfully applied in human and animal populations for preventing deadly diseases.

Unfortunately, this classical approach shows very little efficacy in diseases where antigens remain mainly localized inside cells, such as in some viral and parasitic diseases. The identification of tumor associated antigens (TAA) in human cancers [3,4] triggered an enormous effort in the medical and scientific community to develop "cancer vaccines". Except in the case where viral antigens could be identified [5], the delivery of TAA in various forms by various vectors in association with a variety of adjuvants has led, up to now, to rather disappointing results [6,7]. These studies have revealed several specific difficulties with this type of approach. A primary difficulty is that most TAA are cell-associated and probably not delivered efficiently to professional APCs. While TAA can include proteins [3,4] that are coded by the host and overexpressed in cancer cells (HER2, wild type p53), some are expressed in fetal development (CEA) and/or select tissues, but not widely expressed in adult life such as the cancer–testis antigen family. Others are expressed with somatic mutations (RAS, p53) or translational modifications (MUC1). However, in general, they are poorly antigenic or expressed in an immunosuppressive environment. "Cancer vaccines" are supposed to be used mainly

as therapeutic vaccines when a state of TAA immune-tolerance is established, a situation quite different from that encountered in classical vaccines where xenogeneic antigens are delivered to naïve individuals. Although new immunomodulatory reagents that may reverse tolerance in advanced cancer patients are being developed for cancer immunotherapy, strategies to enhance the potency of cancer vaccines to break established tolerance are essential for vaccines that may be given to a wide range of cancer patients

The lactadherin C1C2 domain is a lipid binding domain, related to the C1C2 domain of factor V. It is responsible for the specific addressing of lactadherin to exosomes as deletion in this domain abolishes exosome addressing [1,8]. It has recently been shown that soluble proteins including intracellular proteins, when fused to the C1C2 domain of lactadherin are no longer found intracellularly but are released in extracellular compartment, almost exclusively associated to exosomes [1,9]. As exosomes transfer intracellular antigens directly to antigen presenting cells (APCs) [2], it was proposed that targeting intracellular antigens to exosomes would increase their trafficking to APCs and therefore stimulate their immunogenicity [1]. These principles were tested in a recent study that compared the tumorigenicities of ovalbumin antigen expressing cells [9]. In the study, the malignant cells expressing the C1C2-lactadherin domain ovalbumin fusion protein released the ovalbumin protein bound to exosomes in contrast to cell expressing unmodified ovalbumin. The authors also found that cells expressing the C1C2-fusion albumin were strikingly less tumorigenic if tested in immune-competent mice but kept their tumorigenity in immune-suppressed mice. Furthermore, some animals treated with cells expressing C1C2-ovabulin fusion could become immune against the cells expressing the unmodified ovalbumin. These results suggest that despite a tumor cell environment, the C1C2 fusion protein could induce an effective anti-tumor immune response most likely mediated by trafficking to exosomes [9].

In order to test the possibility of using this targeting strategy to improve the potency of vaccines, we generated recombinant adenoviral vectors expressing the extracellular domain (ECD) of carcinoembryonic antigen (CEA) or HER2 linked to the C1C2 domain of lactadherin in addition to native unlinked ECD versions of CEA and HER2. We tested the efficacy of these viruses using mice made transgenic for these antigens to mimic the state of immune-tolerance found in human patients. We found that adenoviral expression of a C1C2 modified CEA/ECD and HER2/ECD resulted in significantly higher protein expression in exosomal fractions compared to non-targeted CEA in both murine cell lines and antigen presenting cells. We also found that secreting the ECD of CEA or HER2 *in vivo* as a vesicle-associated form was superior in inducing antigen specific immune responses in naïve and tolerant animals and enhanced anti-tumor immune responses. Our results thus provide insight into the low immunogenicity of soluble TAAs in cancer patients and suggest new means to improve anti-tumor immune responses for vaccines targeting cancer or potentially other diseases.

2. Materials and methods

2.1. C1C2 cloning and Ad vector construction

Briefly, the extracellular domain of either human CEA (nt 1-2025) or human HER2/neu (nt 1-1953) were inserted into the mouse Lactadherin expression plasmid p6mLC1C2 as described [1] to create exosomal cassettes containing the leader signal and C1C2 domains of mouse lactadherin fused in-frame to the respective constructs. Vectors were created using the pAdEasy system [10] and all

stocks titered using AdEasy viral titer kit (Stratagene, Santa Clara, CA).

2.2. In vivo experiments

C57BL/6J and BALB/c mice were obtained from Jackson Labs (Bar Harbor, MA), human CEA-transgenic mice were a kind gift from Jeff Schlom (National Cancer Institute, Bethesda, MD), and HER2 transgenic mice were obtained from Dr. Wei-Zen Wei (Wayne State University, Detroit, MI). Adenoviral vectors were administered via the footpad at indicated times of 4–12-week-old mice. All animal work was performed in accordance with Duke IACUC approved protocols.

2.3. ELISPOT and antibody procedures

Mouse IFN-gamma ELISPOT assay (Mabtech Inc., Cincinnati, OH) was performed according to according to published methods [11]. Briefly, harvested splenocytes were stimulated with CEA peptide mix (2.6 μg/ml: BD Bioscience, San Jose, CA), HER2 overlapping peptide mixtures (1 μg/ml of 15mer peptides overlapping by 11 amino acids for HER2) or irrelevant HIV gag or CMV pp65 antigen controls (2.6 μg/ml: BD Bioscience, San Jose, CA). PMA (50 ng/ml) and Ionomycin (1 μg/ml) were used as positive controls for splenocyte responsiveness. Anti-HER2 IgG antibodies were detected by FACS analysis of BT474 and SKBR3 HER2+ cells using PE-conjugated anti-Mouse IgG (Dako, Cat # R0480) as a secondary detection antibody. CEA ELISA used recombinant CEA (TriChem Resources, Inc., West Chester, PA, 10ug/ml) as the capture antigen and an anti-mouse IgG secondary antibody (Jackson Immunoresearch, West Grove, PA) as the detection antibody.

2.4. In vitro assays

The human BT474 and SKBR3 HER2+ breast cancer lines and the murine JAWSII DC lines were obtained, tested for contamination (cellular and mycoplasma), and maintained according to ATCC recommendations. The human-HER2 expressing 4T1 mouse mammary tumor line (4T1-HER2) was kindly provided by Dr. Michael Kershaw (Peter MacCallum Cancer Centre, East Melbourne, Victoria, Australia). Murine bone marrow derived dendritic cells (bmDCs) were prepared and cultured with standard methods using GM-CSF (10 ng/ml) and IL-4 (10 ng/ml) (PeproTech, Rocky Hill, NJ).

For assessment of exosome protein expression, cleared supernatants were harvested and exosomes concentrated using standard ExoQuick (SBI Biosciences, Mountain View, CA) procedures [12]. Briefly, cleared supernatants (centrifuged at $3000 \times g$ for 15 min) were filtered using a .45um PVDF filter and mixed with ExoQuick precipitation solution and incubated overnight at 4 °C. After incubation, precipitated exosomes were centrifuged at $1500 \times g$ for 30 min at 4 °C following ExoQuick protocols. Concentrated exosomal fractions were resuspended in then quantified used a BCA assay (Thermo Fisher, Rockford, IL), and subjected to western blot analysis using anti-CEA (Cell Signaling Technology, Danvers, MA) and tsg101 as an exosome marker loading control (Abcam, Cambridge, MA) antibodies.

For exosome-capture ELISA to measure CEA and HER2 protein levels, supernatants from transduced cells were used in an anti-CD81 cross-capture ELISA [13] with monoclonal anti-CD81 (BioLegend, San Diego, CA) as a capture antibody and a polyclonal anti-CEA rabbit Ab (AbCam, Cambridge, MA) or an anti HER2 (N-terminal) rabbit Ab (Santa Cruz Biotechnology, Santa Cruz, CA), and an anti-rabbit HRP linked antibody (AbCam, Cambridge, MA) as the detection antibody set. In all experiments, uninfected control

Fig. 1. Exosomal Adenoviral Vectors. (A) Design of adenoviral vectors encoding CEA/ECD and HER2/ECD exosomal constructs and controls. (B) Ad transduced (MOI = 2000) JAWSII and bmDCs supernatant CEA expression at 24 and 48 hpi. (C) and (D) Ad-transduced (MOI = 2000) JAWSII cells 24 hpi (C) and 48 hpi (D) supernatants were assessed using an exosome-specific ELISA, which employed a CD81 capture antibody to isolate exosomes and CEA-specific detection antibody (C) and HER2-specific detection antibody (D) to assess exosomal CEA and HER2 expression. In all experiments, '*' and '**' denotes conditions that showed $p < 0.05$ and $p < 0.01$, respectively, compared to control Ad-LacZ transduction and '#' and '##' denote conditions that showed $p < 0.05$ and $p < 0.01$, respectively to Ad-CEA/ECD or Ad-HER2/ECD treatment. $N = 3$ and error bars = SD.

wells were performed simultaneously to monitor and control for background absorbance.

For cellular proliferation assessments, HER2+ BT474 human mammary tumor cells were cultured with serum of Ad immunized mice (Ad-HER2/ECDC1C2 or control at 1:20 dilution with Trastuzumab (Herceptin) (1 μg/ml) as a positive control for 6 days (with a media change at day 3) and measured by MTT (absorbance 550 nm).

To assess complement-dependent cytotoxicity (CDC), sera from mice immunized as above was diluted (1:100) and co-incubated with target cells (BT474) at 37 °C for 1 h and 1:100 diluted rabbit serum as the source of complement. After 2.5 h incubation, cytotoxicity was measured using the CytoTox 96 Non-Radioactive Cytotoxicity Assay (Promega) to measure LDH release in the culture media as evidence of cytotoxicity.

3. Results

3.1. Construction of adenoviral vectors targeting CEA and HER2 to exosome and exosome associated expression of CEA

To assess the effect of exosomal secretion on virally expressed tumor associated antigens (TAAs), we generated a series of recombinant adenoviral vectors expressing the extracellular domain of carcinoembryonic antigen and HER2 in addition to a control LacZ. Identical antigen constructs coupled to a C1C2 domain, previously demonstrated to target antigens to exosomal compartment [1,9] were then generated to assess the effect of antigen exosomal targeting (Fig. 1A).

Immortalized and bmDC-derived murine dendritic cells were then transduced with the various Ad-CEA vectors and exosome concentrated supernatants (using ExoQuick) assessed for CEA expression at 1 and 2 days post-transduction (dpi) by western blot analysis (Fig. 1B). These results revealed a dramatic enhancement of CEA expression in extracellular exosome fractions compared to CEA and CEA/ECD controls (Fig. 1B). To further confirm CEA antigen presence in the exosomal fraction, we used an exosomal capture ELISA assay to isolate CD81+ exosome fractions and measure CEA protein levels (Fig. 1C). These assays confirmed our western blot analysis, demonstrating that only in exosomal fractions from JAWSII cells transduced with Ad-CEA/ECDC1C2 did we detect significant levels of CEA protein, thus demonstrating the C1C2 domain effectiveness in enhancing TAA exosome targeting. Similar experiments using Ad-HER2ECD and Ad-HER2/ECDC1C2 adenoviral vectors confirmed the secretion of HER2 in exosomal fractions (Fig. 1D), thus confirming that lactadherin C1C2 targeting of tumor antigen in adenoviral vector could effectively target these proteins to secreted exosomal vesicles.

3.2. Enhancement of T-cell responses to CEA/ECD by targeting to exosomes

To determine the immunologic effects of the C1C2 modification, we vaccinated C57BL/6J mice with the various Ad-CEA or control adenoviral vectors and assessed CEA specific immune responses by CEA specific ELISPOT and ELISA at 2 weeks post-transduction (wpi). Both ELISPOT and ELISA analyses demonstrated that anti-CEA immunity in Ad-CEA/ECDC1C2 was significantly enhanced compared to Ad-CEA/ECD vectors (Fig. 2A). To determine if similar differences in anti-CEA responses could be seen at lower viral doses, Ad-CEA/ECD and Ad-CEA/ECDC1C2 were injected at two lower titers and T-cell and B-cell responses were again assessed by ELISPOT and ELISA assays. Remarkably, we found that Ad-CEA/ECDC1C2 elicited robust T-cell and antibody responses without significant abatement at lower titers, while the strength of Ad-CEA/ECD T-cell and B-cell responses were significantly reduced by the diminished viral titer (Fig. 2B).

We next vaccinated CEA transgenic animals with the Ad-CEA/ECD, Ad-CEA/ECDC1C2 and control vectors to determine the effects of vaccination in a model of CEA tolerance. As expected, the tolerant human CEA transgenic mice were far less responsive to vaccination. While, Ad-CEA/ECDC1C2 vaccinated CEA transgenic mice did have a significant CEA specific T-cell response (Fig. 2C), vaccination with Ad-CEA/ECDC1C2 at this dose did not generate significant anti-CEA antibody responses in CEA transgenic mice (Fig. 2D).
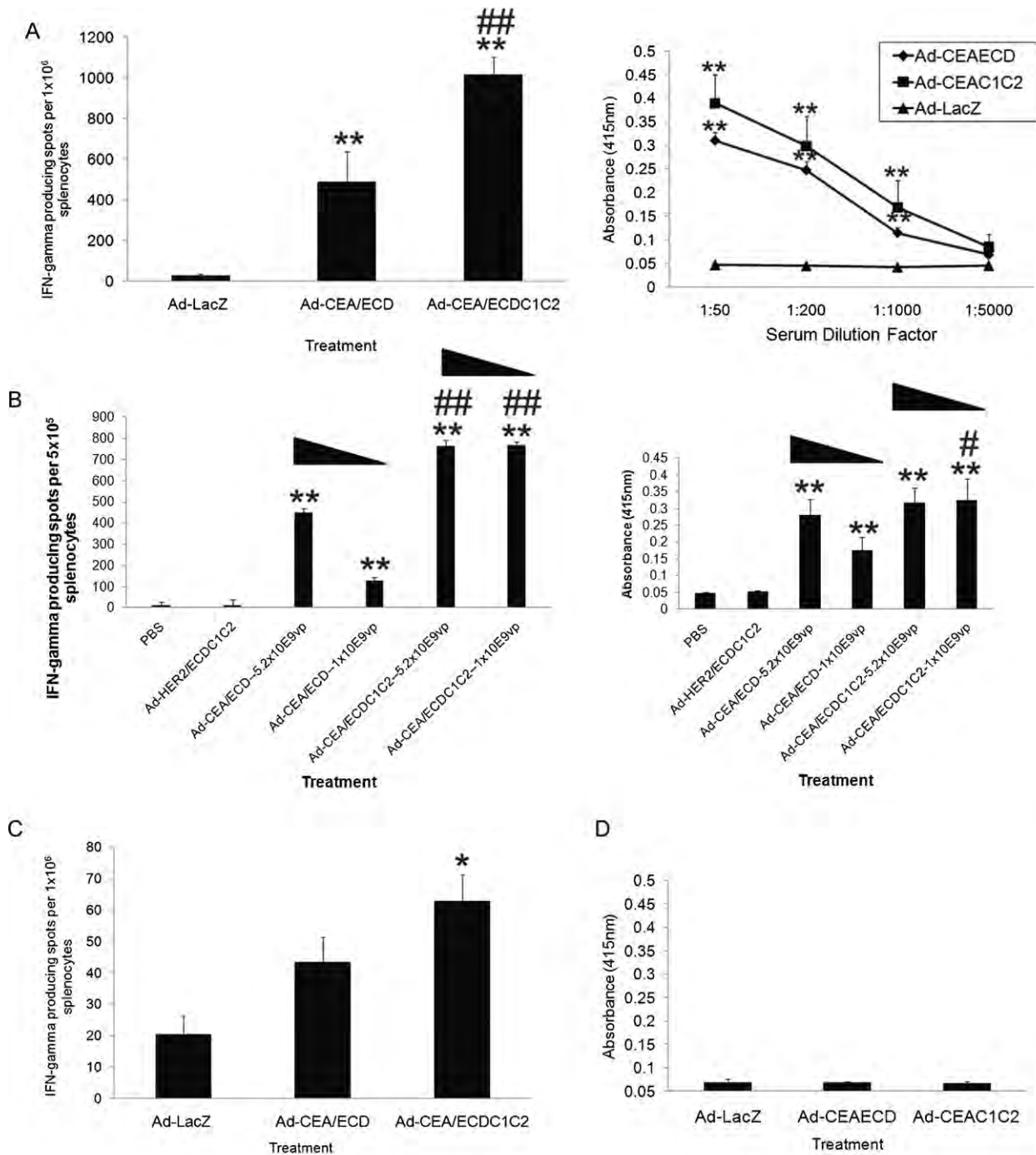
3.3. Enhancement of T and B-cell responses to HER2/ECD by targeting to exosomes

As we demonstrated with CEA exosome targeted vaccines, we found that HER2/ECDC1C2 vaccination elicited significantly greater HER2 specific T-cell (Fig. 3A) and antibody responses compared to wild-type HER2/ECD in vivo (Fig. 3B).

As antibodies that target the extracellular domain of HER2 have proven therapeutic effects, we then assessed the HER2/ECD-specific antibodies in serum for anti-proliferative activity and complement-dependent cytotoxicity. Our results demonstrated a significantly greater inhibition of proliferation (Fig. 3C) and CDC mediated lysis (Fig. 3D) of HER2+ BT474 cells with serum from mice post Ad-HER2/ECDC1C2 vaccination compared to the Ad-HER2/ECD vaccination (Fig. 3C).

To investigate if exosome targeting could enable therapeutic anti-tumor immunity in vivo, we implanted human HER2+ mouse mammary cancer cells (4T1-HER2) into human HER2 transgenic mice and vaccinated tumor bearing mice at the indicated intervals with Ad-LacZ, Ad-HER2/ECD, and Ad-HER2/ECDC1C2. Consistent
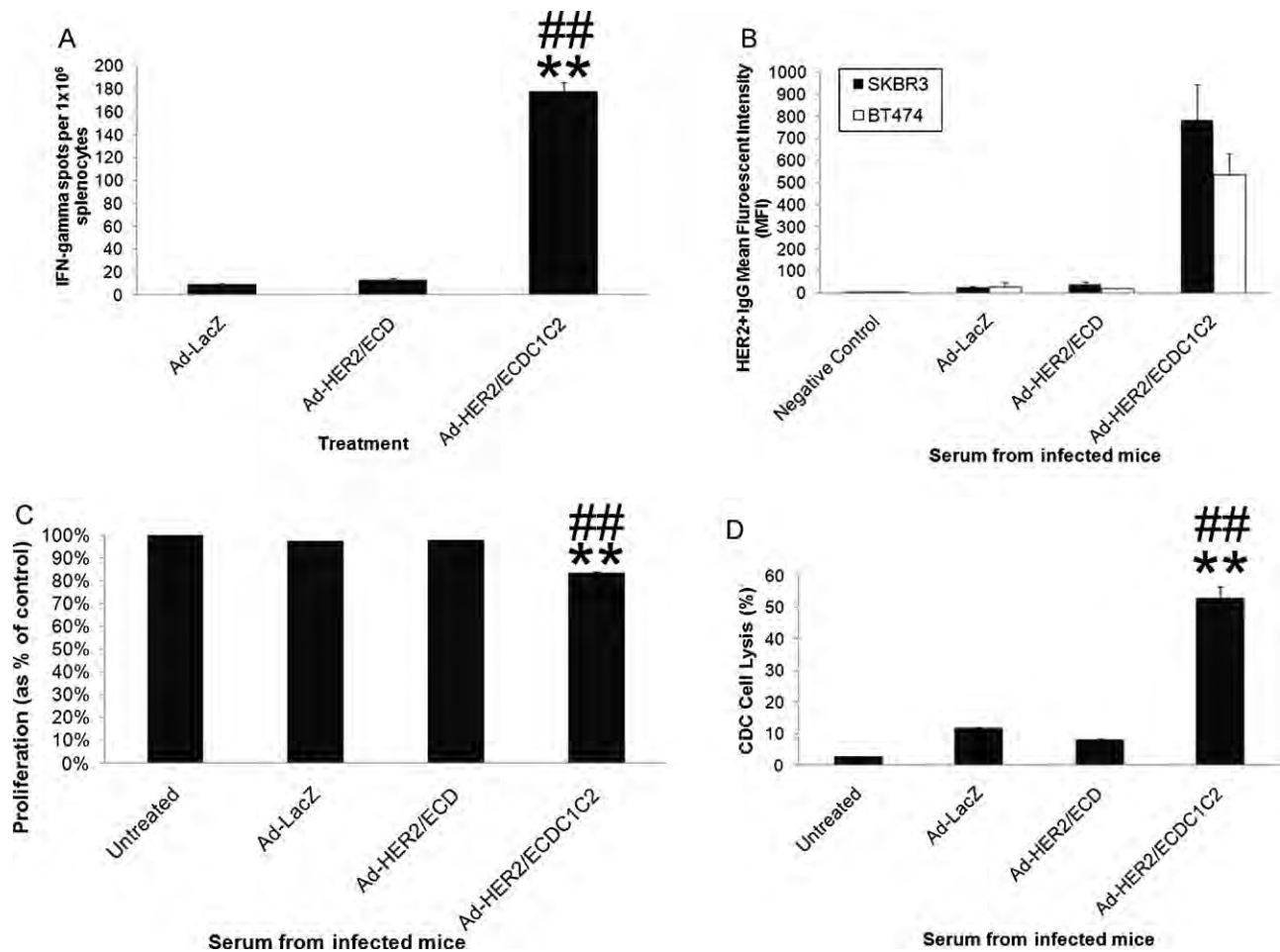
Fig. 2. Vaccination with Ad-CEA C1C2 elicits superior anti-CEA adaptive immune responses. (A) CEA T-cell responses at 14 days post-transduction (dpi) by IFN-γ ELISPOT (on left) and by anti-CEA IgG ELISA (on right) from C57BL/6J Ad vaccinated mice (2.6×10^{10} viral particles). (B) Mice were vaccinated as in (A) but using 5.2×10^9 or 1.05×10^9 vp of the indicated vectors with ELISPOT (on left) and ELISA (on right) performed (1:4000 dilution) at 14 days-post-injection. Triangular bars indicate decreasing viral dose. (C) and (D) ELISPOT And ELISA responses from C57BL/6J human CEA+ transgenic animals were treated and assessed as in (A). In all experiments, '*' and '**' denotes conditions that showed $p < 0.05$ and $p < 0.01$, respectively, compared to control Ad-LacZ transduction and '#' and '##' denote conditions that showed $p < 0.05$ and $p < 0.01$, respectively to Ad-CEA/ECD treatment. $N = 5$ and error bars = SD.

with our previous CEA findings, we found that vaccination with Ad-HER2/ECDC1C2, but not Ad-HER2/ECD, significantly retarded HER2+ tumor growth in transgenic HER2+ mice (Fig. 4A). When vaccinations were repeated against an Ad-CEA/ECDC1C2 control, we again found that Ad-HER2/ECDC1C2 significantly attenuated tumor growth, while Ad-CEA/ECDC1C2 did not, thus indicating the anti-tumor effect was specific to C1C2-tagged HER2 and not due to non-specific effects of C1C2 expression.

4. Discussion

In agreement with previous proposal and observations [1], our study demonstrates that adenoviral transduction of cells in culture with constructs expressing the extracellular regions of different non-mutated TAAs fused to the C1C2 domain of lactadherin promotes high expression of exosome associated antigen in the extracellular medium. It is likely that

Fig. 3. Vaccination with Ad-HER2-C1C2 elicits superior anti-HER2 adaptive responses. (A) Anti-HER2 T-cell responses assessed at 14 days post-transduction (dpi) by IFN-γ ELISPOT in BALB/c mice (2.6×10^{10} vp). Error bars represent standard deviation ($n = 4$ mice per group at each time point). (B) Anti-HER2 antibodies from serum of vaccinated mice (as in A) were measured using FACS to HER2+ cell lines (Average MFI from multiple experiments is shown). (C) Anti-proliferative effects of vaccine induced antibodies were assessed by incubating Serum from C57BL/6J vaccinated mice (injected with 2.6×10^{10} vp, boosted 2.6×10^{10} vp at 14dpi, and harvested at 28dpi) with BT474 HER2+ cells in a MTT proliferation assay ($N = 4$). (D) Complement dependant cytotoxicity (CDC) mediated by vaccine induced antibodies (VIA) was assessed by incubating serum from mice treated as in C) with BT474 HER2+ cells in a CDC assay ($N = 4$). In all experiments, '*' and '**' denotes conditions that showed $p < 0.05$ and $p < 0.01$, respectively, compared to control Ad-LacZ transduction and '#' and '##' denote conditions that showed $p < 0.05$ and $p < 0.01$ respectively to Ad-HER2/ECD treatment. Error bars denote SD.

the same phenomenon occurs *in vivo*. However, at this stage of the investigations, whether a fraction of the fusion proteins associates with other components *in vivo* cannot be ruled out.

The modality of lactadherin trafficking and binding to exosomes, which represent a very small fraction of the total membrane content of a cell is not yet clearly understood. Exosomes reside inside the multivesicular bodies (MVB) and are formed by inward budding

Fig. 4. Vaccination with Ad-HER2-C1C2 elicits superior anti-tumor responses against HER2+ cells in human HER2 transgenic mice. BALB/c HER2+ transgenic mice were implanted with 2×10^4 4T1-HER2+ cells at day zero and vaccinated with 2.6×10^{10} vp of the indicated Ad vectors (A and B) where indicated by arrows (4, 11, and 18 dpi). For all conditions, $N = 6–8$ and error bars denote SE. In all samples, '*' and '**' denotes conditions that showed $p < 0.05$ and $p < 0.01$, respectively, compared to Ad-LacZ (A) or PBS (B) controls. Additionally, '#' and '##' denote conditions that showed $p < 0.05$ and $p < 0.01$, respectively to Ad-HER2/C1C2ECD injected animals (A).

of the MVB membrane [14]. The external surface of exosomes is never in direct contact with cytoplasmic medium. Recently, crystallographic structure of the C2 domain of bovine lactadherin was elucidated [15]. This study indicates that the C1C2 domain forms a high affinity reversible complex with membranes [16] through the intercalation of several aromatic and hydrophobic amino acids in the lipid layer. Since the external surface of exosomes seems to be never in contact with cytoplasmic constituents, lactadherin targeting to exosomes would require its specific transport across the MVB membrane to allow its interaction with the exosomes inside the MVB compartment. Whether selective transport across MVB membrane and specific binding would account for the targeting of lactadherin and its C1C2-fusion analogues to exosomes in cells remains to be examined.

The injection of adenoviruses expressing the C1C2 domain fused to the ECD of either CEA or HER2 results in enhanced antigen-specific immune responses in both naïve and tolerant transgenic animals. This was in contrast to the *in vivo* expression of the soluble antigen not fused to C1C2, which, in naive and tolerant transgenic animals, triggered low or non-detectable immune responses.

Our work demonstrates enhancement of both T-cell and B-cell activation by this targeting process and extends these observations to common human TAAs overexpressed in the context of a viral vector. Furthermore, we demonstrated that TAA targeting to secreted membrane vesicles *in vivo* enhanced immune responses in both naïve and TAA tolerant settings. The utility of the approach to improve recombinant viral vaccines is significant, as these vectors can transduce many cell types and produce protein at much greater levels compare to naked DNA vaccines. Finally, we also found that the heightened immune responses mediated by exosomal targeting also translated into more effective therapeutic anti-tumor responses in a TAA tolerant animal model. The use of a tolerant animal model is critical for mimicking the situation found in human cancers.

The rationale to use exosome targeting is supported by the known physiological properties of exosomes. Indeed, one of the assumed exosome functions is to deliver antigens to antigen presenting cells and exosomes contain a large complex variety of proteins, which could stimulate both adaptive [2,17] and innate [18] immune responses.

It has been observed that exosomes released by some tumor cells could become immunosuppressive [19–21]. Tumors cells can modify the properties and the protein content of the exosomes they release. The ability of some tumor cells to turn exosomes into immunosuppressive vesicles could be one of the factors which allow malignant cells to escape host immunosurveillance, as previously discussed [22]. As viral vectors have been well demonstrated to activate immune responses in innate immune cells, as well as in many types of stromal cells, a viral mediated strategy may be of critical importance to generating exosomes with immunogenic content. As an initial demonstration of this strategy, the modified vaccinia system was shown to induce enhanced immune responses to exosome secreted PSA and PAP antigens in a prostate tumor model [23]. As adenoviral vectors have been demonstrated to be highly immunogenic in comparison to other viral platforms [24,25], we believe that their use could offer significant improvements in the use of exosomal targeting strategies. Thus, while the type of cell and the method of transduction are issues of critical importance for the type of exosome produced, we believe our adenoviral-mediated strategy is capable of significantly enhancing immune responses to exosomal-derived proteins. It must also be underlined that this targeting process allows many different types of protein to be delivered to exosomes, such as interleukins and GM-CSF [1]. In future work, the possibility of co-delivering antigens and adjuvant factors to exosomes to further increase vaccine potency will be investigated.

Finally, our study also suggests that involvement of antigen cross presentation [26] should be considered for vaccine development directed against intracellular antigens and that exosomes as [2] could be one element of this complex and not yet fully characterized process.

In conclusion, this is the first demonstration that viral vaccines can be enhanced by exosomal targeting, specifically demonstrating that both C1C2-fused CEA and HER2 ECD encoded by viral vectors are superior in generating antigen specific T and B-cell response compared to soluble protein in wild type and transgenic animals. In line with this data, endogenous soluble CEA and HER2 ECD found in the circulation of cancer patients are poor immunogens that do not contribute to efficient anti-tumor responses. Modifying tumor antigens to exploit the exosome pathway for cross-presentation may represent a new way to generate effective immune-mediated anti-tumor activity. Significantly, while this work was performed with tumors antigens, this strategy could be also extended to other types of diseases, such as viral and parasitic transductions, to elicit highly effective and specifically targeted therapeutics.

Acknowledgements

References

[1] Delcayre A, Estelles A, Sperinde J, Roulon T, Paz P, Aguilar B, et al. Exosome display technology: applications to the development of new diagnostics and therapeutics. Blood Cells Mol Dis 2005;35(2):158–68.

[2] Théry C, Zitvogel L, Amigorena S. Exosomes: composition, biogenesis and function. Nat Rev Immunol 2002;2(8):569–79.

[3] Finn OJ. Cancer immunology. N Engl J Med 2008;358(25):2704–15.

[4] Steer HJ, Lake RA, Nowak AK, Robinson BWS. Harnessing the immune response to treat cancer. Oncogene 2010;29:6301–13.

[5] Finn OJ, Edwards RP. Human papillomavirus vaccine for cancer prevention. N Engl J Med 2009;361:1899–901.

[6] Finn OJ. Cancer vaccines: between the idea and the reality. Nat Rev Immunol 2003;3:360–441.

[7] Pejawar-Gaddy S, Finn OJ. Cancer vaccines: accomplishments and challenges. Crit Rev Oncol Hematol 2008;67(2):93–102.

[8] Oshima K, Aoki N, Kato T, Kitajima K, Matsuda T. Secretion of a peripheral membrane protein, MFG-E8, as a complex with membrane vesicles. Eur J Biochem 2002;269(4):1209–18.

[9] Zeelenberg IS, Ostrowski M, Krumeich S, Bobrie A, Jancic C, Boissonnas A, et al. Targeting tumor antigens to secreted membrane vesicles in vivo induces efficient antitumor immune responses. Cancer Res 2008;68(4):1228–35.

[10] He TC, Zhou S, da Costa LT, Yu J, Kinzler KW, Vogelstein B. A simplified system for generating recombinant adenoviruses. Proc Natl Acad Sci USA 1998;95(5):2509–14.

[11] Hartman ZC, Wei J, Osada T, Glass O, Lei G, Yang XY, et al. An adenoviral vaccine encoding full-length inactivated human Her2 exhibits potent immunogenicity and enhanced therapeutic efficacy without oncogenicity. Clin Cancer Res 2010;16(5):1466–77.

[12] Taylor DD, Zacharias W, Gercel-Taylor C. Exosome isolation for proteomic analyses and RNA profiling. Methods Mol Biol 2011;728:235–46.

[13] Lamparski HG, Metha-Damani A, Yao JY, Patel S, Hsu DH, Ruegg C, et al. Production and characterization of clinical grade exosomes derived from dendritic cells. J Immunol Methods 2002;270(2):211–26.

[14] Denzer K, Kleijmeer MJ, Heijnen HF, Stoorvogel W, Geuze HJ. Exosome: from internal vesicle of the multivesicular body to intercellular signaling device. J Cell Sci 2000;113:3365–74.

[15] Lin L, Huai Q, Huang M, Furie B, Furie BC. Crystal structure of the bovine lactadherin C2 domain, a membrane binding motif, shows similarity to the C2 domains of factor V and factor VIII. J Mol Biol 2007;371(3):717–24.

[16] Bardelle C, Furie B, Furie BC, Gilbert GE. Membrane binding kinetics of factor VIII indicate a complex binding process. J Biol Chem 1993;268(12):8815–24.

[17] Théry C, Ostrowski M, Segura E. Membrane vesicles as conveyors of immune responses. Nat Rev Immunol 2009;9(8):581–93.

[18] Viaud S, Terme M, Flament C, Taieb J, André F, Novault S, et al. Dendritic cell-derived exosomes promote natural killer cell activation and proliferation: a role for NKG2D ligands and IL-15Ralpha. PLoS One 2009;4(3):e4942.

[19] Koga K, Matsumoto K, Akiyoshi T, Kubo M, Yamanaka N, Tasaki A, et al. Purification, characterization and biological significance of tumor-derived exosomes. Anticancer Res 2005;25:3703–8.

[20] Clayton A, Tabi Z. Exosomes and the MICA-NKG2D system in cancer. Blood Cells Mol Dis 2005;34(3):206–13.

[21] Zhang HG, Grizzle WE. Exosomes and cancer: a newly described pathway of immune suppression. Clin Cancer Res 2011;17(5):959–64.

[22] Delcayre A, Shu H, Le Pecq JB. Dendritic cell-derived exosomes in cancer immunotherapy: exploiting nature's antigen delivery pathway. Expert Rev Anticancer Ther 2005;5(3):537–47.

[23] Rountree RB, Mandl SJ, Nachtwey JM, Dalpozzo K, Do L, Lombardo JR, et al. Cancer Res 2011;71(15):5235–44.

[24] Cubillos-Zapata C, Guzman E, Turner A, Gilbert SC, Prentice H, Hope JC, et al. Differential effects of viral vectors on migratory afferent lymph dendritic cells in vitro predicts enhanced immunogenicity in vivo. J Virol 2011;85(18):9385–94.

[25] Barefoot B, Thornburg NJ, Barouch DH, Yu JS, Sample C, Johnston RE, et al. Comparison of multiple vaccine vectors in a single heterologous prime-boost trial. Vaccine 2008;26(48):6108–18.

[26] Rock KL, Shen L. Cross-presentation: underlying mechanisms and role in immune surveillance. Immunol Rev 2005;207:166–83.

Cancer Research

AACR

HER2 Overexpression Elicits a Proinflammatory IL-6 Autocrine Signaling Loop That Is Critical for Tumorigenesis

Zachary C. Hartman, Xiao-Yi Yang, Oliver Glass, et al.

Updated version	Access the most recent version of this article at: doi:10.1158/0008-5472.CAN-11-0308
Supplementary Material	Access the most recent supplemental material at: http://cancerres.aacrjournals.org/content/suppl/2011/04/25/0008-5472.CAN-11-0308.DC1.html

Cited Articles	This article cites by 39 articles, 10 of which you can access for free at: http://cancerres.aacrjournals.org/content/71/13/4380.full.html#ref-list-1
Citing articles	This article has been cited by 5 HighWire-hosted articles. Access the articles at: http://cancerres.aacrjournals.org/content/71/13/4380.full.html#related-urls

E-mail alerts	Sign up to receive free email-alerts related to this article or journal.
Reprints and Subscriptions	To order reprints of this article or to subscribe to the journal, contact the AACR Publications Department at pubs@aacr.org.
Permissions	To request permission to re-use all or part of this article, contact the AACR Publications Department at permissions@aacr.org.

HER2 Overexpression Elicits a Proinflammatory IL-6 Autocrine Signaling Loop That Is Critical for Tumorigenesis

Zachary C. Hartman[1], Xiao-Yi Yang[1], Oliver Glass[1], Gangjun Lei[1], Takuya Osada[1], Sandeep S. Dave[2], Michael A. Morse[2], Timothy M. Clay[1,3], and Herbert K. Lyerly[1]

Abstract

HER2 overexpression occurs in approximately 25% of breast cancers, where it correlates with poor prognosis. Likewise, systemic inflammation in breast cancer correlates with poor prognosis, although the process is not understood. In this study, we explored the relationship between HER2 and inflammation, comparing the effects of overexpressing wild-type or mutated inactive forms of HER2 in primary human breast cells. Wild-type HER2 elicited a profound transcriptional inflammatory profile, including marked elevation of interleukin-6 (IL-6) expression, which we established to be a critical determinant of HER2 oncogenesis. Mechanistic investigations revealed that IL-6 secretion induced by HER2 overexpression activated Stat3 and altered gene expression, enforcing an autocrine loop of IL-6/Stat3 expression. Both mouse and human *in vivo* models of HER2-amplified breast carcinoma relied critically on this HER2–IL-6–Stat3 signaling pathway. Our studies offer the first direct evidence linking HER2 to a systemic inflammatory mechanism that orchestrates HER2-mediated tumor growth. We suggest that the HER2–IL-6–STAT3 signaling axis we have defined in breast cancer could prompt new therapeutic or prevention strategies for treatment of HER2-amplified cancers. *Cancer Res; 71(13); 4380–91. ©2011 AACR.*

Introduction

Breast cancer is a heterogeneous disease classified into subtypes on the basis of gene expression profiles or biomarker expression (1). A subtype overexpressing HER2 accounts for approximately 25% of breast cancers, and therapeutics targeting HER2, such as trastuzumab and lapatinib, have shown clinical efficacy (2). However, because many tumors are resistant either *de novo* or following therapy, it remains critical to fully understand the molecular and cellular changes elicited by HER2 overexpression during oncogenesis (2–5).

HER2 overexpression has been shown to activate multiple signaling complexes (2–4), which results in a striking dysregulation of the global transcriptome (5). Although these studies have provided a framework for HER2-mediated signaling, the pathways and gene targets critical to HER2 oncogenesis remain incompletely understood. Recent studies have

shown that inflammatory pathways and genes [such as interleukin-6 (IL-6) and IL-8] are strongly upregulated by several different oncogenes and are critical to their transformative capacity (6–9). Of note, rat ErbB2 (HER2 homolog) transgenic animals develop tumors with inflammatory patterns by gene expression profiling (10, 11), and these patterns correspond to the proinflammatory pattern of gene expression found in human tumors. Furthermore, clinical studies have shown the activation of inflammatory genes within breast cancer biopsies, whereas several circulating inflammatory cytokines have been found in the serum of breast cancer patients (12–14), with high levels of IL-6 and IL-8 associated with a poor prognosis (12, 13, 15–18).

To investigate whether HER2-mediated signaling could elicit inflammation critical for oncogenesis, we compared gene expression patterns of cells overexpressing wild-type HER2 to a kinase-inactivated HER2 (19). We documented that HER2 overexpression consistently elicited an inflammatory transcriptional signature, including marked elevation of IL-6 expression, which was required for HER2-mediated transformation. HER2-mediated secretion of IL-6 triggered Janus-activated kinase 1 (JAK1)–Stat3 signaling in an autocrine manner, resulting in amplified IL-6 activation of Stat3 in HER2^{+} cells and, significantly, enhanced HER2-mediated transformation. These findings were confirmed in the MMTV-*neu* mouse model and a human HER2–amplified breast carcinoma. In sum, we show that HER2 overexpression initiates a HER2–IL-6–Stat3 signaling loop required for HER2-mediated oncogenesis, providing a possible molecular basis for the clinical and pathologic inflammatory markers seen in breast cancer patients. This suggests that IL-6 targeted

American Association for Cancer Research

therapies could have significant impact on HER2-overexpressing cancer prevention or therapies.

Materials and Methods

Cell lines

Tumor cell lines MCF-10a, MCF-7, 4T1, and 3T3 were obtained from the American Tissue Culture Collection. KPL-4 cells were obtained from the originator, Dr. Kurebayashi (Kawasaki Medical School, Kurashiki, Japan; ref. 20). Human mammary epithelial cells (HMEC) were obtained from Dr. Jeffrey Marks (Duke University, Durham, NC). The 4T1 and 4T1–HER2 cells were obtained from Dr. Michael Kershaw (Cancer Immunology Program, Peter MacCallum Cancer Centre, Victoria, Australia), and all cell lines were validated and tested for contamination by the Duke University Tissue Culture Facility (21).

Adenoviral vector, plasmid, and cell line construction

Adenoviral vectors encoding HER2 and HER2ki were generated as previously described (19). HER2$^+$ cell lines were created through retroviral infection with HER2-expressing vectors. Stat3-Luc reporter cell lines were created by using a lentiviral reporter (SABiosciences). The NF-κB luciferase reporter was purchased from Stratagene, whereas AP-1 and C/EBP reporters were purchased from SABiosciences. Knockdown of JAK1, IL-6, and Stat3 genes was achieved by using retroviral and lentiviral RNA interference constructs purchased from Open Biosystems. A human Stat3 knockdown GFP–expressing lentivirus was kindly provided by Dr. Jaqueline Bromberg (Memorial Sloan-Kettering, New York, NY).

Microarray and quantitative real-time PCR assessments

RNA was extracted by using TRI-Reagent and RNAzol (Molecular Reagents Center, Madison, WI) and purified with an RNeasy Kit (Qiagen). Microarray analysis was conducted with GeneSpring 7.3 and GX10 (Affymetrix) by using datasets deposited at Gene Omnibus Express (GEO) of the National Center for Biotechnology Information (accession numbers GSE13274 and GSE2528). Datasets were analyzed by using the Database for Annotation Visualization and Integrated Discovery (DAVID) by using standard methods (22). MicroRNA (miRNA) arrays were processed from TRI-Reagent cellular extracts as previously described (23). Quantitative real-time PCR (qRT-PCR) was done on an ABI 7300 system by using standard methods and intron spanning primers. Expression differences were assessed by using the comparative cycle threshold (C_T) method against several control genes (*GAPDH*, *β-actin*, *HMBS*, *RN18S*, and *Rpl13*).

In vitro assays and assessments

Proliferation was determined by MTT assay, whereas soft agar assays were done as described (19). Propidium iodide (PI) staining was conducted by fixing cells in 95% EtOH, staining with PI, and assessing DNA content by flow cytometry on a FACScalibur (BD). Luciferase experiments were conducted by transfecting reporters or using stable reporter cell lines and normalizing luminescence with LacZ controls by using a β-Galactosidase Kit (Stratagene) or *Renilla*-transfected controls using a Dual-Luciferase Assay (Promega). ELISAs for IL-6 were done with IL-6 ELISA kits from Biolegend. Kinase inhibitors were purchased from Enzo Life Sciences and Marligen. Western blotting was done using standard methods with antibodies from Cell Signaling Technology and Abcam.

Mouse experiments

Experiments using BALB/c, NOD CB17-Prkdc SCID/J, and FVB/N-Tg(MMTV*neu*)202Mul/J mice (obtained from Jackson Labs) were conducted with Duke University Institutional Animal Care and Use Committee–approved protocols. For HER2 measurement of tumors, excised tumors were enzymatically digested as described below and measured by using a HER2-PE labeled antibody (BD Biosciences). For xenograft experiments, cells were injected s.c. into the flank of nonobese diabetic severe combined immunodeficient (NOD/SCID) mice (at indicated concentrations) measured by using calipers with volumes calculated by the formula [v = width*width* (length/2)]. For live imaging experiments, mice were anesthetized with the use of isoflurane, injected with 2.85 mg luciferin (in 100 μL of dH$_2$O), and monitored with a Xenogen IVIS 100 *in vivo* bioluminescence imaging system. Statistical differences were calculated with a mixed effects regression model using autoregressive covariance. Excised tumors were digested into single cell suspensions using a mix of collagenase (1 mg/mL), DNAse (20 U/mL), and hyaluronidase (100 μg/mL) at 37°C for 3 to 5 hours, run through a cell strainer (80 μm; BD), and cultured under standard conditions.
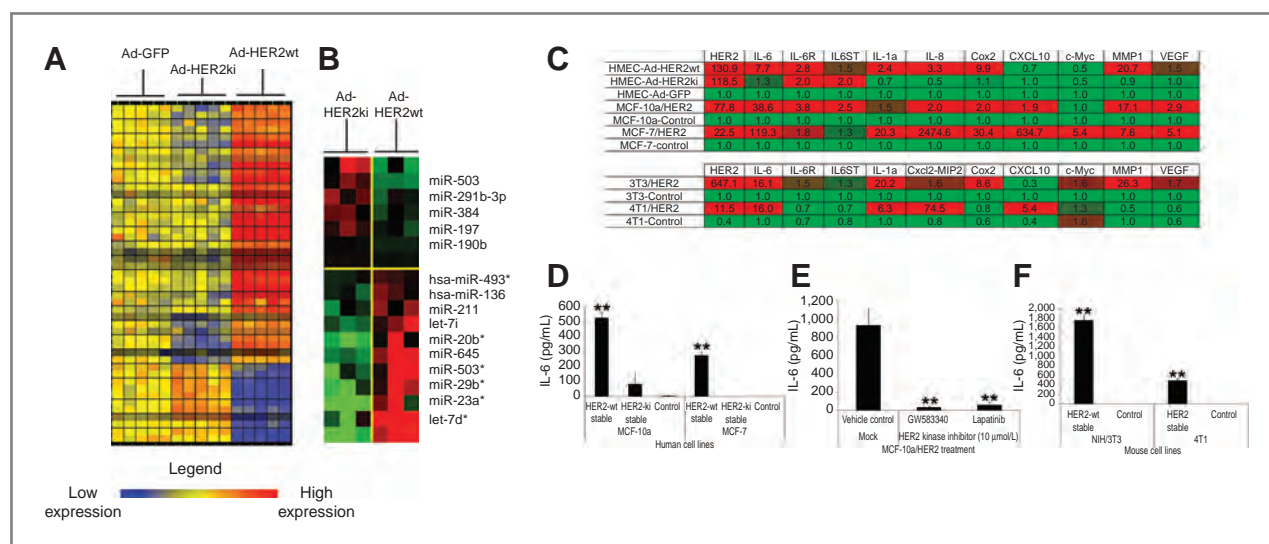
Results

Overexpression of HER2 elicits the activation of a broad inflammatory profile that includes IL-6

Although we have previously reported that global HER2-mediated gene expression changes were dependent on HER2 phosphorylation (19), we now report that a high proportion of these significantly affected genes ($P < 0.05$, >3-fold expression difference) are inflammatory type genes (53 of 424 probesets, ~12.5%; Fig. 1A) that require HER2 overexpression and phosphorylation for their overexpression (Fig. 1A). Concurrent examination of the miRNA profile also revealed significant differences in a cluster of miRNAs (Fig. 1B), which included the expression of different let-7 isoforms, recently shown to affect IL-6 expression (Fig. 1B; ref. 7).

We also investigated HER2-induced inflammatory gene expression in immortalized (MCF-10a) and transformed (MCF-7) human breast cells. We found that HER2 overexpression significantly induced the expression of specific inflammatory genes across different types of human breast cells (Fig. 1C), as well as murine fibroblasts (NIH/3T3) and transformed murine mammary tumor cells (4T1; Fig. 1C). As in human cells, expression of HER2 elicited significant activation of inflammatory gene expression, indicating that HER2 induction of inflammatory gene transcription is independent of species and cell type.

We next examined the impact of HER2 expression on IL-6 protein expression and secretion, showing that supernatants

Figure 1. HER2 expression mediates an inflammatory response and expression of IL-6 across multiple cell types. A, microarray heat map of significantly dysregulated mRNA inflammatory genes (A) and miRNAs (B), $n = 3$–5, multiplicity of infection (MOI) = 150, 16 hours post-treatment. C, qRT-PCR analysis of inflammatory genes in Ad-infected HMECs (as in A) and HER2wt, HER2ki, and control stably infected cell lines ($n = 5$; MOI = 150, 16 hours post-treatment). In all heat maps, red represents high expression and green represents low expression. D, IL-6 secretion from stably infected MCF-10a and MCF-7 cells ($n = 4$). E, IL-6 secretion from HER2-stable MCF-10a cells treated with lapatinib, a lapatinib analogue, or control vehicle (10 μmol/L assessed 24 hours post-treatment, $n = 4$). F, IL-6 secretion from stably infected NIH/3T3 and 4T1 cells ($n = 4$). For C–E, $n = 5$; bars, SD. *, $P < 0.05$ from controls; **, $P < 0.01$ from controls.

from HER2-overexpressing human mammary cells contained high levels of IL-6 (Fig. 1D), whereas treatment with small molecule HER2 inhibitors ablated IL-6 (Fig. 1E). HER2 overexpression in NIH/3T3 and murine 4T1 cells induced similar elevations of IL-6 (Fig. 1F).

HER2-mediated upregulation of IL-6 is dependent upon the parallel activation of multiple signaling pathways that activate several IL-6 transcription factors

To identify HER2–IL-6 responsive pathways, we focused on known downstream kinases and transcription factors. We exposed HER2-expressing MCF-10a cells (MCF-10a-HER2) to a variety of specific kinase inhibitors and assessed IL-6 secretion, finding that specific inhibition of mitogen-activated protein kinase (MAPK), c-*jun* NH kinase (JNK), phosphoinositide 3-kinase (PI3K), Akt, and Src reduce secretion of IL-6 (Fig. 2A). Although PKC inhibition reduced IL-6 secretion, inhibition of the mTOR pathway actually enhanced the HER2-mediated secretion of IL-6. Inhibition of other kinases, such as GSK3B, had no effect on the level of HER2-mediated IL-6 secretion (Fig. 2A, data not shown). To investigate IL-6 transcriptional regulation, we used luciferase reporters for the dominant transcription factors present in the IL-6 promoter complex (NF-κB, AP-1, and C/EBP). In MCF-10a cells, we found that although HER2 strongly induced NF-κB and AP-1 reporters, it had no effect on C/EBP expression (Fig. 2B). However in 3T3 cells, HER2 expression induced the 3 dominant transcription factors (NF-κB, AP-1, and C/EBP), suggesting that HER2 induction of NF-κB and AP-1 is cell type independent but that C/EBP induction may be cell type dependent (Fig. 2C). As NF-κB was strongly induced in both cell types, we directly assessed the importance of NF-κB in HER2-mediated IL-6 secretion through

pharmacologic disruption of NF-κB signaling in MCF-10a–HER2 cells and found a dose-dependent inhibition of IL-6 secretion (Fig. 2D). Collectively, these results showed that HER2 overexpression activates multiple pathways which synergistically result in the secretion of IL-6 through the activation of multiple transcription factors (Fig. 2E).

Secretion of IL-6 is required for HER2-mediated transformation and tumor growth *in vivo*

To determine whether IL-6 secretion was required for HER2-mediated transformation, we inhibited IL-6 expression in 3T3–HER2 transformed cells by stable IL-6KD (Supplementary Fig. S1) and assessed *in vivo* growth in NOD/SCID mice. IL-6 inhibition significantly attenuated *in vivo* tumor growth (Fig. 3A and B) and 3T3–HER2–IL-6KD tumors that eventually developed had reacquired baseline IL-6 expression (compared with control 3T3–HER2 cells; Fig. 3C). In addition to the significant role IL-6 has in HER2-mediated transformation, we also investigated its role in the behavior of transformed mammary cells. In transformed 4T1 mammary carcinoma cells, we found that overexpression of HER2 (4T1–HER2) yielded a significant *in vivo* growth advantage compared with non–HER2-expressing 4T1 cells (Fig. 3D, data not shown), which could be inhibited by blocking IL-6 expression (Supplementary Fig. S1), suggesting that IL-6 also plays a key role in HER2-facilitated growth in transformed cells.

HER2-induced secretion of IL-6 can act in an autocrine fashion to elicit Stat3-mediated gene expression and signaling
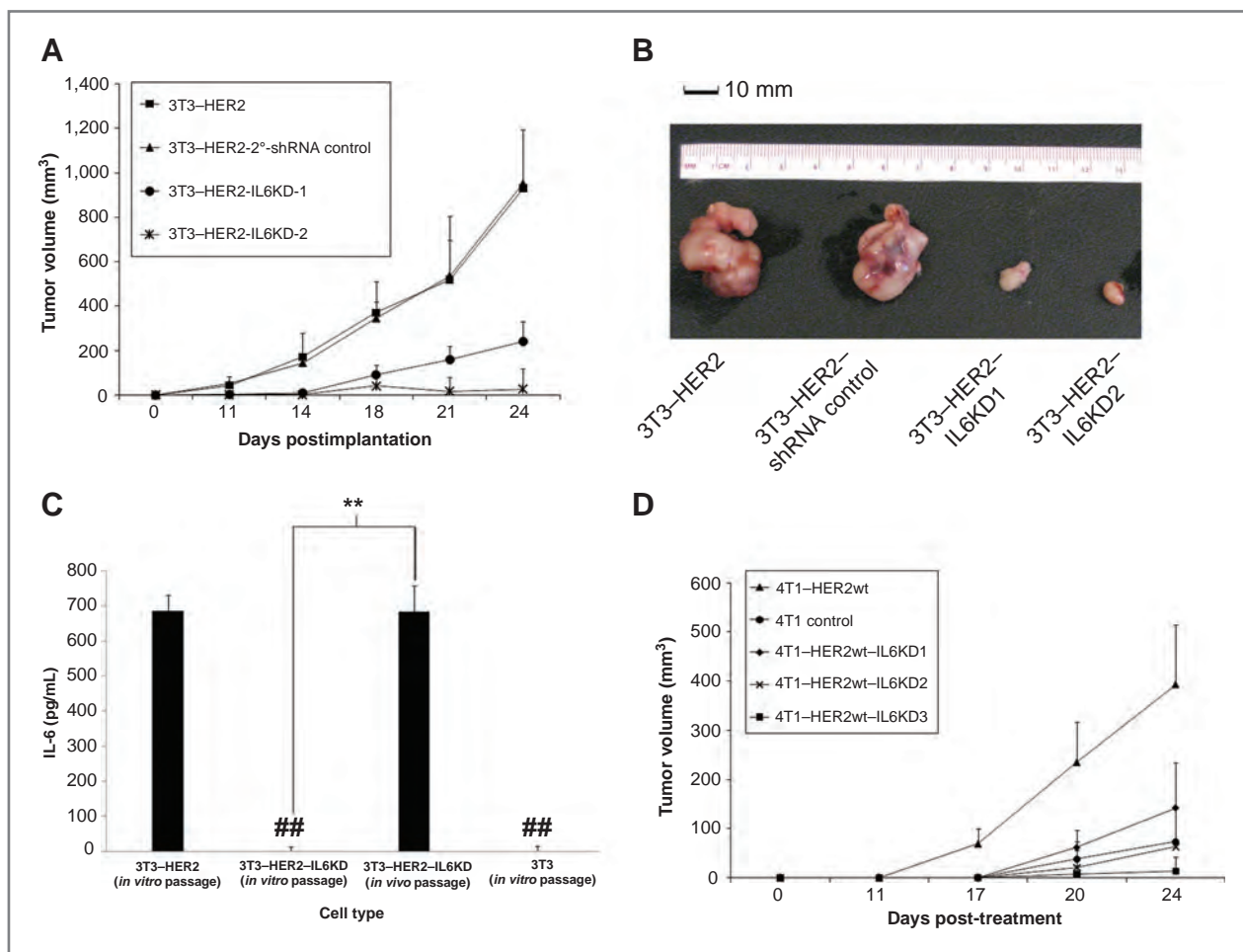
We next determined whether IL-6 had autocrine effects on HER2-transformed cells *in vitro*. *In vitro* assessment of

Figure 2. Transcriptional regulation of HER2-mediated IL-6 expression. A, kinase inhibition (10 µmol/L) of IL-6 secretion in MCF-10a–HER2 cells ($n = 3$; 24 hours post-treatment, bars, SD). B and C, NF-κB, AP-1, and C/EBP activity in MCF-10a and MCF-10a–HER2 cells (B) or NIH/3T3 or NIH/3T3–HER2 cells (C). In all samples, luciferase expression measured 24 hours post-treatment, $n = 4$, bars, SD. D, NF-κB inhibition of IL-6 secretion in MCF-10a–HER2 cells ($n = 4$; 24 hours post-treatment, bars, SD). *, $P < 0.05$; **, $P < 0.01$ in comparison with controls. DMSO, dimethyl sulfoxide. E, schematic diagram of the signaling pathways regulating HER2-induced transcriptional upregulation of IL-6. MEK, MAP/ERK kinase.

cellular proliferation revealed no difference in growth or cell-cycle changes between control and IL-6KD 3T3–HER2 cells (Fig. 4A), nor were any differences detected between these cell types in cell-cycle regulation (Fig. 4B). However, studies of anchorage-independent growth revealed significant growth attenuation by inhibition of IL-6 expression, thus signifying the importance of autocrine IL-6 signaling (Fig. 4C). We thus focused on Stat3, the dominant transcription factor induced by IL-6. Using a lentiviral Stat3 luciferase reporter, we found that HER2 expression significantly induced the activation of Stat3 compared with control 3T3 cells and, furthermore, that inhibition of IL-6 expression ablated Stat3 induction (Fig. 4D). These results were specific

for IL-6 induction of Stat3, as tandem investigations using transient transfection revealed that HER2-mediated activation of Stat3, but not Stat1, was dependent upon IL-6 secretion (Supplementary Fig. S2). To further elucidate and confirm that IL-6 activation of Stat3 was mediated by an IL-6–IL-6R–IL6ST signaling complex via JAK kinases, we stably expressed a mutant IL6ST receptor and inhibited JAK1 expression in 3T3–HER2 Stat3–luciferase cells (Supplementary Fig. S3). In the absence of exogenous IL-6 stimulation, inhibition of IL6ST, JAK1, or Stat3 in 3T3–HER2 cells, all significantly inhibited Stat3 activation (Fig. 4E), as previously shown by the inhibition of IL-6 expression itself (Fig. 4D). Notably, in the presence of

Figure 3. IL-6 is required for HER2-mediated tumor growth *in vivo*. A, 3T3–HER2 cells were modified with control and IL-6KD lentiviruses and implanted (1×10^5 cells) via s.c. injection into NOD/SCID mice and tumor volume measured over time ($n = 5$; bars, SE). B, visual representation of IL-6KD growth attenuation at day 24 of representative resected tumors. C, IL-6 secretion in tumor cells from resected tumors in comparison with *in vitro* passaged counterparts ($n = 5$; bars, SD). D, 4T1–HER2 and 4T1 cells were modified with control and IL-6KD lentiviruses and implanted (1×10^5 cells) via s.c. injection into NOD/SCID mice, and tumor volume was measured over time ($n = 5$; bars, SE). *, $P < 0.05$; **, $P < 0.01$ in comparison with controls.

exogenous IL-6 stimulation, we also found that inhibition of these signaling nodes critically inhibited Stat3 induction (Fig. 4E).

We next assessed the role of IL-6 on the expression of other inflammatory genes in 3T3, 3T3–HER2, and 3T3–HER2–IL-6KD cells by qRT-PCR and found that IL-6 inhibition did not affect certain genes such as *c-myc* and *COX2* but that the expression of other genes was significantly attenuated (Fig. 4F). In particular, we had noted that MMP1 was significantly enhanced by IL-6 secretion, so we examined several other MMP genes known to play a role in oncogenesis (ref. 24; Fig. 4G). We found that multiple MMP genes were significantly affected by inhibition of IL-6 secretion, thus showing that HER2-mediated IL-6 secretion elicits autocrine activation of Stat3, perturbing cellular gene expression.

As previous studies have illustrated IL6ST–HER2 interactions in different cell types, we also sought to determine whether HER2 expression could enhance autocrine IL-6–

mediated signaling (3, 25). Treatment of 3T3 and 3T3–HER2 cells revealed a nearly identical time course of activation, but at early time points, Stat3 appeared more phosphorylated in HER2-expressing cells in comparison with controls (Fig. 4H). Identical IL-6 treatment of 3T3–HER2–JAK1KD cells confirmed that the enhanced Stat3 activation was being achieved through a JAK1-dependent pathway in 3T3–HER2 cells and not by alternative mechanisms (Fig. 4H). To quantify Stat3 induction, we stably infected cells with Stat3–luciferase reporters, selected 3T3, and 3T3–HER2 cells that had equivalent basal activation of Stat3 (Fig. 4I) and found that IL-6 treatment activated Stat3 signaling to a significantly greater extent in HER2-expressing cells. As 3T3 cells had minimal expression of IL-6Rα (by fluorescence-activated cell sorting, data not shown), we hypothesized that HER2 amplification of IL-6–Stat3 signaling could be potentially abrogated by greater IL-6Rα expression. To test this hypothesis, we overexpressed

Figure 4. HER2-elicited IL-6 is critical for anchorage-independent growth and autocrine-mediated Stat3 activation *in vitro*. A, 3T3–HER2 were stably infected and growth monitored by MTT assay ($n = 6$; bars, SD). B, 3T3 and modified 3T3 cells were plated at equal densities and cell-cycle phases assessed by PI at 24 hours postplating. The average distribution of populations ($\sim 5 \times 10^5$ cells) is represented. C, indicated 3T3 cells were plated in 0.3% agar at a concentration of 5×10^4 cells/mL and colony growth assessed at 3 weeks ($n = 3$; bars, SD). D, 3T3–Stat3–Luc stable cells were modified to express HER2 and stably infected with IL-6 knockdown or control vectors. Equal populations of cells were then plated and Stat3 activation assessed by luciferase assay ($n = 6$; bars, SD). E, 3T3–Stat3–Luc–HER2 cells were modified to express a cytoplasmic domain truncated IL6ST (IL6STdn) or knocked down for JAK1 or Stat3 expression, treated with IL-6 (10 ng/mL) and luciferase activity assessed 24 hours post-treatment ($n = 6$, bars, SD; ##, $P < 0.01$ in comparison with IL-6–treated controls). F and G, 3T3, 3T3–HER2, and 3T3–HER2–IL-6KD cells were plated at equal densities and expression assessed by qRT-PCR of inflammatory (F) and MMP genes. G, $n = 4$; bars, SD; *, $P < 0.05$; **, $P < 0.01$ from 3T3 controls. #, $P < 0.05$; ##, $P < 0.01$ between 3T3–HER2–IL-6KD and 3T3–HER2 controls). H, 3T3, 3T3–HER2, and 3T3–HER2–JAK1KD cells were treated with IL-6 (10 ng/mL) and Stat3 phosphorylation (pY705) analyzed at indicated time points. I, 3T3–Stat3–Luc, 3T3–Stat3–Luc–HER2, and 3T3–Stat3–Luc–HER2–IL-6Rα, and 3T3–Stat3–Luc–IL-6Rα–modified cells were treated with IL-6 and Stat3 activation assessed by luciferase assay 24 hours post-treatment ($n = 6$; bars, SD; *, $P < 0.05$; **, $P < 0.01$ in comparison with untreated controls. #, $P < 0.05$; ##, $P < 0.01$ from 3T3 control cells). *, $P < 0.05$; **, $P < 0.01$ in comparison with controls.

IL-6Rα in both 3T3 and 3T3–HER2 Stat3–luciferase cells and found that Stat3 activation was again enhanced in HER2-expressing counterparts (Fig. 4I). Furthermore, we found that although IL-6Rα expression increased baseline Stat3 signaling in both cell types, it had a significantly greater effect in cells expressing HER2 upon IL-6 addition. These results suggested that, in addition to stimulating IL-6 secretion, HER2 expression enhances the activation of Stat3 signaling by IL-6. Collectively, these data showed that HER2 expression plays a critical dual role in the activation of an autocrine IL-6–Stat3 signaling complex.

HER2–IL-6 activation of Stat3 significantly enhances tumor growth *in vivo*

To investigate the importance of HER2–IL-6–Stat3 signaling *in vivo*, we first assessed the level of phosphorylated Stat3 in extracted tumor tissue. We found that 3T3–HER2 cells displayed modest phosphorylation of Y705 *in vitro*, whereas *in vivo* samples from 3T3–HER2 tumor displayed much higher levels of phosphorylated Stat3 (Fig. 5A). Notably, they also displayed a different pattern of activation in multiple forms of phosphorylated Stat3 as well as different isoforms of unphosphorylated Stat3 (data not shown). Having observed significantly enhanced Stat3 phosphorylation
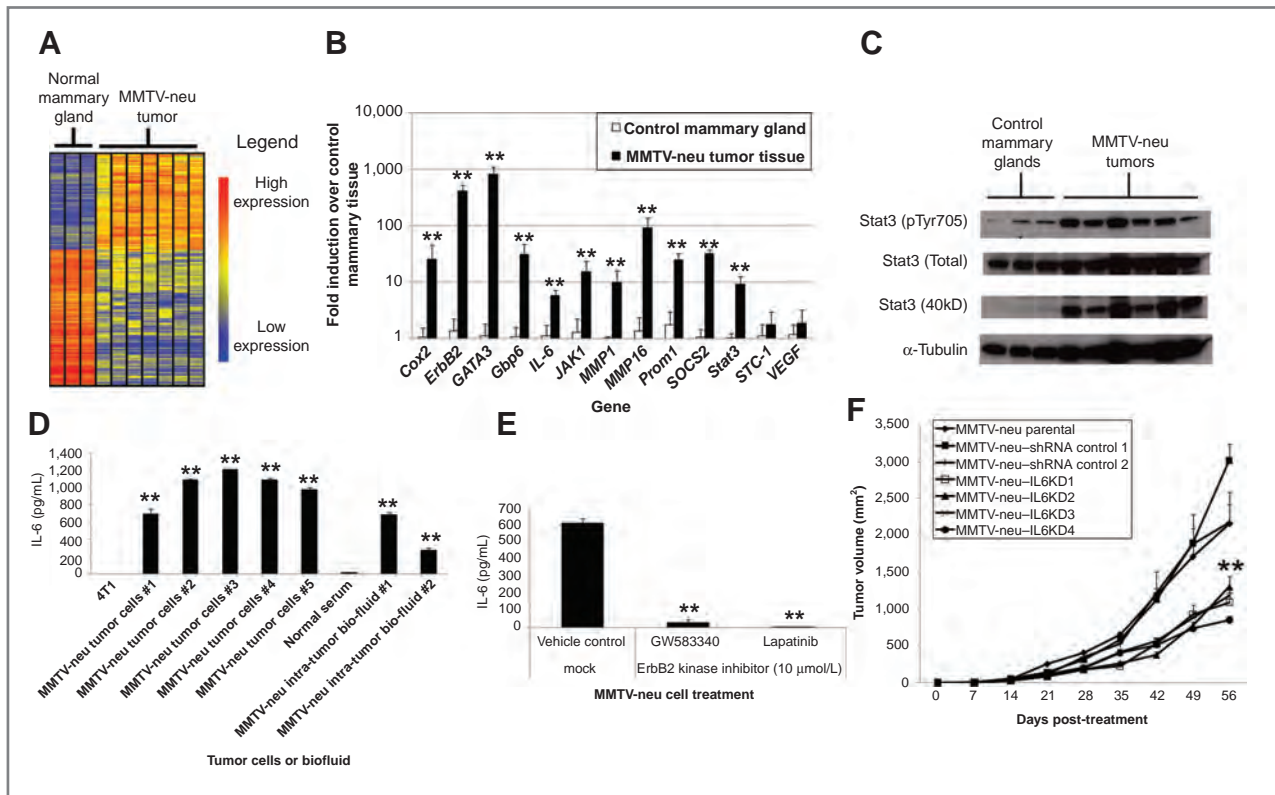
Figure 5. IL-6 activation of Stat3 is critical for HER2-mediated growth *in vivo*. A, total cell extracts from 3T3 and 3T3–HER2 (from *in vitro* cultures or xenografts biopsies) were subjected to Western analysis to determine total and phosphorylated Stat3 expression (pY705). B, 3T3–Stat3–Luc–HER2 and 3T3–Stat3–Luc–HER2–IL-6KD cells (1×10^5) were implanted in mice and Stat3 activation assessed by Xenogen luciferase imaging 11 days post-treatment ($n = 5$; 2–3 representative mice are shown). C, whole cell lysates from 3T3–Stat3–Luc–HER2–LacZ cells which were implanted in mice (sacrificed 24 days post-treatment) or passaged (for corresponding 24 days) were assessed for Stat3 activation, normalized to LacZ expression (samples from individual replicates shown, bars, SD). D, qRT-PCR from 3T3, 3T3–HER2, and 3T3–HER2 xenografts (sacrificed at 25 dpi) to determine MMP gene expression ($n = 4$; bars, SD; [#], $P < 0.05$; [##], $P < 0.01$ between *in vitro* and *in vivo* conditions). E, the indicated types of Stat3KD and control 3T3–HER2 cells (1×10^5) were implanted via s.c. injection into NOD/SCID mice and tumor volume measured over time ($n = 5$, bars, SE). *, $P < 0.05$; **, $P < 0.01$ in comparison to controls.

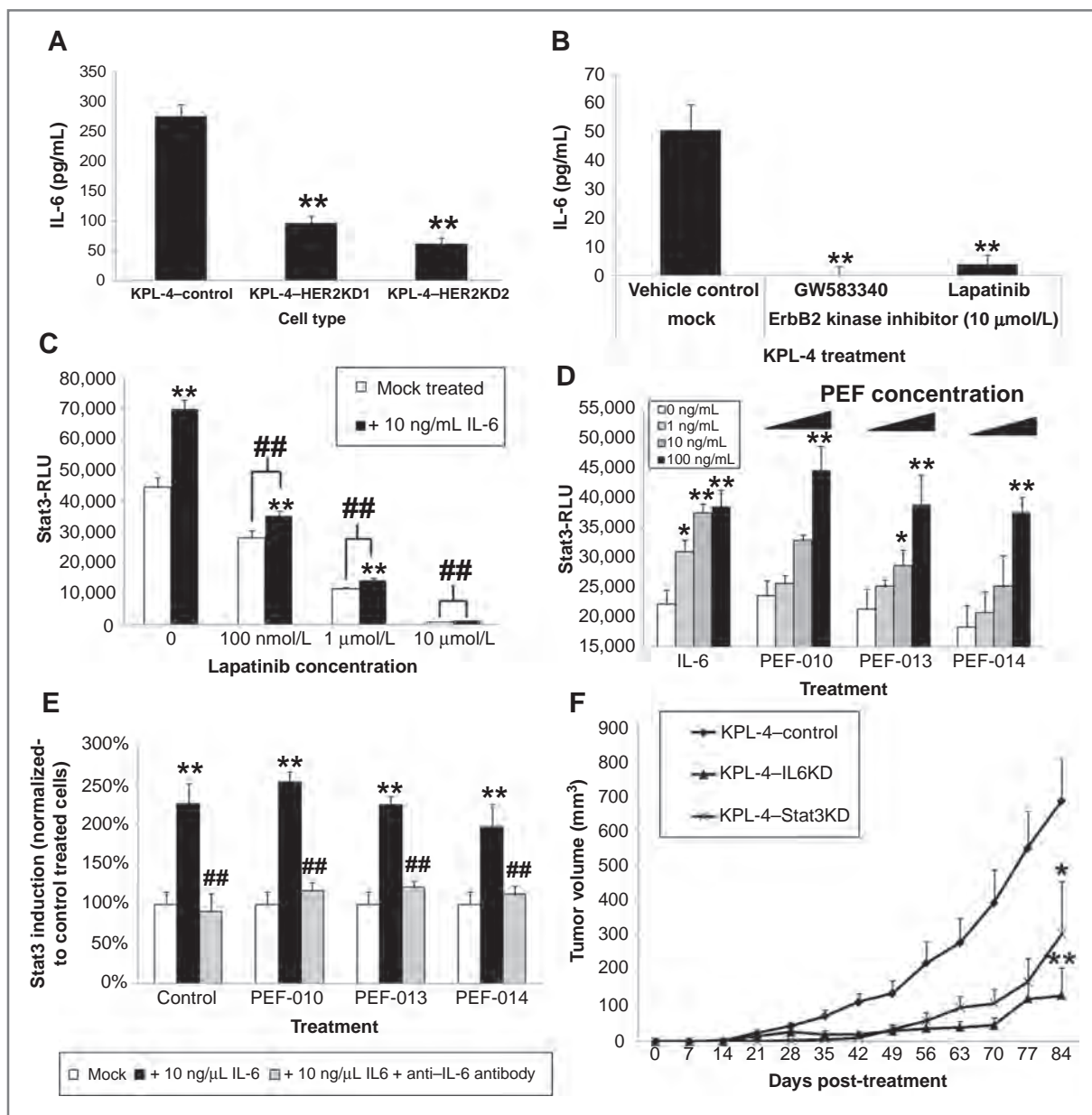in whole tumors *in vivo*, we next wanted to determine whether IL-6 could mediate autocrine activation of Stat3 specifically within 3T3–HER2 tumor cells *in vivo*. We constructed 3T3–HER2 and 3T3–HER2–IL-6KD cell lines with either a Stat3–Luc reporter or LacZ control reporter. When these cells were implanted in mice, striking differences were noted in the level of Stat3 activation 14 days post-treatment with the use of Xenogen imaging (Fig. 5B, Supplementary Fig. S4), consistent with differences seen *in vitro*. When tumors were excised and Stat3-mediated luciferase activation compared with identically *in vitro* passaged cells (all normalized with LacZ), we found that Stat3 was significantly more active in 3T3–HER2 cells under *in vivo* conditions compared with those same cells under *in vitro* conditions (Fig. 5C). As these results suggested a more significant activation of Stat3 *in vivo*, we next assessed the expression of IL-6 affected MMP genes *in vitro* and *in vivo*. Although certain genes (*MMP1* and *MMP7*) were not strongly affected by the greater level of Stat3 activation in

vivo, we did find that the expression of other MMP genes (*MMP3*, *MMP10*, and *MMP12*) was significantly enhanced *in vivo* (Fig. 5D). We then inhibited Stat3 expression in 3T3–HER2 cells (Supplementary Fig. S5) and compared *in vivo* growth with control 3T3–HER2 cells (Fig. 5E). We found that Stat3 inhibition did significantly retard tumor growth, although not to the extent observed when IL-6 secretion was inhibited.

ErbB2 induction of IL-6 plays a critical role in an endogenous model of ErbB2-mediated oncogenesis

The MMTV-*neu* mouse model spontaneously develops mammary carcinomas dependent upon expression of activated ErbB2 (the rat homolog of HER2). Using published microarray datasets of developing MMTV-*neu* tumors (26), we found that a significant portion of genes were dysregulated in ErbB2+ tumors in comparison with control mammary gland tissue (Fig. 6A, ~5% 309 probes with $P < 0.05$, >3 fold), of which approximately 10% (31 of 309 probesets) had

Figure 6. ErbB2-mediated induction of IL-6 plays a critical role in an endogenous ErbB2-mediated model of breast cancer. A, heat map depiction of significantly dysregulated genes (1-way ANOVA with $P < 0.05$, >3-fold difference) in MMTV-*neu* tumors. B, qRT-PCR from MMTV-*neu* tumors and control mammary glands ($n = 5$, bars, SD). C, Western blot analysis of lysates of MMTV-*neu* tumors and control mammary glands. D, tumor cells from MMTV-*neu* tumors were isolated, cultured, and assessed for IL-6 secretion in comparison with a non-ErbB2 transformed mammary carcinoma cell line (24 hours postplating). Fluid samples from tumors as well as control mice were also tested for IL-6 concentration by ELISA. In all samples, $n = 3$; bars, SD. E, tumor cells from MMTV-*neu* mice were passaged for 3 months, mock or ErbB2 kinase inhibitor treated, and IL-6 secretion assessed 24 hours post-treatment ($n = 3$; bars, SD). F, MMTV-*neu* tumor cells were modified by IL-6KD or control lentiviral infection and implanted (1×10^6 cells) via s.c. injection into NOD/SCID mice and tumor volume measured over time ($n = 5$; bars, SE). *, $P < 0.05$; **, $P < 0.01$ in comparison with controls.

immune-related functions. Quantitative RT-PCR analysis confirmed these findings (Fig. 6B), revealing strong induction of several relevant inflammatory mediators including IL-6, Stat3, and SOCS2. Western blots of control and transformed MMTV-*neu* mammary tissue revealed tumor Stat3 activation, further confirming this IL-6 inflammatory phenotype (Fig. 6C). Although IFN and inflammatory signatures have been reported in MMTV-*neu* tumors (10, 11), we focused on IL-6 expression in tumor cells and biofluid from multiple MMTV-*neu* tumors and compared these with a transformed non–ErbB2-expressing murine breast cancer (4T1; Fig. 6D). MMTV-*neu* tumor cells secreted high levels of IL-6, and peritumoral fluid contained significant amounts of IL-6 (Fig. 6D). Exposure of MMTV-*neu* tumor cells to ErbB2 inhibitors ablated IL-6 secretion (Fig. 6E), and IL-6KD MMTV-*neu* tumor cells were significantly growth attenuated compared with control infected or uninfected MMTV-*neu* cells (Fig. 6F). Our findings thus showed that endogenous ErbB2 expression supports an inflammatory phenotype, typified by IL-6 secretion, which plays an important role in MMTV-*neu* mammary tumor growth *in vivo*.

ErbB2-mediated IL-6 expression in human tumor cells causes Stat3 activation and facilitates oncogenic growth

To ascertain the relationship between spontaneously amplified ErbB2 and IL-6 secretion in human cells, we used the human KPL-4 breast cancer line, which overexpresses HER2 and secretes IL-6. When HER2 was stably knocked down, we found a significant, but not complete reduction of IL-6 secretion (Fig. 7A and Supplementary Fig. S7). As the high endogenous HER2 expression in KPL-4 cells was not completely knocked down by short hairpin RNA (Supplementary Fig. S7), we next used pharmacologic inhibition of HER2 (Fig. 7B), which resulted in a near complete ablation of IL-6 expression, showing the importance of HER2 signaling in promoting IL-6 secretion in HER2-expressing tumor cells.

KPL-4 cells were then stably infected with Stat3–luciferase reporters and then treated with IL-6 in tandem with HER2 kinase inhibitors to assess Stat3 activation (Fig. 7C). These studies revealed that HER2-inhibited cells had lower basal levels of Stat3 activation, correlating with their lower levels of IL-6 secretion (Fig. 7C). More significantly, we found that high

Figure 7. HER2-mediated secretion of IL-6 in human mammary carcinoma cells is critical for Stat3 activation and *in vivo* tumor growth. A, KPL-4 cells (endogenously HER2+) were knocked down for HER2 expression and IL-6 secretion assessed ($n = 6$; bars, SD). B, KPL-4 were treated with HER2 inhibitors (10 µmol/L) or DMSO and IL-6 secretion assessed at 24 hours ($n = 4$; bars, SD). C, KPL-4–Stat3–Luc stable cells that were exposed to varying concentrations of IL-6 in the presence or absence of 10 µmol/L lapatinib for 24 hours and Stat3 activation assessed ($n = 6$; bars, SD; #, $P < 0.05$; ##, $P < 0.01$ from DMSO control–treated KPL-4 and KPL-4+IL-6 counterparts). D, KPL-4–Stat3–Luc stable cells were exposed to varying concentration of IL-6 (as indicated) and pleural effusion fluid (consisting of increasing concentrations of 0, 0.25%, 2.5%, and 25% of total media volume indicated by increasing bars) for 24 hours, after which Stat3 activity was quantified by luciferase assay ($n = 6$; bars, SD). E, KPL-4–Stat3–Luc cells were treated with 10 ng/mL of IL-6 and PEF (at a 10 ng/mL IL-6 concentration, which represented 25%, 58%, and 100% of respective PEF concentrations), along with either mock treatment with 1 ng/mL of an anti–IL-6 neutralizing antibody or 1 µg/mL of a control immunoglobulin G (IgG) antibody. After a 24-hour incubation, Stat3 activity was quantified by luciferase assay ($n = 6$; bars, SD; #, $P < 0.05$; ##, $P < 0.01$ from IL-6+IgG–treated counterparts). F, the indicated types of modified KPL-4 cells (5×10^5) were implanted via s.c. injection into NOD/SCID mice and tumor volume measured over time ($n = 5$; bars, SE). *, $P < 0.05$; **, $P < 0.01$ in comparison with untreated controls.

concentrations of IL-6 were not able to activate Stat3 in HER2-inhibited cells, suggesting that HER2 plays a prominent role in the IL-6–mediated activation of Stat3. These studies used levels of IL-6 (10 ng/mL) that approximated levels that

we found in pleural effusions from breast cancer patients (Supplementary Fig. S8). When KPL-4–Stat3–Luc cells were directly exposed to malignant pleural effusions, we again observed significant activation of Stat3 (Fig. 7D), which

was inhibited by addition of neutralizing IL-6 antibody (Fig. 7E).

Finally, to determine whether HER2-mediated expression of IL-6 was critical for the growth of human HER2$^+$ breast carcinomas *in vivo*, both IL-6 and Stat3 were stably knocked down in KPL-4 cells, which were then implanted in mice (Fig. 7E, Supplementary Fig. S9) and assessed for tumor growth. The growth of Stat3KD cells was significantly inhibited, whereas IL-6KD cells displayed the most dramatically inhibited tumor growth, again suggesting that both autocrine and paracrine modes of IL-6 signaling likely play important roles in human tumor growth.

Discussion

Although oncogenes such as *Ras, src, myc,* and *EGFR* are known to trigger inflammatory pathways critical for oncogenesis (6–9, 27), the relationship between HER2/*neu* and inflammation had previously been speculative (28). In this study, we documented that HER2 overexpression activates multiple inflammatory pathways, including the secretion of IL-6, which we identify as critical for HER2-mediated transformation. We found that several pathways downstream of HER2 synergistically affected IL-6 expression and showed that secreted IL-6 elicited autocrine Stat3 activation. We also found that Stat3 activation was enhanced in HER2-expressing cells and associated with cellular transcriptional changes, as well as anchorage-independent growth. Studies with endogenously arising ErbB2 tumors also revealed that ErbB2–IL-6–Stat3 activation enhances tumor growth, signifying that these phenomena were not limited to a cellular model of HER2-mediated transformation. Likewise, investigation of a human breast carcinoma line with amplified HER2 also showed that HER2-mediated IL-6 expression was critical for autocrine Stat3 activation, signaling amplification, and human tumor growth *in vivo*. In sum, these experiments reveal that HER2 activation and amplification of autocrine IL-6–Stat3 signaling are critical to its oncogenic capacity.

We found that inflammatory related genes encompass approximately 10% of the most significant transcriptional changes induced by the overexpression of HER2 and that this inflammatory transcriptional response occurs in various cell types at different stages of transformation. The inflammatory effect on cellular properties is likely dependent upon cellular context as oncogene-induced inflammatory pathways (such as IL-6) can lead to autocrine-induced cellular senescence in nonimmortalized cells (29), whereas inflammatory genes can enhance cellular oncogenicity in tumor cells (9, 30–33). In addition, inflammatory responses can influence other cells (such as fibroblasts, adipocytes, or immune cells) and modulate tumor-mediated immunity.

Our study is the first to show that overexpression of kinase active, but not inactive, HER2 induces IL-6 secretion and is thus dependent upon HER2 phosphorylation and preservation of multiple signaling pathways downstream of HER2. HER2 activation correlated with NF-κB and AP-1 activation, and NF-κB was critical to IL-6 expression. These findings are similar to those observed in the RAS-mediated activation of

IL-8 (9), which we also found to be induced by HER2, suggesting that oncogene-mediated cytokine gene expression is dependent on multiple coordinated signaling pathways. Although this does not exclude the influence of other factors in the activation of IL-6 (such as let-7 involvement; ref. 7), it shows that interference with many signaling nodes downstream of HER2 can perturb IL-6 expression and thus implies the possibility of therapeutic intervention against HER2-mediated IL-6 secretion at multiple levels.

Our investigation also revealed that IL-6 secreted in response to HER2 expression was critical for HER2-mediated transformation and activation of Stat3 *in vitro* and *in vivo*, a finding corroborated by other studies that show IL-6 mediation of transformative properties in mammary epithelial and tumor cells (7, 33). Collectively, these findings suggest that HER2–IL-6–Stat3 activation is a critical component of HER2-mediated oncogenesis, although a full evaluation of Stat3-mediated effects may vary on the basis of cell type. Notably, we found that HER2 plays an additional role in the IL-6–Stat3 signaling axis, through the amplification of Stat3 signaling after IL-6 treatment. Although the exact nature of this role is unknown, previous studies have documented the involvement of HER2 with the IL6ST receptor (3, 25), suggesting that HER2 expression on the cell surface could be an important part of the IL-6–IL6ST–IL-6Rα complex. As such, HER2 could play a critical dual role in this pathway acting as an initiator and amplifier of cellular IL-6 signaling. However, it should also be noted that in multiple contexts, our knockdown of Stat3 did not fully recapitulate the suppression of tumor growth achieved with IL-6 knockdown.

We found that Stat3 was more highly activated in tumor cells *in vivo* in comparison with identical cells *in vitro*, consistent with the high levels of activated Stat3 reported in different types of tumor biopsies (34, 35). Although we found that tumor cell Stat3 activation was directly associated with tumor cell IL-6 expression *in vitro* and *in vivo*, stronger Stat3 activation *in vivo* could be a product of infiltrating cells as well as environmental stimuli that would provide additional sources or stimulations to permit Stat3 activation. For instance, the presence of high levels of soluble IL-6Rα *in vivo* (36) could permit IL-6 trans signaling in tumor cells, as IL-6Rα could be a limiting activating factor in certain cell types. Although it is unclear whether pharmacologic HER2 inhibition could alleviate Stat3 activation *in vivo*, our data suggest that such an approach may provide Stat3 suppression through inactivation of HER2-mediated IL-6 secretion, as well as abrogation of HER2-mediated enhancement of IL-6–Stat3 signaling. In sum, our finding of enhanced Stat3 signaling in HER2$^+$ tumor cells *in vivo* supports the importance of Stat3 activation in tumor cell populations in clinical settings.

Finally, although multiple studies have shown IL-6 expression in breast cancer patients and linked expression with certain subsets and grades of malignancy (12, 14, 37, 38), the source and mechanisms generating IL-6 in cancer patients has been undetermined. Likewise, other studies have determined that many breast cancers have activated Stat3, although the activators and significance of Stat3 in these

tumors remains unknown (34, 39). Our study shows that HER2 overexpression activates a transcriptional inflammatory profile, which includes the significant secretion of IL-6 in multiple cell types, as well as in a mouse model of ErbB2 overexpression and in a human HER2$^+$ breast carcinoma line. We further found that secreted IL-6 was critical for HER2-mediated oncogenesis and was mediated by autocrine activation of Stat3 in tumor cell populations, which was enhanced by cellular HER2 expression and in *in vivo* contexts. Thus, our findings show a potential origin and mechanism for IL-6 expression and its relevance to breast cancer progression. Although further study of HER2-mediated inflammation is needed, these findings suggest that therapeutic targeting of IL-6–Stat3 activation could augment existing prevention strategies and treatments of HER2$^+$ cancers.

References

1. Polyak K. Breast cancer: origins and evolution. J Clin Invest. 2007;117:3155–63.
2. Wang SC, Lien HC, Xia W, Chen IF, Lo HW, Wang Z, et al. Binding at and transactivation of the COX-2 promoter by nuclear tyrosine kinase receptor ErbB-2. Cancer Cell 2004;6:251–61.
3. Grant SL, Hammacher A, Douglas AM, Goss GA, Mansfield RK, Heath JK, et al. An unexpected biochemical and functional interaction between gp130 and the EGF receptor family in breast cancer cells. Oncogene 2002;21:460–74.
4. Guo W, Pylayeva Y, Pepe A, Yoshioka T, Muller WJ, Inghirami G, et al. Beta 4 integrin amplifies ErbB2 signaling to promote mammary tumorigenesis. Cell 2006;126:489–502.
5. Staaf J, Ringner M, Vallon-Christersson J, Jonsson G, Bendahl PO, Holm K, et al. Identification of subtypes in human epidermal growth factor receptor 2–positive breast cancer reveals a gene signature prognostic of outcome. J Clin Oncol 2010;28:1813–20.
6. Ancrile B, Lim KH, Counter CM. Oncogenic Ras-induced secretion of IL6 is required for tumorigenesis 3. Genes Dev 2007;21:1714–9.
7. Iliopoulos D, Hirsch HA, Struhl K. An epigenetic switch involving NF-kappaB, Lin28, Let-7 MicroRNA, and IL6 links inflammation to cell transformation. Cell 2009;139:693–706.
8. Gao SP, Mark KG, Leslie K, Pao W, Motoi N, Gerald WL, et al. Mutations in the EGFR kinase domain mediate STAT3 activation via IL-6 production in human lung adenocarcinomas. J Clin Invest 2007;117:3846–56.
9. Sparmann A, Bar-Sagi D. Ras-induced interleukin-8 expression plays a critical role in tumor growth and angiogenesis. Cancer Cell 2004;6:447–58.
10. Speers C, Tsimelzon A, Sexton K, Herrick AM, Gutierrez C, Culhane A, et al. Identification of novel kinase targets for the treatment of estrogen receptor-negative breast cancer. Clin Cancer Res 2009;15:6327–40.
11. Herschkowitz JI, Simin K, Weigman VJ, Mikaelian I, Usary J, Hu Z, et al. Identification of conserved gene expression features between murine mammary carcinoma models and human breast tumors. Genome Biol 2007;8:R76.
12. Salgado R, Junius S, Benoy I, Van Dam P, Vermeulen P, Van Marck E, et al. Circulating interleukin-6 predicts survival in patients with metastatic breast cancer. Int J Cancer 2003;103:642–6.
13. Nicolini A, Carpi A, Rossi G. Cytokines in breast cancer. Cytokine Growth Factor Rev 2006;17:325–37.
14. Kozlowski L, Zakrzewska I, Tokajuk P, Wojtukiewicz MZ. Concentration of interleukin-6 (IL-6), interleukin-8 (IL-8) and interleukin-10 (IL-10) in blood serum of breast cancer patients. Rocz Akad Med Bialymst 2003;48:82–4.
15. Zhang GJ, Adachi I. Serum interleukin-6 levels correlate to tumor progression and prognosis in metastatic breast carcinoma. Anticancer Res 1999;19:1427–32.
16. Bachelot T, Ray-Coquard I, Menetrier-Caux C, Rastkha M, Duc A, Blay JY. Prognostic value of serum levels of interleukin 6 and of serum and plasma levels of vascular endothelial growth factor in hormone-refractory metastatic breast cancer patients. Br J Cancer 2003;88:1721–6.
17. Bozcuk H, Uslu G, Samur M, Yildiz M, Ozben T, Ozdogan M, et al. Tumour necrosis factor-alpha, interleukin-6, and fasting serum insulin correlate with clinical outcome in metastatic breast cancer patients treated with chemotherapy. Cytokine 2004;27:58–65.
18. Benoy IH, Salgado R, Van Dam P, Geboers K, Van Marck E, Scharpe S, et al. Increased serum interleukin-8 in patients with early and metastatic breast cancer correlates with early dissemination and survival. Clin Cancer Res 2004;10:7157–62.
19. Hartman ZC, Wei J, Osada T, Glass O, Lei G, Yang XY, et al. An adenoviral vaccine encoding full-length inactivated human Her2 exhibits potent immunogenicty and enhanced therapeutic efficacy without oncogenicity. Clin Cancer Res 2010;16:1466–77.
20. Kurebayashi J, Otsuki T, Tang CK, Kurosumi M, Yamamoto S, Tanaka K, et al. Isolation and characterization of a new human breast cancer cell line, KPL-4, expressing the Erb B family receptors and interleukin-6. Br J Cancer 1999;79:707–17.
21. Kershaw MH, Jackson JT, Haynes NM, Teng MW, Moeller M, Haya-kawa Y, et al. Gene-engineered T cells as a superior adjuvant therapy for metastatic cancer 1. J Immunol 2004;173:2143–50.
22. Huang dW, Sherman BT, Tan Q, Kir J, Liu D, Bryant D, et al. DAVID bioinformatics resources: expanded annotation database and novel algorithms to better extract biology from large gene lists. Nucleic Acids Res 2007;35:W169–75.
23. Zhang J, Jima DD, Jacobs C, Fischer R, Gottwein E, Huang G, et al. Patterns of microRNA expression characterize stages of human B-cell differentiation. Blood 2009;113:4586–94.
24. Kessenbrock K, Plaks V, Werb Z. Matrix metalloproteinases: regulators of the tumor microenvironment. Cell 2010;141:52–67.
25. Qiu Y, Ravi L, Kung HJ. Requirement of ErbB2 for signalling by interleukin-6 in prostate carcinoma cells. Nature 1998;393:83–5.
26. Landis MD, Seachrist DD, Montanez-Wiscovich ME, Danielpour D, Keri RA. Gene expression profiling of cancer progression reveals intrinsic regulation of transforming growth factor-beta signaling in ErbB2/Neu-induced tumors from transgenic mice. Oncogene 2005;24:5173–90.
27. Soucek L, Lawlor ER, Soto D, Shchors K, Swigart LB, Evan GI. Mast cells are required for angiogenesis and macroscopic expansion of Myc-induced pancreatic islet tumors. Nat Med 2007;13:1211–8.
28. Grivennikov S, Karin M. Autocrine IL-6 signaling: a key event in tumorigenesis? Cancer Cell 2008;13:7–9.
29. Kuilman T, Michaloglou C, Vredeveld LC, Douma S, van Doorn R, Desmet CJ, et al. Oncogene-induced senescence relayed by an

interleukin-dependent inflammatory network. Cell 2008;133: 1019–31.

30. Grivennikov SI, Karin M. Inflammation and oncogenesis: a vicious connection. Curr Opin Genet Dev 2010;20:65–71.

31. Naugler WE, Sakurai T, Kim S, Maeda S, Kim K, Elsharkawy AM, et al. Gender disparity in liver cancer due to sex differences in MyD88-dependent IL-6 production. Science 2007;317:121–4.

32. Park EJ, Lee JH, Yu GY, He G, Ali SR, Holzer RG, et al. Dietary and genetic obesity promote liver inflammation and tumorigenesis by enhancing IL-6 and TNF expression. Cell 2010;140:197–208.

33. Sansone P, Storci G, Tavolari S, Guarnieri T, Giovannini C, Taffurelli M, et al. IL-6 triggers malignant features in mammospheres from human ductal breast carcinoma and normal mammary gland. J Clin Invest 2007;117:3988–4002.

34. Diaz N, Minton S, Cox C, Bowman T, Gritsko T, Garcia R, et al. Activation of stat3 in primary tumors from high-risk breast cancer patients is associated with elevated levels of activated SRC and survivin expression. Clin Cancer Res 2006;12:20–8.

35. Yu H, Pardoll D, Jove R. STATs in cancer inflammation and immunity: a leading role for STAT3. Nat Rev Cancer 2009;9:798–809.

36. Jones SA, Richards PJ, Scheller J, Rose-John S. IL-6 transsignaling: the in vivo consequences. J Interferon Cytokine Res 2005;25:241–53.

37. Benoy I, Salgado R, Colpaert C, Weytjens R, Vermeulen PB, Dirix LY. Serum interleukin 6, plasma VEGF, serum VEGF, and VEGF platelet load in breast cancer patients. Clin Breast Cancer 2002;2:311–5.

38. Knupfer H, Preiss R. Significance of interleukin-6 (IL-6) in breast cancer (review). Breast Cancer Res Treat 2007;102:129–35.

39. Berishaj M, Gao SP, Ahmed S, Leslie K, Al Ahmadie H, Gerald WL, et al. Stat3 is tyrosine-phosphorylated through the interleukin-6/glycoprotein 130/Janus kinase pathway in breast cancer. Breast Cancer Res 2007;9:R32.

Clinical Cancer Research

AACR

An Adenoviral Vaccine Encoding Full-Length Inactivated Human Her2 Exhibits Potent Immunogenicty and Enhanced Therapeutic Efficacy without Oncogenicity

Zachary C. Hartman, Junping Wei, Takuya Osada, et al.

Updated version	Access the most recent version of this article at: doi:10.1158/1078-0432.CCR-09-2549
Supplementary Material	Access the most recent supplemental material at: http://clincancerres.aacrjournals.org/content/suppl/2010/03/01/1078-0432.CCR-09-2549.DC1.html

Cited Articles	This article cites by 39 articles, 17 of which you can access for free at: http://clincancerres.aacrjournals.org/content/16/5/1466.full.html#ref-list-1
Citing articles	This article has been cited by 1 HighWire-hosted articles. Access the articles at: http://clincancerres.aacrjournals.org/content/16/5/1466.full.html#related-urls

E-mail alerts	Sign up to receive free email-alerts related to this article or journal.
Reprints and Subscriptions	To order reprints of this article or to subscribe to the journal, contact the AACR Publications Department at pubs@aacr.org.
Permissions	To request permission to re-use all or part of this article, contact the AACR Publications Department at permissions@aacr.org.

An Adenoviral Vaccine Encoding Full-Length Inactivated Human Her2 Exhibits Potent Immunogenicty and Enhanced Therapeutic Efficacy without Oncogenicity

Zachary C. Hartman[1], Junping Wei[1], Takuya Osada[1], Oliver Glass[1], Gangjun Lei[1], Xiao-Yi Yang[1], Sharon Peplinski[1], Dong-Wan Kim[5], Wenle Xia[2], Neil Spector[2], Jeffrey Marks[1], William Barry[3], Amy Hobeika[1], Gayathri Devi[1], Andrea Amalfitano[6], Michael A. Morse[2], H. Kim Lyerly[1], and Timothy M. Clay[1,4]

Abstract

Purpose: Overexpression of the breast cancer oncogene *HER2* correlates with poor survival. Current *HER2*-directed therapies confer limited clinical benefits and most patients experience progressive disease. Because refractory tumors remain strongly *HER2+*, vaccine approaches targeting *HER2* have therapeutic potential, but wild type (wt) *HER2* cannot safely be delivered in imunogenic viral vectors because it is a potent oncogene. We designed and tested several HER2 vaccines devoid of oncogenic activity to develop a safe vaccine for clinical use.

Experimental Design: We created recombinant adenoviral vectors expressing the extracellular domain of HER2 (Ad-HER2-ECD), ECD plus the transmembrane domain (Ad-HER2-ECD-TM), and full-length HER2 inactivated for kinase function (Ad-HER2-ki), and determined their immunogenicity and antitumor effect in wild type (WT) and HER2-tolerant mice. To assess their safety, we compared their effect on the cellular transcriptome, cell proliferation, anchorage-dependent growth, and transformation potential *in vivo*.

Results: Ad-HER2-ki was the most immunogenic vector in WT animals, retained immunogenicity in HER2-transgenic tolerant animals, and showed strong therapeutic efficacy in treatment models. Despite being highly expressed, HER2-ki protein was not phosphorylated and did not produce an oncogenic gene signature in primary human cells. Moreover, in contrast to HER2-wt, cells overexpressing HER2-ki were less proliferative, displayed less anchorage-independent growth, and were not transformed *in vivo*.

Conclusions: Vaccination with mutationally inactivated, nononcogenic Ad-HER2-ki results in robust polyclonal immune responses to HER2 in tolerant models, which translates into strong and effective antitumor responses *in vivo*. Ad-HER2-ki is thus a safe and promising vaccine for evaluation in clinical trials. *Clin Cancer Res; 16(5); 1466–77. ©2010 AACR.*

Human epidermal growth factor receptor 2 (*HER2*), overexpressed in 25% to 30% of breast cancers, is a well-known oncogene that is strongly associated with more aggressive tumors and poorer overall patient survival (1). A

Authors' Affiliations: ¹Duke Comprehensive Cancer Center, Departments of Surgery, ²Medicine, Division of Medical Oncology, ³Biostatistics and Bioinformatics, and ⁴Immunology, Duke University Medical Center, Durham, North Carolina; ⁵Division of Medical Oncology, Department of Internal Medicine, Seoul National University Hospital, Seoul, Korea; and ⁶Department of Microbiology and Molecular Genetics, Michigan State University, East Lansing, Michigan

major contributor to tumorigenicity, *HER2* is the target of multiple clinical therapies, such as the anti-*HER2* antibody trastuzumab and the HER2 kinase inhibitor lapatinib. Although both have shown some measure of efficacy in the clinic, their effects are limited and do not affect *HER2* expression in treated patients (2, 3). Thus, given the limitations of current treatments and their inability to affect *HER2* expression, targeting *HER2* with T cells and antibodies induced by cancer vaccines represents a promising and potentially effective strategy to treat patients refractory to lapatinib and trastuzumab (4, 5).

Numerous phase I and phase II breast cancer vaccine studies have been conducted (6) which have used proteins, peptides, modified tumor cells, and dendritic cells loaded with breast tumor antigens to elicit antitumor immune responses to tumor-associated antigens, such as HER2. Although some of these studies have shown beneficial clinical outcomes, by and large they have only achieved modest anti-HER2 immune responses. To elicit maximal therapeutic immunity, a vaccine must break immunologic tolerance to a self-expressed tumor-associated antigen

as well as elicit strong polyclonal antibody and T-cell responses to multiple epitopes across the tumor-associated antigen of interest, yet possess a high safety profile. Of the many vaccine platforms utilized, recombinant adenoviruses show great promise of fulfilling these criteria in a cancer vaccine platform. Recombinant adenoviruses are widely used in clinical gene therapy and vaccine applications with an extensive safety profile and well-documented history of eliciting strong transgene-specific adaptive immune responses (6–9). Thus, to elicit maximal antitumor responses, we focused on using an adenoviral platform to target the well-validated breast cancer oncogene, *HER2*.

Although we wished to incorporate the *HER2* gene into adenoviral vectors for therapeutic vaccination against *HER2*, the use of a wild-type *HER2* (*HER2-wt*) oncogene raised serious safety concerns regarding its tumorigenicity (10, 11). HER2 is a well-documented member of the ErbB family of tyrosine-kinase receptors and functions in tandem with different binding partners to elicit multiple signaling pathways that enable tumorigenesis (12). HER2 is also known to bind and elicit signaling with other non-ErbB family members as well as to directly activate transcription by nuclear translocation and binding (13, 14). To potentially eliminate the oncogenic potential and maximize the immunologic potential encoded by full-length HER2, we constructed and tested the immunogenicity of several vectors potentially ablated for HER2 kinase function. One vector contained a mutation in the HER2 ATP binding site (HER2-ki) whereas two others were truncated either before or after the transmembrane domain to completely eliminate the HER2 intracellular signaling domain. We hypothesized that these functionally inactivated oncogenes could

be used in the adenoviral platform to elicit strong adaptive immune responses that would show efficacy against metastatic HER2+ mammary tumors in both naïve and tolerant preclinical models. We further hypothesized that strong overexpression of the most promising inactivated *HER2* gene would be nononcogenic and thus safe for future clinical use.

Our results revealed that the recombinant adenoviral vectors expressing full-length HER2 inactivated for kinase function (Ad-HER2-ki) and expressing the extracellular domain of HER2 plus the transmembrane domain (Ad-HER2-ECD-TM) were highly effective in eliciting significant T-cell and antibody responses to HER2 in naïve mouse models compared with plasmid vaccination with HER2-ki constructs, thus validating the immunologic efficacy of the adenoviral platform. In contrast, we did not observe any induction of HER2-specific T-cell or antibody responses in HER2-ECD–vaccinated animals. Although the strong immune responses from both Ad-HER2-ki and Ad-HER2-ECD-TM vectors translated into significantly retarded tumor growth in naïve animals, our studies revealed that Ad-HER2-ki–vaccinated animals had the most significant HER2-specific T-cell responses as well as the most significant antitumor response. When animal models with tolerance to HER2+ were used, Ad-HER2-ki vaccination elicited only slightly diminished T-cell and antibody responses along with significant antitumor responses. Subsequent investigation into the oncogenicity associated with strong overexpression of HER2-ki revealed no evidence of its oncogenic functionality in terms of phosphorylation or transcriptional signature in primary human cells. We also found no evidence of its oncogenicity in enabling enhanced cellular proliferation, anchorage-independent growth, or transformation *in vivo*. Thus, our results strongly suggest that Ad-HER2-ki is an effective and safe vaccine that could show therapeutic efficacy in future clinical trials.

Materials and Methods

Cell lines. Tumor cell lines MCF-10a and 3T3 were obtained from the American Tissue Culture Collection (ATCC), and were maintained according to ATCC recommendations. The human-HER2 and control 4T1 cells were kindly provided by Dr. Michael Kershaw (Cancer Immunology Program, Peter MacCallum Cancer Centre, Victoria, Australia; ref. 15).

Adenoviral vector and cell line construction. The LTR-2/erbB2 plasmid was provided by Dr. L. E. Samelson (National Cancer Institute, Bethesda, MD) and HER2-ki (K753A) was created by quick-change mutagenesis. Adenoviral vectors were generated using standard cloning techniques as previously described (16, 17). Ad-Ras (H-Ras G12V) was kindly provided by Dr. Joseph Nevins, Duke University, Durham, NC. HER2+ cell lines were created through retroviral infection and/or plasmid transfection of 3T3 and MCF-10a cell lines and selection with hygromycin (500 ug/mL). Cell expression of HER2 was tested and confirmed in selected cells by Fluorescence-activated cell sorting (FACS) analysis using a

HER2-phycoerythrin–labeled antibody (BD Biosciences; Supplementary Table S3).

Microarray and quantative real time-PCR assessments. Cellular RNA was extracted using TRI-Reagent (Molecular Reagents Center) and further purified by using a RNeasy kit (QIAGEN). RNA quality was assessed using an Agilent Lab-on-a-Chip 2100 Bioanalyzer (Agilent Technologies) and samples were processed for HG-U133+ v2.0 Affymetrix microarray hybridization according to standard protocols at the Duke Microarray Facility. Datasets were deposited at National Center for Biotechnology Information's Gene Omnibus Express (GEO) in a MIAME-compliant form (along with complete details of all procedures) as accession number GSE13274. Datasets were analyzed using Genespring 7.2 and the Database for Annotation Visulaization and Integrated Discovery (DAVID) using standard methods (18).

Real-time PCR was carried out with an ABI 7300 system using standard methods and intron spanning primers described in Supplementary Table S2. Expression differences were assessed using the comparative cycle threshold (C_T) method against *GAPDH* and *β-actin* control genes.

Assessment of HER2-mediated phosphorylation, proliferation, and anchorage-independent growth in vitro. Proliferation of stable cells was determined by MTT assay using 5,000 cells/well over the course of 3 d (against control counterparts) in 96-well plates. MTT growth assessments were done using a Bio-Rad plate reader after cell solubilization in DMSO. Soft agar assays for stable and adenovirus-infected MCF-10A cells were done as described in O'Hayer and Counter, 2006, with adenovirus-infected MCF-10a cell infected at a multiplicity of infection of 150 (19). Briefly, 50,000 cells/well were plated in 0.3% soft agar (on a base of 0.6% soft agar) and allowed to grow for a period of 2 wk in DMEM with 10% FCS (3T3 cells) or DMEM:F12 with 5% horse serum and mammary epithelial growth medium singlequot growth additives (Clonetics; MCF-10a cells). At the end of this time, colonies of >15 cells were counted and scored. Western blots of infected human mammary epithelial cells (HMEC) were done using standard procedures with HER2 phosphorylation assessed using a HER2-phospho specific antibody (20).

Mouse experiments. Experiments using BALB/c, NOD CB17-Prkdc SCID/J, and SCID-B6.129S7-Rag1(tm1Mom) mice (obtained from Jackson Labs) were done in accordance with Duke Institutional Animal Care and Use Committee–approved protocols. Human HER2-transgenic mice (kindly provided by Dr. Wei-Zen Wei, Wayne State University, Detroit, MI; ref. 21) were crossed with BALB/c mice (Jackson Labs) to permit implantation of 4T1-HER2 tumors and genotyped by PCR as previously described (15). For HER2 measurement of 4T1-HER2 tumors, excised tumors were enzymatically digested as previously described (22, 23) and measured using a HER2-PE–labeled antibody (BD Biosciences). Stable 3T3 cells were injected s.c. into the flank of NOD-SCID mice (1×10^6 or 1×10^5 cells/animal) as previously described and measured after 28 d. Tumor measurements were made using calipers and volumes cal-
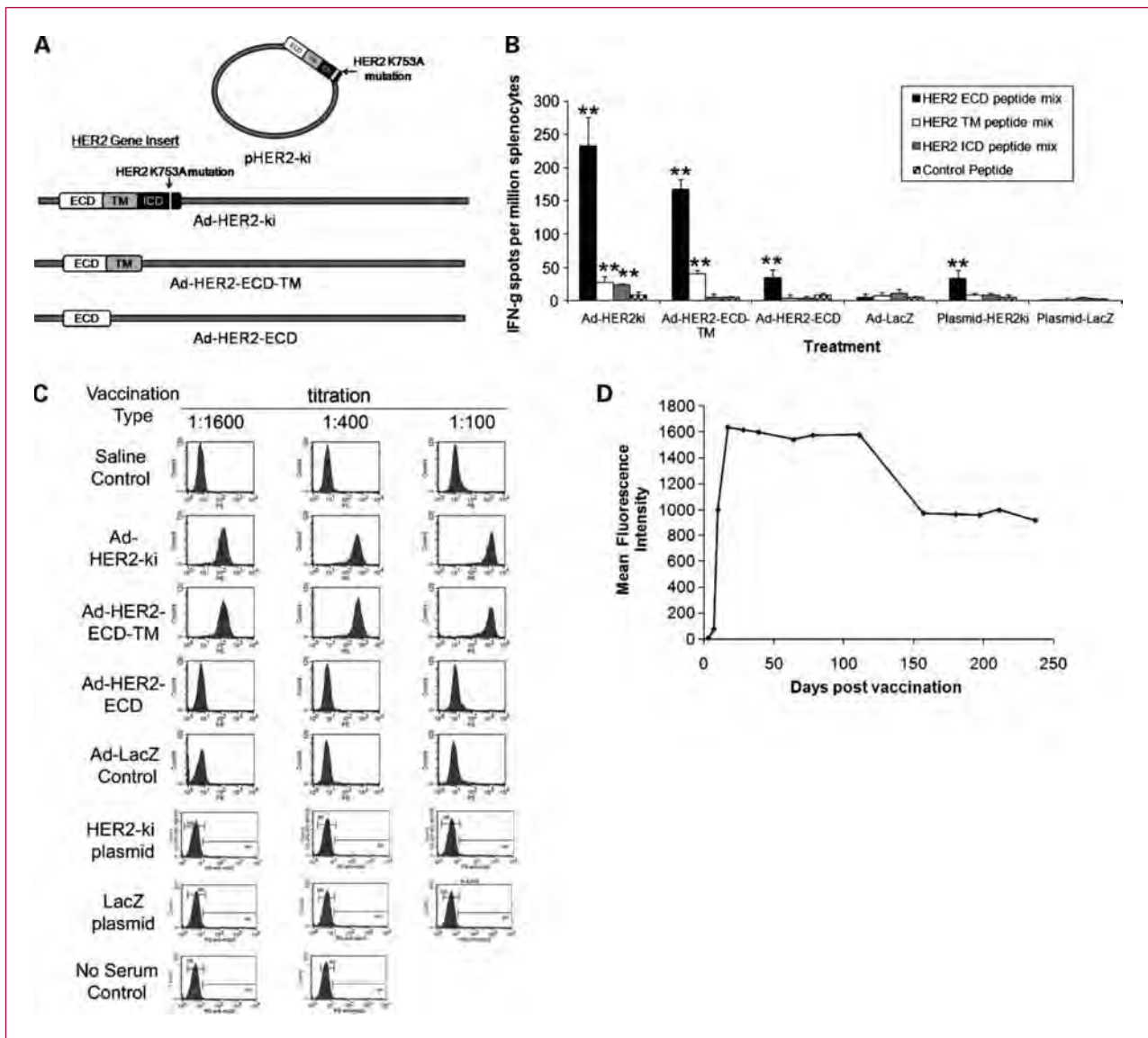
culated using the formula [v = width × width × (length / 2)] whereas statistical differences were calculated using a mixed effects regression model using autoregressive covariance.

Assesment of vector immunogenicity in vivo. Immunogenicity experiments involved footpad injection of Ad-HER2-ki, Ad-HER2-ECD-TM, Ad-HER2-ECD, and Ad-LacZ vectors (2.6×10^{10} particles/mouse) in transgenic and naïve animals. Plasmid injection was done by injecting 100 μg of plasmid DNA in 50 μL of PBS i.m. as previously described. Fourteen days postinjection, mice were euthanized and splenocytes and sera were collected for analysis. IFN-γ ELISPOT assays (Mabtech Inc.) were done according to the manufacturer's instructions using overlapping HER2 peptide mixes (2.6 μg/mL; BD Biosciences) as stimulating antigens and HIV-irrelevant overlapping peptide mixes as negative controls (BD Biosciences). Phorbol 12-myristate 13-acetate (50 ng/mL) and ionomycin (1 μg/mL) served as a positive control for splenocyte responsiveness. Antibodies were assessed by a flow cytometry adapted methodology reported by Piechocki et al. (24). Briefly, 3×10^5 cells (mouse 4T1-HER2, HER2+; mouse 4T1, HER2-) were incubated with diluted (1:100, 1:400, 1:1,600) mouse serum for 1 h at 4°C, washed with 1% bovine serum albumin–PBS, stained with PE-conjugated antimouse IgG (Dako) for 30 min at 4°C, washed, and then samples were analyzed on a BD LSRII or BDFACScalibur flow cytometer and results were represented as histograms or mean fluorescence intensity. Epitope mapping was done using spotted peptide arrays of 14 mer peptides overlapping by four amino acids representing the full length of the human HER2 protein or portions of the full-length human HER2 protein on cellulose membranes using a Spot Robot ASP 222 (AbiMed) and done as described (25).

Results

Development of recombinant adenoviral vectors expressing inactivated forms of human HER2. To maximize adaptive immune responses against multiple epitopes of human HER2 while disabling its oncogenic potential, we developed three different adenoviral vectors, one encoding a full-length inactive form of human HER2 and two others encoding truncated forms of human HER2, either before or after the transmembrane region (and thus no intracellular signaling domain; Fig. 1A). The truncated forms of HER2 were produced by deleting the HER2 intracellular domain coding region after amino acid 684 for Ad-HER2-ECD-TM (nucleotide position 2084) and after amino acid 653 for Ad-HER2-ECD (nucleotide position 1959). To mutationally inactive human HER2, we mutated a key residue in the ATP binding region (K753A) to render the tyrosine kinase inactive (Fig. 1A; ref. 26). The K753A mutation had been previously shown to reduce HER2 phosphorylation, but its full impact on HER2 function and oncogenicity was undetermined at this time.

Immunization with Ad-HER2-ki and Ad-HER2-ECD-TM but not Ad-HER2-ECD elicits strong functional T-cell and antibody responses in naïve mice. As previous studies had

Fig. 1. Ad-HER2-ki and Ad-HER2-ECD-TM vaccination elicit robust HER2-specific cellular and polytypic humoral responses *in vivo*, with long-term maintenance of antibody responses. A, diagram of adenoviral and plasmid-based HER2 vectors constructed and compared in this study. All vectors utilized an identical cytomegalovirus immediate early promoter to drive transgene expression. B, IFN-γ ELISPOT responses at 2 wk postimmunization (wpi) in adenovirus- or plasmid-vaccinated animals (2.6×10^{10} vp or 100 μg of plasmid per mouse; $n = 5$). *, $P < 0.05$; **, $P < 0.01$ from control peptide stimulation. Error bars, SD. C, FACS analysis using 4T1-HER2 cells to detect HER2-specific IgG antibodies from adenovirus- or plasmid-vaccinated animals at 2 wpi at different dilutions ($n = 5$ mice, pooled composite results shown). D, composite mean fluorescence intensity FACS assessment of HER2-specific IgG responses after single Ad-HER2-ki vaccination at day 0 (2.6×10^{10} vp per mouse) of C57BL/6 mice ($n = 3$; 1:100 dilution composite results shown).

reported widely differing efficiencies in the induction of HER2-specific immune responses, we first wanted to determine the strength of T-cell and antibody responses to the modified forms of HER2 using the adenoviral vaccine platform in comparison with the previously reported immunogenicity of HER2-ki plasmid- based vaccination (Fig. 1A; ref. 26). Naïve mice were vaccinated with a single dose of the vaccines and after two weeks, T-cell and antibody responses were assessed by ELISPOT assays and FACS assays (to show antibody binding to HER2+ human

breast tumors), respectively. We found that Ad-HER2-ki and Ad-HER2-ECD-TM elicited highly significant responses compared with control vaccinations, but that Ad-HER2-ECD and plasmid-based HER2-ki vaccination elicited far weaker responses (Fig. 1B). ELISPOT assays showed that T-cell responses were strongest to epitopes in the extracellular domain of HER2 (ECD) and weakest to the intracellular and transmembrane domains (ICD and TM) in both Ad-HER2-ki and Ad-HER2-ECD-TM adenoviral vaccinations. As expected, T-cell responses to ICD domain

epitopes were only present in the Ad-HER2-ki–vaccinated animals and were not observed in animals vaccinated with Ad-HER2-ECD-TM, which was ICD truncated. Differences in T-cell responses between Ad-HER2-ki– and Ad-HER2-ECD-TM–vaccinated animals were mostly minor, but T-cell responses to the ECD and TM regions were slightly more robust in Ad-HER2-ki–vaccinated animals. In contrast, HER2-ki plasmid and Ad-HER2-ECD vaccination showed only weak responses to the ECD domain and ICD/TM were completely absent.

Our assessment of HER2-specific IgG responses mirrored our ELISPOT assessments, with both Ad-HER2-ki and Ad-HER2-ECD-TM vaccination eliciting highly significant levels of HER2-specific antibodies compared with control vector (Fig. 1C). Interestingly, plasmid-based vaccination with HER2-ki and adenoviral vaccination with HER2-ECD were both unable to elicit significant quantities of HER2-specific antibodies compared with control vaccinations.

Because antibody efficacy is a function of its targeted epitope, the antibody isotype, and the duration of the humoral response, we next investigated these aspects of our Ad-HER2-ki and Ad-HER2-ECD-TM vaccine-induced antibodies (VIA). Isotype-specific ELISA indicated the presence of multiple antibody isotypes from both vaccinations, with all IgG subtypes predominanting, modest levels of IgM, and with low concentrations of IgA and IgE isotypes (data not shown). Epitope mapping revealed that Ad-HER2-ki elicited IgG antibodies that specifically bound multiple epitopes in the intracellular and extracellular regions of HER2 (Table 1), which Ad-LacZ did not elicit, thus showing a polyclonal HER2-specific adaptive response against full-length HER2. Lastly, we investigated the longevity of the polyclonal antibody response by immunizing wild-type C57BL/6 mice with Ad-HER2-ki and periodically assessing HER2-specific IgG antibody levels at different times postinjection by FACS (Fig. 1D). We

found that peak antibody responses represent a titer of 1:25,000 based upon ELISA at day 78 (data not shown) and that although antibody responses gradually diminished, a single immunization resulted in considerable (roughly ~50%) HER2-specific antibody levels seven months after injection. Thus, vaccination using Ad-HER2-ki is sufficient to elicit robust levels of polyclonal antibodies that are part of a long-lived response that is significant at seven months postinjection.

In sum, the Ad-HER2-ki and Ad-HER2-ECD-TM vectors elicited significantly greater T-cell and antibody responses in comparison with Ad-HER2-ECD and HER2-ki plasmid-based vaccination.
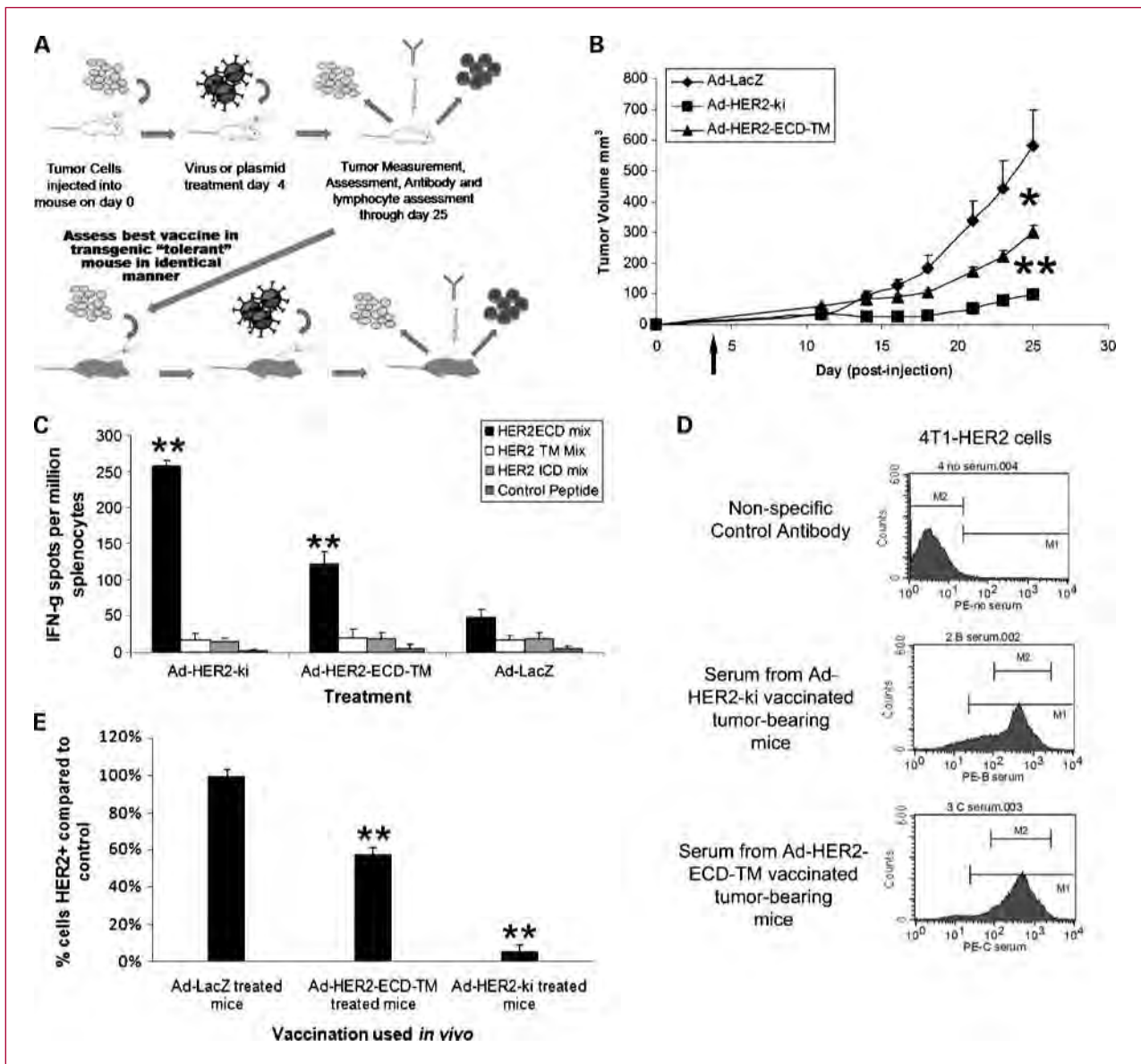
Ad-HER2-ki and Ad-HER2-ECD-TM vaccines are effective against HER2+ tumors **in vivo.** Although both Ad-HER2-ki and Ad-HER2-ECD-TM were able to efficiently induce polyclonal T-cell and humoral immunity, it was unknown if these responses could effectively inhibit aggressive HER2+ tumor growth *in vivo*. To assess the antitumor effect of these vectors, an aggressive herceptin-resistant (ref. 15; Supplementary Fig. S1) HER2+ metastatic mouse mammary carcinoma line (4T1-HER2) was implanted in mice, which were subsequently vaccinated with either Ad-HER2-ki, Ad-HER2-ECD-TM, or with a control vector (Ad-LacZ; Fig. 2A). This approach effectively mimicked conditions seen in patients, as 4T1-HER2 cells were not solely dependent on HER2 for growth, but grew aggressively and could initiate metastases. Furthermore, once the most promising vector was determined in the naïve model, that vector could be tested using the same approach in the more stringent HER2 transgenic mouse model that mimics the human HER2 tolerance seen in patients (Fig. 2A).

Using the naïve model, we found that mice receiving a single vaccination with either Ad-HER2-ki or Ad-HER2-ECD-TM showed significant retardation in tumor growth compared with the control Ad-LacZ (Fig. 2B). Comparison of the two vectors revealed that Ad-HER2-ki gave a significant protective advantage in blunting tumor growth compared with Ad-HER2-ECD-TM and a more significant advantage when compared with Ad-LacZ control animals. Assessment of T-cell responses and antibody responses in vaccinated animals revealed that although HER2-specific IgG responses were not significantly different T-cell responses showed significant differences (Fig. 2C and D). In all tumor-bearing animals, HER2 peptide stimulation of splenocytes produced significant responses compared with unstimulated controls, indicating that aggressive HER2+ tumor growth had elicited a baseline level of T-cell activation in naïve animals against HER2 epitopes, which had been unable to curtail tumor growth. The domain-specificity of activated T-cell epitopes mirrored that of vaccinated non–tumor-bearing animals (Figs. 1B and 2C), in that ECD responses were dominant in all groups. Significantly, though, we observed that the dominant ECD-specific responses of Ad-HER2-ki and Ad-HER2-ECD-TM were significantly greater than control-vaccinated animals and directly correlated with the strength of the antitumor effect observed in vaccinated animals.

Table 1. HER2-VIA antibody epitopes

Epitope(s) position	Protein region
29-50	ECD
365-385	ECD
405-420	ECD
577-595	ECD
605-630	ECD
817-840	ICD
909-940	ICD
941-965	ICD
989-1040	ICD
1061-1085	ICD
1097-1160	ICD
1169-1190	ICD
1195-1211	ICD
1229-1245	ICD

Fig. 2. Vaccination using Ad-HER2-ECD-TM and Ad-HER2-ki significantly inhibits HER2+ tumor growth in naïve mice *in vivo*. A, schematic representation of vaccination and antitumor assessment strategy in both naïve and tolerant models. B, antitumor effect of vaccines in naïve model. BALB/c mice (*n* = 8) were implanted with 2×10^4 4T1-HER2+ cells on day 0 and were vaccinated via footpad with 2.6×10^{10} particles of Ad-HER2-ki (□), Ad-HER2-ECD-TM (Δ), or control Ad-LacZ (◊), on day 4 (arrow). *, $P < 0.05$; **, $P < 0.01$. Error bars, SD. C, activation of HER2-specific T-cells correlates with the strength of tumor regression in vaccinated tumor-bearing animals. IFN-γ ELISPOT assay employed different overlapping pools of HER2-specific epitopes for various HER2 domains at a concentration of 1 μg/mL per million splenocytes (*n* = 8 vaccinated animals). *, $P < 0.05$; **, $P < 0.01$ compared with control. Error bars, SD. D, top, HER2-specific IgG antibody responses are equivalent between vaccinated tumor-bearing animals and HER2 is selected against in tumors of vaccinated animals. Pooled composite FACS analysis using 4T1-HER2 cells to detect HER2-specific IgG antibodies from adenovirus-vaccinated animals at 25 dp implantation (dilution 1:100; *n* = 8). Bottom, HER2 expression on tumor cells from treated animals show evidence of anti-HER2-specific selection. Explanted 4T1-HER2 cells from vaccinated animals (*n* = 8; cell explanted 25 d postimplantation) were assessed using HER2-specific FACS.

Although Ad-HER2-ki– and Ad-HER2-ECD-TM–vaccinated animals had significantly repressed tumor growth, tumors in these animals were not fully eliminated. We hypothesized that if HER2-specific responses were attributable for the diminished growth, then the 4T1 tumor outgrowths in these animals would have a reduced level of HER2 expression as a result of immunoselection induced by vaccination.

We further hypothesized that if the HER2-specific cytotoxic T-cells were the major selective pressure on tumors, then the level of HER2 expression in the remaining tumor cells would inversely correlate with the strength of anti-HER2 T-cell responses we observed in vaccinated animals. Tumors from vaccinated animals were excised and dissociated, and HER2 expression determined quantitatively by FACS.
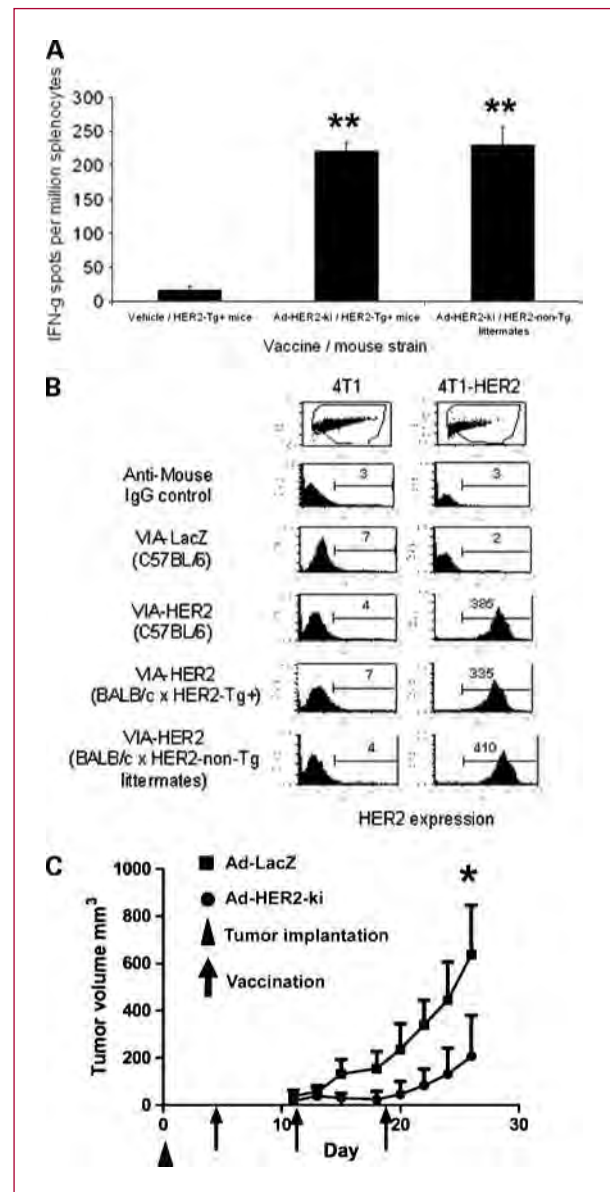
Supporting the hypothesis, we found that HER2 expression was significantly diminished in both Ad-HER2-ECD-TM– and Ad-HER2ki–vaccinated animals (compared with Ad-LacZ control), being lowest in Ad-HER2-ki–vaccinated animals (about 5% displaying expression comparable with control-vaccinated animals; Fig. 2D). Thus, HER2 expression was indeed found to be inversely associated with HER2-specific T-cell responses, strongly suggesting that HER2-specific T-cells were predominantly responsible for the efficacy of Ad-HER2-ki and Ad-HER2-ECD-TM vaccinations.

Ad-HER2-ki vaccine effectiveness against HER2+ tumors in a tolerant in vivo model. As tolerance to self-antigen is a major impediment to the successful clinical use of vaccines, we sought to determine if our most promising vaccine (Ad-HER2-ki) could be as effective in its immune induction and antitumor effects in a mouse with tolerance to human HER2+ (21). To first determine if immune responses elicited by Ad-HER2-ki vaccination were comparable in a tolerant setting, we vaccinated naïve and human HER2 transgenic animals with Ad-HER2-ki and assessed T-cell and antibody induction using ELISPOT and HER2-specific FACS. Our ELISPOT results revealed that HER2+ transgenic animals produced nearly equivalent HER2-specific T-cell responses compared with naive controls (Fig. 3A). Similarly, FACS analysis of mouse serum for HER2-specific antibodies showed similar levels of specific binding to HER2+ cells (but not parental HER2- cells) between vaccinated HER2 transgenic mice, non-HER2 transgenic littermates, and wild-type C57BL/6 mice (Fig. 3B). As expected, serum from Ad-LacZ–vaccinated mice did not significantly bind to HER2+ cells, showing that antibody responses were HER2 specific in Ad-HER2ki–vaccinated mice.

As immune responses in naïve and tolerant mice were nearly equivalent, we next wished to determine if the therapeutic effect elicited by the induction of HER2 immunity after Ad-HER2-ki vaccination was equivalent in tolerant animals. To determine therapeutic effect in tolerant animals, transgenic animals with tolerance to HER2+ were injected with the same dose of 4T1-HER2+ cells and vaccination with Ad-HER2-ki was given at 4 days postimplantation as previously done in naïve counterparts (Fig. 3C). We found that as with immune responses, Ad-HER2-ki vaccination was again able to significantly blunt the growth of 4T1-HER2+ tumors with similar kinetics in tolerant animals. It should be noted, however, that it required repeated dosing to achieve these effects in tolerant mice, whereas a single vaccination was sufficient in wild-type (WT) mice (Fig. 2B). Indeed, tumors from Ad-HER2-ki–vaccinated HER2+ transgenic mice outgrew slightly quicker after the initial tumor regression compared with naïve Ad-HER2-ki vaccinated mice (Figs. 2B and 3C), despite three vaccinations. Thus, our results indicate that Ad-HER2-ki is a potent antitumor vaccine against aggressive non–HER2-dependent tumor growth in a tolerant preclinical model.
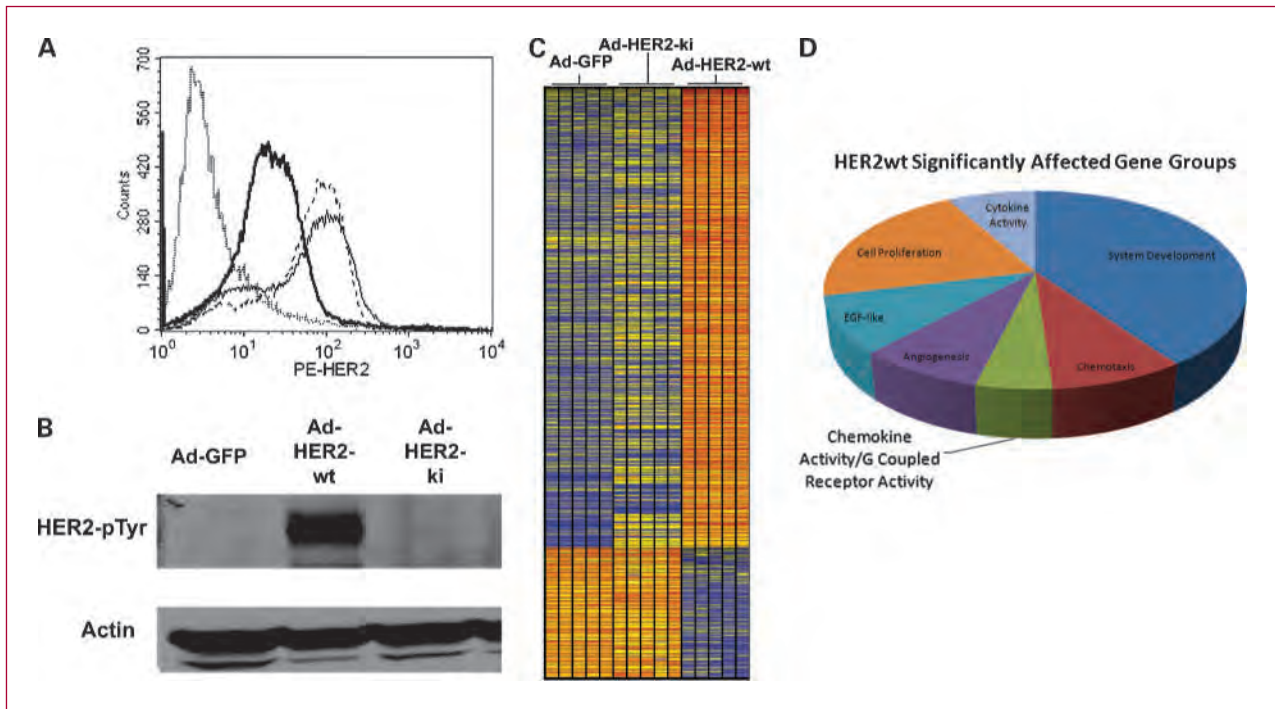
Oncogenic signaling deficiency after overexpression of kinase inactivated HER2. As our preclinical studies of immunogenicity and therapeutic effectiveness had revealed Ad-HER2-ki to be the most promising candidate for a human HER2 vaccine, we next wanted to determine if HER2-ki was truly nononcogenic. As strong overexpression of HER2 is known to be an early causative event in breast cancer, it was of the utmost importance to understand if

Fig. 3. Ad-HER2-ki significantly inhibits HER2+ tumor growth in transgenic mice with tolerance to HER2+ *in vivo*. A, IFN-γ ELISPOT responses at 2 wpi in Ad-HER2-ki– or Ad-LacZ–injected human-HER2-transgenic (HER2-Tg+) and nontransgenic (HER2-Tg-) littermates. A pool of epitopes to full-length human HER2 was used to stimulate splenocytes (*n* = 5). *, *P* < 0.05; **, *P* < 0.01. Error bars, SD. B, FACS analysis using 4T1 or 4T1-HER2 cells to detect HER2-specific IgG antibodies from mice vaccinated with Ad-HER2-ki or Ad-LacZ (2 wpi, *n* = 5). *, *P* < 0.05; **, *P* < 0.01. Error bars, SD. C, vaccination using Ad-HER2-ki inhibits the growth of established 4T1-HER2 tumors in human HER2-transgenic mice. Human HER2 transgenic mice (*n* = 5) were implanted with 2×10^4 4T1-HER2+ cells on day 0 (Δ) and were vaccinated with 2.6 × 10 E^{10} particles of Ad-HER2-ki (○) or Ad-LacZ (□), on days 4, 11, and 18 (arrows). Regression analysis *P* < 0.0001. Error bars, SD.

Fig. 4. Equivalent expression of HER2-wt and HER2-ki but differential phosphorylation and oncogenic signaling capacity. HMECs were serum starved for 36 h, infected with Ad-HER2-wt, Ad-HER2-ki, or Ad-GFP at a multiplicity of inflection of 150. A, FACS analysis at 18 hpi using anti-HER2 PE-labeled antibody revealed surface expression of human HER2 infected with the Ad-HER2-wt (thin dotted line), Ad-HER2-ki (thin solid line), or Ad-GFP (thick solid line) vectors. B, Western blots done on infected HMECs at 18 hpi using anti-HER2 pTyr705 and actin antibodies. C, a hierarchically clustered heatmap of significantly affected genes ($P < 0.05$ with Benjamini-Hochberg Multiple Testing Correction, filtered by >3-fold difference) where each gene probe is represented by a single row and each column denotes an individual infected sample ($n = 5$ for all conditions). The more transcriptionally active a gene is, the greater the intensity of the shade of red, whereas less active genes are depicted by greater intensity of shades of blue. D, HER2-wt significantly dysregulated genes ($P < 0.05$ with Benjamini-Hochberg Multiple Testing Correction) with >3-fold difference from control (Ad-GFP) were interrogated for their functional classification using DAVID as described in Materials and Methods. The most significantly affected gene groups are displayed in proportional representation to the number found in those groups to be dysregulated by HER2-wt.

the single amino acid mutation could fully block phosphorylation and oncogenic signaling in the context of strong adenoviral overexpression.
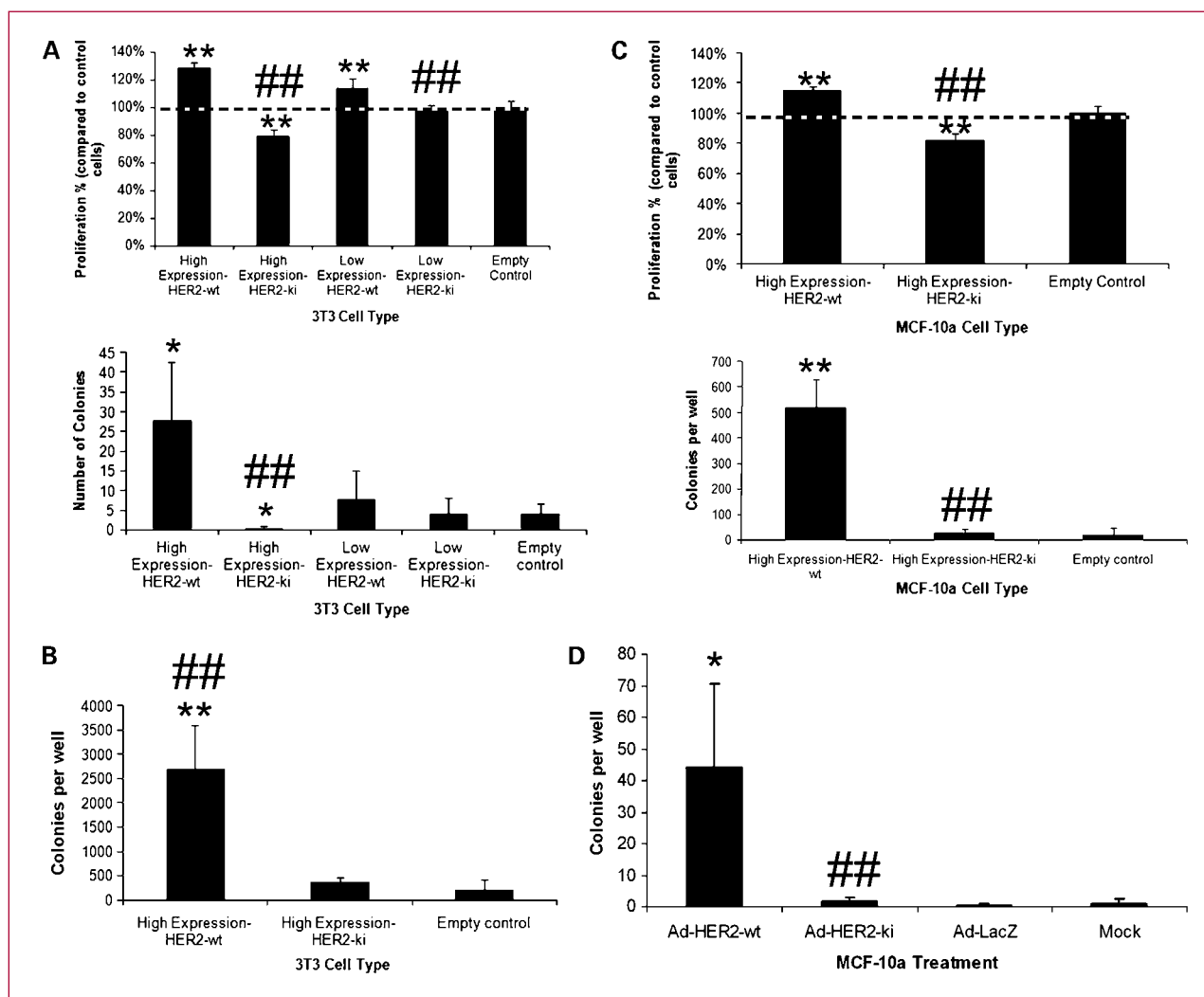
To initially determine if there were differences between HER2-ki (kinase inactive) and HER2-wt (wild-type) expression and phosphorylation, we infected primary HMECs with Ad-HER2-ki or Ad-HER2-wt. Although infection with both vectors resulted in similar levels of high surface expression of HER2 as shown by FACS analysis and Western blot analysis (Fig. 4A, Supplementary Fig. S2), we could detect no evidence of HER2 phosphorylation in Ad-HER2-ki–infected HMECs, in contrast to Ad-HER2-wt–infected HMECs (Fig. 4B, Supplementary Fig. S2). We next examined the signaling consequences of this phosphorylation defect through a comparison of transcriptome profiles from Ad-HER2-wt–, Ad-HER2-ki–, and Ad-GFP control–infected HMECs. Using one-way ANOVA ($P < 0.05$ with Benjamini-Hochberg false discovery rate multiple testing correction) additionally filtered for genes with a >3-fold difference, we found that 423 genes were statistically different between the Ad-HER2-wt and Ad-GFP, whereas only 21 were different between Ad-HER2-ki and Ad-GFP (Fig. 4C). Subsequent investigation

of nine representative gene targets by quantitative real-time PCR (Supplementary Table S1 and S2) revealed a high degree of array concordance and confirmed our transcriptome findings. A functional analysis of HER2-wt revealed significant overrepresentation and clustering into seven Gene Ontology (GO) groups: systems development, epidermal growth factor (EGF)-like, cytokine activity, chemotaxis, chemokine activity/GPCR activity, proliferation, and angiogenesis (Fig. 4D). These findings suggest that much of the oncogenic potential attributed to HER2 kinase activity could be mediated through inflammatory and chemotaxis pathways (an area currently under investigation in our lab), as well as through more established angiogenic and EGF typical pathways. In sum, immunoblot and transcriptome assessments indicate the vast majority of cellular pathway activation mediated by HER2-wt are critically dependent upon phosphorylation and kinase functionality, strongly suggesting a critical oncogenic signaling deficit in HER2-ki.

Diminished proliferation and anchorage-independent growth of kinase-inactive HER2. Although immunoblots and transcriptome analysis revealed strong HER2-ki signaling deficiencies, it was unknown if these would diminish oncogenic function. To assess HER2 oncogenic function *in vitro*,

we constructed several stable HER2-wt and HER2-ki 3T3 fibroblasts lines that had different levels of HER2 expression (retrovirally selected lines expressed high levels of HER2 and are denoted as "high expression" whereas plasmid transfection selected lines expressed lower levels of HER2 and are denoted as "low expression"; Supplementary Table S3) and tested their proliferative and transformative capacity *in vitro*. We found that HER2-wt significantly augmented 3T3 proliferation in an expression-sensitive manner (Fig. 5A). In contrast, we found that strong HER2-ki expression significantly reduced cell proliferation, whereas weak HER2-ki expression had no effect on proliferation (Fig. 5A). Likewise, high-expression stable HER-wt 3T3 formed colonies in soft agar, whereas high-expression

stable HER2-ki 3T3 cells formed colonies at a significantly reduced basal rate compared with control cells (Fig. 5A). Thus, HER2-wt enhanced cell proliferation and transformation *in vitro*, whereas HER2-ki inhibited proliferation and transformation *in vitro*. Although statistically significant, these colony formation differences were modest and only apparent in highly expressed lines. Thus, to elicit a more sensitive measure of *in vitro* transformation, EGF (an ErbB family growth factor) was used to enhance HER2 soft agar colony formation (27). Although EGF addition enhanced colony formation of all cell types (Fig. 5A and B), only HER2-wt cell displayed significantly enhanced anchorage-independent growth over control cells (Fig. 5A and B). Thus, even in the presence of EGF, HER2-ki displays

Fig. 5. Diminished proliferation and anchorage-dependent growth of HER2-ki–expressing 3T3 and MCF-10a cells. A, stable 3T3 cells were assessed for proliferation by MTT assay 72 h after plating ($n = 6$) or for anchorage-independent growth by soft agar assay 2 wk after plating (5×10^4 cells/well in 2 mL, 2-wk assessment, $n = 3$). B, soft agar assay was done as described in A but in the presence of EGF (10 ng/mL) with cells cultured for 3 wk (5×10^4 cells/well in 2 mL, 2-wk assessment, $n = 3$). C, stable MCF-10a cells were assessed for proliferation by MTT assay 72 h after plating ($n = 5$) or for anchorage-independent growth by soft agar assay 2 wk after plating ($n = 3$). D, MCF-10a cells were assessed for anchorage-independent growth after adenoviral vector infection (multiplicity of infection = 150; $n = 3$). *, $P < 0.05$; **, $P < 0.01$, compared with control cells, all samples. #, $P < 0.05$; ##, $P < 0.01$ to HER2-wt stable or infected cells. Error bars, SD.

Table 2. Tumorgenicity assays show lack of oncogenic potential of the HER2-ki gene

3T3 clone	Tumor formation at 28 d (1 × 10⁶ cells)	Tumor formation at 28 d (1 × 10⁵ cells)
3T3-high expression/HER2 wild-type	10/10 mice	50/50 mice
3T3-high expression/HER2-ki	0/10 mice	0/30 mice
3T3-empty vector	1/10 mice	0/30 mice
3T3 cells	0/10 mice	0/30 mice

a significant transformation deficiency compared with HER2-wt.

Having determined a proliferative and transformative defect in HER2-ki expressing mouse fibroblasts, we extended our investigation to a more relevant human cell type using engineered immortalized (but nontransformed) human breast epithelial cells (MCF-10a) to express either HER2-wt or HER2-ki. As before, we found that HER2-wt cells grew at a significantly enhanced rate whereas HER2-ki cells displayed a significant repression of proliferation compared with control cells (Fig. 5C). Additionally, we determined that HER2-wt cells formed significantly more colonies in soft agar compared with HER2-ki cells and control cells (Fig. 5C).

Finally, we wished to explore if adenovirus-mediated delivery and oncogene overexpression impacted human cell transformation *in vitro*. Although unlikely, it remained possible that in the context of an inflammatory response and heavy overexpression of HER2-ki, the minor dysregulation observed in our microarray could impact transformative capacity. We infected MCF-10a cells with HER2-wt, HER2-ki, and control GFP adenoviral vectors, and assessed anchorage-independent growth in soft agar. Although adenovirus-mediated overexpression of HER2-wt elicited anchorage-independent growth in those cells, Ad-HER2-ki–infected cells were unable to form more colonies than Ad-GFP–infected cells or uninfected controls (Fig. 5D). Thus, adenovirus-mediated delivery did not significantly alter transformative capacity of HER2-ki.

Collectively these *in vitro* data show that the signaling defects conferred by the mutation of HER2-ki ablate the enhanced proliferation and anchorage-independent growth elicited by the *HER2* oncogene. These defects were observed across different expression contexts and different cell types and thus strongly suggest that HER2-ki is a functionally ablated oncogene.

Lack of tumorigenicity in immunodeficient xenografts. Because HER2-ki had shown significant signaling and functional defects *in vitro*, we hypothesized that it would have a reduced oncogenic transformation potential *in vivo*. To assess this, stable HER2-ki, HER-wt, and control 3T3 cells were implanted in immunodeficient mice and tumor formation was assessed. Data from five independent experiments are summarized in Table 2, which shows that although all mice injected with 3T3 cells expressing the wild-type human HER2 gene (*HER2-wt*) developed tumors, mice injected with 3T3 cells expressing the kinase inactive gene (*HER2-ki*) did not develop tumors. Even at the highest concentrations of injected cells, the basal rate of spontaneous 3T3 transformation in control 3T3 cells proved higher than HER2-ki–expressing cells. Thus, the slightly greater transformation potential observed in control 3T3 cells suggests that HER2-ki expression has a negative effect on 3T3 transformation *in vivo*. These findings show that HER2 kinase function and downstream signaling are critical to its transformative capacity *in vivo* and further show that the transformative capacity of HER2-ki is ablated and its expression is safe *in vivo*.

Discussion

More than 20 years after its discovery, therapeutic strategies to target the human oncogene *HER2* are achieving measures of efficacy in the clinic, through use of the HER2-specific monoclonal antibody trastuzamab and the HER2/EGF receptor selective kinase inhibitor lapatinib. However, many tumors have *de novo* resistance to these therapies and the majority of tumors that initially respond to them eventually become refractory to treatment. In spite of this, these tumors retain HER2 expression, thus permitting the use of alternative anti-HER2 approaches as potential adjunct therapies. Along these lines, several HER2 vaccines have been developed that utilize protein or peptide fragments of either the intracellular and/or extracellular domain. In our study, we compare the use of several possible inactivated HER2 vaccines and report the strong efficacy of an adenoviral vector that encodes a kinase-inactive full-length *HER2* gene in an attempt to maximize immunotherapeutic anti-HER2 efficacy and concomitantly minimize HER2 oncogenic potential.

Although the oncogenic potential of HER2 is well documented, there have been few in-depth studies investigating the oncogenic effect of kinase-inactive HER2. HER2 is well known to signal in cooperation with the ErbB family of tyrosine kinase receptors, but has also been documented to translocate to the nucleus to activate genes such as *Cox-2* (13). Other reports have also documented HER2 to be involved with other signaling receptor families (28), thus broadening the potential mechanisms whereby HER2 promotes oncogenesis. Our study shows that overexpression of a kinase inactive HER2 (HER2-ki) results in a complete block of HER2 phosphorylation and has a dramatic impact on cellular signaling as measured by transcriptome dysregulation, in spite of high levels of

HER2 expression. We also found that HER2-ki does not confer any proliferative or transformative potential to cells, in the context of different expression capacities, different cell lines, as well as in *in vitro* and *in vivo* settings. Although some genes were dysregulated by expression of HER2-ki and reversion mutations could potentially occur with the single HER2-ki mutation, our investigation strongly suggests that HER2-ki is a functionally inactivated oncogene and thus safe for use in humans.

Beyond safety, our study also shows that Ad-HER2-ki is able to induce strong adaptive immune responses against HER2 that translate into effective antitumor immunity *in vivo*. Although previous studies have used a variety of different vaccination strategies that target ErbB2/HER2, none have targeted the human full-length HER2 using an adenoviral vector and extended these findings to a HER2-tolerant model. Indeed, studies that have used similar vaccine strategies to target ErbB2/HER2 have all utilized the rat *neu* gene (HER2 homolog) in mice, which is recognized as a foreign transgene (*neu*) and thus more immunogenic than a self-antigen (29–32). A number of studies using the rat *neu* have also looked at prevention of spontaneous tumors in various rat *neu*-transgenic mouse models (32–36). Although the data show that these vaccine strategies can be effective in reducing or preventing the development of mammary tumors, the physiologic relevance of these tumor models has been questioned (37). Additionally, the *neu*T model has been shown to be more responsive to DNA vaccination than the human HER2-transgenic model used in the present study, likely because the spontaneous *neu* tumors seem to be completely dependent upon *neu* for growth and are more sensitive to anti-*neu* antibodies (38). For these reasons, we chose to use the more rigorous tolerance model provided by the human HER2-transgenic mice using 4T1-HER2+ cells, an aggressive and metastatic mouse tumor that is not completely dependent on HER2 for growth. Vaccination with Ad-HER2-ki in this model elicited the generation of strong T-cell and antibody responses comparable with those elicited in naïve mice. Ad-HER2-ki vaccination was able to strongly limit HER2+ cancer growth and elicited strong selection against HER2 expression in residual tumor mass. Because 4T1 cells are not dependent on HER2, it is possible that HER2-dependent models would offer even stronger evidence of Ad-HER2-ki efficacy. Our results indicate that the induction of HER2-specific T-cells highly correlates with antitumor efficacy and anti-HER2 tumor selection in multiple vaccines, strongly suggesting that vaccine efficacy is dependent upon the strong induction of HER2-specific T-cells. Of relevance for future clinical studies, we were also able to show Ad-HER2-ki antitumor effects against an aggressive HER2+ breast cancer in a human HER2-tolerant mouse model that most closely resembles the state of immunologic tolerance to human HER2 that exists in cancer patients.

In sum, our study shows the importance of HER2 kinase function in oncogenesis as well as the safety and efficacy of Ad-HER2-ki and Ad-HER2-ECD-TM for therapeutic vaccination against HER2+ breast cancer. Based on these findings, we are actively pursuing the use of Ad-HER2-ki in clinical studies to determine the safety and efficacy of this approach in patients with HER2+ breast cancer. Although adenoviral vaccines in humans with pre-existing anti-Ad5 immunity have lacked efficacy, we recently described a modified Ad5 platform that overcomes this barrier (39). If successful, our strategy of targeting active oncogenes with inactive oncogene vaccines could become a significant therapeutic option in the treatment of different oncogene-dependent cancers.

Disclosure of Potential Conflicts of Interest

Grant Support

References

1. Paik S, Hazan R, Fisher ER, et al. Pathologic findings from the National Surgical Adjuvant Breast and Bowel Project: prognostic significance of erbB-2 protein overexpression in primary breast cancer. J Clin Oncol 1990;8:103–12.
2. Konecny GE, Pegram MD, Venkatesan N, et al. Activity of the dual kinase inhibitor lapatinib (GW572016) against HER-2-overexpressing and trastuzumab-treated breast cancer cells. Cancer Res 2006;66: 1630–9.
3. Tuma RS. Lapatinib moves forward in inflammatory and early HER2-positive breast cancer trials. J Natl Cancer Inst 2007;99:348–9.
4. Ritter CA, Perez-Torres M, Rinehart C, et al. Human breast cancer cells selected for resistance to trastuzumab *in vivo* overexpress epidermal growth factor receptor and ErbB ligands and remain dependent on the ErbB receptor network. Clin Cancer Res 2007;13:4909–19.
5. Martin AP, Miller A, Emad L, et al. Lapatinib resistance in HCT116 cells is mediated by elevated MCL-1 expression and decreased BAK activation and not by ERBB receptor kinase mutation. Mol Pharmacol 2008;74:807–22.
6. Wilson JM. Adenoviruses as gene-delivery vehicles. N Engl J Med 1996;334:1185–7.
7. Barouch DH, Nabel GJ. Adenovirus vector-based vaccines for human immunodeficiency virus type 1. Hum Gene Ther 2005;16:149–56.
8. Tatsis N, Ertl HC. Adenoviruses as vaccine vectors. Mol Ther 2004; 10:616–29.
9. Kozarsky KF, Wilson JM. Gene therapy: adenovirus vectors. Curr Opin Genet Dev 1993;3:499–503.
10. Di Fiore PP, Pierce JH, Kraus MH, Segatto O, King CR, Aaronson SA. erbB-2 is a potent oncogene when overexpressed in NIH/3T3 cells 21. Science 1987;237:178–82.

11. Hudziak RM, Schlessinger J, Ullrich A. Increased expression of the putative growth factor receptor p185HER2 causes transformation and tumorigenesis of NIH 3T3 cells. Proc Natl Acad Sci U S A 1987; 84:7159–63.

12. Moasser MM. Targeting the function of the HER2 oncogene in human cancer therapeutics. Oncogene 2007;26:6577–92.

13. Wang SC, Lien HC, Xia W, et al. Binding at and transactivation of the COX-2 promoter by nuclear tyrosine kinase receptor ErbB-2. Cancer Cell 2004;6:251–61.

14. Wang SE, Narasanna A, Perez-Torres M, et al. HER2 kinase domain mutation results in constitutive phosphorylation and activation of HER2 and EGFR and resistance to EGFR tyrosine kinase inhibitors. Cancer Cell 2006;10:25–38.

15. Kershaw MH, Jackson JT, Haynes NM, et al. Gene-engineered T cells as a superior adjuvant therapy for metastatic cancer. J Immunol 2004;173:2143–50.

16. Amalfitano A, Hauser MA, Hu H, Serra D, Begy CR, Chamberlain JS. Production and characterization of improved adenovirus vectors with the E1, E2b, and E3 genes deleted. J Virol 1998;72:926–33.

17. Hartman ZC, Black EP, Amalfitano A. Adenoviral infection induces a multi-faceted innate cellular immune response that is mediated by the toll-like receptor pathway in A549 cells. Virology 2007;358: 357–72.

18. Huang DW, Sherman BT, Tan Q, et al. DAVID Bioinformatics Resources: expanded annotation database and novel algorithms to better extract biology from large gene lists. Nucleic Acids Res 2007;35:W169–75.

19. O'Hayer KM, Counter CM. A genetically defined normal human somatic cell system to study ras oncogenesis *in vivo* and *in vitro*. Methods Enzymol 2006;407:637–47.

20. Xia W, Gerard CM, Liu L, Baudson NM, Ory TL, Spector NL. Combining lapatinib (GW572016), a small molecule inhibitor of ErbB1 and ErbB2 tyrosine kinases, with therapeutic anti-ErbB2 antibodies enhances apoptosis of ErbB2-overexpressing breast cancer cells. Oncogene 2005;24:6213–21.

21. Piechocki MP, Ho YS, Pilon S, Wei WZ. Human ErbB-2 (Her-2) transgenic mice: a model system for testing Her-2 based vaccines 1. J Immunol 2003;171:5787–94.

22. duPre' SA, Redelman D, Hunter KW, Jr. Microenvironment of the murine mammary carcinoma 4T1: endogenous IFN-gamma affects tumor phenotype, growth, and metastasis. Exp Mol Pathol 2008;85: 174–88.

23. DuPre SA, Redelman D, Hunter KW, Jr. The mouse mammary carcinoma 4T1: characterization of the cellular landscape of primary tumours and metastatic tumour foci. Int J Exp Pathol 2007;88:351–60.

24. Piechocki MP, Pilon SA, Wei WZ. Quantitative measurement of anti-ErbB-2 antibody by flow cytometry and ELISA. J Immunol Methods 2002;259:33–42.

25. Frank R, Overwin H. SPOT synthesis. Epitope analysis with arrays of synthetic peptides prepared on cellulose membranes. Methods Mol Biol 1996;66:149–69.

26. Wei WZ, Shi WP, Galy A, et al. Protection against mammary tumor growth by vaccination with full-length, modified human ErbB-2 DNA 3. Int J Cancer 1999;81:748–54.

27. Riedel H, Massoglia S, Schlessinger J, Ullrich A. Ligand activation of overexpressed epidermal growth factor receptors transforms NIH 3T3 mouse fibroblasts. Proc Natl Acad Sci U S A 1988;85:1477–81.

28. Qiu Y, Ravi L, Kung HJ. Requirement of ErbB2 for signalling by interleukin-6 in prostate carcinoma cells. Nature 1998;393:83–5.

29. Park JM, Terabe M, Steel JC, et al. Therapy of advanced established murine breast cancer with a recombinant adenoviral ErbB-2/neu vaccine. Cancer Res 2008;68:1979–87.

30. Lachman LB, Rao XM, Kremer RH, Ozpolat B, Kiriakova G, Price JE. DNA vaccination against neu reduces breast cancer incidence and metastasis in mice. Cancer Gene Ther 2001;8:259–68.

31. Wang X, Wang JP, Rao XM, Price JE, Zhou HS, Lachman LB. Prime-boost vaccination with plasmid and adenovirus gene vaccines control HER2/neu+ metastatic breast cancer in mice. Breast Cancer Res 2005;7:R580–588.

32. Tegerstedt K, Lindencrona JA, Curcio C, et al. A single vaccination with polyomavirus VP1/VP2Her2 virus-like particles prevents outgrowth of HER-2/neu-expressing tumors. Cancer Res 2005;65: 5953–7.

33. Gallo P, Dharmapuri S, Nuzzo M, et al. Adenovirus vaccination against neu oncogene exerts long-term protection from tumorigenesis in BALB/neuT transgenic mice. Int J Cancer 2007;120:574–84.

34. Renard V, Sonderbye L, Ebbehoj K, et al. HER-2 DNA and protein vaccines containing potent Th cell epitopes induce distinct protective and therapeutic antitumor responses in HER-2 transgenic mice. J Immunol 2003;171:1588–95.

35. Cipriani B, Fridman A, Bendtsen C, et al. Therapeutic vaccination halts disease progression in BALB-neuT mice: the amplitude of elicited immune response is predictive of vaccine efficacy. Hum Gene Ther 2008;19:670–80.

36. Park JM, Terabe M, Sakai Y, et al. Early role of CD4+ Th1 cells and antibodies in HER-2 adenovirus vaccine protection against autochthonous mammary carcinomas. J Immunol 2005;174:4228–36.

37. Andrechek ER, Hardy WR, Siegel PM, Rudnicki MA, Cardiff RD, Muller WJ. Amplification of the neu/erbB-2 oncogene in a mouse model of mammary tumorigenesis. Proc Natl Acad Sci U S A 2000;97:3444–9.

38. Jacob J, Radkevich O, Forni G, et al. Activity of DNA vaccines encoding self or heterologous Her-2/neu in Her-2 or neu transgenic mice. Cell Immunol 2006;240:96–106.

39. Osada T, Yang XY, Hartman ZC, et al. Optimization of vaccine responses with an E1, E2b and E3-deleted Ad5 vector circumvents preexisting anti-vector immunity. Cancer Gene Ther 2009;16:673–82.

Synergism from combined immunologic and pharmacologic inhibition of HER2 *in vivo*

Michael A. Morse[1,2], Junping Wei[3], Zachary Hartman[3], Wenle Xia[1], Xiu-Rong Ren[4], Gangjun Lei[3], William T. Barry[6], Takuya Osada[3], Amy C. Hobeika[3], Sharon Peplinski[3], Haixiang Jiang[7], Gayathri R. Devi[2,3], Wei Chen[2,4], Neil Spector[1,2], Andrea Amalfitano[8,9], H. Kim Lyerly[2,5] and Timothy M. Clay[2,10]

[1] Division of Medical Oncology, Department of Medicine, Duke University Medical Center, Durham, NC

[2] Duke Comprehensive Cancer Center, Duke University Medical Center, Durham, NC

[3] Division of Surgical Sciences, Department of Surgery, Duke University Medical Center, Durham, NC

[4] Division of Gastroenterology, Department of Medicine, Duke University Medical Center, Durham, NC

[5] Division of General Surgery, Department of Surgery, Duke Comprehensive Cancer Center, Duke University Medical Center, Durham, NC

[6] Department of Biostatistics and Bioinformatics, Duke University Medical Center, Durham, NC

[7] Department of Pediatrics, Duke University Medical Center, Durham, NC

[8] Department of Microbiology and Molecular Genetics, Michigan State University, East Lansing, MI

[9] Department of Pediatrics, Michigan State University, East Lansing, MI

[10] Division of Surgical Sciences, Department of Surgery, and Department of Immunology, Duke University Medical Center, Durham, NC

The monoclonal antibody trastuzumab and the EGFR/HER2 tyrosine kinase inhibitor lapatinib improve the clinical outcome of patients with HER2-overexpressing breast cancer. However, the majority of metastatic cancers will eventually progress, suggesting the need for other therapies. Because HER2 overexpression persists, we hypothesized that the anti-HER2 immune response induced by cancer vaccines would be an effective strategy for treating trastuzumab- and lapatinib-refractory tumors. Furthermore, we hypothesized that the antibody response could synergize with lapatinib to enhance tumor inhibition. We developed a recombinant adenoviral vector expressing a kinase-inactive HER2 (Ad-HER2-ki) to use as a cancer vaccine. Vaccine-induced polyclonal HER2-specific antiserum was analyzed for receptor internalization and signaling effects alone and in combination with lapatinib. Ad-HER2-ki vaccine-induced potent T cell and antibody responses in mice and the vaccine-induced polyclonal HER2-specific antiserum mediated receptor internalization and degradation much more effectively than trastuzumab. Our *in vitro* studies demonstrated that HER2 vaccine-induced antibodies effectively caused a decrease in HER2 expression, but when combined with lapatinib caused significant inhibition of HER2 signaling, decreased pERK and pAKT levels and reduced breast tumor cell proliferation. In addition, a known mechanism of resistance to lapatinib, induction of survivin, was inhibited. The combination of Ad-HER2-ki plus lapatinib also showed superior antitumor efficacy *in vivo*. Based on these results, we feel clinical studies using this approach to target HER2-overexpressing breast cancer, including trastuzumab- and lapatinib-resistant tumors is warranted.

Tumor Immunology

The human epidermal growth factor receptor (HER) 2, over-expressed in 20–30% of breast cancers, is associated with more aggressive tumors and inferior overall survival.[1] Combinations of the anti-HER2 antibody trastuzumab and chemotherapy lengthen survival in metastatic HER2-overexpressing breast cancer.[2] However, progressive disease typically occurs within 1 yr. Lapatinib, a potent reversible inhibitor of HER2 and EGFR tyrosine kinases,[3] in conjunction with chemotherapy, enhances time to progression in these patients.[4] Unfortunately, responses to lapatinib are generally short lived and progression remains a significant clinical problem.

Intriguingly, the overexpression of HER2 persists in trastuzumab and lapatinib-refractory tumors,[5,6] and thus, targeting HER2 with T cells and antibodies induced by cancer vaccines is a potentially effective strategy. More than a dozen phases I and II studies of cancer vaccines have been conducted in breast cancer patients.[7] These vaccines have included proteins, peptides, modified tumor cells and dendritic cells loaded with breast tumor antigens. In these studies,

HER2 has been demonstrated to be immunogenic, with a suggestion that immunized patients had an improved clinical outcome.[8–12] Although we saw promising results following immunization with HER2-protein loaded dendritic cells,[13] such approaches are limited to specialized centers with cell processing expertise, and a more feasible approach to immunize patients would be the use of recombinant viral vectors encoding HER2.

Among the many vectors being studied, recombinant adenovirus (Ad) is the most widely used in clinical gene therapy applications including vaccines, having demonstrated the ability to induce immune responses in many clinical studies.[14–17] The commonly used Ad5 serotype has an extensive safety profile in the vaccine setting.[18–20] Although we wished to incorporate the HER2 gene into Ad vectors for therapeutic vaccination against HER2, there is potential concern that the full length molecule may be oncogenic.[21,22] Therefore, we generated a recombinant adenovirus encoding full length human HER2 with a kinase-inactivating mutation (Ad-HER2-ki) and demonstrated that it was nononcogenic and activated HER2-specific T cells and polyclonal antisera [called HER2-vaccine-induced antibodies (HER2-VIA)] with potent antitumor activity in murine models (Hartman et al., manuscript submitted). Interestingly, HER2 specific polyclonal antisera mediate receptor internalization and degradation much more effectively than trastuzumab, the monoclonal antibody targeting HER2 (manuscript in preparation).

Because lapatinib is now commonly used to treat patients with advanced HER2 overexpressing breast cancer that has become refractory to trastuzumab and because of our promising preclinical data suggesting that HER2-specific antibodies were synergistic when combined with lapatinib,[23] it was our intention to develop a vaccine strategy that could be used synergistically with lapatinib in humans. Therefore, we studied the effect of lapatinib combined with HER2-VIA on HER2-expressing cell lines. We then evaluated whether lapatinib would affect the induction of an immune response in vivo. Next, we assessed the antitumor activity of the Ad-HER2-ki vaccine in conjunction with lapatinib. We observed that the HER2-VIA had enhanced antisignaling and antiproliferative activity in the presence of lapatinib, so that Ad-HER2-ki could induce potent HER2-specific immune responses when administered with lapatinib and the combination resulted in greater antitumor activity in vivo than either agent alone.

Material and Methods
Reagents
Lapatinib was obtained from the Duke University Medical Center Pharmacy. The tablets were pulverized and then mixed with water at a concentration of 5 mg/mL. Similarly, trastuzumab and rituximab (as an antibody control) were obtained from the pharmacy and used as reconstituted. HER2 peptide mixes were synthesized by Jerini Peptide Technologies (Berlin, Germany) as 15mers overlapping by 11 amino acids.

Cell lines
The human breast cancer cell line Au565 (HER2+) was obtained from American Type Culture Collection (ATCC, Manassas, VA) and cultured in RPMI medium 1640 with 10% heat-inactivated FBS. Human breast cancer cell lines BT474 (HER2+) and SK-BR-3 (HER2+) were obtained from the Duke University Comprehensive Cancer Center Cell Culture Facility and were grown in Dulbecco's modified Eagle's medium (DMEM) supplemented with 10% FBS. The mouse breast cancer cell line 4T1 was purchased from ATCC. 4T1-HER2 was kindly provided by Dr. Michael Kershaw (Cancer Immunology Program, Peter MacCallum Cancer Centre, Victoria, Australia)[24] and maintained in DMEM with penicillin/streptomycin and 10% FBS.

Adenovirus vector preparation
Construction of the E1-, E3-Ad vector containing the human full length HER2 with an inactivating mutation in the kinase domain (Ad-HER2-Ki-) or beta-gal Lac-Z antigen under the control of human CMV promoter/enhancer elements was performed as previously described.[25] The LTR-2/erbB2 plasmid was provided by Dr. L.E. Samelson, (NCI, Bethesda, MD), and the HER2-ki sequence with a K753A mutation to a key residue in the ATP binding region to render the tyrosine kinase inactive[26] was created using Quik-Change mutagenesis (Stratagene, La Jolla, CA).

Mice
C57BL/6 and BALB/c mice were purchased from Jackson Labs (Bar Harbor, ME). All work was conducted in accordance with Duke IACUC-approved protocols.

Induction of HER2-VIA
C57BL/6 mice were vaccinated via footpad injection with Ad-Lac-Z or Ad-HER2-ki vectors (2.6×10^{10} particles/mouse). Fourteen days later, mice were euthanized and sera were collected and stored at -80°C.

MTT assay to detect cell proliferation
To assess VIA effects on proliferation, HER2+ cells (Au565 at 5000 cells per well in a 96-well plate) were cultured with purified HER2-ki-VIA or control serum (1:50 dilution) for 3 d and assessed by 3-(4, 5-dimethylthiazol-2-yl)-2,5-diphenyl tetrazoliumbromide (MTT) assay. Trastuzumab (Herceptin; 10 μg/mL) was used as a positive control, and sera from mice receiving Ad-LacZ vaccine or saline were used as negative controls.

Western blotting to analyze pathway inhibition
AU565 cell extracts were prepared by scraping cells off petri dishes, washing cell pellets 2× in phosphate buffered saline (PBS) and then resuspending pellets in two-packed-cell volumes of RIPA buffer (150 mM NaCl, 50 mM Tris-HCl, pH 7.5, 0.25% (w/v) deoxycholate, 1% NP-40, 5 mM sodium

orthovanadate, 2 mM sodium fluoride and a protease inhibitor cocktail). Protein concentrations were determined using a modification of the Bradford method (Bio-Rad Labs, Hercules, CA). Equal amounts of proteins (50 μg) were resolved by 4–15% gradient SDS polyacrylamide gel electrophoresis. After transfer, the membranes were then probed with specific antibodies recognizing target proteins [pTyr (Sigma), HER2, Akt, pAkt, Erk 1/2, pErk1/2, (Cell Signaling, Beverly, MA) survivin, and actin (Sigma, St. Louis, MO)] and IRDye 800 conjugated anti-rabbit or mouse IgG or Alexa Fluor 680 anti-rabbit IgG and were visualized using the Odyssey Infrared Imaging System (LI-COR, Lincoln, NE).

Immunogenicity of lapatinib plus Ad-HER2-ki
Eight-wk-old female C57BL/6 mice received lapatinib (75 mg/kg/d) by oral gavage or vehicle (saline) daily beginning on day 0. Beginning on day 7, mice were vaccinated with 2.6 × 10^{10} particles of Ad-HER2-ki or Ad-LacZ. Fourteen days postinjection, mice were euthanized and splenocytes and sera were collected for analysis by ELISPOT and flow cytometry.

ELISPOT analysis
IFN-γ ELISPOT assays (Mabtech, Cincinnati, OH) performed according to the manufacturer's instructions. Splenocytes (500,000 cells/well) were added to the well, and HER2 peptide mix (2.6 μg/mL was used; BD Bioscience, San Jose, CA) was used as a stimulating antigen. HIV peptide mix (BD Bioscience) was used as a negative control, and a mixture of PMA (50 ng/mL) and Ionomycin (1 μg/mL) was a positive control of the assay.

Analysis of anti-HER2 antibody binding by ELISA
Human breast tumor cell lines (BT474, SKBR3, MCF-7) were harvested, washed and 3 × 10^5 cells were suspended in 100 μL 1% BSA-PBS and incubated with HER2-VIA or LacZ-VIA (1:100, 1:1000, 1:5000) for 30 min at 4°C. Cells were washed twice with 2 mL of 1% PBS-BAS and stained with HRP-conjugated anti-human IgG (109-035-088; Jackson ImmunoResearch Labs, West Grove, PA; 1:5000) in 100 μL 1% BSA-PBS for 30 min at 4°C. After two times washing with 1% BSA-PBS, 150 μL TMB substrate was added and cells were incubated for 15 min at room temperature. Hundred microliters of supernatant was transferred into a 96-well plate. The absorbance was measured on plate reader at 660 nm.

Analysis of anti-HER2 antibody binding by Flow cytometry
We have adapted a methodology reported by Wei *et al.*[27] to measure anti-HER2 VIA in vaccinated mouse serum by flow cytometry. Briefly, 3 × 10^5 cells (mouse 4T1-HER2, HER2+; mouse 4T1, HER2-) were incubated with diluted (1:100, 1:1000, 1:10,000) mouse serum (HER2-VIA or LacZ-VIA) for 1 hr at 4°C, washed with 1% BSA-PBS, stained with PE-conjugated anti-mouse IgG (Dako, Cat R0480) for 30 min at 4°C

and washed again. Samples were analyzed on a BD LSRII flow cytometer with results represented as histograms.

Complement dependent cytotoxicity assay
The HER2-VIA or LacZ-VIA in sera from mice immunized as above was diluted (1:100) and co-incubated with target cells (4T1 and 4T1-HER2) at 37°C for 1 hr and 1:100 diluted rabbit serum as the source of complement. After 2.5 hr incubation, cytotoxicity was measured using the CytoTox 96 Nonradioactive Cytotoxicity Assay (Promega; per manufacturer's instructions) to measure LDH release in the culture media as evidence of cytotoxicity. Percent cell lysis is denoted with error bars representing SD.

Measuring antibody-dependent cellular cytotoxicity
Effector cells for the antibody-dependent cellular cytotoxicity (ADCC) assays were obtained by mincing murine spleens, passing the cells through a nylon sieve, lysing the red blood cells and culturing the remaining cells in RPMI 1640 containing mouse IL-2 (1000 U/mL) for 3 d. Nonadherent cells were removed by washing the flask gently with PBS twice. The adherent cells were supplemented with fresh RPMI 1640 medium containing IL-2 and cultured for three additional days. The adherent cells were then harvested and used as effector cells for ADCC assay. One million target (4T1-HER2) cells were labeled with 100 μCi of ^{51}Chromium at 37°C for 1 hr. The labeled target cells were washed three times with culture medium, counted and plated (10^4/well in 100 μL medium) into V-bottomed 96-well microtiter plates, then incubated with either HER2-VIA (1:100), control LacZ-VIA (1:100) or trastuzumab (20 mg/mL) at 4°C for 20 min. Effector cells were add to the plates containing target cells and incubated for another 4 hr. The effector:target (E:T) ratio was 20:1. After incubation, the plates were centrifuged for 5 min at 500g, and 100 μL supernatant was removed from each well for counting of radioactivity in a spectrometer (Auto-gamma; Packard, Meriden, CT). The cytotoxicity of each sample was determined as follows: Lysis (%) = (experimental − target spontaneous)/(target maximum − target spontaneous)*100%.

Assessment of HER2 localization and internalization
Construction of fluorescent HER2 construct: the HER2-YFP was constructed by using a LTR-2/erbB-2(HER2) construct as PCR template[21] and pcDNA3.1-mYFP construct as vector (gift from Roger Y. Tsien, University of California at San Diego). HER2 was PCR amplified by using the primers 5′-CCCAAGCTTAGCACCATGGAGCTGGCGGCC-3′ and 5-CCGCTCGAGCACTGGCACGTCCAGACCCAG-3′ and inserted into the vector by Hind III and XhoI restriction sites. The authentication of HER2 cDNA was verified by sequencing. HEK293 cells were maintained in MEM medium supplemented with 10% FBS and 100 units of penicillin and streptomycin. The day before transfection, 0.3 million HEK293 cells were seeded into fibronectin-coated 35-mm glass bottom dishes (MatTek). HER2YFP DNA was

Tumor Immunology

transfected into cells using FuGENE 6 (Roche). Twenty-four hours after transfection, cells were treated with 100 µg/mL of HER2-VIA, LacZ-VIA or trastuzumab in culture medium for live cell imaging using Zeiss laser scanning microscopy (LSM-510).

Murine model of antitumor activity of lapatinib plus Ad-HER2-ki

Eight-wk-old female BALB/c mice were implanted with 30,000 4T1-HER2 mouse mammary tumor cells expressing human HER2 on day 0. Mice received lapatinib (75 mg/kg/d) by oral gavage daily beginning on day 0, and they were randomized (n = 8 or 9 mice per group) to be vaccinated weekly with 2.6×10^{10} particles of Ad-HER2-ki or Ad-LacZ on days 4, 11 and 18. Tumor volume was measured, once it became palpable every 2 d using calipers, and is reported for day 29 when mice were euthanized in accordance with humane endpoints for tumor size as stated in the Duke IACUC policy.

Statistical analyses

To analyze tumor volume measurements, a cubic root transformation was applied to stabilize the variance such that residuals are normally distributed (data not shown).[28] An ANOVA test was used to assess statistical differences in day 29 volume measurements, and step-down Student t-tests were applied to five pairwise treatment comparisons of interest, using Bonferroni corrected p values. Longitudinal growth models were estimated for changes in tumor volume across time, using mixed effects models. The covariance structure was estimated with a time-continuous autoregressive model that was determined to be optimal by the Bayesian Information Criteria. Fixed effects were considered for the interaction of Treatment with a quadratic trend across day, and the likelihood ratio test was highly significant ($\chi^2 = 51.5$ with 8 df; $p < 0.0001$), such that one concludes there is a distinct treatment difference in tumor growth over time. Wald-type tests are reported for the linear and quadratic trends within treatment. Analyses were performed using R version 2.8.1. For all tests, statistical significance was set at $p < 0.05$.

Results

Ad vector encoding kinase-inactivated HER2 induces potent T cell and antibody responses

We have developed a recombinant adenoviral vector expressing full length human HER2 with a single amino acid mutation that eliminates kinase activity (Ad-HER2-ki) but retains the kinase domain to enhance T cell immunogenicity conferred by the intracellular domain. When wild type C57BL6 mice were vaccinated with Ad-HER2-ki, splenocytes from vaccinated mice were demonstrated by ELISPOT to recognize an overlapping human HER2 peptide mix, whereas splenocytes from mice receiving control Ad-LacZ vaccine or saline showed no reactivity to the HER2 peptide mix (Fig. 1a). To measure HER2-specific antibody responses, binding of VIA

in mouse serum was tested against HER2 strongly expressing (BT474, SKBR3) and weakly expressing (MCF-7) cell lines (Fig. 1b). The serum of mice vaccinated with the Ad-HER2-ki had binding titers of 1:5000, whereas the serum of mice receiving the control Ad-LacZ vaccine showed only background levels of binding. The HER2-VIA recognized greater than 14 epitopes in the intracellular and extracellular domain (Hartman et al., manuscript submitted), demonstrating that the antibody responses are polyclonal.

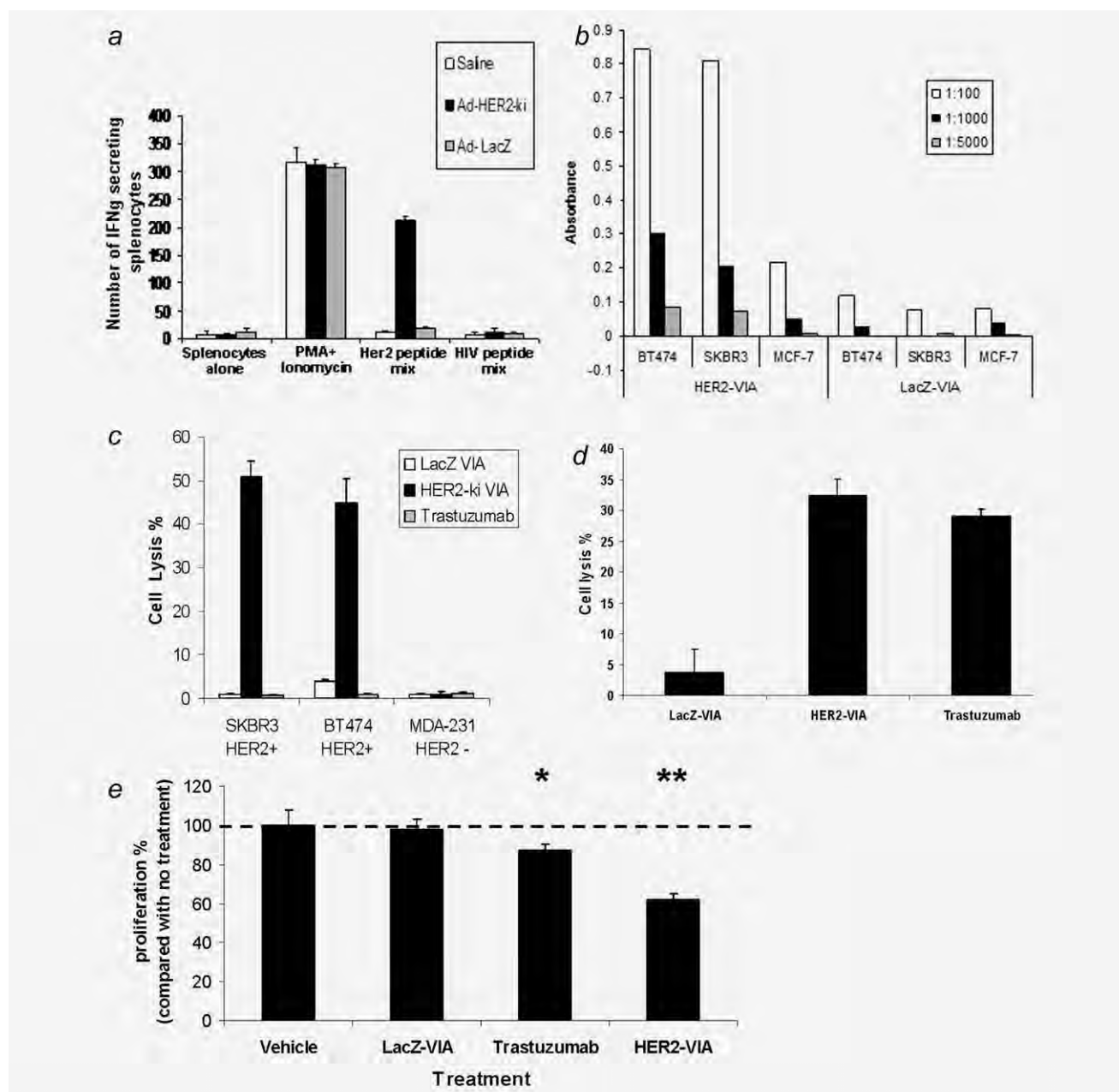### VIA against HER2 (HER2-VIA) lyse HER2+ breast tumor cells

Direct antibody-mediated tumor cell killing is a powerful potential mechanism of action of VIA. We evaluated the capacity of VIA against HER2 to mediate complement-dependent cytotoxicity (CDC) and ADCC. Trastuzumab did not mediate CDC but the HER2-VIA exhibited strong CDC against SKBR3 and BT474 human breast tumor cells, while control LacZ-VIA showed no effect (Fig. 1c). The effect was HER2-specific, because there was no CDC against the HER2 negative cell line MDA-231. To evaluate ADCC, we cultured mouse NK cells with HER2-VIA or LacZ-VIA and the human HER2-expressing 4T1 mammary tumor line (4T1-HER2) as a target. HER2-VIA and trastuzumab mediated significant and equivalent levels of ADCC (Fig. 1d). These data demonstrate that the Ad-HER2-ki induced polyclonal sera contain polyclonal antibodies with an extended spectrum of activity compared with trastuzumab.

VIA against HER2 inhibit proliferation of HER2+ cell lines

Although immunization with Ad-HER2-ki was able to efficiently induce humoral immunity *in vivo*, we also wished to determine whether the antibodies could inhibit HER2+ tumor cell proliferation as has been ascribed to trastuzumab. We found that when highly HER2+ human breast cancer cells (SKBR3) were cultured with HER2-VIA from the sera of Ad-HER2-ki vaccinated mice, their proliferation was significantly inhibited compared with cells cultured with control LacZ-VIA (Fig. 1e). Indeed, the inhibition of proliferation was greater than with trastuzumab. Similar results were obtained with other HER2+ human breast cancer cell lines, BT474 and AU565 (data not shown), thus demonstrating the antiproliferative effect of the VIA against HER2 *in vitro*.
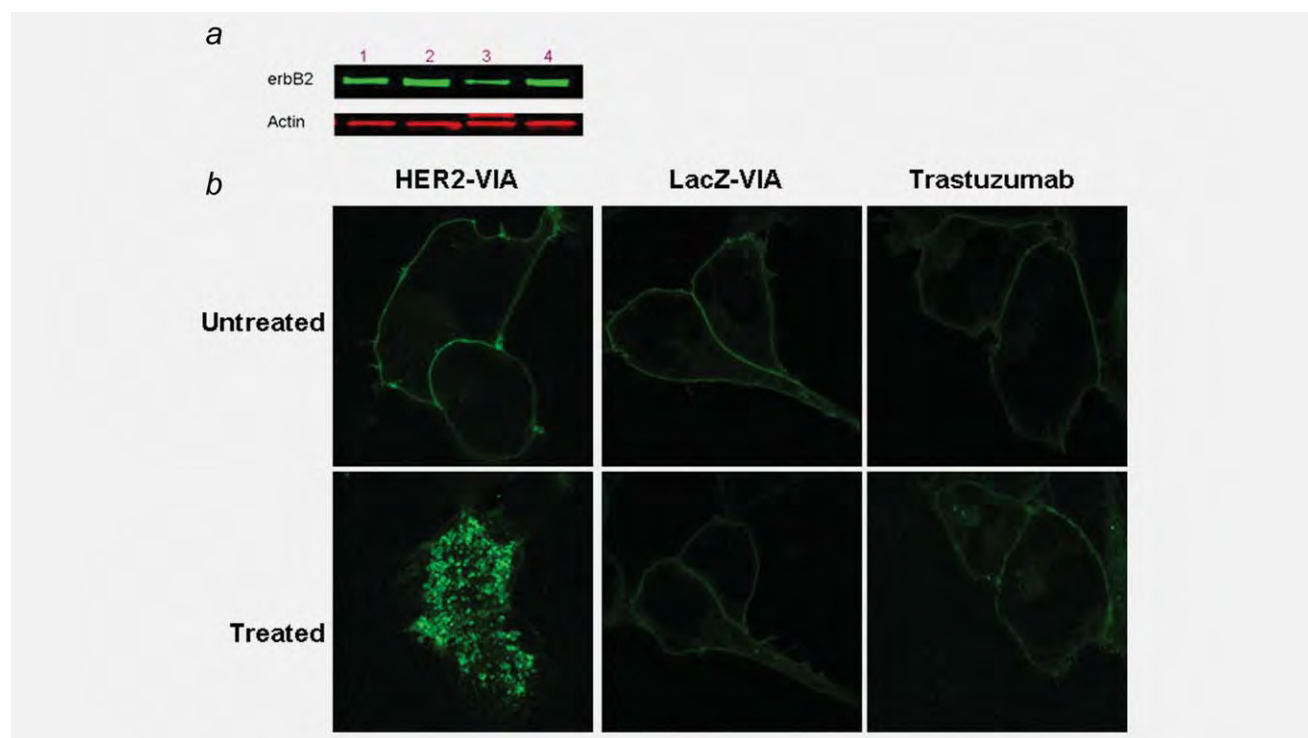
VIA against HER2 mediate HER2 receptor internalization

Growth factor receptor downregulation has been proposed as a mechanism for the inhibition of tumor growth mediated by monoclonal antibodies. To ascertain whether receptor downregulation was caused by HER2-VIA, we next investigated HER2 expression levels in highly HER2+ SKBR3 cells after exposure to serum VIA against HER2. Analysis by Western blotting revealed a decrease in HER2 protein levels in cells exposed to HER2-VIA relative to untreated cells or cells exposed to LacZ-VIA (Fig. 2a). This loss of HER2 expression suggested that HER2 was being internalized and degraded

Figure 1. (*a*) HER2-specific T cell responses in vaccinated mice. Pooled splenocytes obtained from C57BL/6 mice (n = 8 per treatment group) 14 d after injection of Ad-HER2-ki, Ad-LacZ or saline were tested in an interferon-gamma ELISPOT, and the number of responding T cells (±SD) was determined. The number of responding cells per 500,000 splenocytes in response to the antigen stimulus (*x*-axis) is shown. (*b*) HER2-specific T cell responses in vaccinated mice. Serum obtained from the same mice as in A at 14 d post injection of Ad-HER2-ki or Ad-LacZ was mixed with the listed cell lines shown on the *x*-axis. Binding of anti-HER2 antibodies was detected by ELISA. Absorbance was measured at 660 nm. (*c*) Polyclonal anti-HER2 VIA (Ad-HER2-VIA) mediates CDC *in vitro*. Pooled serum (8 mice per group) from C57BL/6 mice immunized with Ad-HER2-ki or Ad-LacZ or trastuzumab (10 μg/mL), was mixed with HER2 overexpressing cell lines (BT474 and SKBR3) or a HER2 negative cell line (MDA-231) and then rabbit complement was added. The percentage lysis of the cells (±SD) was determined by Chromium release assay. (*d*) Polyclonal Ad-HER2-VIA mediates ADCC *in vitro*. NK cells derived from C57BL/6 mice were cultured with the anti-HER2 VIA, anti-LacZ VIA or trastuzumab, and the cell line 4TI-HER2. The percentage lysis of the cells (±SD) was determined by Cytox 96 assay. (*e*) Antiproliferative effect of HER2-VIA on HER2+ SKBR3 proliferation. HER2+ SKBR3 cells were cultured with HER2-VIA, LacZ-VIA, trastuzumab (10 μg/mL) or saline, and an MTT assay was used to determine proliferation. Statistical analysis comparing samples to the vehicle alone treatment: *trastuzumab $p = 0.010$; **HER2-VIA $p > 0.0001$.

Figure 2. Polyclonal anti-HER2 VIA (Ad-HER2-VIA) lead to HER2 receptor internalization and degradation. (*a*) Western blots of ErbB2, in SKBR3 cells at 72 hr after designated treatments. (1 = no treatment, 2 = lapatinib 0.2 μ*M*, 3 = HER2-VIA (1:50), 4 = LacZ-VIA (1:50). (*b*) HER2-GFP transfected HEK293 cells were plated onto collagen-coated plastic dishes with glass bottoms and cultured overnight. Confocal images of cells expressing HER 2-GFP were acquired using Zeiss laser scanning microscopy (LSM-510). Cells were left untreated (top row) or treated for 1 hr with HER2-VIA (bottom left), LacZ-VIA (bottom middle), or trastuzumab (bottom right). Representative images of three independent experiments are shown.

after exposure to HER2-VIA. To confirm this, we sought to visualize HER2 receptor internalization. By using fluorescently labeled endogenous HER2 in HEK293 cells, we observed dramatic internalization and aggregation of the receptor within 1 hr after exposure to HER2-VIA, but not with exposure to trastuzumab or control LacZ-VIA (Fig. 2*b*).

HER2 VIA enhance the antisignaling effect of lapatinib

Because of our published evidence of synergy between VIA and small molecule inhibition of HER2, we performed Western blot analysis on the human HER2+ breast tumor cell line Au565 treated with lapatinib and serum from mice immunized with the Ad-HER2-ki vaccine to evaluate the downstream effects of this combination (Fig. 3*a*). As expected, lapatinib reduced pTyr (as an indicator of pHER2), pErk and pAKT levels, but did not alter HER2 expression. Trastuzumab had a minimal effect on HER2 expression, even in the presence of lapatinib. In contrast, serum HER2-VIA reduced the level of HER2 protein and the combination of lapatinib and serum VIA against HER2 reduced HER2 protein and pTyr, pErk and pAKT expression. In addition, the combination of lapatinib plus the HER2-VIA resulted in loss of survivin expression. Similar effects were observed in experiments with the cell lines SKBR3 and BT474 (data not
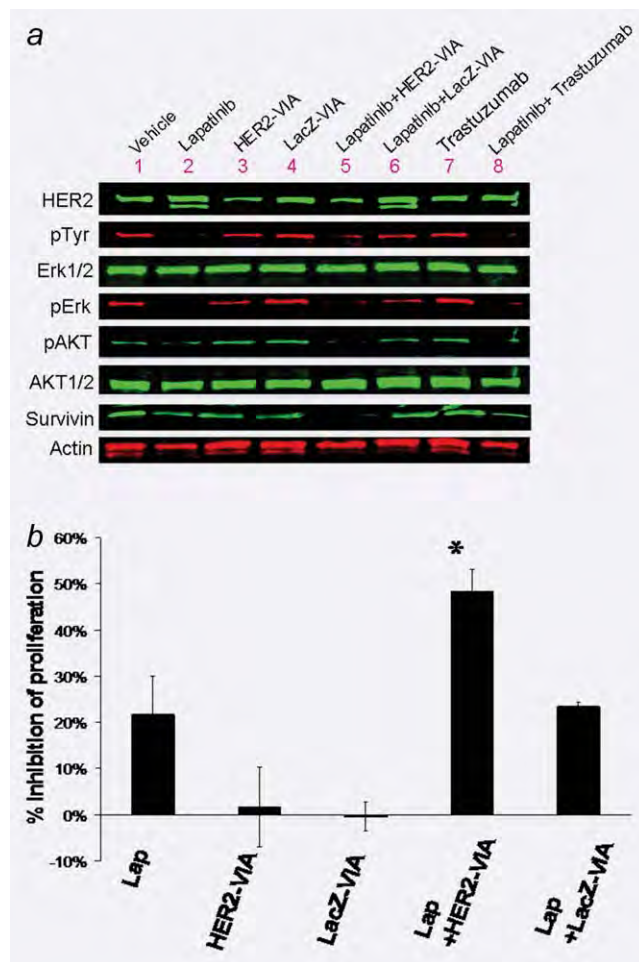
shown). These data demonstrate that lapatinib and the polyclonal HER2-VIA induced by immunization against HER2 have different effects on HER2+ breast cancer cell lines and that combining the two agents results in additional perturbation of tumor cell signaling.

HER2 VIA enhance the antiproliferative effect of lapatinib

Having demonstrated that the HER2-VIA inhibited proliferation of HER2-expressing cell lines (Fig. 1*e*), we wanted to determine whether there would be additional benefit for the addition of lapatinib to the HER2-VIA, for which, we cultured the AU565 and BT474 cells with HER2-VIA and lapatinib. As demonstrated in Figure 3*b*, lapatinib plus the HER2-VIA resulted in greater inhibition of proliferation of AU565 than lapatinib alone at this sub-maximal dose. Similar results were obtained for the BT474 (data not shown). These data demonstrate that the HER2-VIA contain antibodies that synergize with lapatinib to reduce the proliferation of HER2-expressing cell lines.

Immune responses to the Ad-HER2-ki vaccine are not impaired by lapatinib

Little is known about the effect of lapatinib on the immune response to cancer vaccines *in vivo*. BALB/c mice were

Figure 3. HER2-VIA enhances antisignaling and antiproliferative effects of lapatinib. (*a*) AU565 breast cancer cells were incubated with lapatinib, HER2-VIA, LacZ-VIA and trastuzumab with or without lapatinib. Lysates were analyzed by Western blot for HER2, pTyr (all phosphorylated tyrosines), ERK1/2, pERK, pAKT, AKT1/2 and survivin. VIA were used at a dilution of 1:50; lapatinib was at 0.1 μM; and trastuzumab was at 10 μg/mL. (*b*) Au565 cells (1 × 10^4) cells were treated with VIA (1:50 dilution) with or without lapatinib (0.1 μM) for 3 d. Live cells were measured using a thiazolyl blue (MTT) cell proliferation assay by reading A^{485}, and the mean percent inhibition of proliferation ±SD is represented. All treatments were performed in triplicate.

treated with lapatinib or vehicle for 21 d by oral gavage daily beginning on day 0 and were vaccinated at day 7 with Ad-HER2-ki, Ad-LacZ or vehicle. The magnitude of the day 21 HER2-specific T cell response to Ad-HER2-ki, measured by an interferon gamma ELISPOT using mouse splenocytes incubated with a HER2 polypeptide mix, was identical, irrespective of whether mice were receiving lapatinib or vehicle (Fig. 4*a*). These data demonstrate that concurrent lapatinib does not diminish T cell responses to the Ad-HER2-ki vaccine. Similarly, we studied the induction of anti-HER2 antibody responses in the setting of lapatinib. The HER2-VIA

bound to HER2 expressing tumor cells to the same extent, regardless of whether activated in the presence, or absence, of lapatinib (Fig. 4*b*). Furthermore, HER2-VIA from mice treated with lapatinib or vehicle and vaccinated with the Ad-HER2-ki were tested for CDC and ADCC *in vitro*. Lapatinib administration had no effect on the ability of the Ad-HER2-ki to induce VIA capable of lysing HER2+ 4T1 tumor cells by CDC (Fig. 4*c*) or ADCC (Fig. 4*d*). These data indicate no negative effect of lapatinib on induction of antibody responses to Ad-HER2-ki.
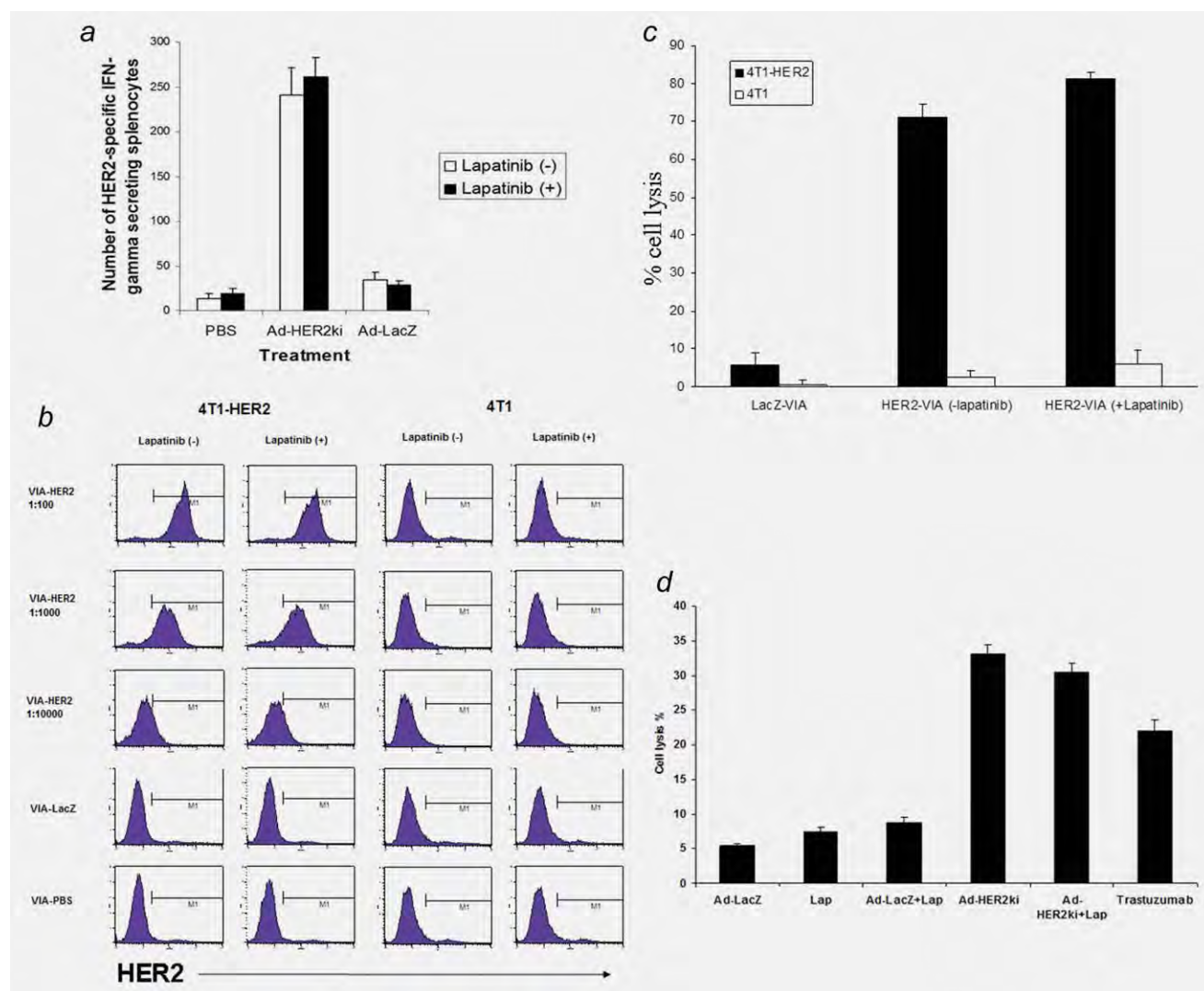
Ad-HER2-ki vaccine plus lapatinib leads to greater tumor regression than either therapy alone in a treatment model

To demonstrate efficacy of a combination of lapatinib and vaccination, we administered lapatinib simultaneously with Ad-HER2-ki immunizations to mice bearing HER2 expressing breast tumor cells and evaluated tumor growth over time (Fig. 5*a*–5*c*). In vehicle-treated animals, tumor growth reached an average volume of 968 mm^3 at day 29, and treatment arms with Ad-HER2-ki vaccine and lapatinib showed general tumor control (ANOVA $F_{4,37} = 4.84$, $p = 0.003$). Although the step-down tests of single agent antitumor activity were not statistically significant at the α = 0.05 level after adjusting for multiple comparisons ($t = 0.94$ and 2.68, for lapatinib and Ad-HER2-ki, respectively), the combination of both resulted in the greatest tumor control ($t = 4.42$, adjusted $p = 0.003$). Distinct differences are observed in the average tumor growth profile of each treatment over time (Fig. 5*b*), as indicated by the highly significant interaction between treatment and a quadratic trend across day ($p < 0.0001$). Among mice receiving vehicle control, tumor growth increased linearly on the cube-root scale (slope = 0.3, $p = 0.019$), while mice receiving Ad-HER2-ki vaccine alone or in combination with lapatinib showed a significant attenuation in volume from day 10 to day 20 before similar growth patterns returned ($p = 0.015$ and 0.02, respectively). These data demonstrate synergistic antitumor activity for the combination of Ad-HER2-ki and lapatinib on tumor growth in treating established tumors. By comparing final tumor volume at day 29 (Fig. 5*c*), when the study reached humane endpoints, a highly significant decrease in tumor volume was observed when compared with the lapatinib plus Ad-LacZ control with the lapatinib plus Ad-HER2-ki vaccine ($p = 0.0009$).

Discussion

Tumors that progress on trastuzumab and lapatinib continue to express high levels of HER2, leading us to propose targeting HER2+ tumors using a cancer vaccine strategy. We have developed an adenoviral vector vaccine expressing a kinase-inactive, full length human *HER2* gene (Ad-HER2-ki), which we have demonstrated is nononcogenic (Hartman et al., manuscript submitted). We now establish that this vector induces HER2-specific T cell responses and polyclonal antibody responses capable of mediating ADCC and CDC. In
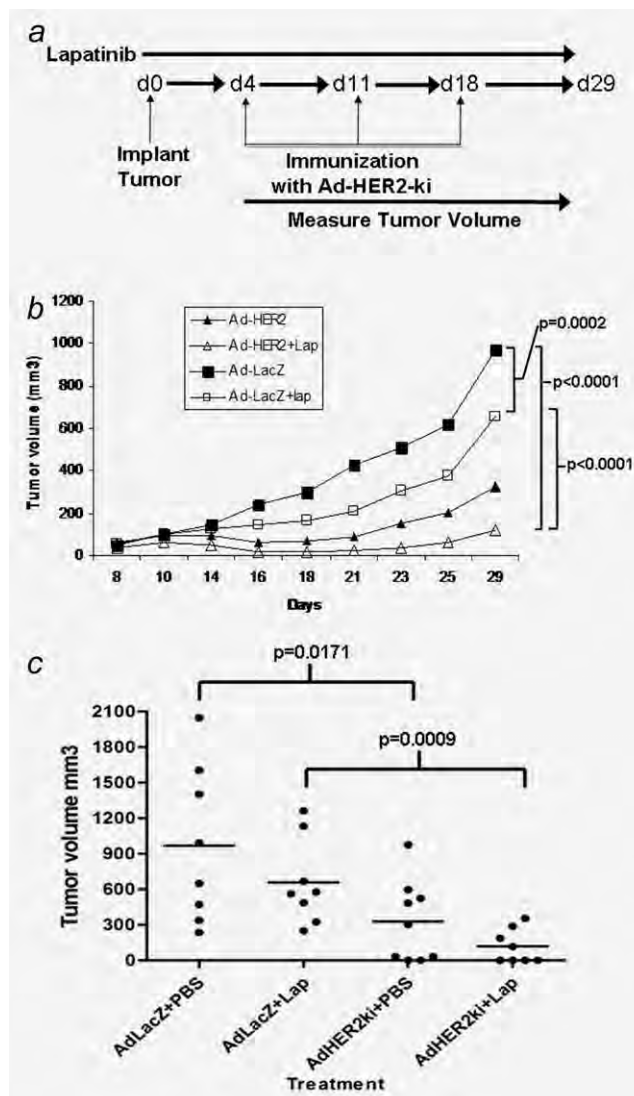
Tumor Immunology

Figure 4. T cell, antibody and cytolytic responses to immunization with Ad-HER2-ki vaccine are not impaired by lapatinib treatment. (*a*) Wild type C57BL/6 mice, treated with lapatinib (75 mg/kg/d) or vehicle (PBS), were vaccinated with Ad-HER2-ki, Ad-LacZ, or vehicle (PBS). The magnitude of the immune response to HER2 was measured by IFN$_\gamma$ ELISPOT. The mean number of IFN$_\gamma$ producing cells per 500,000 splenocytes is represented $\pm$SD. (*b*) Mouse 4T1-HER2 (HER2+) and 4T1 (HER2-) were incubated with diluted HER2-VIA or LacZ-VIA, stained with PE-conjugated anti-mouse IgG and samples analyzed by flow cytometer. The histogram representing the mean fluorescent intensity (MFI) for each treatment is shown. (*c*) 4T1 or 4T1-HER2 cells were incubated mouse HER2-VIA (from mice treated with or without lapatinib as in Figure 1*a* or LacZ-VIA (1:50) along with rabbit serum as a source of complement. Supernatant from the cultures were taken for the CDC assay. The percentage of lysis was calculated by the following formula: lysis (%) = (experimental-target spontaneous)/(target maximum-target spontaneous) * 100%. (*d*) NK cells derived from C57BL6 mice were cultured with the cell line SKBR3 and serum from mice treated with Lapatinib, Ad-LacZ, Ad-LacZ plus lapatinib, Ad-HER2-ki, Ad-HER2-ki plus lapatinib. Trastuzumab was used as a control for ADCC activity. The percentage lysis of the tumor cells ($\pm$SD) was determined by Chromium release assay. [Color figure can be viewed in the online issue, which is available at www.interscience.wiley.com.]

addition to these classical immune functions, the antibodies induced by Ad-HER2-ki had potent antiproliferative effects on HER2-expressing tumor cells. We hypothesized that this might be because of receptor downregulation and subsequently demonstrated that the serum HER2-VIA produced significant receptor internalization that did not occur when tumor cells were treated with trastuzumab, distinguishing the polyclonal serum antibodies from conventional monoclonal antibody approaches. Finally, because the monoclonal HER2-

targeting antibody trastuzumab synergizes with lapatinib, we tested whether VIA induced by vaccinations against HER2 would synergize with lapatinib *in vitro* and whether combining lapatinib and Ad-HER2-ki immunization would lead to enhanced control of breast tumors *in vivo*. Our results establish that the combination was superior to either agent alone *in vitro* and *in vivo*.

Several observations in this study require additional commentary. First, much of the activity observed for the Ad-

Figure 5. Synergistic antitumor effect of the administration of Ad-HER2-ki and lapatinib treatment on the growth of established 4T1-huHER2 tumors in BALB/c mice. (*a*) Schema for murine tumor therapy experiment. (*b*) BALB/c mice implanted with 30,000 4T1 mouse mammary tumor cells expressing human HER2 received lapatinib (100 mg/kg/d). Mice were vaccinated weekly for 3 wk with 2.6×10^{10} particles of Ad-HER2-ki or Ad-LacZ. Tumor volume was measured, once tumors became palpable, every 2 d using calipers. Mean tumor volume is represented for each treatment group. (*c*) Data is shown for the various treatment groups at day 29 when mice were euthanized in accordance with humane endpoints for tumor size, per Duke IACUC policy. Bars denote mean tumor size for each group. Circles denote individual mice. Lap = lapatinib.

HER2-ki is likely related to the induction of a polyclonal immune response. For example, the HER2-VIA stimulated by the Ad-HER2-ki mediates both CDC and ADCC. It is widely reported that trastuzumab mediates ADCC but not CDC. Whether these multiple activities of the serum VIA against HER2 are because of different antibodies or are functions of one antibody will be evaluated in future studies aiming to identify the different components of the polyclonal sera. Another activity likely related to the polyclonal characteristics of the sera is the internalization of HER2 induced by the HER2-VIA, a function neither we nor others[29–31] have observed for trastuzumab. Combining two monoclonal antibodies targeting different epitopes on HER2 has been observed to cause HER2 internalization,[30,32] and there is other evidence that supports the ability of multiple antibodies to different epitopes being more efficient at internalizing receptors.[32–34] We have identified 14 epitopes recognized by the HER2-VIA (Hartman et al., manuscript submitted). The importance of the internalization lies in the possibility that internalized receptors may meet one of two fates, either being recycled to the cell surface or degraded. Receptors recycled to the cell surface may continue to stimulate tumor growth, while receptor degradation would block growth factor signaling and clearly be the more desirable outcome for an antitumor strategy. Our preliminary evidence supports the latter for HER2 receptor internalized by HER2-vaccine induced antibody treatment (manuscript in preparation).

The second major observation is that the lapatinib could be administered along with the Ad-HER2-ki and the lapatinib did not affect the immune response to immunization. We are not aware of any other data regarding the effect of lapatinib on the immune response. Some other tyrosine kinase inhibitors have demonstrated negative effects on the immune response, such as sorafenib (which targets raf in the EGFR pathway and other targets) while others, such as sunitinib, have had no detrimental effects.[35,36]

The third major observation is that there was synergy between the lapatinib and the HER2-VIA activated by the Ad-HER2-ki. Although lapatinib and HER2-VIA target the same molecule, their effects on signaling are different. Alone, the HER2-VIA had their greatest effect on HER2 protein levels. As expected, lapatinib interrupted signaling through HER2 and, thus, the phosphorylation of downstream molecules. The combination of the two reagents resulted additionally in a reduction in levels of the antiapoptotic protein survivin, which would result in enhanced tumor cell apoptosis. We previously reported *in vitro* results combining polyclonal antisera from rabbits immunized with a HER2 fusion protein with lapatinib.[23] Thus, although combining lapatinib and trastuzumab has shown favorable clinical results,[37] it is possible that the combination of lapatinib and a polyclonal anti-HER2 antibody response will be superior because of the additional effects provided by polyclonal antibodies over a monoclonal antibody targeting a single epitope. It is also intriguing that lapatinib treatment can lead to stabilization and accumulation of HER2, enhancing trastuzumab-mediated cytotoxicity.[38] We expect similarly that it will potentiate the activity of vaccines targeting HER2.

Collectively, our results strongly support the assessment of Ad-HER2-ki in human clinical trials. The potential benefits of a vaccine strategy over a MAb approach, with the induction of both T cell and polyclonal antibody responses, and

Tumor Immunology

multiple mechanisms of action resulting from polyclonal antibody induction encourage the use of vaccine strategies. There is increasing evidence that cancer vaccines can improve patient survival, renewing enthusiasm for cancer vaccine approaches.[13,39–41] The synergy seen with the vaccine plus lapatinib suggests that there use in combination should also be evaluated clinically. Clinical trials to evaluate the combination are scheduled to open in 2010. These clinical studies will determine if similar levels of cellular and humoral immune response can be induced in breast cancer patients to those seen in our animal model and whether the vaccine results in clinical efficacy. More broadly, we believe our results suggest that targeting receptor molecules using vaccines as a means to perturb signaling offers new opportunities to target cancer beyond the conventional lytic killing of tumors by the immune system.

Acknowledgements

References

1. Paik S, Hazan R, Fisher ER, Sass RE, Fisher B, Redmond C, Schlessinger J, Lippman ME, King CR. Pathologic findings from the National Surgical Adjuvant Breast and Bowel Project: prognostic significance of erbB-2 protein overexpression in primary breast cancer. *J Clin Oncol* 1990;8:103–12.

2. Slamon DJ, Leyland-Jones B, Shak S, Fuchs H, Paton V, Bajamonde A, Fleming T, Eiermann W, Wolter J, Pegram M, Baselga J, Norton L. Use of chemotherapy plus a monoclonal antibody against HER2 for metastatic breast cancer that overexpresses HER2. *N Engl J Med* 2001;344:783–92.

3. Xia W, Mullin RJ, Keith BR, Liu LH, Ma H, Rusnak DW, Owens G, Alligood KJ, Spector NL. Anti-tumor activity of GW572016: a dual tyrosine kinase inhibitor blocks EGF activation of EGFR/ erbB2 and downstream Erk1/2 and AKT pathways. *Oncogene* 2002;21:6255–63.

4. Geyer CE, Forster J, Lindquist D, Chan S, Romieu CG, Pienkowski T, Jagiello-Gruszfeld A, Crown J, Chan A, Kaufman B, Skarlos D, Campone M, et al. Lapatinib plus capecitabine for HER2-positive advanced breast cancer. *N Engl J Med* 2006;355:2733–43.

5. Ritter CA, Perez-Torres M, Rinehart C, Guix M, Dugger T, Engelman JA, Arteaga CL. Human breast cancer cells selected for resistance to trastuzumab *in vivo* overexpress epidermal growth factor receptor and ErbB ligands and remain dependent on the ErbB receptor network. *Clin Cancer Res* 2007;13:4909–19.

6. Martin AP, Miller A, Emad L, Rahmani M, Walker T, Mitchell C, Hagan MP, Park MA, Yacoub A, Fisher PB, Grant S, Dent P. Lapatinib resistance in HCT116 cells is mediated by elevated MCL-1 expression and decreased BAK activation and not by ERBB receptor kinase mutation. *Mol Pharmacol* 2008;74:807–22.

7. Emens LA, Reilly RT, Jaffee EM. Breast cancer vaccines: maximizing cancer treatment by tapping into host immunity. *Endocr Relat Cancer* 2005;12: 1–17.

8. Peoples GE, Gurney JM, Hueman MT, Woll MM, Ryan GB, Storrer CE, Fisher C, Shriver CD, Ioannides CG, Ponniah S. Clinical trial results of a HER2/neu (E75) vaccine to prevent recurrence in high-risk breast cancer patients. *J Clin Oncol* 2005;23:7536–45.

9. Disis ML, Schiffman K, Guthrie K, Salazar LG, Knutson KL, Goodell V, dela Rosa C, Cheever MA. Effect of dose on immune response in patients vaccinated with an her-2/neu intracellular domain protein-based vaccine. *J Clin Oncol* 2004;22: 1916–25.

10. Murray JL, Gillogly ME, Przepiorka D, Brewer H, Ibrahim NK, Booser DJ, Hortobagyi GN, Kudelka AP, Grabstein KH, Cheever MA, Ioannides CG. Toxicity, immunogenicity, and induction of E75-specific tumor-lytic CTLs by HER-2 peptide E75 (369–377) combined with granulocyte macrophage colony-stimulating factor in HLA-A2+ patients with metastatic breast and ovarian cancer. *Clin Cancer Res* 2002;8:3407–18.

11. Salazar LG, Fikes J, Southwood S, Ishioka G, Knutson KL, Gooley TA, Schiffman K, Disis ML. Immunization of cancer patients with HER-2/neu-derived peptides demonstrating high-affinity binding to multiple class II alleles. *Clin Cancer Res* 2003;9:5559–65.

12. Disis ML, Gooley TA, Rinn K, Davis D, Piepkorn M, Cheever MA, Knutson KL, Schiffman K. Generation of T-cell immunity to the HER-2/neu protein after active immunization with HER-2/neu peptide-based vaccines. *J Clin Oncol* 2002;20:2624–32.

13. Morse MA, Hobeika A, Osada T, Niedzwiecki D, Marcom PK, Blackwell KL, Anders C, Devi GR, Lyerly HK, Clay TM. Long Term Disease-Free Survival and T Cell and Antibody Responses in Women with High-Risk HER2+ Breast Cancer Following Vaccination Against HER2+. *J Transl Med* 2007;5:42–51.

14. Wilson JM. Adenoviruses as gene-delivery vehicles. *N Engl J Med.* 1996;334:1185–7.

15. Barouch DH, Nabel GJ. Adenovirus vector-based vaccines for human immunodeficiency virus type 1. *Hum Gene Ther* 2005;16:149–56.

16. Tatsis N, Ertl HC. Adenoviruses as vaccine vectors. *Mol Ther.* 2004;10:616–29.

17. Kozarsky KF, Wilson JM. Gene therapy: adenovirus vectors. *Curr Opin Genet Dev* 1993;3:499–503.

18. Reyes-Sandoval A, Fitzgerald JC, Grant R, Roy S, Xiang ZQ, Li Y, Gao GP, Wilson JM, Ertl HC. Human immunodeficiency virus type 1-specific immune responses in primates upon sequential immunization with adenoviral vaccine carriers of human and simian serotypes. *J Virol* 2004;78: 7392–99.

19. Hensley SE, Cun AS, Giles-Davis W, Li Y, Xiang Z, Lasaro MO, Williams BR, Silverman RH, Ertl HC. Type I interferon inhibits antibody responses induced by a chimpanzee adenovirus vector. *Mol Ther* 2007;15:393–403.

20. Barouch DH, Pau MG, Custers JH, Koudstaal W, Kostense S, Havenga MJ, Truitt DM, Sumida SM, Kishko MG, Arthur JC, Korioth-Schmitz B, Newberg MH, et al. Immunogenicity of recombinant adenovirus serotype 35 vaccine in the presence of pre-existing anti-Ad5 immunity. *J Immunol* 2004;172:6290–7.

21. Di Fiore PP, Pierce JH, Kraus MH, Segatto O, King CR, Aaronson SA. erbB-2 is a potent oncogene when overexpressed in NIH/3T3 cells. *Science* 1987;237:178–82.

22. Hudziak RM, Schlessinger J, Ullrich A. Increased expression of the putative growth factor receptor p185HER2 causes transformation and tumorigenesis of NIH 3T3 cells. *Proc Natl Acad Sci U S A* 1987; 84:7159–63.

23. Xia W, Gerard CM, Liu L, Baudson NM, Ory TL, Spector NL. Combining lapatinib (GW572016), a small molecule inhibitor of

ErbB1 and ErbB2 tyrosine kinases, with therapeutic anti-ErbB2 antibodies enhances apoptosis of ErbB2-overexpressing breast cancer cells. *Oncogene* 2005;24:6213–21.

24. Kershaw MH, Jackson JT, Haynes NM, Teng MW, Moeller M, Hayakawa Y, Street SE, Cameron R, Tanner JE, Trapani JA, Smyth MJ, Darcy PK. Gene-engineered T cells as a superior adjuvant therapy for metastatic cancer. *J Immunol* 2004;173: 2143–50.

25. Hodges BL EH, Everett RS, Ding EY, Serra D, Amalfitano A. Adenovirus vectors with the 100K gene deleted and their potential for multiple gene therapy applications. *J Virol* 2001;75:5913–20.

26. Akiyama T, Matsuda S, Namba Y, Saito T, Toyoshima K, Yamamoto T. The transforming potential of the c-erbB-2 protein is regulated by its autophosphorylation at the carboxyl-terminal domain. *Mol Cell Biol.* 1991;11:833–42.

27. Piechocki MP, Pilon SA, Wei WZ. Quantitative measurement of anti-ErbB-2 antibody by flow cytometry and ELISA. *J Immunol Methods* 2002;259(1–2):33–42.

28. Vlotides G, Siegel E, Donangelo I, Gutman S, Ren SG, Melmed S. Rat prolactinoma cell growth regulation by epidermal growth factor receptor ligands. *Cancer Res* 2008;68: 6377–86.

29. Longva KE, Pedersen NM, Haslekas C, Stang E, Madshus IH. Herceptin-induced inhibition of ErbB2 signaling involves

reduced phosphorylation of Akt but not endocytic down-regulation of ErbB2. *Int J Cancer* 2005;116:359–67.

30. Hommelgaard AM, Lerdrup M, van Deurs B. Association with membrane protrusions makes ErbB2 an internalization-resistant receptor. *Mol Biol Cell* 2004;15:1557–67.

31. Austin CD, De Maziere AM, Pisacane PI, van Dijk SM, Eigenbrot C, Sliwkowski MX, Klumperman J, Scheller RH. Endocytosis and sorting of ErbB2 and the site of action of cancer therapeutics trastuzumab and geldanamycin. *Mol Biol Cell* 2004;15: 5268–82.

32. Friedman LM, Rinon A, Schechter B, Lyass L, Lavi S, Bacus SS, Sela M, Yarden Y. Synergistic down-regulation of receptor tyrosine kinases by combinations of mAbs: implications for cancer immunotherapy. *Proc Natl Acad Sci U S A* 2005;102: 1915–20.

33. Roepstorff K, Grovdal L, Grandal M, Lerdrup M, van Deurs B. Endocytic downregulation of ErbB receptors: mechanisms and relevance in cancer. *Histochem Cell Biol* 2008;129:563–78.

34. Kirisits A, Pils D, Krainer M. Epidermal growth factor receptor degradation: an alternative view of oncogenic pathways. *Int J Biochem Cell Biol* 2007;39:2173–82.

35. Zhao W, Gu YH, Song R, Qu BQ, Xu Q. Sorafenib inhibits activation of human peripheral blood T cells by targeting LCK phosphorylation. *Leukemia* 2008;22: 1226–33.

36. Hipp MM, Hilf N, Walter S, Werth D, Brauer KM, Radsak MP, Weinschenk T, Singh-Jasuja H, Brossart P. Sorafenib, but not sunitinib, affects function of dendritic cells and induction of primary immune responses. *Blood* 2008;111:5610–20.

37. O'Shaughnessy KLB J, Burstein H, Storniolo AM, Sledge G, Baselga J, Koehler M, Laabs S, Florance A, Roychowdhury D. A randomized study of lapatinib alone or in combination with trastuzumab in heavily pretreated HER2+ metastatic breast cancer progressing on trastuzumab therapy. *J Clin Oncol* 2008;26(20 suppl): abstract 1015.

38. Scaltriti M, Verma C, Guzman M, Jimenez J, Parra JL, Pedersen K, Smith DJ, Landolfi S, Ramon y Cajal S, Arribas J, Baselga J. Lapatinib, a HER2 tyrosine kinase inhibitor, induces stabilization and accumulation of HER2 and potentiates trastuzumab-dependent cell cytotoxicity. *Oncogene* 2009;28:803–14.

39. Schlom J, Gulley JL, Arlen PM. Paradigm Shifts in Cancer Vaccine Therapy. *Exp Biol Med (Maywood)* 2008;233:522–34.

40. News in brief. *Nat Rev Drug Discov* 2009;8: 346–7.

41. Disis ML, Strickler JH, Wallace D, Goodell V, Salazar LG, Higgins D, Childs J, Tietje K, Dang Y, Slota M. Cellular immune parameters associated with improved long-term survival in advanced stage breast cancer patients after active immunization with a HER2-specific vaccine. *J Clin Oncol* 2008;26(15S):abstract 3015.

Tumor Immunology